Taste and olfactory representations in the human brain

Ivan E. T. de Araujo

DPhil Thesis

Linacre College

University of Oxford

September 2003

Statement

From the five experimental results described in this Thesis (Chapters I, II, III and V), four have been accepted for publication in specialised neuroscience journals as scientific papers (de Araujo et al. 2003a; de Araujo et al. 2003b; de Araujo et al. 2003c; Rolls et al. 2003a). Chapter IV is being prepared for publication.

I hereby state that I performed all the stimulus preparation, pre-scanning psychophysical testing, and subsequent acquisition, pre-processing and statistical modelling of the data presented in Chapters I, II, III and V. In the experiment described in Chapter IV, the intra-venous amphetamine injections administred during scanning were performed by B. Voellm and P. Cowen (Dep. Psychiatry, Oxford). I subsequently performed all of the pre-processing and statistical analyses of the data.

Abstract

Taste and olfactory representations in the human brain

DPhil Thesis – Trinity 2003

Ivan de Araujo

Linacre College

The aim of this Thesis is to investigate the functional neuroanatomy of taste and olfactory processing in the human brain, including where taste-olfactory convergence is represented and which areas respond to these stimuli as a function of their value as reinforcers. Taste and olfactory representations in the human brain were investigated in five functional Magnetic Resonance Imaging studies. First, we have shown that umami tastants activate similar cortical regions of the human taste system to those activated by a prototypical taste stimulus (glucose) and that the psychophysical enhacement produced by combinations of umami tastants is represented in the orbitofrontal cortex. Second, we found that three pleasant (but not unpleasant) odours activated a medial part of the rostral orbitofrontal cortex and that a correlation was found between the subjective pleasantness ratings of the six odours with activation in this medial region of the orbitofrontal cortex. In contrast, the primary olfactory (but not orbital) cortex was correlated with the intensity ratings. Third, unimodal taste and (both retronasal and orthonasal) olfactory inputs were found to converge into a region of the far anterior, agranular insula, where it adjoins the caudal part of the orbitofrontal cortex. Moreover, the pleasantness of flavour is represented in a medial part of the rostral orbitofrontal cortex. Fourth, the medial orbitofrontal cortex was also activated by intra-venous administration of amphetamine, implying that this region is generally involved in reward processing. Fifth, we have shown that water in the mouth activates the same general areas involved in taste processing including the primary taste cortex, and that the medial orbitofrontal cortex and a part of the mid insula respond to water in the mouth as a function of thirst levels whereas the anterior parts of the insular cortex including taste cortex respond to water independently of thirst levels. These new findings imply that the medial part of the human orbitofrontal cortex is a reward-related area involved in particular in the representation of the reinforcing properties of taste and olfactory stimuli (including water in the mouth) whereas a part of the far anterior, agranular insula and adjoining caudal orbitofrontal cortex encode for the sensory properties of these stimuli, in particular taste-olfactory convergence.

Long Abstract

This Thesis aims to investigate a series of questions on the human functional neuroanatomy of taste and olfactory processing by applying functional Magnetic Resonance Imaging (fMRI). The first question concerns the responses, in the human brain, to *umami* tastants such as monosodium glutamate and some ribonucleotides. Umami is considered to be a fifth taste, but it has been largely unknown if taste cortical areas respond to umami stimuli in a similar way to other prototypical tastants such as glucose. A related question concerns how the enhacement of the taste of monosodium glutamate by ribonucleotides (a characteristic effect produced by umami tastants) is represented in the human brain. The characterisation of umami as a fifth taste, at a central level, depends on the clarification of these issues. Second, we investigated how the responses in the human brain to orthonasally delivered odours depend on the hedonic value of the odours, and if the representations of odour valence and intensity in the brain are dissociated. The third question refers to the identification of regions in the human brain receiving convergent taste and olfactory input, and thus supporting the representation of flavour. The representation of the pleasantness of flavour (and the consonance of its components) is a related question. Fourth, we investigated if a different type of substance, M-amphetamine, does activate similar regions of the human brain to those responding to taste and olfactory stimuli as a function of their reward or motivational value. Amphetamine is a potent primary reinforcer, and the effects produced by intra-venous M-amphetamine allows for the inspection of reward-related areas in the human brain that are activated by reinforcing stimuli other than taste or smell. Finally, fifth, we were interested in investigating if water in the mouth does produce activations in brain regions known to respond to taste stimuli, and which brain areas respond to water in the mouth in a thirst-dependent way, and thus where its pleasantness is represented in the human brain.

The fMRI studies corresponding to the investigation of the above issues were described in five experimental Chapters.

Chapter I describes thus an fMRI study on the representation of the taste of *umami* in the human brain. Umami taste stimuli, of which an exemplar is monosodium glutamate (MSG) and which capture what is described as the taste of protein, were shown to activate similar cortical regions of the human taste system to those activated by a prototypical taste stimulus (glucose). These taste regions included the insular cortex (including more anterior parts), and the operculum which jointly constitute part of the primary taste cortex in primates, and the caudolateral

orbitofrontal cortex, a secondary taste cortex in primates. Thus the anterior insula and operculum form part of the human taste cortex as evidenced by the responses to distinct prototypical tastants (umami and glucose). A part of the rostral anterior cingulate cortex was also activated. When the nucleotide 0.005 M inosine 5'-monophosphate (IMP) was added to MSG (0.05 M), the BOLD (blood oxygenation-level dependent) signal in an anterior part of the orbitofrontal cortex showed positive interaction effects (supra-additivity), and this may reflect the subjective enhancement of umami taste that occurs when IMP is added to MSG (a solution containing the main ionic components of saliva, 25 mM KCl + 2.5 mM NaCO3, provides the necessary control for effects such as somatosensory effects and swallowing). These results extend to humans studies showing activation in macaques of single neurons by these umami stimuli, and allow brain areas where activation is related to the perceived enhancement effects of umami tastants to be revealed.

The aim of the study described in Chapter II was to investigate human brain responses to orthonasal olfactory stimulation and the categorisation of these responses by the hedonic value of the odorants. An event-related fMRI study is described where a continuous air-flow olfactometer was used to deliver a total of six different odours, of which three were judged by a panel of subjects as being pleasant (alpha ionone, lynalyl acetate and geranyl acetate) and three as being unpleasant (hexanoic acid, octanol and isovaleric acid; all odours diluted at 5% on propylene glycol). It was found that the three pleasant and the three unpleasant odours activated dissociable parts of the human brain. Pleasant but not unpleasant odours were found to activate a medial region of the rostral orbitofrontal cortex. Further, there was a correlation between the subjective pleasantness ratings of the six odours given during the investigation with activation of a medial region of the rostral orbitofrontal cortex. In contrast, a correlation between the subjective unpleasantness ratings of the six odours was found in regions of the left and more lateral orbitofrontal cortex. Activation was also found in the anterior cingulate cortex, with a middle part of the anterior cingulate activated by both pleasant and unpleasant odours, and a far anterior part of the cingulate cortex showing a correlation with the subjective pleasantness ratings of the odours. Thus the results suggest that there is a hedonic map of the sense of smell in brain regions such as the orbitofrontal cortex. Moreover, a double dissociation was found with the intensity ratings of the odours, which were not correlated with the BOLD signal in the orbitofrontal cortex, but were correlated with the signal in medial olfactory cortical areas including the pyriform and anterior entorhinal cortex. Correlation with the intensity ratings of the odours allowed thus the characterisation of primary (cortical) olfactory areas in humans. These results show thus that the areas of the human brain representing the hedonic or affective properties of odours do not include the primary olfactory areas, and are distinct from the areas encoding the intensity of odours.

Chapter III describes an event-related fMRI study designed to assess directly taste-olfactory interactions in the human brain, with particular interest on the convergence of their inputs into specific cortical sites. Four different stimuli were used including two taste and two olfactory stimuli. In this experiment odorants were delivered retronasally. The stimuli were chosen based on a set of psychophysical tests ran on a panel of subjects previous to the imaging study. These tests are described in the first part of Chapter III. Taste stimuli and the respective concentrations used in the fMRI study were sucrose (saccharin, SIGMA) at 0.5M and MSG (L-glutamic acid, SIGMA) at 0.05M. Olfactory stimuli were strawberry odour (Firmenich) at 20 ppm and 1.9% Methional in propylene glycol (chicken flavour, IFF) at 25 ppm. All stimuli were diluted and delivered in deionised water either as a taste + odour combination or as a simple stimulus. So in this case olfactory stimuli stimulated the retronasal pathway through the posterior nares of the nasopharynx. The tasteless solution was used as a control stimulus. Data analyses demonstrate that both taste and smell were represented in the caudal orbitofrontal cortex, insular cortex and adjoining areas, amygdala, and cingulate cortex. In particular an area of the far anterior, agranular insular cortex was significantly activated by pure taste (sucrose) and strawberry odour. Moreover, this area coincides (within the MNI coordinate system) with the area activated by orthonasal stimulation found in Chapter II and thus represents a site of convergence within the far anterior (agranular) insula for taste and (orthonasal and retronasal) olfactory inputs. Moreover, a comparison between unimodal taste and retronasal stimuli results in activations on the frontal operculum, characterising this area as unimodal primary taste area. Supra-linear interactions between the olfactory and taste stimuli were found in a lateral anterior part of the orbitofrontal cortex. Correlations with consonance and pleasantness (but not intensity) ratings for the smell and taste combinations were also found in a medial anterior part of the orbitofrontal cortex. These results indicate how the human central taste and olfactory systems relate to those of non-human primates and the neural substrate for flavour perception in humans.

The aim of the study described in Chapter IV was to investigate the areas of the human brain activated by intra-venous amphetamine (0.15mg/Kg), and in addition, to relate the brain activation to subjective reports of the degree of "mind-racing" made every minute during scanning. Psychiatrists B. Voellm and P. Cowen from Oxford University performed the amphetamine injections. M-amphetamine (along with other substances known to increase extra-cellular dopamine levels such as cocaine) has its reinforcing and ultimately addictive properties well established and thus helps to characterise the reward-related areas in the human brain by allowing for a comparison with the cortical representations of the reward properties of taste and olfactory stimuli. Two different image analysis models were used to reveal the brain areas modulated by amphetamine. The first was a simple subtractive, categorical analysis designed to

show which areas of the brain were activated by amphetamine. The comparison between the amphetamine condition against the saline (control) condition revealed highly significant activated voxels in the medial orbitofrontal cortex, rostral anterior cingulate cortex, and (ventral) striatum. The second was a correlation analysis, of brain areas where the activation was correlated with the degree of "mind-racing" being reported throughout the experiment. The concept of mind racing was found useful in previous studies with M-amphetamine to define the perceived effects of the drug in otherwise naïve subjects. Activations were found for this analysis in the medial orbitofrontal cortex, bilateral striatum, medio-dorsal thalamus/pulvinar, and anterior cingulate cortex. These results thus demonstrate that the medial orbitofrontal and rostral anterior cingulate cortices (along with other reward-related areas such as the ventral striatum) are activated by a reinforcing stimulus other than taste or smell. It indicates that taste, odours, and other food intake-related stimuli involve human brain areas generally associated with reward processing.

The aim of the fMRI study described in Chapter V is to investigate, in humans, if intra-oral delivery of water does involve similar cortical areas to those activated by prototypical tastants such as glucose and salt, and the modulation of these responses by different levels of hydration. In this study subjects were scanned two times: in the first session subjects were scanned following 6-8 hours of water deprivation, and immediately after were scanned for a second time following drinking (mineral) water to satiety. It was shown, first, that water produces activations in cortical taste areas (in particular the frontal operculum/anterior insula which is the primate primary taste cortex, and the caudal orbitofrontal / secondary taste cortex) comparable to those produced by the prototypical tastants salt (0.1M NaCl) and glucose (0.5M). Second, the activations in the frontal operculum/anterior insula produced by water when thirsty were still as large after the subjects had consumed water to satiety. Thus in the anterior insular (including the far anterior, agranular part of the insula located in the posterior end of the orbital surface) and frontal operculum cortices activations for water were not modulated by the physiological state. Third, in contrast, it was found that a region of the middle part of the insula was also activated by water in the mouth, and further that this activation only occurred when thirsty in that responses to the oral delivery of water in this region were not found after the subjects had drunk water to satiety. Fourth, the responses to water in the medio-caudal orbitofrontal cortex were also found to be modulated by the physiological state of the body. Fifth, further evidence that the reward value or pleasantness of water is represented in the orbitofrontal cortex was that a positive correlation with the subjective ratings of the pleasantness and the refreshing value of the water was found with activations in the caudal and anterior orbitofrontal cortex, and also in the anterior cingulate cortex. Sixth, analyses comparing pre- and post-satiety periods (i.e. when thirsty and when not thirsty) independently of stimulus delivery revealed higher activity levels in the rostral

anterior cingulate cortex. The activity of the rostral anterior cingulate cortex thus also appears to reflect the thirst level or motivational state of the subjects.

The above descriptions, taken together, lead thus to the conclusion that, first, the frontal opercular and anterior insular cortices seem thus to constitute a network in the frontal part of the cortex involved in encoding sensory information on stimuli delivered intra-oral or orthonasally. These regions include the agranular extension of the anterior insula into the caudal part of the orbital surface and the posterior end of the agranular insular cortex, where it adjoins the primary olfactory cortex. The far anterior, agranular part of the insular cortex along with the adjoining caudolateral orbital cortex, is a site for unimodal taste and (retronasal/orthonasal) olfactory convergence whereas a part of the frontal opercular cortex was characterised as a unimodal (taste only) area. The posterior end of the agranular insular cortex, which includes the primary olfactory cortex, encodes the intensity of odorants. Moreover, the stimulus-specific responses in more anterior parts of the insular cortex, including its agranular extension into the orbital surface and the operculum, are not modulated by changes in physiological or homeostatic states (in particular these regions of the cortex do respond to water in the mouth in a way which does not depend on dehydration levels). In contrast, activity in medial parts of the orbitofrontal cortex (including anterior and posterior regions) and in a mid part of the (right) insula seem to be modulated by changes in the reward value of these stimuli possibly as a function of homestatic needs (as in the case of intra-oral water, where dehydration levels were explicitly manipulated; it is possible however that the mid-insular activations were produced by the effects of having a dry mouth when thirsty). These areas seem also to form part of a network involving the rostral anterior cingulate cortex. The results are interpreted under the current knowledge on the functional anatomy of the insular and orbitofrontal cortices as obtained from experimental animals and previous human studies.

This Thesis presents novel findings concerning the representation of taste and smell in the human brain. Some of the brain regions described here have not been systematically investigated electrophysiologically in non-human primates. The results presented here may potentially be used as a basis for new studies at the single-neuron level. This would provide further information on the neural bases of taste and olfactory processing and ultimately on the central mechanisms of food intake control in primates.

Index

Introduction **12**
The Insular and adjoining Orbitofrontal Cortex: Anatomy and Function 14
Anatomy of the primate Insula 14
Orbital and medial prefrontal networks 20
Functions of the Insular and Orbitofrontal Cortex 24
Functions of the Insula 24
Functions of the primate orbitofrontal cortex 28
Somatosensory representation of the oral cavity in the primate cortex 29
Saliva composition 33
Anatomy and function of the cingulate cortex 34
Note on the terminology used in this Thesis 40
Introduction to Methods: Magnetic Resonance Imaging and its Functional variant 41
The basics of MRI 41
The BOLD signal and its physiological substrate 44
Local field inhomogeneities and brain shimming 46
Statistical analysis of activation images 49
Chapter I
The representation of umami taste in the human brain **54**
The organisation and function of the primate gustatory cortex 54
Umami taste 63
The representation of umami taste in the human brain: an event-related fMRI study 64
Materials and Methods 64
Results 66
Discussion 73
Chapter II
Different representations of pleasant and unpleasant odours in the human brain **76**
The organisation of the primate olfactory system 77
Olfactory receptor neurons 77
Organisation of the olfactory cortex in primates 78
Electrophysiology 81
Human studies 82
The representation of pleasant and unpleasant odours in the human brain: an event-related fMRI study 83
Material and Methods 84

Results 87
Discussion 94
Chapter III
Taste-olfaction convergence and the representation of flavour in the human brain 99
The psychophysics of crossmodal taste-olfactory integration 99
Experiment 1 100
Experiment 2 105
Conclusion 110
Taste-olfaction convergence in the human brain: an event-related fMRI study 111
Summary of the imaging study 111
Introduction 111
Materials and methods 113
Results 116
Discussion 128
Chapter IV
Cortical responses to intra-venous amphetamine in naïve subjects 133
Amphetamine and the dopaminergic system 134
The mesocortical dopamine system 134
Effects of amphetamine administration 136
Previous human studies 137
Intra-venous administration of amphetamine: an event-related fMRI study 139
Materials and methods 140
Model 1: On-Off comparison, amphetamine – saline 140
Model 2: Correlation analysis 142
Further analyses: identifying motor contributions 144
The activations in medial orbitofrontal cortex are not motor-dependent 146
Discussion 147
Chapter V
Dehydration and the Taste of Water 150
Introduction: Neural mechanisms of thirst 151
Cellular dehydration 151
Hypovolemia and the renin-angiotensin system 152
The Lamina terminalis 153
Interoception 154
Previous imaging studies 156
Cortical responses to water in the mouth and its modulation by the level of thirst: an event-related fMRI study 157

Summary of the study 157
Introduction 157
Materials and Methods 159
Results 162
Discussion 173
Conclusion 178
Convergence of taste and olfactory inputs into the far anterior, agranular insula 179
Unimodal taste and olfactory areas 182
The orbitofrontal cortex responses to taste 184
Summary 185
Medial orbitofrontal cortex and reward 186
The mid part of the insular cortex 190
Overall Summary 195
References 205

Introduction

Taste and olfactory processing in the human brain has increasingly been the focus of investigation, where methods such as functional neuroimaging (e.g. O'Doherty et al. 2002; O'Doherty et al. 2001b; O'Doherty et al. 2000; Small et al. 1999; Zald et al. 2002; Zald et al. 1998; Zald and Pardo 2000b) and human lesion studies (e.g. Cereda et al. 2002; Pritchard et al. 1999; Small et al. 1997b) have been applied. However, the core of the available data on cortical taste and olfactory processing comes mainly from electrophysiological studies at the single-neuron level in non-human primates (e.g. Critchley and Rolls 1996a; Pritchard et al. 1989; Rolls 1997; Rolls and Scott 2003; Scott et al. 1986a; Yaxley et al. 1988) and rats (e.g. Hanamori et al. 1998), as well as from supporting neuroanatomical data on the gustatory pathways in these species (e.g. Norgren and Leonard 1973; Pritchard et al. 1986). Thus, the human counterpart of most of the known features of cortical representation of taste and olfactory stimuli in non-human primates has yet to be found. In particular for the non-human primate case, the insular and adjoining opercular and orbitofrontal cortices were shown to have a central function in this type of processing. A review of some of the available data on the anatomy and function of these areas follows.

Using both electrophysiological recordings of neuronal responses and horseradish peroxidase (HRP) tracing, Cechetto and Saper (1987) proposed that the ascending pathway for visceral sensory information, including special (gustatory) and general visceral information, is topographically organised at all levels of the rat neuraxis, and in particular at the rat insular cortex. That is, neurons in the most anterior part of the rat insula responded preferentially to taste stimulation, whereas neurons located posterioriorly responded preferentially to general visceral stimulation, and the respective peaks of the of the taste and visceral insular neurons distributions are located approximately 1mm apart from each other. In addition, HRP injections into the gustatory part of the insular cortex retrogradelly labelled neurons in the parvicellular part of the ventroposterior medial thalamic nucleus (VPMpc), a gustatory relay thalamic nucleus whereas injections into the general visceral-responsive part of the insular cortex retrogradelly labelled neurons in a region lateral to VPMpc, in the ventroposterior lateral parvicellular thalamic nucleus (VPLpc). Anterograde injections in these thalamic nuclei revealed a topographic labelling in the insula. These facts lead the authors to conclude that there is a special/general viscerotopic map in the anterior-posterior insular axis of the rat, and that this might result from the connectivity patterns of the thalamo-insular projections.

The extent to which these patterns could also be found in the primate insula is at least not completely clear. Attempts to generalise these results to the primate case face the problem that the homology between the rat and primate case is not always straightforward, as in the case of defining a cytoarchitectonically distinct rat orbital cortex. However an important step was given by Rolls and colleagues, who have found that in macaque monkeys taste-responsive neurons in the anterior insula (and adjoining frontal operculum) are not modulated by hunger (Rolls et al. 1988; Yaxley et al. 1988). This is in contrast with recorded neurons in the hypothalamus and orbital cortex where taste-responsive activity is dependent on the current physiological status of the body (Critchley and Rolls 1996a). However neuronal responses as a function of physiological states in mid and posterior areas of the macaque monkey insula remain to be determined.

Another important comparative topic concerning the functions of the insular cortex refers to the characterisation of convergence sites for gustatory and olfactory inputs. The available anatomical data on the taste and olfactory cortical projections in rats and monkeys including antero and retrograde labelling involving the olfactory bulb and primary olfactory cortex (Carmichael et al. 1994; Sewards and Sewards 2001) indicate that taste and olfactory convergence are likely to be implemented in the more anterior, agranular part of the insula and in the adjoining caudo-medial part of the orbitofrontal cortex. In rats, an area of the cortex situated in the posterior part of the dorsal and ventral agranular insular areas receives direct projections from the main olfactory bulb and pyriform cortex (Behan and Haberly 1999). This region extends into more posterior areas of the insula lying ventral to gustatory regions and is thus a possible site for taste-olfaction integration. Carmichael *et al.* (1994) have demonstrated that olfactory information from the pyriform cortex reaches the anterior (agranular) insula and adjoining caudal orbitofrontal cortex (*e.g.* area 13a) in rhesus monkeys (for a reference, see Fig 0.3); in addition the anterior insula is part of the primary taste cortex in macaque monkeys (Scott and Plata-Salaman 1999). Rolls and his colleagues have shown that taste cells in the orbitofrontal cortex of macaque and rhesus monkeys respond also to olfactory stimuli (Rolls 1997), but the extent to which the insular cortex is involved in this integration remains to be investigated. Kadohisa, Rolls and Verhagen (in preparation) have shown that olfactory inputs into primary gustatory cortex in rhesus monkeys is very weak or absent. A hypothesis to be confirmed is that in primates (including humans) convergence is achieved in more anterior, possibly agranular part, of the insula and so would be an extension of the rat case.

In this work, we used functional magnetic resonance imaging in normal (right handed) human subjects to measure local and transient increases in brain activity following stimulation by taste (including water), olfactory and psychostimulant inputs. We investigated the possible sites of convergence for olfactory and taste inputs, and the responses to taste stimuli under different

physiological states with a special interest in activations located in insular and orbital cortices. The known anatomy of the primate insular cortex and adjacent areas are referred to as much as possible when any intepretation of the data is given. In the remaining of this Introduction a brief overview on the functional anatomy of the rat and primate insula will be given, followed by an introduction to the fMRI methods used in the five subsequent experimental Chapters. The first Chapter investigates the responses, in the human brain, to *umami* tastants such as monosodium glutamate and some ribonucletides and how the enhacement of the taste of monosodium glutamate by ribonucleotides (a characteristic effect produced by umami tastants) is represented in the human brain. Chapter II investigates how the responses in the human brain to orthonasally delivered odours depend on the hedonic value of these odours, and if the representations of odour valence and intensity in the brain are dissociated. The third Chapter is concerned with the identification of regions in the human brain receiving convergent taste and olfactory input, and thus supporting the representation of flavour. The representation of the pleasantness of flavour (and the consonance of its components) is also inspected. Chapter IV investigates if a different type of substance, M-amphetamine, does activate similar regions of the human brain to those responding to taste and olfactory stimuli as a function of their reward or motivational value. Finally, in Chapter V we were interested in investigating if water in the mouth does produce activations in brain regions known to respond to taste stimuli, and which brain areas respond to water in the mouth in a thirst-dependent way, and thus where its pleasantness is represented in the human brain.

The Insular and adjoining Orbitofrontal Cortex: Anatomy and Function

Stimulation of different sensory channels by a variety of compounds including tastants, odours and psychostimulants are known to elicit activity in specific brain areas in humans, such as the orbitofrontal cortex and reviewed in detail for example in (Rolls 2000a). Specific cortical areas activated in the studies to be described in this Thesis are the insular and orbitofrontal cortices. One claim in this work is that the representation of primary reinforcers such as taste, olfactory and psychostimulant stimuli in the human insula and orbitofrontal cortex reveals specific aspects of its functional anatomy. In the following section we describe the basic anatomical and functional features of these regions, as a background to the following Chapters.

Anatomy of the primate Insula

In primates including humans, the insula is placed within the lateral (Sylvian) fissure, covered by the operculum (*i.e.* the system comprising frontal, parietal, Rolandic and temporal opercula). In the Tailarach and Tournoux (1988) atlas, the anterior-posterior axis of the human insular cortex

extends approximately from Y = 20 to Y = -20, which in terms of the Montreal Neurological Institute (MNI) coordinate system (Collins et al. 1994) this corresponds roughly to Y=20.5928 and Y=-20.5928. The MNI coordinate system is the one used in this Thesis to locate brain activations. By covering the insula, the operculum forms at the same time the "lips" of the lateral fissure (Augustine 1996). Cytoarchitectural analyses divide the insula into three distinct fields (Augustine 1996; Cipolloni and Pandya 1999): a rostroventral agranular field, a transitional dysgranular field extending caudodorsally from the agranular field, and more posteriorly a granular field. Preuss and Goldman-Rakic (1989) further divide the agranular insula of macaques into: the periallocortex surrounding the primary olfactory cortex (a zone possessing a *lamina dissecans*) and its neighbouring region lacking the *lamina dissecans*.

Given that there was no classification of the insula proper in terms of Brodmann areas, its cytoarchitectonic divisions have been used in primates as anatomical reference. So, in this Introduction the following names will be used to denote subareas of the primate (macaque monkey) insula (e.g. Mufson and Mesulam 1982): Ia, agranular insula; Id, dysgranular insula; and Ig, granular insula. The agranular part of the insula of macaque monkeys was cytoarchitectonically divided in distinct subareas (Carmichael and Price 1994; Carmichael and Price 1996). These will described in section *Orbital and medial prefrontal networks* below.

Afferent cortical projections in rhesus monkeys

The primate insular cortex is a target of thalamic projections, in particular from the ventroposterior medial nucleus, VPM (Pritchard et al. 1986). Neurons in the parvicellular part of VPM (VPMpc) respond to gustatory stimulation and project to two distinct cortical sites adjacent to the Sylvian fissure, one including a region extending from the caudal part of the orbital cortex to dorsal insula/frontal operculum adjacent to the limiting superior sulcus and a second region located in the pre-central gyrus (Pritchard et al. 1986). Further details on these projections are outlined in the following sections below and in Chapter I. More laterally, the VPM proper projects to more posterior areas in the pre-central gyrus, revealing a topographic organisation of the projections from the medio-lateral dimesion in VPM and VPMpc into the anterior-posterior axis of the pre-central gyrus (Pritchard et al. 1986). Thus, gustatory/somatosensory information from thalamic relay nuclei are conveyed to the insular/opercular complex and subsequentially released to other cortical sites. Mufson and Mesulam (1982) studied the afferent insular connections in old world (rhesus) monkeys with (retrograde) axonal transport methods, the results being as follows.

Injections of horseradish peroxidase (HRP) were applied in the anterior part of the insula, including agranular (Ia) and dysgranular (Idg) sectors. In the frontal lobes, labelled neurons (*i.e.* neurons found to project into this part of the insula) were found in a granular frontal zone, areas 46 and 12 of Walker (Mufson and Mesulam 1982). In the orbital cortex, labelled neurons were found in two granular regions around the medial orbital sulcus corresponding to areas 11 and 13 of Walker, and in the more lateral dysgranular zone comprising area 12 of Walker. More posteriorly some agranular parts were also labelled. Finally, the frontal operculum was found to be heavily labelled with HRP-filled neurons.

The cingulate cortex was also labelled. The most anterior part was found to send rather weak projections to the most anterior part of the insula. Some labelled neurons however were found in area 24 of Walker. In the insula, numerous HRP-positive neurons were found in Ia- (proisocortical) and Idg, that is adjacent to injection. Sparse labelling only was observed in more posterior dysgranular and granular regions. Additional labelling was found in the adjoining prepyriform cortex area (which constitutes in primates part of the primary olfactory cortex), especially layers II and III of its frontal, temporal and insular extensions. Other labelled areas include the temporal and parietal lobes.

HRP injections were also placed in the mid-anterior part of the insula, more precisely in the mid portion of Idg. In the frontal lobes, labelling was almost equivalent to the one observed in the anterior insula case. Labelling was found in areas 11, 12, and 13 in the orbital surface, as well as in the dorsolateral area 46. However, HRP-positive neurons extended further into the ventral bank of the principal sulcus (PS in Fig 0.1). Also, labelled neurons were found in the "orbitofrontal operculum", *i.e.* the opercular part of the caudolateral part of the orbitofrontal cortex, and in the precentral operculum. In the cingulate cortex the results were also similar to the case of the anterior insula, with a few neurons labelled in areas 24 and in the transition zone with the adjoining dorsal part of area 6. Labelled neurons were found in the prepyriform cortex, mainly on its temporal extension although much fewer in the frontal extension. All subdivisions of the insular cortex were labelled, although HRP-positive neurons were found more densely in a part anterior to the injection. Additional labelled sites included the temporal and parietal lobes.

When HRP injections were also placed in the posterior part of the insula (within Ig, but also including caudal Idg), a distinct labelling pattern was found. In the frontal lobes, much fewer HRP-filled neurons were found, including areas 46 and the agranular, dysgranular and granular zones of the orbitofrontal cortex. Some neurons were found in the precentral opercular area. Also, no labelling was found in the pyriform area, indicating thus that only anterior parts of the

insula receive olfactory information from this area. Anterior portions of the insula were densely labelled, and, to a less extent, the sites adjacent to the injection.

The most noticeable change, however, refers to the cingulate area. Throughout labelling was found in areas 23 and 24 of Brodmann, reaching the depths and upper banks of the cingulate sulcus. Additional labelled areas included the temporal and parietal lobes, with the latter depicting a much more dense labelling than in the more anterior cases.

Efferent cortical projections in rhesus monkeys

Mufson and Mesulam have also studied the cortical efferent insular projections in rhesus monkeys (Mesulam and Mufson 1982b). Anterograde tracing was performed with tritiated amino acids (TAA). The first case refers to TAA injection in the anterior part of the insula, extending from Ia-p to Idg. In the frontal lobes, moderate labelling was found in a granular part corresponding to areas 46 and 12 of Walker. Most projections from the anterior insula into the frontal lobes reached the lateral orbitofrontal cortex and the opercular area. In particular, agranular, dysgranular and granular (anterior part of the orbital area) zones of the orbitofrontal cortex were labelled, and the frontal operculum was found also to receive strong projections.

Heavy labelling was found in layers I, II and III of the frontal, temporal and insular extensions of the prepyriform cortex. In the insula, projections reached the adjacent portions Ia-p and Idg. Less marked TAA labelling was found in the more caudal Ig. Moderate projections from the anterior insula were found in the cingulate cortex. Projections were limited to the anterior part of the cingulate gyrus, in its dorsal and sulcal portion. Labelled area corresponds approximately to area 24 of Walker. Additional target areas include subareas of the temporal lobe.

TAA injections were then placed in the posterior insula, entirely within Ig extending to a caudal part of Idg. Only light labelling was found in the frontal lobes, including areas 45 and orbital regions. No labelling was found in the pyriform area. In the insula, anterior parts of Idg and Ia, Ia-p were label-free. However heavy labelling was found in the more posterior regions of the insula, including caudal Ia, Idg and the whole of Ig.

In the cingulate region, extensive labelling was found in areas 23 and 24 of Brodmann, and in general along the dorsal aspect of the mid- and posterior cingulate gyrus, including sulcal banks. Additional target labelled areas included the temporal and parietal lobes.

Finally, TAA injections were placed in the mid-insula, which corresponds to the mid portion of Idg. Concerning the frontal lobes, the pattern of projections to the orbitofrontal cortex was very similar to the anterior insula case. Granular (within areas 11, 12 and 13), dysgranular (within 12) and agranular parts were labelled. The frontal operculum was virtually label-free in this case, indicating thus that projections to this area arise preferentially from the most anterior part of the insula. Exactly the same holds for the pyriform area. In the insula, only the most anterior part of Idg was not labelled. In the cingulate cortex, interestingly, the mid-insula case is also similar to the posterior insula case, in that labelling was found in areas 23 and 24 of Brodmann, and also more dorsally possibly extending to premotor cortical areas. Additional areas labelled include temporal and parietal lobes, where in the latter the opercular part of the parietal cortex was heavily labelled.

In summary, three aspects of the cortical connectivity of the primate (rhesus monkey) insular cortex are of note. First, the anterior part of the insula has strong backprojections with the caudal parts of the orbitofrontal cortex, which could be thus seen as a transition area between the insula and other frontal areas. Second, olfactory processing in the insula seems to be restricted to its anterior agranular part, such that only this part of the insula presented preferential connections with the pyriform area and that gustatory processing seems to mainly involve the anterior insula given the dense projections from this area to the frontal operculum. Finally, the mid and posterior parts of the insular cortex seem to have strong afferent and efferent projections from and to the more medial and posterior areas of the cingulate cortex, in particular areas 23 and 24 of Brodmann. Troughout this Thesis we will explore some of the functional correlates of this findings.

As a reference for the above data, Fig 0.1 shows a series of six coronal slices through the insular cortex of the rhesus monkey, taken from Cipolloni and Pandya's (1999) study on the fronto-parietal operculum of this species. On the top, a lateral view of the rhesus monkey brain. Notice that the insular cortex is visible, and cytoarchitecntonic subdivisions (agranular, dysgranular and granular parts of insular cortices) are shown. Note the location of the gustatory area (labelled *G*) defined as the recepient of projections from the parvicellular part of the ventroposterior medial nucleus of the thalamus (Pritchard et al. 1986). For abbreviations, see Fig 0.1 legend.

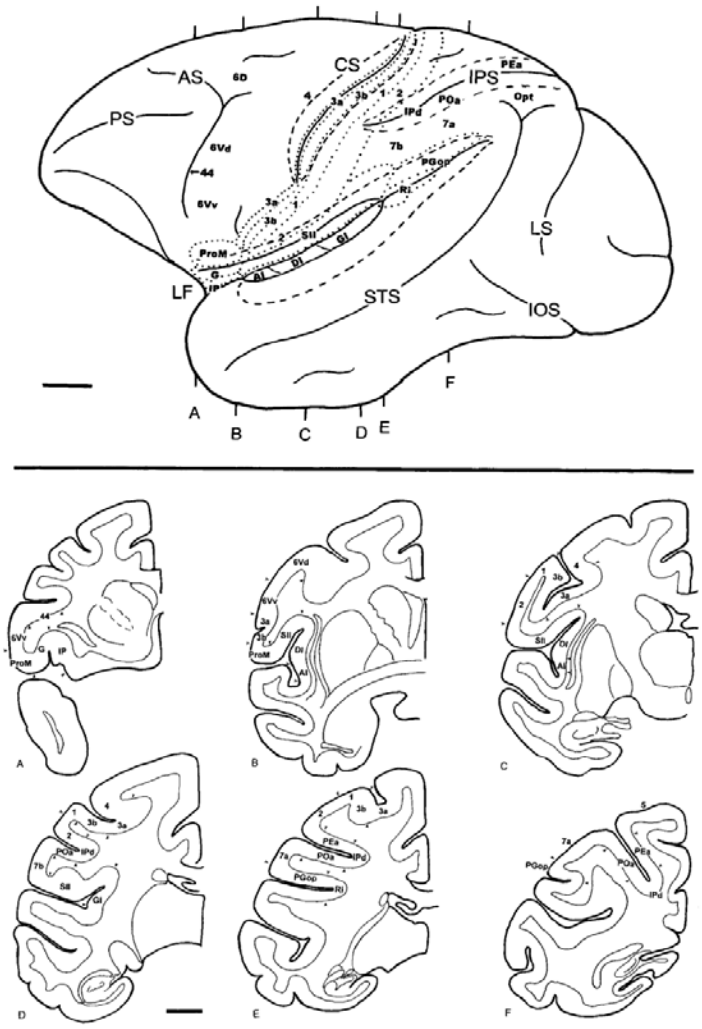


Fig 0.1 After Cipolloni and Pandya (1999). Cipolloni and Pandya (1999) studied the fronto-parietal operculum in rhesus monkeys. In this work they depict a schematic diagram of the lateral surface of the rhesus monkey brain (top), displaying the insular cortex buried within the Sylvian fissure. Notice the labelling of the agranular, dysgranular and granular parts within the insula. On the bottom are shown six slices through the insular cortex, where the subdivisions within the insula and opercula are also labelled. AI, agranular insula; AS, arcuate sulcus; CS, central sulcus, DI, dysgranular insula; G, gustatory area; GI, granular insula, IOS, inferior occiptal sulcus; IP, insula proisocortex; IPS, intraparietal sulcus; LF, lateral (Sylvian) fissure; LS, lunate sulcus; PS, principal sulcus; ProM, motor proisocortical area; Ri, retroinsular area; SII, secondary somatosensory area; STS, superior temporal sulcus; PF, PG, Opt, Pgop, Poa, Pea, Ipd are subdivisions of the parietal cortex; 6D, 6Vd, 6Vv are subdivisions of (premotor) area 6.

Six coronal slices from a human T1 MRI scan locate the insular cortex from posterior to anterior regions, in Fig 0.2. At the top of each figure slice is shown the Y-coordinate in the MNI system (Collins et al. 1994). A saggital slice on the bottom is also given for reference.

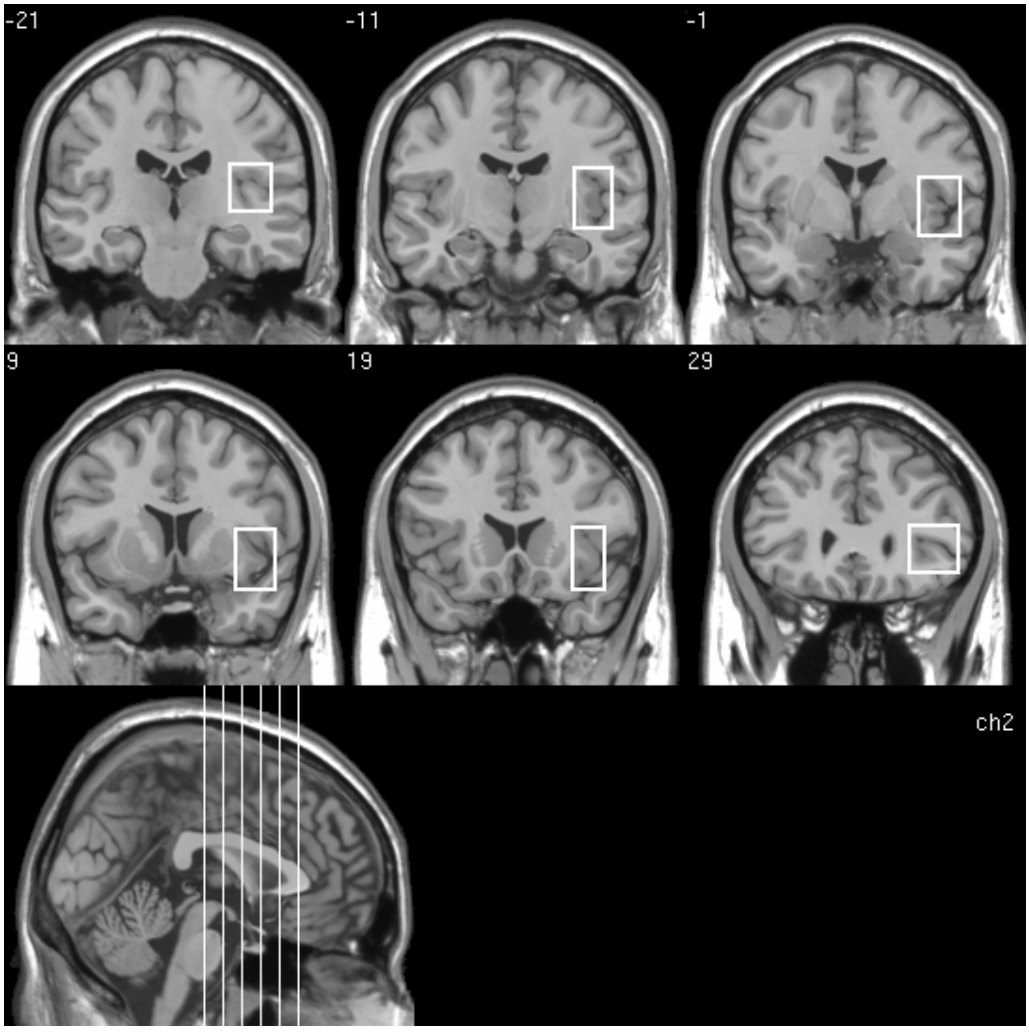


Fig 0.2: Coronal sections showing the location of the (right) insular cortex in the human brain. The first slice (Y= -21) shows the limiting location of the posterior insula at the fundus of the temporal- parietal wall. Coronal sections across the right insular cortex are shown from posterior (Y= - 11) to anterior regions, limited rostrally by the transition area with the orbital cortex (Y= 29). The corresponding Y coordinates are shown above each slice, in the upper left corner. The saggital scan (below on the left) locates the slices.

Orbital and medial prefrontal networks

One of the main regions of interest with respect to the studies presented in this Thesis is the transition zone between the insular and orbitofrontal cortices. Carmichael and Price (1994) studied the architectonic structure of the orbital and medial prefrontal cortex of the macaque monkey with immunohistochemical staining methods. Of particular interest is the transition zone involving the caudal part of the orbital cortex and the adjoining agranular insula of the macaque monkey, recently shown to have a homologous parcelation in humans (see below, and Ongur et

al. 2003). The caudal part of the orbital surface lacks a granular layer IV and thus has been sometimes called the agranular insula, revealing thus the continuity of the agranular cortex lying on the caudal part of the orbital surface with the agranular cortex lying on the lateral fissure (Amaral and Price 1984). Laterally, this area is bordered by the gustatory area *G*, and by the precentral opercular cortex (Preuss and Goldman Rakic 1989). Rostrally, the area is limited by area 13 and by the caudal part of area 12. Importantly, the agranular insula is adjacent to the primary olfactory cortex (the anterior olfactory nucleus and the pyriform cortex). Carmichael and Price (1994) divided the orbital part of the agranular insula into five areas, based on their topographic position: Iai (intermediate agranular insular area); Ial (lateral agranular insular area); Iam (medial agranular insular area); Iapl (posterolateral agranular insular area); and Iapm (posteromedial agranular insular area). Coronal slices from this transition area are shown in Fig 0.3 (Carmichael and Price 1994).

This division of the far anterior agranular insula into five adjoining but distinct areas is part of a cytoarchitectonic analysis of the orbital and medial prefrontal cortex of macaque monkeys with a number of histochemical and immunohistochemical stains. Seventeen areas were recognized in this study (in addition to posterior areas Iai, Ial, Iam, Iapm and Iapl): Walker's areas 10, 11, 12, 13, and 14 (Walker 1940) have been subdivided into areas 10m, 10o, 11m, 11l, 12r, 12l, 12m, 12o, 13m, 13l, 13a, 13b, 14r, and 14c. On the medial wall, areas 32, 25, and 24a,b,c and area 10m were found to have distinctive features.

In a follow-up study, Carmichael and Price (1996) investigated the intrinsic cortico-cortical connections within the prefrontal areas of the macaque monkey as cytoarchitectonically distinguished above. The connectivity pattern led the authors to differentiate between two networks. First, an *orbital network*, consisting of agranular areas Iam, Ial, Iapm, central areas 13l, 13m, 13b, lateral areas 12r, 12l, 12m and the more rostral area 11l. These areas are strongly connected with each other, but not with the medial ones or Iai. Thus, Iai stands out as the only (pre-frontal) agranular insular area not being part of the orbital network. In contrast, a second network, called by the authors the *medial network*, comprises the rostral orbital areas 10o and 11m, the medial wall areas 32, 25, 24(a, b, c), 10m, 14r, and 14c and the posterior area Iai. Areas 12o and 13a, on the caudomedial and caudolateral orbital cortex respectively, were found to have substantial connections with both networks (see Fig 0.3 for reference).

External inputs provide further evidence for a distinction between the orbital and medial networks, as these areas were studied in the macaque monkey with retrograde axonal tracers by Carmichael and Price (1995b). Restricted areas of the lateral and posterior orbital cortex were found to be preferentially targeted by visual, somatosensory, olfactory, gustatory, and visceral-

related inputs. In contrast, the more medial areas received few direct sensory inputs. Orbital area 12l received substantial projection from visual areas in the inferior temporal cortex (TE) whereas 12m received somatosensory input from face, digit, or forelimb regions from cortical somatosensory areas. Areas 13m and 13l received a projection from the opercular part of areas 1-2 and 3b. Areas Iapm and Ial received fibres from the ventral part of (VPMpc) whereas the dorsal part of VPMpc projected to the adjacent gustatory cortex. These restricted inputs from several sensory modalities and the convergent corticocortical connections to orbital areas 13l and 13m suggested to the authors a network related to feeding. In general, the orbital network seems to be preferentially involved in the encoding of different sensory aspects of stimuli. The medial network, on the other hand, was characterised as a visceromotor system providing output control to autonomic and endocrine function (Price 1999).

Also concerning the projections from the insular to the adjacent orbitofrontal cortex, Baylis *et al.* (1995) have used HRP retrograde labelling to determine the afferent projections of the posterior part of the caudolateral orbitofrontal cortex taste area. This area is within the lateral dysgranular field of the caudal orbitofrontal cortex, bounded posteriorly by the limen insula. Labelled cells were found in the primary taste cortex including the frontal operculum and the dysgranular field of the anterior insular cortex. Thalamic labelled cells were found in the mediodorsal nucleus but not in the ventromedial posterior taste relay nucleus, characterising thus the caudal orbitofrontal cortex as a secondary taste cortex. Importantly, labelled cells were found in the agranular part of the caudal orbitofrontal cortex, anterior to the injection site. So the agranular orbital field, which is a part of the orbital cortex receiving olfactory inputs (Carmichael et al. 1994; Carmichael and Price 1994), projects to the dysgranular taste area of the orbital cortex which might thus be involved in the integration of multimodal taste/olfactory information and possibly flavour perception.

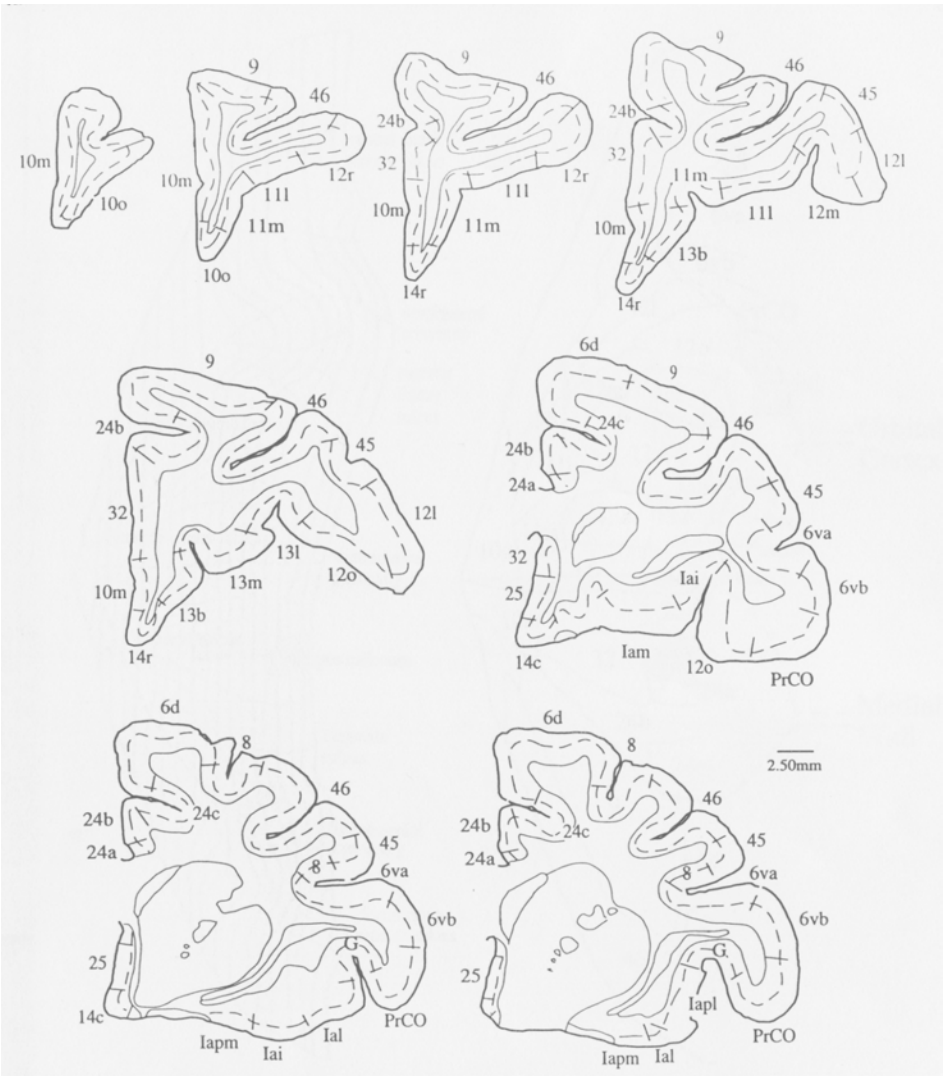


Fig. 0.3. After Carmichael and Price (1994). Architectonic areas in the prefrontal cortex of the macaque monkey including the caudal orbital/agranular insula transition zones. Numbers denote Brodmann areas and their subdivisions as labelled by the authors. G, gustatory cortex; Iai, intermediate agranular insular area; Ial, lateral agranular insular area; Iam, medial agranular insular area; Iapl, posterolateral agranular insular area; Iapm, posteromedial agranular insular area; PrCO, precentral opercular cortex.

In a more recent study, Ongur et al. (2003) investigated the structure of the human orbital and medial prefrontal cortex using five histological and immunohistochemical stains and was correlated with the previous analysis in macaque monkeys (Carmichael and Price 1994) presented above. The have found that all of the areas recognized in the macaque orbital and medial prefrontal cortex have counterparts in humans. Of particular importance to the studies presented here, areas 47/12r, 47/12m, 47/12l, and 47/12s occupy the lateral orbital cortex, corresponding to monkey areas 12r, 12m, 12l, and 12o. The agranular insula (areas Iam, Iapm, Iai, and Ial) extends onto the caudal orbital surface and into the horizontal ramus of the lateral sulcus, the

difference with the monkey being mainly the relative size of the more caudal agranular areas at the expense of a relative increase of the granular areas around the The growth of the frontal pole in humans has pushed area 25 and area 32pl, which corresponds to the prelimbic area 32 in Brodmann's monkey brain map, caudal and ventral to the genu of the corpus callosum. Anterior cingulate areas 24a and 24b also extend ventral to the genu of the corpus callosum. Area 32ac, corresponding to the dorsal anterior cingulate area 32 in Brodmann's human brain map, is anterior and dorsal to the genu. In general, Ongur et al. (2003) hypothetise that the cytoarchitectonic parallel of the macaque monkey orbital and medial prefrontal cortex with the corresponding areas in humans implies that the connectivity (and functional) patterns would also be comparable between monkeys and humans.

Functions of the Insular and Orbitofrontal Cortex

Functions of the Insula

Rats

The agranular, more anterior part of the rat insula was cytoarchitectonically characterised as a taste area by Norgren and colleagues (Kosar et al. 1986a). Multi-unit recordings were used to measure responses to tongue tactile, thermal and gustatory stimuli. The taste cortex in the rat was localized to the agranular insular cytoarchitectural region, in contrast to its traditional assignation to granular insular cortex (e.g. the review in Shi and Cassell 1998). This latter area was rather characterised as responsive to temperature-related stimuli applied to the tongue. In addition, the thalamic relay nucleus conveying lingual somatosensory, thermal, and gustatory information was defined electrophysiologically (Kosar et al. 1986b). These authors subsequently characterised the corresponding thalamic afferent fibres through anterograde tracing of axonal projections in the thalamus. After injections confined to the thalamic gustatory relay, labeled fibers terminated in agranular insular cortex. This confirms the cytoarchitectonic characterisation of the agranular part of the rat insular cortex as a gustatory cortical area. In contrast, the posterior areas of the rat insular cortex seem to be preferentially involved in visceral and autonomic representation. Cechetto and Saper performed a seminal study in which the functional organization of the insular cortex was studied by recording neuronal responses to visceral sensory stimuli (Cechetto and Saper 1987). On the basis of its cytoarchitecture and connections with the thalamus, the insular cortex was subdivided by the authors into a dorsal granular area, an intermediate dysgranular region, and a ventral agranular strip. First, taste responses were characterised. Taste-responsive neurons were located in more anterior areas, primarily in the dysgranular region, whereas unit responses to general visceral modalities were distributed more posteriorly, (thus dorsally) in the granular insular cortex. Gastric mechanoreceptor-responsive units were situated more dorsally

and anteriorly in the granular insular cortex, while cardiopulmonary inputs were located more ventrally and posteriorly.

The authors then studied with retrograde tracing the afferent thalamic fibres of the gustatory and visceral responsive insular cortex. Injections on this dysgranular gustatory part of the insula resulted in retrograde labeling of neurons in the parvicellular part of the ventroposterior medial thalamic nucleus (VPMpc). On the other hand injections into the general visceral insular cortex retrogradely labeled neurons lateral to VPMpc in the ventroposterior lateral parvicellular thalamic nucleus (VPLpc). In addition, anterograde injections into VPMpc and VPLpc verified that their projection to the insular cortex is topographically organized.

In addition, the anatomical localisation of autonomic (in particular cardiovascular) responses elicited in the insular cortex was further examined in Yasui et al (1991), through the use of electrical microstimulation. The efferents from the cardiovascular responsive sites were anterogradely traced. Two distinct patterns of cardiovascular response were elicited following stimulation of the insular cortex: an increase in arterial pressure accompanied by tachycardia and a decrease in arterial pressure with bradycardia. The pressor responses were obtained by stimulation of the rostral half of the posterior insular cortex while depressor sites were located in the caudal part of the posterior insular area. Both types of site were primarily located in the dysgranular and agranular parts of the posterior insular cortex. Gastric motility changes originated from a separate but adjacent region immediately rostral to the cardiovascular responsive sites in the anterior insular cortex. These results by Saper and colleagues, along with those obtained by Norgren and colleagues, demonstrate the relationship of general visceral and special visceral (taste) representations in the rat insular cortex, in that taste responsive areas seem to be localised in the agranular/dysgranular zones of the more anterior insula, whereas (general) visceral representation seems to preferentially involve the more posterior areas of the insula. More precisely, Cechetto and Saper (1987) report that neurons responding to general visceral stimulation are located within the area defined as 2.0mm anterior and 0.5mm posterior to the anterior commisure (AC), peaking around the AC (0.0mm). On the other hand, taste responsive neurons were observed within the area defined as 0.5mm and 2.0mm anterior to AC, peaking at 1.5mm anterior to AC.

More recently, Hanamori *et al* (1998) studied the responses of insular neurons to gustatory, visceral and nociceptive stimuli in rats. In particular, they studied insular neurons responding to gustatory stimulation of the posterior part of the tongue and found that these neurons are located in a region peaking at 1.0mm anterior to AC, posterior to the peak of the taste area found in previous studies but still anterior to the visceral area. In addition these neurons were responsive

also to nociceptive stimulation (tail pinch) and baroreceptor/chemoreceptor stimulation. They raise thus the possibility that there might be neurons in the mid-insula that are located in a taste-visceral overlapping area. In fact, Puskosvas et al (2002) have demonstrated higher cellular metabolism (through c-fos expression) in insular neurons of fluid-deprived rats. In particular they have shown that metabolic activity in these neurons is even higher following water and sodium intake, indicating thus that in addition to the anterior-posterior axis functional dissociation, the insular cortex also contains neurons representing information on taste × visceral interactions and possibly convergence of inputs from these two modalities (see also Ogawa and Wang 2002). Althought a critical comparison was not performed in this study, which refers to the possibility that water ingestion increases insular activity in fluid-replete animals, it gives important insight on the role of the insular cortex in thirst. Finally, it must be noticed that in the rat the posterior part of the dorsal and ventral agranular insular areas (extending possibly to the adjacent posterior agranular part of the insula), lying ventral to the gustatory area, receive direct projections from the olfactory bulb and pyriform cortex (Behan and Haberly 1999). In the nomenclature of Shi and Cassell (1998), this would correspond to the anterior portions of the agranular posterior insular cortex (Sewards and Sewards 2001). So this area of the rat insular cortex presents itself as a candidate for a taste-olfactory integration site.

Primates

Based on the cortical connectivity studies of the rhesus monkey insular cortex decribed above, Mufson and Mesulam propose that the topographic distribution of these connections suggests that the posterodorsal insula is specialized for auditory-somesthetic-skeletomotor function whereas the anteroventral insula is related to olfactory-gustatory-autonomic function (Mesulam and Mufson 1982b). However, as discussed below, whereas gustatory function seems indeed to be represented in more anteroventral parts of the insula, some sympathetic autonomic functions (*e.g.* cardiovascular control) seem also to depend on posterior regions of the insula.

In primates, taste information reaches the cortex through cranial nerves VII, IX and X, which terminate on the rostral part of the nucleus of the solitary tract (Rolls and Scott 2003). Contrary to rat case, where second-order fibres project rostrally to the parabrachial nucleus in the pons, in primates these second-order fibres bypass the parabrachial nucleus only to project through the central tegmental tract and distribute within the parvicellular part of the ventroposterior medial nucleus of the thalamus, VPMpc (Pritchard et al. 2000; Rolls and Scott 2003; Scott and Plata-Salaman 1999). From there, third order fibres project to the frontal area of the operculum and to anterior (agranular/dysgranular) parts of the insula, constituting the primary taste cortex (Pritchard et al. 1986). A second cortical area receiving direct projections form VPMpc is situated within the precentral gyrus, including parts of area 3b (Pritchard et al. 1986). A more complete

account of the taste pathways in primates is given in Chapter I. Rolls, Scott and colleagues (e.g. Yaxley et al. 1988) have performed electrophysiological recordings in primate taste cortex, including the insula. ~6.5% of neurons recorded in this area were responsive to the delivery of one of the five basic tastants in moderate concentrations. Other neurons recorded in this area responded to mouth/jaw movements and sensory stimulation of the mouth (including the tongue).

It is important to note that Yaxley et al (1988) have found that taste neurons in the anterior insula were not modulated by the motivational state of the animal as shown in a sensory-specific satiety type of experiment. Similar findings were made with respect to the frontal operculum (Rolls et al. 1988). This implies that other regions, possibly adjacent to the primary taste cortex such as the orbital cortex and more posterior parts of the insula, must compute the modulation of taste responses by physiological or motivational states (Rolls 1997; Rolls 2000a).

Olfactory input also reaches the insula as shown by retrograde tracer injections studies (Carmichael et al. 1994; Öngur and Price 2000). In primates, as in the case of the rat (Price 1990), there are substantial projections from the primary olfactory cortex into the rostral insula. These injections labelled projections to nine areas in the caudal orbital cortex, including the adjacent agranular insula. Areas Iam (agranular insular cortex, medial part) and Iapm (posteromedial part) receive the densiest projections from pyriform cortex. Areas Iam, Iapm, and adjacent caudolateral orbital cortex (see Fig 0.3) were also the only cortical areas that responded with multiunit action potentials to olfactory bulb stimulation in anesthetized animals (Carmichael et al. 1994).

On the other hand, evidence on the involvement of the insula in representing autonomic and homeostatic states comes from electrophysiological and imaging studies (Bennarroch 1997; Craig 2002; Critchley et al. 2000a; Saper 2002). In fact, in monkeys and humans (as well as in the rat, see above), the insula is involved in the regulation of heart rate and blood pressure in that it contains baroreceptor-related neurons (Zhang and Oppenheimer 2000).

The region of the primate insula characterised as being implicated in cardiovascular control seems to be posterior to the regions containing taste-responsive cells, in that the majority of the baroreceptor-related neurons were located within the dysgranular and granular parts of the insula in layers II, III and V/VI (Zhang et al. 1998). These primate data confirm earlier studies in the rat revealing that specific regions of the insular cortex are involved in visceral and autonomic processing, in that stimulation experiments suggest a discrete localisation within the rostral posterior insula of cardiovascular-related neurons, and electrophysiological studies confirm the

importance of the right posterior insula in the rat as a site of cardiovascular representation, although baroreceptor-related neurons were found in more anterior regions of the insula in primates. In humans, bradycardia and depressor responses were obtained through insular stimulation in pre-operative patients (Oppenheimer et al. 1992).

Responses in medial and posterior areas of the human insular cortex (as measured by functional imaging methods such as functional MRI and positron emission tomography) include sensual touch, noxious stimulation (thermal and chronic pain and a more general somatosensory representation), forced respiration, dynamic exercise and itch (Craig 2002).

The aspects of the insular functions described above (including gustatory, cardiovascular and nonciceptive functions) give evidence for its characterisation as a sensory and motor visceral (including special visceral) area. Further evidence for its role in motor visceral function is provided by its implication in vomiting (Fiol et al. 1988).

Finally, several non-visceral functions of the insular cortex in primates, including humans, were listed in Augustine (1996): motor association (post-stroke recovery, ocular movements), vestibular, language (language-related working memory, auditory processing during speech), and limbic (phobia, aversion) function, include trustworthiness judgements (Winston et al. 2002) although this pattern of activations might involve visceral or autonomic-related components, given that co-activations were observed in areas such as the amygdala, orbitofrontal and anterior cingulate cortices.

Functions of the primate orbitofrontal cortex

The role of the primate (including humans) orbitofrontal cortex in reward processing has been consistently established with different techniques such as electrophysiological recordings and functional neuroimaging. In non-human primates, there is strong evidence at the level of the single neuron that neurons in the orbitofrontal cortex respond in relation to the reward value of taste (Rolls et al. 1989), olfactory, and visual stimuli (Critchley and Rolls 1996b; Rolls 2000a; Rolls et al. 1996b). The caudal part of the orbital cortex, including the regions adjoining the agranular insular cortex, was shown by Rolls and colleagues to be a secondary taste cortex (e.g. Rolls 1997). The area is part of the dysgranular field of the orbital cortex, anterior thus to the insulo-opercular primary taste cortex (see Fig 0.3). Neurons in this region were found to be responsive to stimuli such as glucose, NaCl and HCl. Moreover, the caudal part of the orbital cortex contains neurons responsive to olfactory inputs (Critchley and Rolls 1996a) leading thus to the hypothesis that this region, along with the adjoining agranular part of the insula, could support flavour perception. In fact, bimodal neurons were found in a mediolateral part of the dysgranular orbital cortex in

addition to unimodal taste and odour-responsive neurons (Rolls 1997). Neurons in the orbitofrontal cortex respond to the sight and texture of food, and olfactory responses represent associations of food, which in addition to the fact that rapid visual-taste associations are formed in this region gives evidence for food-intake related multimodal representations in the orbitofrontal cortex (Rolls 1997).

In the specific case of neurons responding to the reward value of taste stimuli, neurons in the macaque monkey orbitofrontal cortex have been shown to respond in a sensory-specific satiety manner, *i.e.* these neurons respond to the taste of a food only if hunger is present (Critchley and Rolls 1996b; Rolls et al. 1996b). Importantly, olfactory inputs into the primate orbitofrontal cortex converge with taste inputs at the single-neuron level, which implicates this region in the representation of flavour (Rolls 1997). Moreover, it has been shown that macaques will learn to self-administer very small quantities of amphetamine to this region (Phillips et al. 1979), and that this is a region where electrical stimulation in macaques is rewarding (Rolls 2000a). In humans, previous functional neuroimaging investigations show that the medial part of the orbitofrontal cortex is an area where activation can be produced by pleasant odour (Anderson et al. 2003; Gottfried et al. 2002), monetary reward (O'Doherty et al. 2001a), and pleasant touch (Rolls et al. 2003b). This region is in an area where high concentrations of dopamine D1 receptors were found, as shown in post mortem binding studies in humans (Hurd et al. 2001). Further evidence, in humans, that the orbitofrontal cortex is involved in reward processing comes from studies making use of a variety of stimuli, such as odour (Anderson et al. 2003; Gottfried et al. 2002; Zald and Pardo 1997, 2000b; Zatorre et al. 1992), olfactory stimuli in a sensory-specific satiety paradigm (O'Doherty et al. 2000), positive and negative feedback (Elliott et al. 1997), taste (O'Doherty et al. 2001b; Small et al. 2001), face attractiveness (Aharon et al. 2001; O'Doherty et al. 2003) and sexually arousing stimuli (Redoute et al. 2000). Further details on the functions of the orbitofrontal cortex will be discussed through the experimental Chapters and in the Conclusion.

Somatosensory representation of the oral cavity in the primate cortex

Besides the anterior insular cortex/frontal operculum, other primate cortical areas respond to the presence of food in the mouth. Understanding somatosensory encoding of intra-oral stimuli is essential to interpret imaging data reporting taste-related activations in the human brain.

For the primate case, the somatotopy of face and oral cavity representation in the somatosensory cortical area 3b has been determined in monkeys with combined cytoarchitectonic analysis and

electrophysiological stimulation in macaque (Manger et al. 1996) and owl and squirrel monkeys (Jain et al. 2001).

Manger and colleagues (Manger et al. 1996) studied the representation of body regions innervated by the trigeminal cranial nerve in the monkey cerebral cortex. Microelectrode recordings following electrical stimulation were used to generate somatosensory maps in the posterior bank of the central sulcus and adjacent regions. The body area covered by the (contralateral) trigeminal nerve is represented in an 8-mm mediolateral extent of area 3b lateral to the representation of the hand constituting thus a representation of most of the contralateral face area. Still in area 3b, a lateral extension to this face area contains representation of ipsilateral intra-oral structures, measuring 6 mm in mediolateral extent so that a rostrocaudal organisation in area 3b emerges, going more caudally from a face representation to more posterior intra-oral responsive sites. The ipsilateral representation forms approximately 40% of the trigeminal representation, consistent with the amount of the ventroposterior medial (VPM) thalamic nucleus devoted to representation of ipsilateral intra-oral structures.

Jain and colleagues studied the somatotopy of area 3b in owl and squirrel monkeys (Jain et al. 2001). In owl monkeys, the caudal part of the face representation in area 3b extended to the upper bank of the lateral sulcus. The representation of the oral cavity is located rostrally to that area, which extends all the way to the most rostral part of the frontal cortex, extending to orbitofrontal cortex just to reach the orbital sulcus. In squirrel monkeys, all areas supporting the representation of face and oral cavity in area 3b are restricted to the lateral surface, and do not extend to the orbitofrontal areas. The linear extent of face and mouth representation areas is comparable to those related to the trunk and limbs.

In both owl and squirrel monkeys, this lateral portion of the lateral part of area 3b subserving face and mouth representations is subdivided in several myelin-rich subareas. In owl monkeys the face areas fold into the upper bank of the lateral sulcus while oral cavity areas extend to the orbitofrontal cortex. In particular the myelin-rich area representing the oral cavity (rostral to the face representation) has in its most caudal part representations for teeth and jaw, and progresses rostrally to tongue, and teeth again, representations. In squirrel monkeys, the same pattern is reproduced, with however a more representative second tongue area lying rostral to the second teeth area, without however reaching the orbital cortex (see Fig 0.4).

The relatively uniform (in a caudal/face-rostral/mouth sense) primate data described above gives some indication about the putative homologous location of face and mouth representations in the human somatosensory cortex. The human primary somatosensory cortex (S1) is located

across the postcentral gyrus. The most characteristic feature of this region is the somatotopic representation of the contra-lateral body surface (Penfield's homunculus, Penfield and Jasper 1954). This initial characterisation was further confirmed by functional neuroimaging studies. Fox and colleagues (Fox et al. 1987) have shown with PET that highly focal S1 responses were seen following stimulation of the cutaneous surfaces of the lips, fingers, and toes. In particular the S1 responses from the three stimulation sites were anatomically distinct and formed a medial-to-lateral homunculus in every subject scanned. More specifically, concerning the mapping of the oral cavity in humans, an initial PET study (Grafton et al. 1991) has shown that tongue movement and stimulation produced activations around the central sulcus near the border with the Sylvian (lateral) fissure.

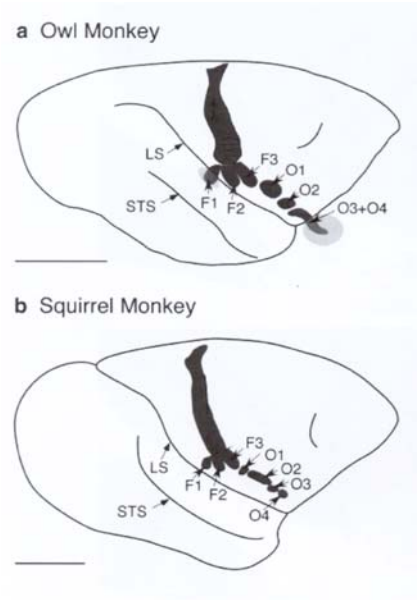


*Fig 0.4 After Jain et al (2001). The locations and myeloarchitectonic features of area 3b. Shaded areas represent the location of area 3b in (**a**) Owl monkeys and (**b**) squirrel monkeys across the central sulcus region. Areas labelled F1, F2, F3 represent face areas whereas O1, O2, O3, O4 represent the oral cavity. In owl monkeys (**a**), oral cavity areas O3 and O4 extend onto the orbitofrontal cortex (lightly shaded area). LS, lateral sulcus, STS, superior temporal sulcus; scale bar = 1cm.*

Urasaki and colleagues (Urasaki et al. 1994) studied motor and sensory cortical tongue representations in patients with intractable epilepsy who have implanted chronic subdural electrode grids. Tongue responses were observed in a wide area 4.5 cm anterior and 3 cm posterior to the central sulcus independently of laterality. In patients with apparently no fronto-parietal lesions, the tongue motor area was located around Sylvian fissure. Analogously, Sakai et al (1995) have shown that mechanical stimulation of the tongue produced activations in the postcentral gyrus adjacent to the Sylvian fissure.

In a more recent PET study, Pardo *et al* (1997) compared the effects of stimulating either the left or right sides of the (protruded) tongue against the effects produced by tongue protrusion only. Significant activations have been found, in particular, in the contralateral central sulcus (including Brodmann Areas 3 and 4) and in the contralateral temporal superior gyrus (BA 42), at the Sylvian fissure. Although this study lacks a control condition in which no motor component by protruding the tongue is involved, it gives some indication on its likely cortical representation.

Overall, there seems to be a homology between the monkey and human cases in that intra-oral representation including representation of the tongue in the somatosensory cortex involves an area which includes the postcentral gyrus extending to the Sylvian fissure, which in the human brain would comprise most of the Rolandic operculum. So, the Rolandic operculum, the opercular part of the Rolandic cortex lying caudal to the frontal operculum (Cipolloni and Pandya 1999) seems to contain in humans (and in the homologous regions of the monkey) a somatosensory representation of the oral cavity, in particular of the tongue.

This is further confirmed by imaging studies where the somatosensory factor of tastants in the mouth have been analysed. In a PET study on cortical activations induced by water in the mouth, Zald and Pardo (Zald and Pardo 2000a) compared the responses produced by intraoral stimulation by water at room temperature against responses produced by motor-related factors such as swallowing. Regional cerebral blood flow increases were detected in particular within the perisylvian and Rolandic (including thus Rolandic operculum) cortices. Although some of these effects were found to be stronger if water in the mouth is not contrasted against swallowing (but against a "closed eyes condition"), a sizeable group of significant activations remained in these areas after comparison. Also, Cerf-Ducastel and colleagues (Cerf-Ducastel et al. 2001) investigated the interaction between lingual-somatosensory and taste effects in an fMRI study. Although a high degree of overlap has been found between the two types of activations, the authors suggest that (pure) taste cortical representation involves preferentially the insular cortex whereas the somatosensory component of flavour involves the Rolandic operculum. In fact, while taste information is conveyed through by the chorda tympany (cranial nerve VII), the glossopharyngeal (cranial nerve IX) and the vagal (cranial nerve X) nerves, lingual somatosensory information related to temperature and tactile stimulation (in addition to chemical transduction stimulation of the perigemmal fibres) is conveyed by the trigeminal nerve (cranial nerve V) for the anterior two thirds of the tongue and cranial nerve IX for the posterior third (Cerf-Ducastel et al. 2001). And as mentioned above, a preferential projecting site for lingual information is the region around the central sulcus proximal to the Sylvian fissure including thus the Rolandic operculum.

It is important to note that the tracing study by Pritchard *et al.* (1986) revealed that the thalamic gustatory relay nucleus VPMpc projects, in addition to the anterior insular/frontal operculum complex, into an area of the pre-central gyrus just rostral to to the somatosensory regions receiving peri- and intra-oral information. These authors then conclude that this part of the pre-central gyrus (which is not contiguous to anterior insula/frontal operculum areas receiving projections form VPMpc) might constitute a primary taste cortex, and its caudal extension towards the lingual somatosensory areas might contain a region of overlap implementing the integration of lingual and gustatory information. The taste-related properties of this area must certainly be further explored.

Saliva composition

The perceptual effects of tastants in the mouth and their cortical representation are modulated by the chemical composition of the saliva, and thus this factor must be controlled for. In particular some salivary constituents such as postassium continuously stimulate taste receptors, resulting in an alteration of taste sensitivity. For example, the taste detection threshold for NaCl is slightly above the salivary sodium concentrations with which the taste receptor is continuously stimulated (Matsuo 2000). Nagler and Nagler (2001) studied the effect of pilocarpine on salivary constituents, and determined in a healthy control group the concentrations of the following salivary variables: sodium (Na), potassium (K), magnesium (Mg), calcium (Ca), phosphate (P). The concentrations of Na and K were measured by flame photometry.

Concentrations are as follows:

Electrolyte (mmol)	Resting			Stimulated		
	Mean	SEM	Range	Mean	SEM	Range
Sodium	7.1	3.2	2–15	6.7	3.0	3–25
Potassium	24.2	5.8	14–38	23.4	1.9	12–29
Calcium	1.0	0.17	0.5–2.5	0.9	0.2	0.5–2.0
Magnesium	0.3	0.065	0.1–0.5	0.21	0.07	0.05–0.45
Phosphate	7.2	1.13	2.66–10.0	6.4	0.66	3.66–9.33

Thus it appears that saliva K concentrations are in the order of 25mM whereas Na concentrations are in the order of 7mM.

Kalk *et al* (2001) used glandular sialometry and sialochemistry to analyse saliva constituents in Sjogren's syndrome patients.

Composition of stimulated glandular saliva in healthy subjects (n=36, mean (SD), in mM/l), for Parotid glands (mean of two sides)/ Submandibular-sublingual glands: Sodium 14(12)/11(6), Potassium 24(6)/17(6), Chloride 16(12)/16(6), Calcium 0.8(0.6)/1.7(0.6), Urea 3.8 (1.2)/2.5 (0.6), Protein (g/l) 0.6(0.6)/0.8(0.6), and Protein (g/min) 0.3(0.3)/0.4(0.3). In particular, K

concentrations match thus the ones found in Nagler and Nagler (2001). In addition, Christersson *et al* (2000) performed rheological measures on human saliva and found a coefficient of 1.9 mPas. Notice that 1 centiPoise (cP) = 1 milliPascal-second (mPa.s).

Anatomy and function of the cingulate cortex

Another region of interest in this study is the (anterior) cingulate cortex, given its rich set of connections with both visceral and motor systems, as will be seen.

In primates including humans, the cingulate cortex can be seen as a continuous ring of cortex around the medial wall of the cerebral hemisphere, covering the corpus callosum, in such a way that it is uninterrupted by any of the major sulci (Morecraft and Van Hoesen 1998), occupying thus ~2/3 on the medial wall of each cerebral hemisphere. This region has been often referred as part of the "limbic lobe" and its subdivisions have been referred to following this terminology (Paus 2001). Here we will follow cytoarchitectonic criteria including labelling subdivisions with Brodmann's areas.

Rostro-caudally, the cingulate cortex can be divided into two cytoarchitectonically distinct areas: an anterior, agranular region (the "ACC") comprising Brodmann areas (BAs) 33, 24, 25, 32 and a posterior, granular region comprising BAs 23, 26, 29, 30 31 (Paus 2001). A dorso-ventral distinction can also be determined based on the degree of laminar differentiation between the old periallocortical ventral area (*i.e.* around the corpus callosum) including BA 33 and the proisocortical more dorsal areas including BAs 24, 25 and 32.

Vogt and colleagues studied the cytoarchitecture and anatomical connections of cingulate cortex in rhesus monkeys (Macaca mulatta, Vogt and Pandya 1987; Vogt et al. 1987). Concerning the cytoarchitecture (Vogt et al. 1987), BA area 24 was shown to have three subdivisions: "24a", which is adjacent to the callosal sulcus and also has the least laminar differentiation; "24b", which has more clearly defined layers II, III, and V, and finally "24c", which forms the lower bank of the anterior cingulate sulcus, shown to have a particularly dense layer III. Three subareas were also found in area 23: "23a" is adjacent to the callosal sulcus and has the thinnest layers II-IV, which have the same cell density as layers V and VI; "23b" has the largest pyramids in layers IIIc and Va, and finally "23c", in the depths of the posterior cingulate sulcus, has the broadest external and thinnest internal pyramidal layers. The more posterior areas 29 and 30 are located in the posterior depths of the callosal sulcus, and have a special status concerning granularity. Two divisions of area 29 were apparent: a granular layer adjacent to layer I (named by the authors area 29a-c), and another with differentiation of layers III and IV (named area 29d). On the other hand area 30 was found to be apparently dysgranular (layer IV).

Further differentiations within the anterior cingulate cortex were found following injections of the retrograde tracer horseradish peroxidase (HRP). The results allowed differentiations within the cingulate subdivisions accordingly to their thalamic afferents (the terminology of the authors are still being followed here). Area 25 received thalamic input mainly from the midline parataenial (Pt), central densocellular (Cdc), and reuniens nuclei as well as from the dorsal parvicellular division of the mediodorsal nucleus (MDpc). On the other hand, areas 24a and 24b received most thalamic afferents from fusiform and multipolar cells in the Cdc and Pf nuclei with fewer from the ventral anterior (VA) and MDpc and MD densocellular (MDdc) nuclei. Most input to 24c appeared to originate in VA, MDdc, and Li. Area 29 received the most dense input from the anteroventral (AV), anterodorsal (AD), and laterodorsal (LD) nuclei. Areas 23a and 23b, in contrast, did not receive AV, AD, or LD input, but the greatest proportion of their thalamic afferents arose in AM.

Concerning cortical and allocortical afferents, these have been studied by Vogt and Pandya (Vogt and Pandya 1987), and also provide further light on the cingulate subdivisions. Projections were studied with horseradish peroxidase and tritiated amino acid tracers. Cortical input to area 25 originated in the frontal lobe in lateral areas 46 and 9 and orbitofrontal areas 11 and 14. Area 25 also received afferents from cingulate areas 24b, 24c, and 23b, from rostral auditory association areas TS2 and TS3, from the subiculum and CA1 sector of the hippocampus, and from the lateral and accessory basal nuclei of the amygdala. Areas 24a and 24b received afferents from areas 25 and 23b of cingulate cortex, but most were from frontal and temporal cortices, including areas 9, 11, 12, 13, and 46; temporal polar area TG as well as lateral and basal amygdalar nuclei; superior temporal sulcus; agranular insular cortex; posterior parahippocampal cortex / subiculum. Autoradiographic cases indicated that area 24c received input from the insula, parietal cortex, temporal pole, and frontal areas 12 and 46. Area 24 was not found to be a target of amygdalar afferents. The following projections were observed both to and within posterior cingulate cortex. Area 29a-c received inputs from area 46 of the frontal lobe and the subiculum and in its turn area 30 received projections from this area, as well as from the posterior parietal cortex and temporal cortex. Areas 23a and 23b received inputs mainly from prefrontal areas 46, 9, 11, and 14, parietal areas, and superior temporal cortex. Anterior cingulate areas 24a and 24b and posterior areas 29d and 30 projected to area 23.

More recently, Morecraft and Van Hoesen (1998) have studied, with retrogade and anterograde tracing in rhesus monkeys, the projections to areas 24c and 23c, also called "motor cingulate cortex" and referred to M3 and M4 respectively, in this study (on the projections from these areas to spinal chord and related areas, see below). Concerning retrograde labelling for area 24c, it has been observed that the heaviest projections come intrisincally from area 24c itself. Strong

labelling was also observed in area 23c, whereas other cingulate areas have depicted only moderate, if any, labelling.

Of particular interest in the retrograde studies are projections from the insular cortex to area 24c. In particular, labelling in the anterior parts of the insula was only moderate, and confined to its inferior portion (*i.e.* Iap and Idg). On the other hand at midlevels of Idg labelling was substantial only inferiorly. Also of interest are the projections from the dysgranular, posterior part of the orbitofrontal cortex, whereas only a few neurons in the granular part were labelled. Other labelled areas include temporal pole, entorhinal, perirhinal and parahippocampal cortices.

The pattern of projections from the insula into area 23c were different from those found for area 24c. In this case, whereas the most anterior areas were not labelled, moderate label was found in the superior part of Idg and heavy labelling in the superior part of Ig. In general heavy projections from the granular part of the insular cortex were observed in 23c. This preferentially granular origin of projections into 23c was also observed with respect to the orbitofrontal cortex. Projections from parietal and temporal lobes, entorhinal, perirhinal and parahippocampal cortices were also observed. These projections might indicate that the cingulate cortex plays a role in visual-cue based spatial orientation (de Araujo et al. 2001). Interestingly, intracingulate projections were found to be widespread, in that most subdivisions of the cingulate cortex were labelled with respect to 23c.

On the other hand a more complete appreciation of cingulate functions can be given if the projection targets of the cingulate cortex are revealed. Two major sets of projections are of interest. The first concerns corticospinal projections originanting from the cingulate area. Morecraft *et al.* (1997) studied these projections in rhesus monkeys. Methods included injections of biotinylated dextran amine involving the arm representation of 24c and 23c. In 24c cases, contralateral terminal label occurred in the lateral part of laminae V and VI of the intermediate zone including the reticulated marginal border. On the other hand, 23c cases demonstrated contralateral terminal labeling in the medial part of the dorsal and intermediate zones (laminae III, IV, V and VI) giving evidence thus of two distinct, but well-defined cingulospinal systems controlling voluntary movement through superior limbs.

The second set of projections refers to visceromotor activity. In rats and cats, (the homologous to) area 25 projects to the nucleus of the solitary tract and to the dorsomotor nucleus of the vagus (Hurley et al. 1991), the latter being a brainstem area involved in feeding, sexual and cardiovascular responses as elicited by vagus nerve information. Also, area 25 projects to the sympathetic thoracic intermediolateral cell column (Hurley et al. 1991). Area 24 does not contain

similar projection sites, but could however contribute to visceral control trhough its projections to area 25. In primates (macaque monkeys), visceral control by cingulate areas 25 and 32 are mainly implemented through projections to the amygdala (Carmichael and Price 1995a) and to the hypothalamus (Ongur et al. 1998), the homeostasis-control centre of the brain. In this study, it has been shown that areas 25 and 32 send the heaviest cortical projections to all parts of the hypothalamus, especially the anterior hypothalamus and the ventral medial hypothalamic nucleus. It should be noticed that posterior orbital areas also project selectively to the lateral hypothalamic area (Carmichael and Price 1995a).

Approximate locations of human cingulate subdivisions, in terms of Brodmann areas, are shown in Fig 0.4. It should be noted however that a great variability across individuals in sulcal patterns is observed in human cingulate cortex (Paus 2001).

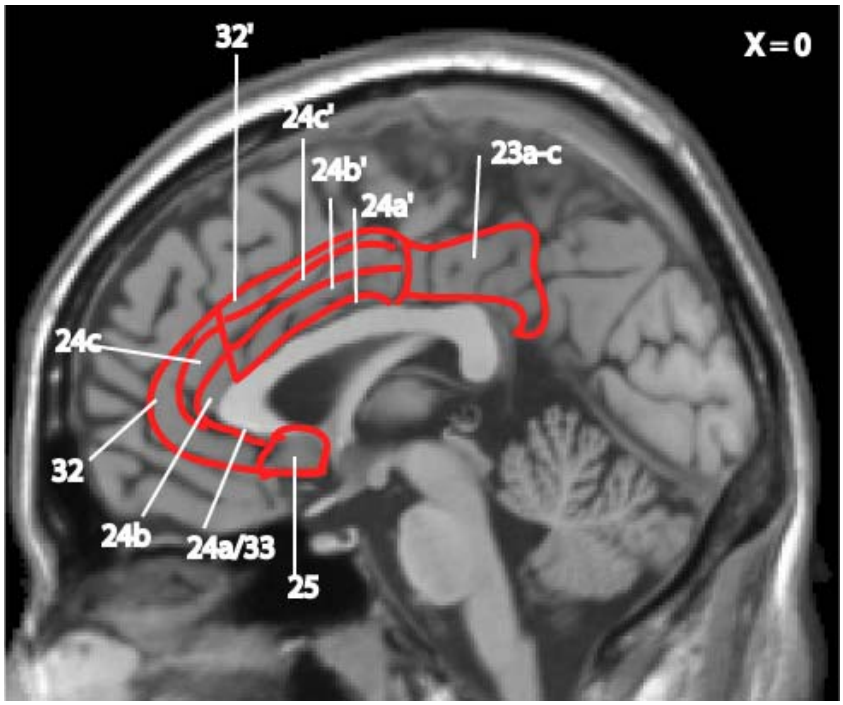


Fig 0.5 Approximate locations of cingulate subareas on an MRI saggital scan through the medial wall of the human brain (X=0) based on Paus (2001), Bush et al (2000) and Devinsky et al (1995)

Given the complexity of the cingulate cortex cytoarchitectonic and hodological structures, it is not surprising that the functions of the primate cingulate cortex are rather hard to characterise. Concerning mainly the human anterior cingulate cortex, an organisational effort has been attempted by classifying cingulate subdivision areas as performing "affective" or "cognitive"

functions (Bush et al. 2000; Paus 2001). Roughly, the cognitive division would comprise the more dorsal areas 24b'-c' and 32', (*i.e.* the cingulate areas immediately dorsal to areas 24b-c and 32) whereas the affective division would include the more rostral-ventral areas 24a-c 25, 32 and 33. In functional neuroimaging studies, the cognitive division has been preferentially activated in tasks involving stimulus-response associations in which the appropriate response depends on processing competing streams of information such as Stroop-like tasks, as well as tasks involving attentional and working memory mechanisms (Bush et al. 2000), whereas the affective division responds preferentially during "emotional processing".

"Cognitive" and "emotional" are rather vague terms with respect to their ability to characterise the actual functions of cingulate cortex subregions. For example the "emotional stroop task" (Bush et al. 2000) hardly seems to be an "affective" equivalent of the "cognitive" stroop-task. Also, it seems rather difficult to experimentally separate the "cognitive" and "emotional" components in tasks involving functions such as social interactions and vocalisation, known to require the anterior cingulate cortex of primates including humans (Devinsky et al. 1995).

It seems however that there is consistent evidence that the rostral part of the primate anterior cingulate cortex is involved in complex response-selection tasks (Hadland et al. 2003a; Rushworth et al. 2002), its anatomical substrate probably being the corticospinal projection fields, which integrate information from other frontal areas including supplementary motor areas. Also, the involvement of the more ventrorostral areas 25 and 32 of the anterior cingulate cortex in visceromotor functions seem also to be well documented (Devinsky et al. 1995), specially given its projections to central autonomic areas including the hypothalamus. In fact, early stimulation studies in monkeys show clear autonomic alterations, such as changes in blood pressure and heart/respiratory rates. The cingulate cortex has been recently found to be important in nociception, including the effects of placebo trials in perceived pain (Petrovic et al. 2002; Petrovic et al. 2000). The role of the cingulate cortex in nociception might be related to a high responsivity to the cholicystokinin (CCK) peptide, known to be involved in the chemical transmission of nociceptive information across the central nervous system (Skinner et al. 1997). More generally, functional neuroimaging studies in normal subjects and lesion studies in macaque monkeys have evidenced the role of the cingulate cortex in affective processing and social interaction. Monkeys sustaining cingulate lesions were impaired in social interaction-related activities, and were also impaired with respect to facial expressions and vocalisation (Hadland et al. 2003b), further confirming previous primate data (Devinsky et al. 1995). Analogously, recent imaging data have demonstrated the involvement of the cingulate in autonomic and homeostatic processing (Craig 2002; Craig et al. 2000; Critchley et al. 2000a; Denton et al. 1999b). Given the role of the cingulate cortex in action-reward associations in non-human primates (Hadland et al.

2003a), one is lead to the hypothesis that the representation of primary rewards in the cingulate cortex is required for appropriate behavioural action.

In a recent study, Ongur et al. (2003) investigated the human orbital and medial prefrontal cortex structure using five histological and immunohistochemical stains, and correlated the findings with a previous similar analysis performed on macaque monkeys (Carmichael and Price 1994). Ongur et al. note that Brodmann's area 32 in humans is not equivalent to area 32 in monkeys: Brodmann called the human area 32 the "dorsal anterior cingulate area", but he called the monkey area 32 the "prelimbic area", noticing that the two are not homologous (Brodmann 1909). This leads Ongur et al. to call the human area 32 as "32ac" ("anterior cingulate area 32"). Thus, homology between lesion studies on area 32 in monkeys can be only partially generalised to the human case. On the other hand, thy notice that, as in monkeys (Carmichael and Price 1994), area 24 can be divided into three zones (24a, 24b, 24c), but only areas 24a and 24b are present rostral and ventral to the genu of the corpus callosum.

In summary, there is clear evidence that the insular and cingulate cortices are anatomically connected to a network involving visceral and homeostatic-related processing through areas such as the hypothalamus. The extent to which these areas perform similar functions in the human brain largely remains to be determined, and this thesis attempts to make a contribution to this topic.

Note on the terminology used in this Thesis

For the purpose of consistency, the terminology employed throughout this Thesis has to be established, in particular with respect to the subvidivisons of the insular cortex. We define the *far anterior, (agranular) part of the insula* as the insular cytoarchitectonically distinct regions indentified in macaque monkeys (Carmichael and Price 1994; Carmichael and Price 1996; Price 1999) as Iai, Ial, Iam, Iapl and Iapm (see above for details and Fig 0.3). Thus we distinguish this far anterior, agranular part of the insula, which is part of the most posterior part of the orbital surface, from the adjoining regions usually called "anterior insula", which possibly contains in addition its gustatory part (area G, Carmichael and Price 1994; Mesulam and Mufson 1982a; Pritchard et al. 1986; Yaxley et al. 1990) and the adjoining (pre-central) opercular cortex. Regions Iai, Ial, Iam and Iapm were recently indentified in humans (Ongur et al. 2003) and together constitute what is being called the *far anterior, (agranular) part of the human insula* in this Thesis (Iapl is possibly posterior to the orbital region investigated by Ongur et al. 2003). In addition, we call *mid-insula* the part of the insular cortex posterior to the limen insula (~5mm) and dorsal to the medial limb of the inferior limiting sulcus, as defined for macaque monkeys by Mesulam and Mufson (1982a). By the expression *orbital surface* (or *orbital cortex*) we denote the area of the primate prefrontal cortex which includes the orbitofrontal cortex (Petrides and Pandya 1994; Rolls 2000a) and its agranular extension into the anterior insular cortex as defined above.

Introduction to Methods: Magnetic Resonance Imaging and its Functional variant

The basics of MRI

The field of nuclear magnetism, on which lie the foundations of the *magnetic resonance imaging* (MRI) technique, is a vast and complex area of research obviously impossible to cover in this type of document. So only a description of the basic mechanisms of MRI will be given, sufficient for the understanding of the main ideas behind its functional variant, *fMRI*. The following description is based on Heeger and Ress (2002), Logothetis (2002) and Thompson *et al* (2003).

Atomic nuclei possessing an odd number of protons (such as the hydrogen nucleus, ^1H) are thought to behave as magnetic dipoles, being formally represented as two-dimensional vectors, called *magnetic dipole moment* and denoted by μ. The physical substrate for the existence of these dipoles is the fact that, as shown by quantum mechanics, protons possess angular momentum or *nuclear spin*. It is known from quantum theory that atomic nuclei have specific energy levels that are formally related to a quantity called *spin quantum number,* which quantifies the nuclear spin and is denoted by S. In particular we have that $S(^1H) = ½$. In general, the number of energy states of a nucleus is given by 2S+1, so that hydrogen has two energy states denoted as ½ and -½.

Under normal (earth-like) magnetic field strengths the magnetic dipoles are randomly oriented; however, when exposed to higher external fields, the dipoles line up and "precess" around the field's direction, creating a uniform organisation given by this main external magnetic field. The rate at which the proton precesses around the external magnetic field is given by the *Larmor equation*:

$$f = \gamma B_0/2\pi$$

where f is the resonance frequency in Hz, γ is a constant, called the gyromagnetic ratio, and B_0 is the external magnetic field. For hydrogen protons, $\gamma = \gamma (H) = 42.6$ MHz/Tesla. For example, in a 1.5 Tesla field, the precessional frequency of hydrogen as given by the Larmor relationship is 64MHz. Notice that as the field strength increases, so does the precessional frequency of hydrogen protons (in a 3 Tesla field, 127.8 MHz).

Given that the isotope ^1H has two states with orientation either parallel (lower energy) or antiparallel (higher energy) to the main magnetic field, the tissue magnetisation used by MRI is

due to the small excess of the isotope population in the lower energy level (~1/100000 in a 1.5 Tesla field). Nuclear MR is related to the frequency-specific excitation produced by the transitions between these two (^{1}H) different energy states. The reason why MRI works is that it is possible to measure the emission of energy after excitation as the whole system returns to equilibrium.

Frequency-specific excitation is achieved through emission of radio-frequency (RF) pulses. RF pulses are oscillating electromagnetic fields, normally in the order of 100 MHz (so within the radio-frequency bandwidth). Bloch and colleagues (Bloch 1946; Bloch et al. 1946) were the first to observe the electromotive force received through a coil induced by the precession of nuclear moments around the main magnetic field B_0 and perpendicular to B_1, the field induced by the RF pulse. This is the basic mechanism on which lie MRI methods: an RF pulse is applied through a coil in order to excite the nuclear spins and cause the tissue magnetisation to *nutate* on the transverse plane (*i.e.* to move in a spiral-like form around the B_0 direction down to the B_1 direction). The arbitrary angle by which the magnetisation can be rotated is called the *flip angle* and is denoted by θ. The optimum angle is called the *Ernst angle* θ_E, which is given by the relationship

$$\cos \theta_E = \exp(-TR/T_1)$$

where TR is the *repetition time*, the time between two successive RF excitations, and T_1 is the longitudinal relaxation time (*i.e.* the time it takes for the spins to realign along the longitudinal axis, also called the *spin-lattice* relaxation time).

Once the RF pulse is turned off, the magnetisation is again subject uniquely to the external field B_0, and returns to its equilibrium state (the state of lower energy) emitting energy at same radio-wave frequency. So, as the system returns to equilibrium and emits energy as determined by the magnitude of the RF pulse, a voltage is induced in an RF receiver coil, having the characteristics of a "damped cosine" function. This voltage is called the FID signal ("free-induction decay" signal) and is the main signal from which an image can be displayed.

In analogy to the T_1 measure, T_2 reflects spin dephasing on the perpendicular ("xy" as opposed to the main "z" direction given by B_0) and is known as transverse or "spin-spin" relaxation time. However, transverse magnetisation decays faster than what could be expected from the spin-spin relaxation alone, as occurring in a perfectly homogeneous magnetic field. So typically the FID has a T_2* reflecting the effective transverse relaxation time, where field inhomogeneities are taken into account.

The process described above, however, can account only for the general mechanism allowing the elicitation of the FID signal. How spatial encoding can be achieved? The idea is to superimpose linear-field gradients on the main magnetic field. The gradients are time-changing alternations of the magnetic field along a chosen dimension such as $\partial B_0/\partial X$. Superposing then a linear-field gradient to B_0, the Larmor relationship becomes

$$f = \gamma(B_0 + (\partial B_0/\partial X)X + (\partial B_0/\partial Y)Y + (\partial B_0/\partial Z)Z).$$

A range of Larmor frequencies are thus determined by the gradient application, providing exact spatial information. Gradient schemes are arbitrarily chosen in any dimension for slice selection (G_{ss}), readout (G_{ro}), and phase encoding (G_{pe}). The readout gradient is applied at the same time as the MR data are acquired while the phase encode gradient encodes the second dimension in the plane. Given an image with $N_{ro}N_{pe}$ pixels, N_{ro} points are sampled with the same readout gradient G_{ro}, and for phase encoding the gradient G_{pe} is incremented N_{pe} times. So, for each readout step, the collected signal is formed by the same frequencies differing only in their phases as determined by each phase-encoding step. The acquired data matrix with dimensions $N_{ro} \times N_{pe}$ is termed the *K-space*. The quantity

$$\gamma \int G_{ro,pe,ss} dt$$

gives the image in the inverse spatial domain and Fourier transform applied on the K-space determines the appropriate frequencies, angles and amplitudes. In particular, the amplitude of the central point of the K-space determines the signal-to-noise ratio (SNR) of the global image. For a field of view of dimensions $D_{ro} \times D_{pe}$ the SNR is given by

$$SNR \approx [(d\, D_{ro}D_{pe})/(\sqrt{}\, N_{ro}\, N_{pe})]\sqrt{}NEX$$

where d is the slice thickness and NEX is the number of excitations.

To accomplish fMRI (the details of which will be discussed below) one needs a faster acquisition method as compared to usual scanning protocols such as spin-echo (SE). The fastest scanning technique used in fMRI is *echo-planar imaging*, EPI (Mansfield et al. 1994; Mansfield and Harvey 1993; Stehling et al. 1991). To be able to perform EPI, hardware modifications need to be carried out, in particular the installation of *high performance gradients*. In *single-shot* EPI the entire K-space is filled in one shot with readout gradient during one T2* decay. In *multi-shot* EPI, multiple excitations are used. Single-shot EPI allows oscillating frequency-encoding gradient pulses and

complete K-space filling after a single RF pulse. On the other hand, in multi-shot EPI, the readout is divided into multiple "shots" or segments (Ns), such that

$$N_y = N_s \times ETL$$

where ETL (echo train length) is the number of lines in each segment. This is why this technique is also known as "*segmental* EPI". In multi-shot EPI, less stress is placed on the gradients compared with single-shot EPI. However, it takes longer to be performed, and so is more susceptible to motion artefacts.

The BOLD signal and its physiological substrate

The non-invasive brain imaging technique known as *blood oxygen level dependent functional magnetic resonance imaging* - BOLD fMRI - relies on the relationship between neuronal activity and haemodynamics. As in classical MRI, the fundamental BOLD signal is detected from hydrogen atoms that absorb the energy that is applied through a RF pulse. Exposed to higher external magnetic fields, these atoms, after being excited by the RF pulse emit energy at the same (radio frequency) while returning to their equilibrium state.

The measured radio-frequency signal decays over time, partly because of inhomogeneities in the external magnetic field. The greater the inhomogeneity, the weaker the image intensity, because the hydrogen atoms will experience slightly different magnetic fields, and within the T_2^* time their radio-frequency emissions will end up cancelling each other out. BOLD signal results from local, transient changes in inhomogeneities in the magnetic field, the key point being that these changes depend on the level of blood oxygenation.

S. Ogawa discovered the contrast mechanism reflecting the blood oxygenation level by observing signal dropouts from blood vessels when applying spin-echo sequences in experimental animals (Ogawa et al. 1990; Ogawa et al. 1992). As is currently known, this is due to the field inhomogeneities induced by deoxyhaemoglobin, which acts as an endogenous contrast (Logothetis 2002). Haemoglobin consists of two pairs of polypeptide chains (*globin*), forming the *haem* group. In deoxyhaemoglobin, the iron Fe^{2+} is in a paramagnetic state, given that four of its six outer electrons are unpaired and act as exogenous paramagnetic agents. When oxygenated, however, the haem iron changes to low-spin state through receiving oxygen electrons. The result is that a decrease in local deoxyhaemoglobin turns this region into less paramagnetic (with more hydrogen protons in low-spin state), increasing field homogeneity and so image intensity (Heeger and Ress 2002).

As reviewed in Heeger and Ress (2002), the current haemodynamic response model relies on the fact that a transient increase in neuronal activity leads to an increased consumption in oxygen and increased metabolic demand. This results in an initial decrease in local oxyhaemoglobin concentrations and increased deoxyhaemoglobin concentration (the "initial dip"). This increased neuronal activity elicits after approximately 2 seconds a large increase in blood flow, which is proportional to the amount of consumed glucose (necessary for cell metabolism). However, the blood flow overcompensates the amount of oxygen being used, leading then to an excessive provision of oxygen, giving rise to the BOLD signal which is observed in fMRI.

There are some grounds to believe that the transient local increase in blood flow, and ultimately the BOLD effect, results from neuronal activity. A possible line of explanation for that is as follows (Heeger and Ress 2002). First, blood flow increase is proportional to increase in glucose consumption and also, glucose metabolism has been shown to be linked to synaptic activity (Schwartz et al. 1979). In addition to that, it has been suggested that increases in brain activations are related to glycolysis, which is a non-oxidative form of glucose metabolism (Heeger and Ress 2002). This would explain the proportional amount of glucose consumption with respect to blood flow increase, which is not true for oxygen consumption. In fact, astrocytes rely on glycolysis to be able to consume glucose and release lactate, which corresponds to their neurotransmitter recycling function.

On the other hand, it has been also argued that the increase in blood supply does indeed provide the extra amount of oxygen needed by the neurons during (increased) activity. Given that oxygen extraction through passive diffusion is less efficient at higher flow rates, the mismatch between oxygen consumption and blood flow supply becomes not hard to explain. In favour of this view, is the fact the oxygen consumption does increase with neuronal activity (Davis et al. 1998).

More recently, new evidence has emerged linking directly the BOLD effect with oxygen consumption in the brain. Thompson *et al* (2003) performed simultaneous measurements of tissue oxygenation and single-cell recordings in the cat visual cortex, and found that increases in spike rate were coupled to decreases in tissue oxygenation, providing thus a concrete relationship between oxidative brain metabolism and the BOLD signal. The authors argue that fMRI resolution could be much improved by using information from the initial period where a decrease in oxygenation (*i.e.* a proportional increase in deoxyhaemoglobin concentration, the "initial dip") is detected. To show this, they used the measured decrease in oxygenation to predict the orientation selectivity and ocular dominance of neurons neighbouring those being recorded, reaching thus localisation of neuronal activity at a columnar level. In general, this study is a step

forward in establishing the fact that the initial dip is actually caused by metabolic activity following increases in neuronal spiking rates, and that the relative increase in oxygenated blood flow measured with fMRI works in fact as a compensatory mechanism. This opens thus the possibility that the "initial dip" could be used as a higher-resolution parameter for brain activity measurement with fMRI.

The relationship between neuronal activity and the BOLD effect is being uncovered by the work of Logothetis and colleagues, through the use of a series of simultaneous electrophysiological recordings and fMRI measurements in non-human primates (Logothetis 2002; Logothetis et al. 2001). The results so far show that the BOLD signal, acting as a contrast mechanism, does reflect neuronal activity as elicited by an external stimulus. For stimuli presentation of short durations, BOLD responses were found to be linearly related to neuronal activity, although vascular variability implies that neural signals have a higher SNR. However, the significance of the linear relationship seems to depend on the method used to record the neural signal. In particular, the haemodynamic response seems to be better correlated with local field potential measurements than with multi-unit activity recording, which allowed Logothetis to conclude that the BOLD activation seems to reflect better the incoming input and local processing in a given area, rather than spiking activity (Logothetis 2002).

Further evidence linking the BOLD signal to changes in neuronal spiking activity was provided in Smith *et al* (2002). In this study, which measured brain activity following forepaw stimulation in the anesthesised rat, the energetic component from the BOLD signal was related to spiking activity by sequential measurements of changes in spiking activity $\Delta\nu/\nu$ (through extra-cellular recording in a neuronal ensemble) and localised changes in brain energy metabolism, $\Delta CMR_{O2}/CMR_{O2}$ (detected through combined fMRI BOLD measurements, cerebral blood volume, and transverse relaxation rates of tissue water, at 7 Tesla). The results show that $\Delta CMR_{O2}/CMR_{O2} \approx \Delta\nu/\nu$, and given that $\Delta CMR_{O2}/CMR_{O2}$ had the same high spatial and temporal as the fMRI signal, the authors concluded that the BOLD signal when converted into $\Delta CMR_{O2}/CMR_{O2}$ measurements correlates with changes in spiking activity.

Local field inhomogeneities and brain shimming

Performing fMRI experiments in higher magnetic fields (e.g. >2 Tesla) leads to improvements in SNR, increasing the likelihood of observing activations (henceforth meaning local and transient increases in BOLD signal) in brain areas in which some *a priori* hypothesis has been formulated. However, subject-specific geometric and magnetic susceptibility variations within the human head lead to local distortions in the B_0 field (Li et al. 1996) particularly in the vicinity of air-bone tissue interfaces (e.g. sphenoid/ethmoid sinus and petrous bone regions). The rapid imaging

methods used in fMRI, namely echo planar imaging (EPI) and spiral methods, are particularly vulnerable to the resulting susceptibility artifacts of geometric distortion and localised signal loss (Ojemann et al. 1997).

This problem is particularly serious for investigators interested in regions such as the orbitofrontal cortex, which is the case for several of our studies. In collaborative work with FMRIB (Oxford University) physicist James Wilson and colleagues, a method was presented for automatic shimming of the brain, which greatly improves signal recovery in regions such as the human orbitofrontal cortex. The details of this technique have been outlined in Wilson, Jenkinson, de Araujo *et al* (2002). In this work experimental evidence was given based on an olfactory fMRI study, and whose group analysis and main findings are presented in Chapter II of this Thesis. Essentially, the technique involves calculating a target function representing the amount of field homogeneity, which has thus to be minimised through the use of appropriate statistical methods. Specific values resulting from such analysis are thus used to parameterise changes in hardware settings through the use of a shim current constrained algorithm.

To optimise the static magnetic field B_0, a homogeneity target function must be minimised with knowledge of the *in-vivo* B_0 variation, the shim coil basis functions and, if required, a weighted ROI map. Once the optimal shim coil currents are determined, the input to the shim coil amplifiers is updated and the scanner resonance frequency adjusted.

The implementation used in the present study utilises a shim current constrained algorithm devised by Wen *et al.* (1995), with the modification of a conventional least squares target function (Hu et al. 1995; Prammer et al. 1988; Reese et al. 1995; Schneider and Glover 1991; Tropp et al. 1989; Webb and Macovski 1991), *L*, defined as:

$$L = \sqrt{\sum_{\mathrm{VOI}} S_{\mathrm{W}} \left[B_0(x,y,z) - \langle B_0 \rangle \right]^2} \ , \qquad [1]$$

where $\langle B_0 \rangle$ is the average static field within the volume of interest and S_W is equal to unity at all points in space for global brain shimming. So, essentially, *L* is a function of the difference (in field strength) between all points in space *(x,y,z)* (located in the appropriate volumes of interest) and the mean field strength $\langle B_0 \rangle$. S_W on its turn represents a "weight" applied to the points in a given volume of interest. Practically, the minimisation of this target function has the effect of placing the volume of interest as close to resonance as possible, so reducing spatial distortion effects. The main point of interest here is that the original target function used by Wen *et al.* (1995), *D*, is effectively a measure of local signal loss artefact. This additional B_0 homogeneity

measure was then used as a parameter in the analysis described in Wilson *et al* (2002).

We applied this technique (*i.e.* minimising the function *L* with respect to both a volume of interest defined as the inferior frontal cortex, where $S_W > 1$ for the voxels within this region, and a global shimming where S_W is set as $S_W = 1$ at all points in space) in one subject scanned for the orthonasal olfactory task described in Chapter II. For this particular subject half of the scans were acquired under global shimming of the magnetic field, whereas the other half was acquired under application of local shimming in the inferior frontal cortex.

Generally the results of comparing a global field shimming against local field shimming (applied the inferior frontal cortex) were as follows. For the inferior frontal ROI, improvements of 19.3% in L and 30.3% in D were found post-local shim as compared to post-global shim. The resulting reduction in image distortion and signal loss artefacts of the raw EPIs were representative of a larger sample. The mean odour intensities during the studies, as rated by the subject, were 0.87 for the post-olfaction shim and 0.85 for the post-global shim (paired t-test, t=0.330, df=31, not significant, $p>0.4$). Thus there is no significant difference in these intensity means, indicating habituation effects of the subject to the odours were minimal between studies.

An example of a significant activation (obtained by using local shimming) in the medial orbitofrontal cortex is shown in Fig 0.6 for the comparison odour (hexanoic acid) – control (pure air). In the top row, left, is shown a coronal slice through the orbitofrontal cortex (red bars) for the comparison odour-control tested in the images acquired under local shimming. A significant activation ($p<0.0001$ uncorrected for multiple comparisons) was found in a region of the medial orbitofrontal cortex, extending dorsally into the medial wall (with respect to the methods used for testing significance of activation images, see the next section). The corresponding field map is show in the same top row, right.
No significant activations were found in this region (or any other inferior frontal region) for the global shimming case (at $p<0.01$ uncorrected), as depicted in Fig 0.6, bottom row, left. In the same bottom row, right, is the corresponding field map (note the loss of signal intensity in the orbitofrontal region). The slices shown in the bottom row are exactly the same as in the top row. The activation images were overlayed on the structural scan taken from the subject, normalised to the standard MNI space (see next section for more details on normalisation).

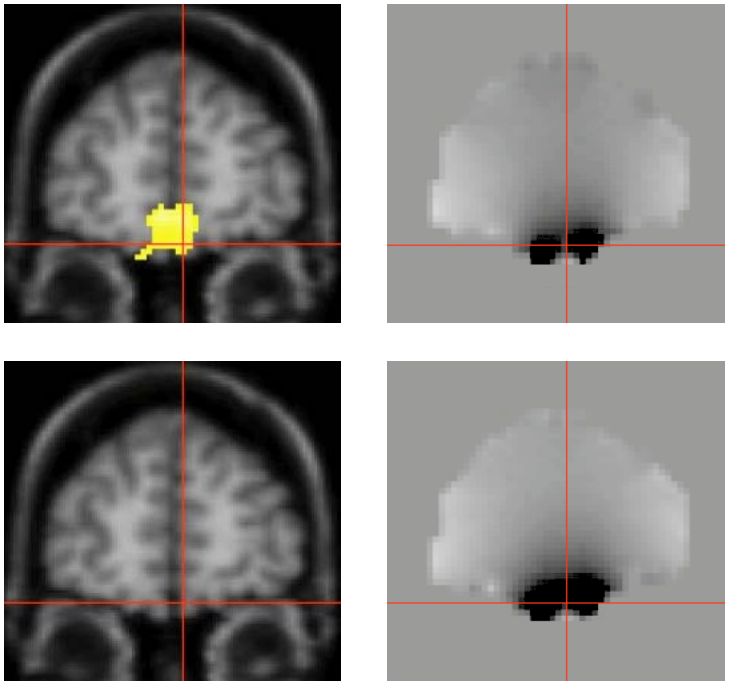


Figure 0.6: Activated voxels in the comparison (Odour – Control) for Hexanoic acid in one subject. A single slice of normalised MNI-space containing the orbitofrontal cortex is shown following (a) an olfaction shim, and (b) a global shim. The activation visible in (a) has a cluster size of 259 voxels with the peak at [x,y,z]=[-6,40,-26] and a maximum Z-score of 4.35 (p<0.0001, uncorrected). No significant activations were obtained in the orbitofrontal cortex after application of the global shim. B_0 maps of the brain transformed into MNI-space obtained post-olfaction shim and post-global shim are displayed in (c) and (d) respectively. The B_0 range is –150 (white) to 110 Hz (black). This figure is also presented in Wilson et al (2002).

Statistical analysis of activation images

Following data acquisition and pre-processing (this step includes operations such as motion correction, spatial and temporal filtering and normalisation of functional images to a standard stereotaxic space; given the variability of the parameters the specifics will be given in each of the experimental chapters), activations in specific brain areas as revealed by fMRI are inferred from the time-series data that usually contain large amounts of noise (random error). This section briefly reviews the basic statistical methods used to infer activations in the studies that constitute this Thesis. The formalism is based on Friston (1995a) and Worsley (2001).

The HRF response function

If we denote by s(t) a function of time that describes the behaviour of an external stimulus (normally s(t) is a binary function representing the delivery or presentation of a given stimulus), we can model the BOLD response at a specific voxel by a function x(t) which is assumed to peak at 6 seconds and normally occurs between 3 and 10 seconds following stimulus delivery. The delay of the response is modelled by a *haemodynamic response function* – *HRF* – which is denoted by h(t) and is used to convolve past stimulus values:

$$X(t) = \int_{+} h(u)s(t-u)du$$

where "$\int_{+}$" denotes the integral being calculated over the set of non-negative real numbers. The HRF function h(t) on its turn is modelled as a difference of two gamma functions (Friston et al. 1995b):

$$h(t) = (t/d_1)^{a_1}\exp(-(t-d_1)/\ b_1) - c(t/d_2)^{a_2}\exp(-(t-d_2)/\ b_2)$$

where: $d_j = a_j b_j$ is the time to the peak, and $a_1 = 6$, $a_2 = 12$, $b_1 = b_2 = 0.9$ seconds and $c = 0.35$.

Univariate linear modelling

BOLD responses are estimated by univariate (i.e. each voxel is independently modelled) linear modelling, where it is assumed that responses to different conditions or stimuli (including rest or control condition) have different magnitudes, denoted as β_1, β_2, etc. in such a way that their sum corresponds to the final BOLD response. The general form is then

$$X_{i1}\beta_1 + X_{i2}\beta_2 + \ldots + X_{im}\beta_m .$$

for *m* different responses X_{ij}, j = 1,…,*m* and fixed time point *i*.

For, say, time point *i*, the observed response Y_i is described thus as

$$Y_i = X_{i1}\beta_1 + X_{i2}\beta_2 + \ldots + X_{im}\beta_m + \varepsilon_i$$

where ε_i is the random (normally distributed) error (remember that these expressions refer to a single voxel).

The next step is to estimate the magnitudes of the β's. To accomplish that, classical least square methods are used (Worsley 2001) through calculation of the pseudoinverse of the design matrix,

i.e., the matrix $[X_{ij}]^{-1}$. If we call β the vector of length *m* containing the values of the estimators as given by the least-square method, let's denote the efficient estimator (Worsley 2001) of β as $\boldsymbol{\beta}$.

In order to be able to detect an effect, we need to make inferences based on comparisons between the values of β. In a simple on-off design, the effect to be tested is $\beta_1 - \beta_2 > 0$, where for example β_1 refers to the stimulus delivery estimate and β_2 to the rest condition. In general these comparisons are expressed as vectors of the same length of β, called *contrasts* and denoted here by "c". The T statistic has then the form

$$t = c\boldsymbol{\beta}/(\sqrt{\mathbf{Var}(c\boldsymbol{\beta})})$$

where $\mathbf{Var}(c\boldsymbol{\beta})$ is the variance of $c\boldsymbol{\beta}$. In other terms, the activation effect is assessed by comparing, through the definition of a contrast vector applied on the vector of parameter estimates, the contribution of specific explanatory variables (*e.g.* stimulus presentation versus rest condition).

t-statistics images are then usually converted into z statistical images, where the theoretical t distribution (taking into account the relevant number of degrees of freedom) is transformed into a unit-variance Gaussian distribution. The voxel values resulting from this transform (the z statistical image) form an "image process", called a *statistical parametric map*, or *SPM*. Friston (1996) interprets the SPMs as spatially extended statistical processes.

A particular application of the general linear approach to fMRI data series involves using a fixed-effect analysis. In a group analysis, this implies in assuming that each subject gives a fixed contribution to the significance of the activation. This presents the obvious problem of overestimating the contribution of a specific subject in the group effect. *Random-effects* (or "component variance") analyses involve linear models equivalent to *n*-factor ANOVA model where subject × condition interactions are taken into account by considering the "subject" factor as a random factor (so that this constitutes more precisely a *mixed-effects*, or ANOVA type III, linear model). In other words, these are second-level statistical tests that take into account inter-subject variability, by for example performing one-sample t-tests on the voxel values as defined by the *individual* Z-maps. In this case the degree of freedom is *n*-1, where *n* is the number of subjects. This type of analysis allows the activation effects to be generalised to an entire population (which gave origin to the sample) given that subject × condition interactions are being accounted for (see below).

An alternative method for assessing the significance of group effects is known as *conjunction analysis* (Friston et al. 1999a) and is used throughout this thesis. Random effects (*i.e.* variance between subjects) can be seen as subject × condition interactions (Friston et al. 1999b), where condition-specific activations are specified by linear contrasts. Subject × condition interactions on their turn are a special case of session-by-contrast interactions, assuming that a different subject is scanned in each section. Conjunction analysis proposes to assess the joint significance of several different contrasts (*i.e.* hypotheses) through the significance of their combination so that individual voxels indicating interactions among contrasts are eliminated. In some way, conjunction analysis can be seen as a technique that reveals the main effects of different effects or contrasts subtracted from interaction terms (Price and Friston 1997).

Friston *et al* (1999a) show, through binomial expansion analysis, that the probability (under the null hypothesis) *P(n)* of a conjunction of effects (given a contrast) over *n* subjects occurring by chance is

$$P(n) = [\alpha(1 - \gamma) + \beta\gamma]^n.$$

where $1 - \alpha$ is the test specificity (*i.e.* α is the P value of the test), β its power or sensitivity and γ is the proportion of the population (where the sample originated from) showing the effect.

It is clear that an upper bound for the estimation of *P(n)* is given when $\beta=1$, with respect to a critical proportion of the population γ_c:

$$P(n \mid \gamma \leq \gamma_c) \leq [\alpha(1 - \gamma_c) + \gamma_c]^n$$

This conditional probability effectively gives a P value corresponding to how "typical" an effect is, as defined by the critical parameter γ_c. If we fix $P(n \mid \gamma \leq \gamma_c) = \alpha_c$ with $\alpha_c > \alpha$, γ_c will satisfy the relationship

$$\gamma_c \geq ((\alpha_c)^{1/n} - \alpha)/1\text{-}\alpha.$$

Note that $\gamma_c \rightarrow 1$ as $n \rightarrow +\infty$. Thus a confidence interval for the estimated proportion of the population producing an effect can be given.

In summary, a typical analysis of a pre-processed time series fMRI data as used in this thesis is as following. First, each event *e* is modelled by a delta function of the form

δ_e (t) ≡ 1 if t = time onset for event e;

δ_e (t) ≡ 0 if $t \neq$ time onset of event e;

where $0 \leq t \leq T$ and T is total time (*e.g.* in seconds) of the experiment.

Thus there is one specific δ_e corresponding to each of a number of event types (*e.g.* odour, pure air, etc.). Given the complete set of events *e,* the values of δ_e might be seen as corresponding to the entries in $[X_{ij}]$. Then, the regressors of interest representing the event types are obtained through convolution of the δ_e with the haemodynamic response function *h(t)* depicted above. The result of convolving the δ_e functions with the haemodynamic response function *h(t)* results in a new function defined over $0 \leq t \leq T$ which constitutes the core of the model to be tested. Normally, the first-order time-derivatives of these functions are also included to account for shifts in latency of responses. Possibly, the effects of some covariate of interest (*e.g.* subjective pleasantness ratings) might be calculated by modulating the relevant regressors with the values of these parameters ("parametric modulation"). Finally, after least-square estimation of parameters estimates, comparisons are carried out through t-tests between the relevant parameter estimates. t-values are then transformed into Gaussian z-values. The resulting image is a statistical parametric mapping (*spm*). In a group analysis, these *spm*s might be entered into mixed effects (ANOVA type III) or conjunction analyses.

A note should be given on the corrections for the number of comparisons made (since the model is univariate, there is one comparison made for each voxel increasing thus the occurrence probability of type I errors). Spatial smoothing *e.g.* with a Gaussian filter introduces correlations between neighbouring voxel values, in such a way that they can no longer be considered as independent observations. A *resel* (resolution element) is an image unit where the FWHM value of the Gaussian smoothing is taken into account. If we have an image with *npixels* pixels, the number of resels is *npixels*/FWHM^2. This is the value taken into account for calculating corrected p-values in *spm*'s. If the number of resels is known, it is possible to estimate the most likely value of the Euler characteristic (roughly, the number of significant clusters) at any given threshold (*e.g.* Z=4.0). The calculation of the likelihood of the Euler characteristic (the actual corrected p-value) given the number of resels and a threshold is based on random field theory techniques (Worsley et al. 1992).

In the analyses presented in this Thesis, the SPM99b software (Wellcome Department of Imaging Neuroscience, London) was used to implement linear models as outlined above, which thus constitute a well-validated method for fMRI data analysis.

Chapter I

The representation of umami taste in the human brain

In this chapter we describe an fMRI study on the representation of the taste of *umami* in the human brain. Umami taste stimuli, of which an exemplar is monosodium glutamate (MSG) and which capture what is described as the taste of protein, were shown using fMRI to activate similar cortical regions of the human taste system to those activated by a prototypical taste stimulus (glucose), as we will be seen in this Chapter. These taste regions included the insular/opercular cortex and the caudolateral orbitofrontal cortex. A part of the rostral anterior cingulate cortex was also activated. When the nucleotide 0.005 M inosine 5'-monophosphate (IMP) was added to MSG (0.05 M), the BOLD (blood oxygenation-level dependent) signal in an anterior part of the orbitofrontal cortex showed synergism, and this may reflect the subjective enhancement of umami taste that occurs when IMP is added to MSG. These results extend to humans, studies showing activation in macaques of single neurons by these umami stimuli, and allow brain areas where activation is related to the perceived enhancement effects of umami tastants to be revealed.

The first section gives a brief description of gustatory representation in the primate (including human) brain. The next section gives a brief account of the main properties of the characteristic taste of umami and finally a description of an fMRI study investigating the representation of umami taste in the human brain.

The organisation and function of the primate gustatory cortex

Anatomy

The "gustatory sense" in mammals is the set of sensations elicited through stimulation of taste buds, located on the tongue and on other areas in the oral cavity (such as the soft palate, the naso-pharynx system, and the larynx). The tongue is rather than anything a muscle, but whose

surface is covered by different types of papillae ("bumps"). Most papillae do not contain taste buds, but fungiform, foliate, and vallate papillae do. Each of those contains a variable number of taste buds (ranging from ~5 in fungiform papillae to ~5000 in vallate papillae). These on their turn are ovoid structures formed by ~100 modified epithelial cells, most of which are taste receptor cells. Taste receptor cells contain microvillar processes that extend to a small opening (the taste pore) where they are exposed to chemical stimuli. At specific regions of the taste bud, these receptor cells make synapses with visceral sensory fibres from the facial (VII), glossopharyngeal (IX) and vagal (X) cranial nerves (Norgren 1990).

Taste receptor cells make use of several methods to convey (or "transduce") information on the structure of chemical stimuli into electrical signals (that will be later conveyed through the cranial nerves to the central nervous system). Corresponding to the multiple taste qualities (e.g. sweet, salty, sour, bitter and umami) there might be different transduction processes (Matsunami et al. 2000; Montmayeur et al. 2001; Montmayeur and Matsunami 2002).

The transduction process for the prototypical salty stimulus, sodium chloride (NaCl), does not involve receptor molecules. Na^+ channels in the receptor cells allow inflow of Na^+ ions, depolarising the cell. Similarly, the operative agent in sour taste transduction is H^+, which also acts to depolarise taste receptor cells. Sweet taste transduction differs from the previous ones in that sweet compounds bind to G protein-coupled receptor molecules that (through a second messenger) decrease K^+ conductance in other parts of the cell. Bitter-sensitive taste receptor cells use both ligand-gated channels and G-protein coupled receptors. This allows taste receptor cells to be depolarised by a rather broad range of chemicals, such as quinine, which binds to ligand-gated K^+ channels. Chaudhari and colleagues (Chaudhari et al. 2000) have recently found a G protein-coupled receptor specific for glutamate in lingual tissue taste buds.

The electrical signals conveying information on the chemical properties of tastants are then sent to the rostral division of the Nucleus of the Solitary Tract (NST) of the medulla, the principal visceral sensory nucleus of the brainstem, via cranial nerves VII, IX and X. In the rat, second-order fibres (*i.e.* NST afferents) project ipsilaterally to the gustatory parabrachial nuclei in the pons, proceeding then to the parvicellular part of the ventroposterior medial nucleus of the thalamus (VPMpc). In primates, however, the NST projection fibres bypass the PBN only to join the central tegmental tract and synapse directly into VPMpc (Pritchard et al. 2000; Rolls and Scott 2003), whereas the PBN seems to be dedicated to convey general visceral information (*e.g.* from the vagus) to specialised thalamic nuclei (Pritchard et al. 2000), which might include VPM (Pritchard et al. 1989). Thalamic afferents then project to gustatory cortex (Scott and Plata-Salaman 1999). However, in the rat, parabrachial fibres also reach directly forebrain areas such as

the lateral hypothalamus and the central nucleus of the amygdala, giving gustatory information direct access to motivational and reinforcement-related areas including the dopaminergic system (through direct projections from the central nucleus of the amygdala, Fudge and Haber 2000).

The primary taste cortex in macaques can defined in terms of VPMpc afferents (Scott and Plata-Salaman 1999; Scott et al. 1986a). Pritchard et al. (1986) have studied the efferent projections of the VPMpc of the monkey, *macaca fascicularis* with tritiated amino acid autoradiography. Two discrete cortical areas were characterised as a target of VPMpc projections. First, labelled cells were located in the ipsilateral insular-opercular cortex adjacent to the superior limiting sulcus and extending as rostrally as the caudolateral orbitofrontal cortex (but see Baylis et al. 1995). Moreover, further projections were located within the primary somatosensory cortex, in the precentral gyrus subjacent to the anterior subcentral nucleus (*i.e.* a precentral extension of SI). This area is anterior to the VPM projection sites representing somatosensory information and is adjacent or overlapping with the cortical somatotopic sites for the face and oral cavity (Jain et al. 2001). Thus this area might be a target of VPM and VPMpc projection fibres and thus implement the convergence in the cortex of the somatosensory and gustatory aspects of stimuli delivered in the mouth (See Figs 1.1 and 1.2).

Scott (e.g. Scott and Plata-Salaman 1999) defines the anterior limit of the primary taste cortex in the macaque as the junction of the orbitofrontal and opercular cortices, from which it extends 4.0 mm posteriorly. The mediolateral extension is defined ~16-19 mm lateral to the midline in an average adult macaque. The dorsal limit is defined as ~6 mm above the lateral fissure. The insular cortex, in the depth of the Sylvian fissure, has been divided into four rostrocaudal subdivisions (Cipolloni and Pandya 1999): the most rostral portion has been designated the insular proisocortex; adjacent to it is the agranular subdivision of the insula, followed caudally by the dysgranular and the granular insular areas. In these terms, The VPMpc nucleus projects to the opercular and insular regions of the granular and dysgranular insula, and extends to adjacent agranular portions of the insula.

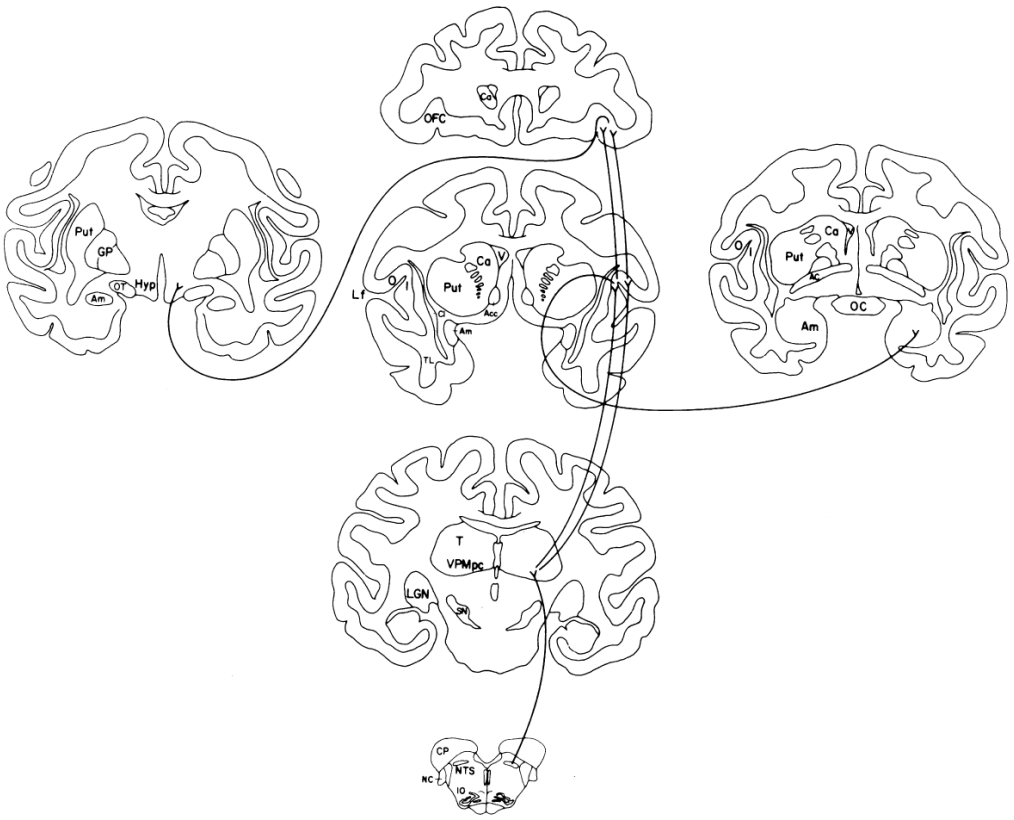


Fig 1.1 After Scott and Plata-Salaman (1999), where the anatomy of the central gustatory system of the cynomolgus monkey is reviewed. In the middle column are shown the projections from the brainstem nucleus of the solitary tract, from there to the ventral posterior medial thalamic nucleus (pars parvocellularis), and then to primary taste cortex (frontal operculum/anterior insula, and to the secondary taste cortex (caudolateral orbitofrontal cortex). In the left is shown the orbitofrontal projections conveying taste information into the hypothalamus, and in the right the projections from primary taste cortex to the amygdala. AC, anterior commissure; Acc, nucleus accumbens; Am, amygdala; Ca, caudate nucleus; Cl, claustrum; CP, cerebellar peduncle; GP, globus pallidus; Hyp, hypothalamus; I, Insula; IO, inferior olive; Lf, lateral (Sylvian) fissure; LGN, lateral geniculate nucleus of the thalamus; NC, nucleus cuneatus; NTS, nucleus of the solitary tract; O, operculum; OC, optic chiasm; OFC, orbitofrontal cortex; OT, optic tract, Put, putamen; SN, substantia nigra; T, thalamus; TL, temporal lobe; V, ventricle; VPMpc, ventral posterior medial thalamic nucleus (pars parvocellularis).

One of the projections from this primary taste cortex is to the central nucleus of the amygdala from where gustatory information reaches the basal forebrain, lateral hypothalamus (Scott and Plata-Salaman 1999) and dopaminergic cells in the substantia nigra pars compacta and ventral tegmental area (Fudge and Haber 2000; Scott et al. 1993). Fibres also project anteriorly to the dysgranular caudolateral orbitofrontal region, a secondary taste cortical area (Baylis et al. 1995; Rolls et al. 1990). This transition zone including the more anterior parts of the primary taste

cortex and the adjoining caudolateral orbitofrontal cortex is also dubbed "area G" by Carmichael and Price (1996). Taste neurons in the caudolateral orbitofrontal cortex form connections laterally with visual areas in the inferior temporal cortex and importantly converge with more medial cells receiving projections from primary olfactory cortex, which might have implications for the perception of flavour (Rolls 1997; Rolls and Baylis 1994). Taste cells in caudal orbitofrontal cortex project to the caudate nucleus (where taste information is distributed throughout the striatum) and lateral hypothalamus (Öngur and Price 1998; Scott and Plata-Salaman 1999), which in turn communicates directly with the central nucleus of the amygdala. The central nucleus of the amygdala on its turn projects back to the NST (Price and Amaral 1981). The described circuit could then form a complex neural network integrating information on the identity of individual tastants with their hedonic and motivational properties (Fig 1.1).

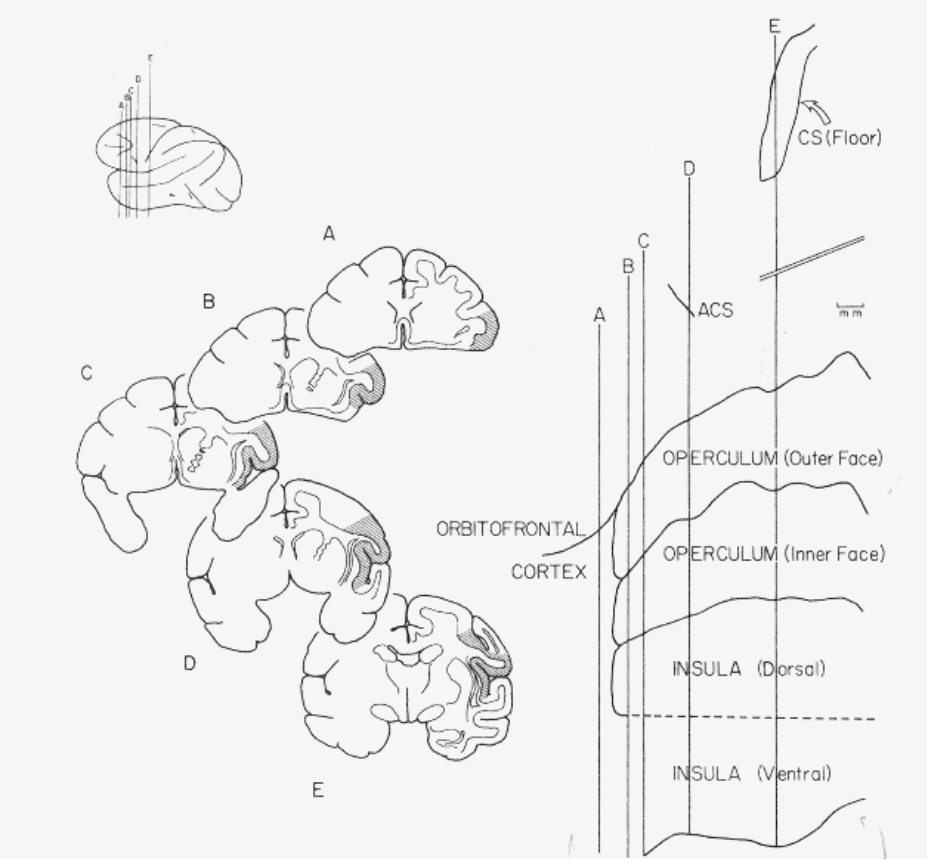


Fig 1.2 After Pritchard et al (1986) VPMpc projections into the cortex of the monkey, macaca fascicularis. The two cortical sites were found to receive direct projections from VPMpc, including the caudolateral orbitofrontal cortex/insular/opercular complex, and the area within the precentral gyrus subjacent to the anterior subcentral nucleus. On the top left, a reference for the anteroposterior location of the slices. CS: central sulcus.

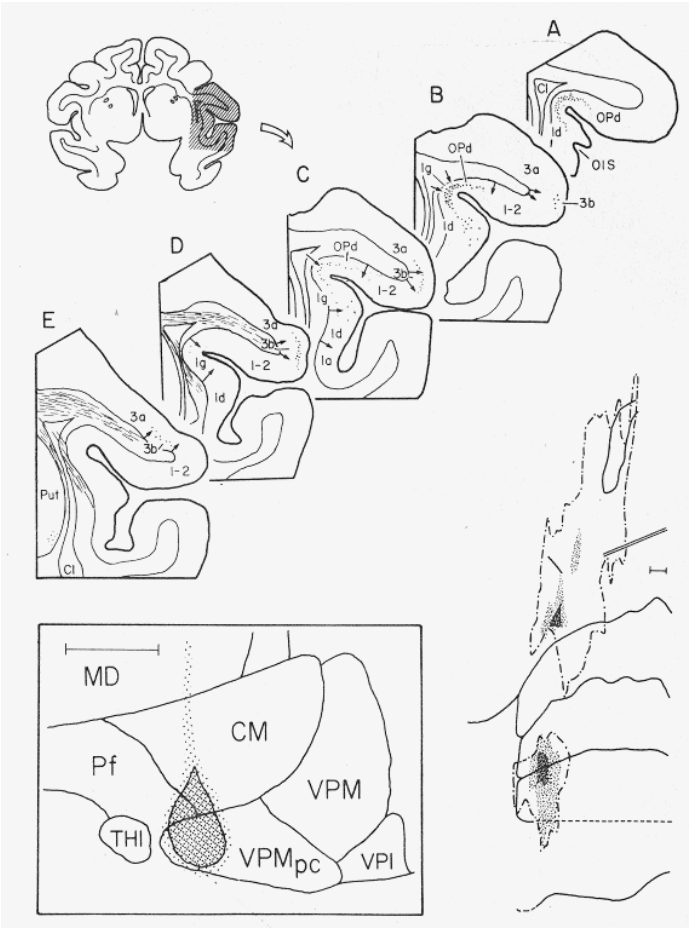


Fig 1.3 After Pritchard et al (1986). Details of the projections from the VPMpc into cortical areas, including the caudolateral orbitofrontal cortex, the insular/opercular complex and the precentral gyrus, including area 3b which is part of the somatosensory cortex. Top: Slices A-E progress anteroposteriorly and depict the terminal sites of the anterograde autoradiographic injection as the dots pointed by the arrows. Bottom left: injection site in the VPMpc; right: corresponding orthographic projection. Cl, claustrum; CM, central medial nucleus of the thalamus; MD, medial dorsal nucleus of the thalamus; Ia, agranular insula; Id, dysgranular insula; Ig, granular insula; OIS, orbitoinsular sulcus; Opd, dysgranular operculum; Pf, parafascicular nucleus; Put, putamen; VPI, ventroposteroinferior nucleus of the thalamus; THI, habenular interpenducular tract.

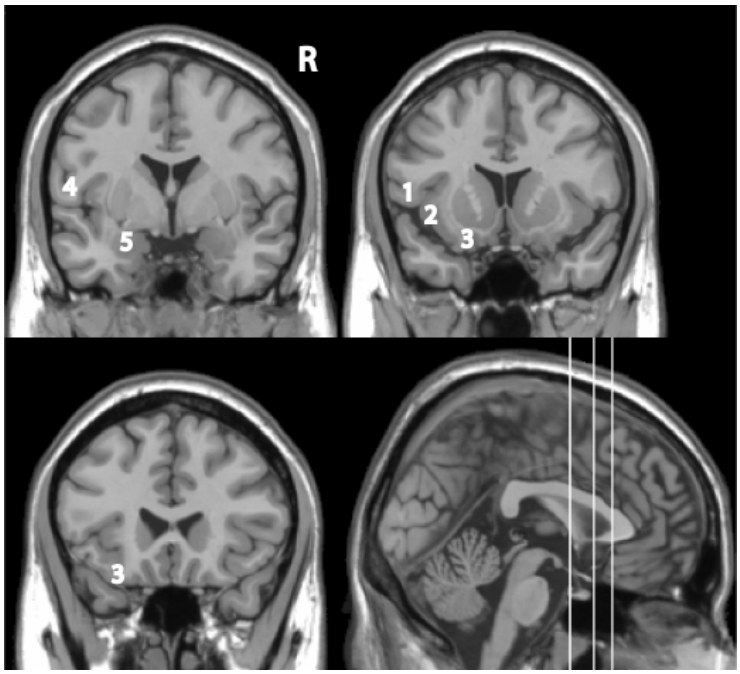


Figure 1.4: Coronal MRI slices through the human insular/frontal opercular cortices. On the top right is shown a part of the frontal operculum (1), the anterior insula (2, both part of the primary taste cortex in primates) and the caudal orbitofrontal cortex (3), a part of the secondary taste cortex in primates. The most posterior slice, on the top left, depicts a part of the Rolandic operculum (4), a part of the operculum posterior to the frontal operculum putatively involved in intra-oral somatosensory representation in humans (see Introduction); the amygdala (5) can also be seen in this slice. The secondary cortical taste area (the orbotofrontal cortex) conveys taste information to the amygdala. In the bottom left, a more anterior region of the caudal orbitofrontal cortex is shown, probably depicting a dysgranular transition area with the insular cortex. On the bottom right these slices are indicated in a saggital image for orientation.

Electrophysiology

Unlikely the rat, where NST taste-responding cells seem to interact with physiological need and satiety signals (e.g. gastric distention, Glenn and Erickson 1976), some NST taste cells in primates are unaffected by satiety, as shown for example by reversing the incentive value of glucose in a sensory-specific satiety type of experiment (Yaxley et al. 1985). The rationale for this finding in primates is that in this species the NTS is sufficiently more complex in order to contain taste-only (as in not modulated by the physiological state) responsive cells (Scott et al. 1986b).

In both frontal opercular and dysgranular insula the responses of gustatory neurons are significantly more specific to individual stimuli than in NST and VPMpc (Sewards and Sewards 2001). However, despite its name, a small proportion of cells in the primary taste cortex do actually respond exclusively and consistently to taste stimuli (Scott and Plata-Salaman 1999;

~6.5%, Scott et al. 1986a), while a higher proportion (~23%) responded during tongue or jaw movements, for example. In these recording studies taste neurons in the anterior insula/frontal operculum area were sparsely distributed, and generate actions potentials in the order of 200-500 μV. Also, neurons in this area seem not to be affected by satiety and other motivational signals (Yaxley et al. 1988). These results suggest that information on tastant identity and its hedonic value are segregated in the primate brain, including possibly humans.

In fact, in the secondary taste cortex (orbitofrontal cortex), neurons responding to taste stimuli (e.g. glucose) are modulated by hunger as demonstrated in sensory-specific satiety experiments (Rolls 2000a; Rolls et al. 1989). Interaction between taste and motivational information was also found in central nucleus of the amygdala cells (Yan and Scott 1996) and in lateral hypothalamus (Rolls et al. 1986). Humans are likely, as monkeys, to process gustatory information independently from hedonics in the primary gustatory cortex.

Human studies

Ageusia (lack of gustatory sense) was found in patients having suffered bullet wounds in the opercular cortex (Bernstein 1940) turning it into a likely brain region for taste processing in humans. Penfield and Faulk (1955) described a patient presenting an aura of unpleasant taste which seemed to be caused by a tumour in the insular cortex. More interestingly, electrical stimulation of the insula in patients undergoing epilepsy surgery resulted in reported taste perception. In addition, gustatory sensations were reported in patients with insular lesions (Cascino and Karnes 1990). Also, detection and recognition deficits in patients undergoing temporal lobe resection (for epilepsy treatment) have been reported (Small et al. 1997b). More recent human lesion studies have further confirmed the role of the insular cortex in taste processing (Cereda et al. 2002; Pritchard et al. 1999). In particular these studies provide evidence that taste quality and intensity recognition is impaired by lesions in either side of the human brain, suggesting thus that taste processing is bilateral in humans, in analogy to the non-human primate case.

A recent review of neuroimaging studies in humans has been reported (Small et al. 1999), including PET (normally with the $[O_{15}]H_2O$ bolus or the $[O_{15}]CO_2$ inhalation method) and fMRI studies. These studies revealed a wide distribution of activity peaks in the insular and opercular cortices, including frontal and parietal operculae. However, no precise location for the peaks within these areas could be found. Also, orbitofrontal cortex activity, specifically the caudal orbitofrontal cortex, was observed in some studies. In general, a lateralised pattern of activity in the right hemisphere was observed, which probably derives thus from threshold setting in the

analyses, given the current evidence on taste processing as provided by the lesion studies (Cereda et al. 2002; Pritchard et al. 1999).

Some studies were dedicated to the hedonic aspects of taste processing. One study for example investigated the possible separation of salt and glucose representations in the human brain and concluded that this separation exists (up to some degree of certainty as given by the spatial smoothing of the data) in a more anterior region of the orbitofrontal cortex (O'Doherty et al. 2001b). It has also been found activations in the amygdala for both stimuli. Another study has used PET to investigate the representation of aversive gustatory stimulation with saline, using also chocolate as a contrasting stimulus (Zald et al. 1998). Aversive saline activated the right amygdala, the left caudolateral orbitofrontal cortex and the dorsal part of anterior cingulate cortex. Chocolate (thought here to represent a pleasant taste, although being a complex mixture) activated the posterior cingulate robustly, in addition to the cingulate area being activated by saline. An intrinsic problem with this study, however, is the fact that water was used as a control stimulus. Besides being a rewarding stimulus under certain physiological conditions (e.g. after delivery of saline), water does not contain most of the ionic components of saliva, which turns it into an inappropriate stimulus to be used in a neuroimaging taste study. Also, some of the amygdala activation could be due to retronasal olfactory stimulation by the chocolate compound.

More interestingly, the areas of the primate brain more generally involved in reward processing seem to be necessary, in addition to primary taste areas, to implement reward learning and expectation of reward when the unconditioned stimulus is a taste reward. These areas are likely to involve the midbrain dopaminergic system. This has been shown to be the case in monkeys (Schultz et al. 1997; Schultz et al. 2000) and in humans (O'Doherty et al. 2002).

In general, neuroimaging studies might have met other caveats. For example, swallowing needs to be cued to avoid motor-related confounds. Also, fMRI studies normally require special techniques to minimise signal dropout in the orbitofrontal cortex (Wilson et al. 2002). Finally, the lateralised responses in the right hemisphere remain to be explained, as the explanation based on the fact that some left opercular areas have speech and other language-related functions (Small et al. 1999) is not convincing, given the relatively limited extent of speech areas as compared with those found to be activated in taste imaging studies. In fact, it will be shown below that fMRI studies on taste can reveal significant activations in the left hemisphere.

Umami taste

Recently, the taste referred to by the Japanese word *umami* has come to be recognised as a "fifth taste" (Baylis and Rolls 1991; Kawamura and Kare 1987) (after sweet, salt, bitter and sour; umami captures what is sometimes described as the taste of protein). In fact, multidimensional scaling methods in humans (Yamaguchi and Kimizuka 1979; Yoshida and Saito 1969) have shown that the taste of glutamate (as its sodium salt monosodium glutamate, MSG) cannot be reduced to any of the other four basic tastes. Umami taste is found in a diversity of foods like fish, meats, milk, tomatoes and some vegetables, and is produced by the glutamate ion and also by some ribonucleotides (including inosine and guanosine nucleotides), which are present in these foods.

Specific receptors for glutamate in lingual tissue with taste buds have been recently found (Chaudhari et al. 2000). A G protein-coupled receptor that couples negatively to a cAMP cascade shows an unusual concentration-response relationship. The similarity of its properties to monosodium glutamate taste led Chaudhari and colleagues to suggest that this receptor is a taste receptor for glutamate.

Besides their effects as unique tastants, umami substances also present synergism, *i.e.,* when two umami substances are mixed, the mixture effect is stronger than the sum of the effects given by the two substances. The synergism characteristic of umami occurs when MSG is combined with the ribonucleotide inosine 5'-monophosphate, IMP (or with its guanosine equivalent). The result of combining these two taste stimuli is a synergistic (i.e. supra-additive) effect in the subjective experience of taste intensity (Rifkin and Bartoshuk 1980; Yamaguchi 1967). Glutamate is high in concentration in foods such as tomatoes, green vegetables, fish and is relatively high in human breast milk; and nucleotides are present in for example meat and in some fish such as tuna (Yamaguchi and Ninomiya 2000). The mixture of these components underlies the rich taste characteristic of many cuisines.

Some fibres in the taste nerves of rodents have been shown to have selective responses to umami tastants such as monosodium glutamate (Ninomiya and Funakoshi 1987), and in macaques it has been shown that single neurons in both the primary taste cortex in the insular / frontal opercular region, and in the secondary taste cortex in the orbitofrontal cortex, are selectively activated by monosodium glutamate (Baylis and Rolls 1991; Rolls 2000b) or by glutamic acid or by IMP (Rolls et al. 1996a). Nothing is known however about the cortical responses in humans to umami substances, or how their synergistic interactions are represented in the human brain. We designed

an event-related functional Magnetic Resonance Imaging (fMRI) experiment to investigate these questions.

The representation of umami taste in the human brain: an event-related fMRI study

Materials and Methods

Subjects

Ten healthy right-handed subjects (of which 6 were males) participated in the study. Written informed consent from all subjects and ethical approval were obtained before the experiment.

Stimuli and experimental design

Solutions consisted of either 0.05 M MSG (the monosodium salt of L-glutamic acid), or 0.005 M (IMP, inosine 5'-monophosphate which in this experiment was used in a form without sodium ions), or of a combination of the two (MSGIMP made to contain a concentration of 0.05 M MSG and 0.005 M IMP), or glucose (1.0M). These concentrations of MSG and IMP were chosen based on psychophysical investigations we performed on human subjects that indicated that enhancement was exhibited at these concentrations (see Results). Furthermore, these concentrations are close to a midpoint of the sensitivity curves of single neurons to these stimuli in macaques (Baylis and Rolls 1991; Rolls et al. 1996a). The glucose was used in order to reveal the brain areas activated by an exemplar of a prototypical type of taste, sweet, so that we could determine whether the umami stimuli activated similar areas. Glucose was used as the exemplar (rather than sucrose) because it has been used as the taste stimulus in many previous neurophysiological and some neuroimaging studies (O'Doherty et al. 2001b; Rolls et al. 1989; Rolls et al. 1990; Yaxley et al. 1990), in which the effects of feeding to satiety were often of interest to investigate the brain mechanisms underlying appetite. Glucose was used in those studies because it is rapidly absorbed and can act as a satiety signal without further metabolism (Rolls et al. 1986).

The experimental protocol consisted of an event-related interleaved design using these four taste stimuli as well as a tasteless control solution, which was delivered to the subject's mouth through

five polythene tubes that were held between the lips. Each tube of approximately 1 meter in length was connected to a separate reservoir via a syringe and a one-way syringe valve (supplied by Fisher Scientific Ltd., UK).

At the beginning of each taste delivery, one of the four stimuli chosen by random permutation, was delivered in 0.75 ml aliquots to the subject's mouth. Swallowing was cued by a visual stimulus after 10 seconds (following initial instruction and training). After a random delay of 2 – 10 seconds, a tasteless control solution (using the main ionic components of saliva: 25 mM KCl + 2.5 mM $NaHCO_3$) (O'Doherty et al. 2001b) was administered in exactly the same way and the subject was cued to swallow again after 10 seconds. There was then a 2 – 10 second random delay period until the next taste was delivered. The tasteless solution was used as the comparison condition for the taste solution, and allowed non-taste effects such as somatosensory effects produced by liquid in the mouth, and the single tongue movement made to distribute the liquid throughout the mouth, to be controlled for. This taste trial was repeated for each of the four tastes, and the whole cycle was repeated 12 times. It was a feature of the experimental design that a tasteless solution was used to control for non-taste (including somatosensory) effects of placing solutions in the mouth, and that all activations analyzed took this into account by subtraction. The tasteless solution also provided a rinse for the preceding tastant.

During the experiment subjects were asked to rate each of the taste stimuli for intensity using a visual analog scale anchored at -2 for very weak, and +2 for very intense.

fMRI data acquisition

Images were acquired with a 3.0-T VARIAN/SIEMENS whole-body scanner at the Centre for Functional Magnetic Resonance Imaging at Oxford (FMRIB), where 14 T2* weighted EPI slices were acquired every 2 seconds (TR=2). We used the techniques that we have developed over a number of years to carefully select the imaging parameters in order to minimise susceptibility and distortion artefact in the orbitofrontal cortex as described in detail by Wilson et al. (Wilson et al. 2002). The relevant factors include imaging in the coronal plane, minimising voxel size in the plane of the imaging, as high a gradient switching frequency as possible (960 Hz), a short echo time of 25 ms, and local shimming for the inferior frontal area.

The matrix size was 64 x 64 and the field of view was 192 x 192 mm. Continuous coverage was obtained from +60 (A/P) to –38 (A/P). Acquisition was carried out during the task performance which lasted a total of 25 minutes and 28 seconds, yielding 764 volumes in total. A whole brain T2* weighted EPI volume of the above dimensions and an anatomical T1 volume with slice thickness 6 mm and in-plane resolution of 0.75 x 0.75 mm was also acquired. The acquisition

protocol used in this study is similar to that used in previous studies from our laboratory in which we used fMRI to image the orbitofrontal cortex.

fMRI data analysis

The imaging data were analysed using SPM99 (Wellcome Department of Cognitive Neurology, London). Pre-processing of the data used SPM99 realignment, reslicing with sinc interpolation, normalisation and spatial smoothing with a 10 mm full width at half maximum isotropic Gaussian kernel and global scaling. The time series at each voxel were high-pass and low-pass filtered with a haemodynamic response kernel. A general linear model was then applied to the time course of activation of each voxel and linear contrasts were defined to test the specific effects of each condition. Voxel values for each contrast resulted in a statistical parametric map of the *t* statistic, which was then transformed into the unit normal distribution (SPM z). Group effects were assessed by conjunction analyses of subject-specific contrasts. Reported p-values based on this group analysis for *a priori* regions of interest (i.e. the insula and the orbitofrontal cortex) were corrected for the number of comparisons made within each region (Worsley et al. 1996). Checks were performed using the estimated motion as a covariate of no interest to rule out the possibility of the observed results being due to motion-related artefact. Conjunction analysis (Friston et al. 1999a) was then performed to reveal significant common activations for each effect of interest.

Results

Behavioral data

The taste intensity ratings (using a visual analog scale anchored at -2 for very weak, and +2 for very intense) taken in the experiment were -0.75±0.38 for IMP (mean±s.e.m.), 0.46±0.36 for MSG, 0.92±0.35 for MSG+IMP (MSGIMP), and 1.5±0.50 for glucose. Statistically it was shown that the intensity of the taste of umami produced by the mixture of MSG and IMP was greater than that produced by the MSG alone (even if the rating scales are taken as implying that the threshold is at –2 on the rating scale used, paired $t=1.95$, $df=9$, $p<0.04$ one-tailed). We refer to this as taste enhancement within the domain of umami taste. Although the effect is not supralinear (or "synergistic") (if the rating scales are taken as implying that the threshold is at –2 on the rating scale used) on average across subjects with the relatively small number of subjects used, supralinearity has been found when larger psychophysical studies are performed (Rifkin and Bartoshuk 1980).

fMRI data

Responses to umami taste

The effects of umami taste as produced by the prototypical stimulus 0.05 M monosodium glutamate (MSG) on cortical activation in the group analysis are shown in Fig. 1.5 row 3, the activations produced by IMP (0.005 M) are shown in Fig. 1.5 row 2, and the activations produced by the sweet tastant 1 M glucose are shown in Fig. 1.5 row 1. For all stimuli, activation of the insular-opercular taste cortex, which is the putative human primary taste cortex, and the orbitofrontal cortex, were found. The activation produced by IMP shows that umami, even when the solution administered contains no sodium ions, activates these areas of the cerebral cortex.

Activation was also found by all these taste stimuli in the group analysis in a part of the rostral anterior cingulate cortex, as shown in Fig. 1.5 right column, ACC and discussed in the Discussion.

To analyze whether there are areas of overlap of the activations produced by the umami stimuli and the glucose used as a prototypical taste stimulus, we show in Fig. 1.5 row 5 the conjunction across stimulus conditions and subjects (Friston et al. 1999a) of the effects produced by MSG, IMP, MSGIMP and glucose. Activations (significant at the $p<0.05$ level, corrected for multiple comparisons) were found at the rostral border of the insula, which by comparison with the macaque is likely to be the primary taste cortex, and in a part of the orbitofrontal cortex, which is likely to be a secondary taste cortical area (Baylis et al. 1995; Rolls et al. 1990). The analysis thus shows that rather similar cortical areas were activated by the glucose and umami taste stimuli, providing evidence that umami is specifically activating regions that are demonstrably activated by classical taste stimuli.

Fig.1

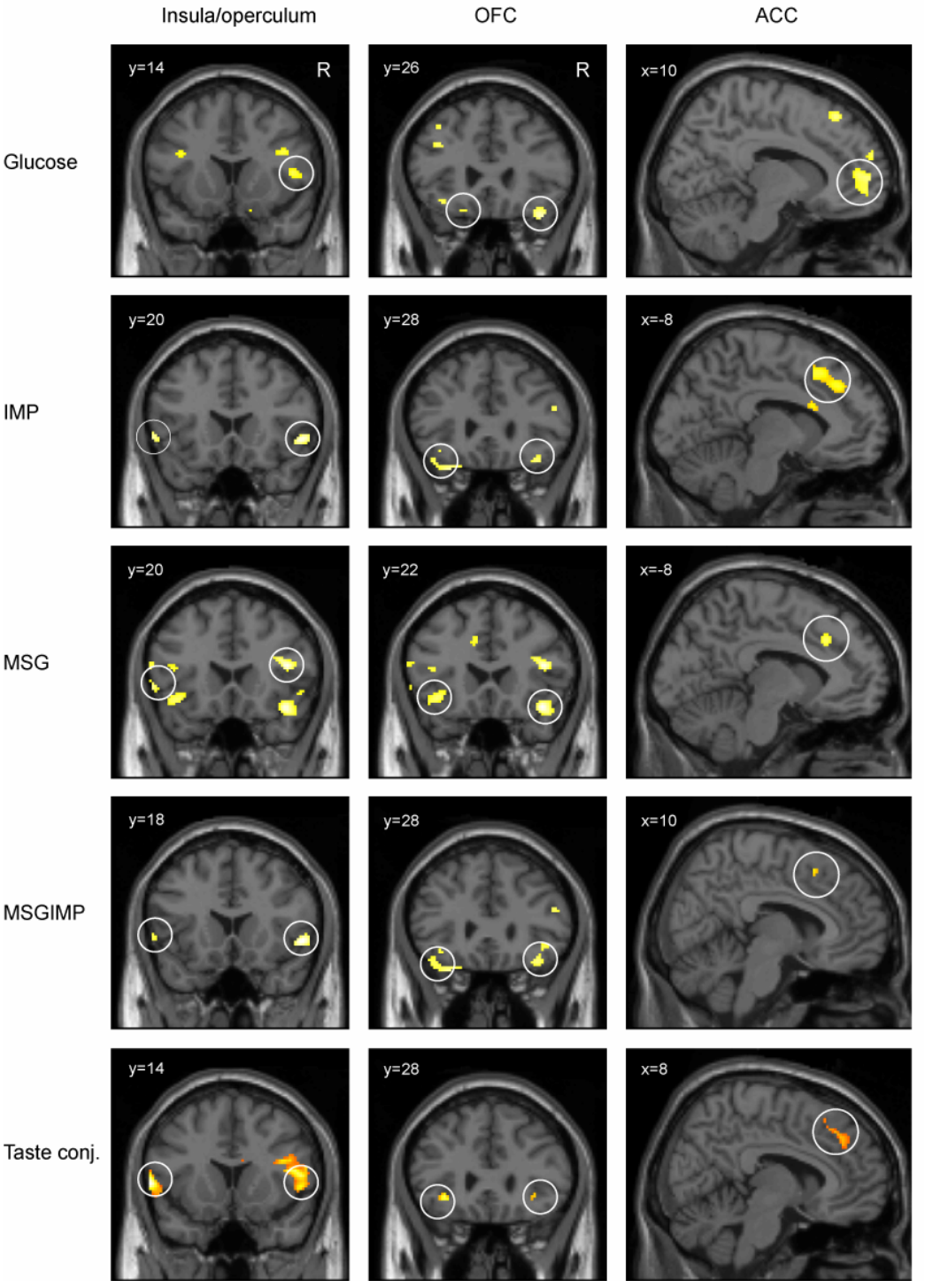

Insula/operculum
OFC
ACC
Glucose
IMP
MSG
MSGIMP
Taste conj.
y=14
R
y=26
R
x=10
y=20
y=28
x=-8
y=20
y=22
x=-8
y=18
y=28
x=10
y=14
y=28
x=8

Figure 1.5. Activations produced in the rostral insula/operculum, the orbitofrontal cortex (OFC), and the anterior cingulate cortex (ACC) by the tastants 1 M Glucose, 0.005 M inosine 5'-monophosphate (IMP), 0.05 M monosodium glutamate (MSG), and by a combination of the MSG and IMP (MSGIMP), and by the conjunction of all tastants. In the group analysis used, the peak of each of these activations is significant at p<0.05 corrected (S.V.C.), but to show the full extent (circled) of the activated regions of these brain structures, the Figure shows the activations thresholded at p<0.001 uncorrected. The group size included all subjects in all cases except for the IMP condition for the OFC brain area, where one subject was not included because no activation was found in the OFC in this condition, and interestingly the subject reported a low perceived intensity of the IMP. The y and x values are with respect to the MNI coordinate system (Collins et al. 1994).

To reveal the main effects produced by the three umami stimuli (umami taste), we show in Fig. 1.6 the conjunction across stimulus conditions and subjects (Friston et al. 1999a) of the effects produced by MSG, IMP and MSGIMP. Significant activations (at the p<0.05 corrected for multiple comparisons) were found in the primary taste cortex (insula/operculum), putative secondary taste cortex (caudolateral orbitofrontal cortex) and in a region of the rostral anterior cingulate cortex. Activations are summarised in Table 1.1.

Fig.2

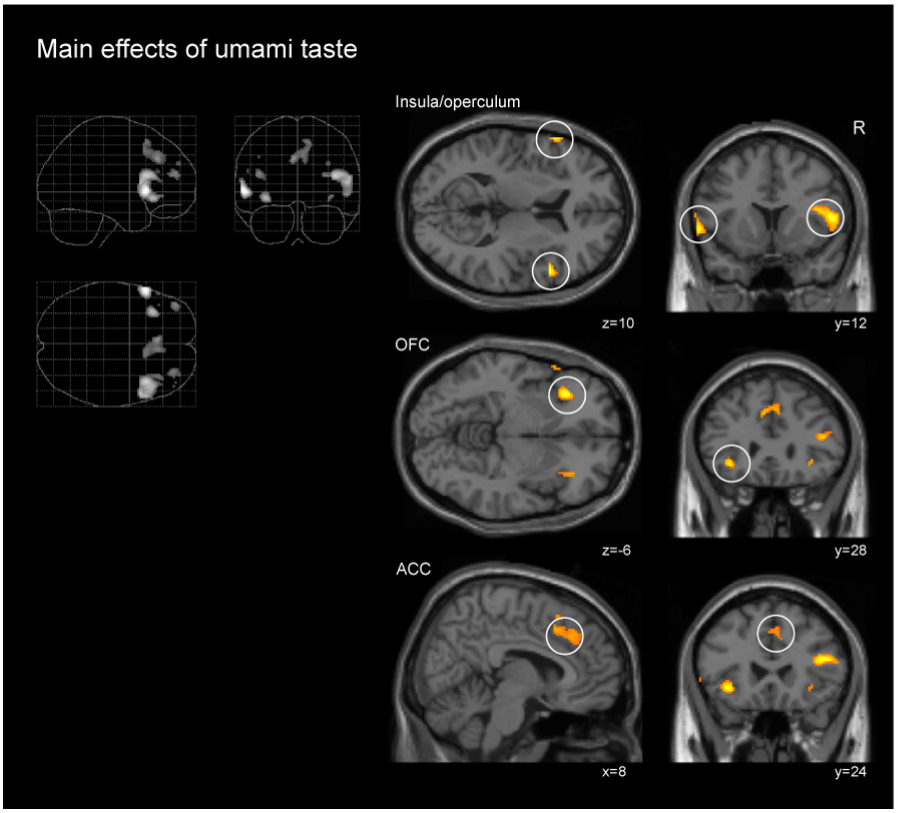


Figure 1.6. Cortical activations produced by umami tastants. Group conjunction statistical analysis was applied to reveal common areas activated by the umami tastants (IMP, MSG, MSGIMP). Left: the results from the SPM99 analysis are shown in a glass brain. Right above: axial and coronal section through the primary taste cortex (x,y,z=54,12,10; z=5.21; -58,18,2; z=6.15, with z=4.5 corresponding to a group corrected p value of <0.05) are shown with the activations thresholded at p<0.0001 for extent. Right middle: axial and coronal section through the caudal orbitofrontal cortex (-34, 26, -6; z=4.84). Right bottom: saggital and coronal section through the anterior cingulate cortex (-4, 30, 36; z=4.35, S.V.C.).

Side/Location	MNI	Z	p
L Frontal Operculum	[-58 18 2]	6.15	p<.01c
R Frontal Operculum	[42 18 15]	5.21	p<.05c
L Caudal OFC	[-34 26 –6]	4.84	p<.05c
R Ant. Ins.	[34 24 –5]	3.75	p<.001u
L Superior Cing	[-4 30 36]	4.35	p<.0001u

Table 1.1 – Main effects of umami taste. c, corrected for multiple comparisons ; u, uncorrected for multiple comparisons.

The only significant difference in activation between glucose and umami stimuli (as revealed by masking the statistical maps at $p<0.05$) was found in a ventral part of the rostral anterior cingulate cortex, which was activated reliably by glucose but not by any of the umami stimuli. This activation is shown in Fig. 1.5, third column of the first row. Given the role of this region of the ACC in motivation and emotion-related behaviour (Bush et al. 2000), it is notable that the glucose stimulus was clearly rated as being the most pleasant tastant to all subjects (mean pleasantness ratings (± s.e.m.): glucose = 1.54 ± 0.17, MSGIMP = 0.5 ± 0.31, MSG = 0.22 ± 0.32, IMP = -0.4 ± 0.32 with +2 = very pleasant, -2=very unpleasant). Comparisons performed subsequent to an ANOVA showed that the glucose was significantly more pleasant than any of the umami stimuli ($p<0.0001$ in each case using a post hoc pairwise t-test comparison).

The combination of MSG and IMP

Given the evidence that inosine 5'-monophosphate, IMP (or its guanosine equivalent) and MSG can show synergism psychophysically (Rifkin and Bartoshuk 1980), we performed an SPM contrast to investigate whether any brain areas are significantly more strongly activated by the MSGIMP combination than by the sum of the effects of MSG alone and IMP alone. Figure 1.7 shows the results of a stringent group analysis (based on the conjunction of activations in individual subjects (Friston et al. 1999a)) thresholded for the group conjunction test at $p<0.001$, which reveals a significant cluster with 30 voxels in the left lateral orbitofrontal cortex (x,y,z=-44,34,-18; z=3.49). Furthermore it was found that this activation is significant using corrected statistics ($p<0.05$ with a small volume correction). Thus supra-linear additivity in the BOLD

signal was found in this anterior part of the orbitofrontal cortex (Fig. 1.7). The supra-linear additivity in the BOLD signal is further demonstrated by the timecourses for each of the umami taste stimuli in this significant cluster of voxels in the orbitofrontal cortex, as shown in Fig. 1.8a. (The timecourses across all ten subjects are shown in Fig 1.8a with respect to the tasteless solution.) This shows in these voxels a greater activation by MSGIMP than by either alone. For comparison, Fig. 1.8b shows the timecourses for the largest peak in the main effects comparison for umami taste for the insular /operculum taste region shown in Fig. 1.6, and it is evident that the MSGIMP response was not especially prominent in the insular/opercular taste cortex.

Fig.3

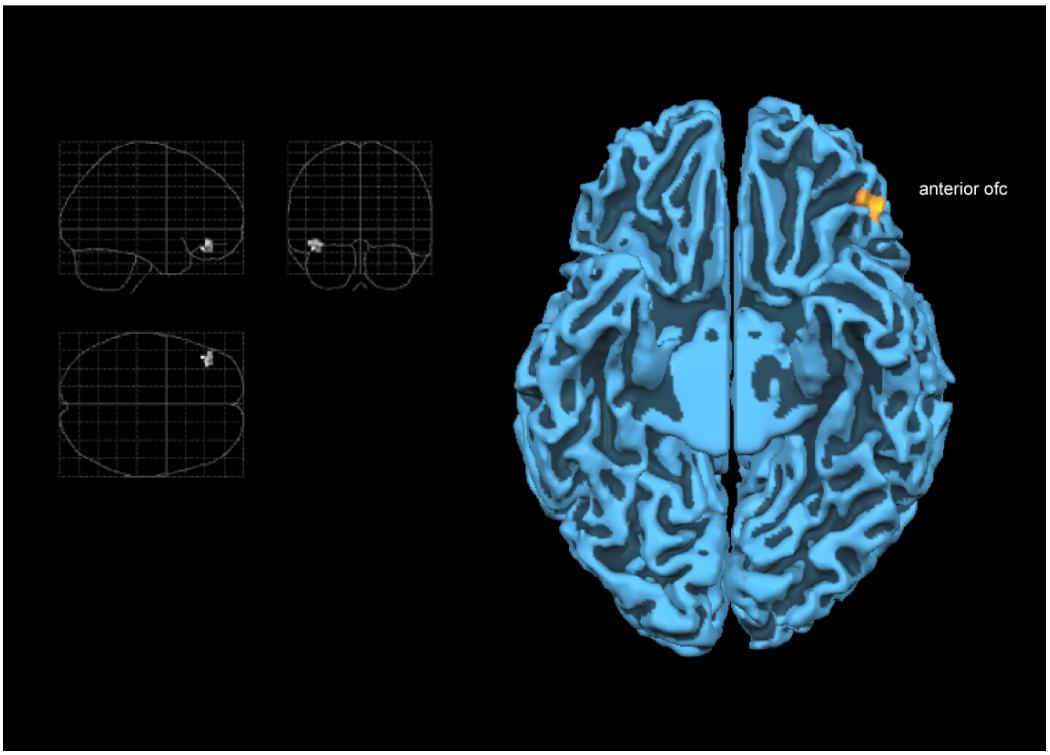


Figure 1.7. Effects produced by a combination of umami tastants. Results of an SPM analysis to show brain regions where significantly larger activations were found to the combination taste stimulus MSG and IMP (MSGIMP) than to the sum of the activations produced by MSG and IMP delivered separately. The statistical analysis revealed a region of the orbitofrontal cortex (-44,34,-18; $z=3.49$, $p<0.05$ corrected for multiple comparisons with S.V.C). Left: the unmasked results in a glass brain. Right: the activation in the anterior orbitofrontal cortex (OFC) is shown rendered on the ventral surface of human cortical areas with the cerebellum removed.

Fig.4

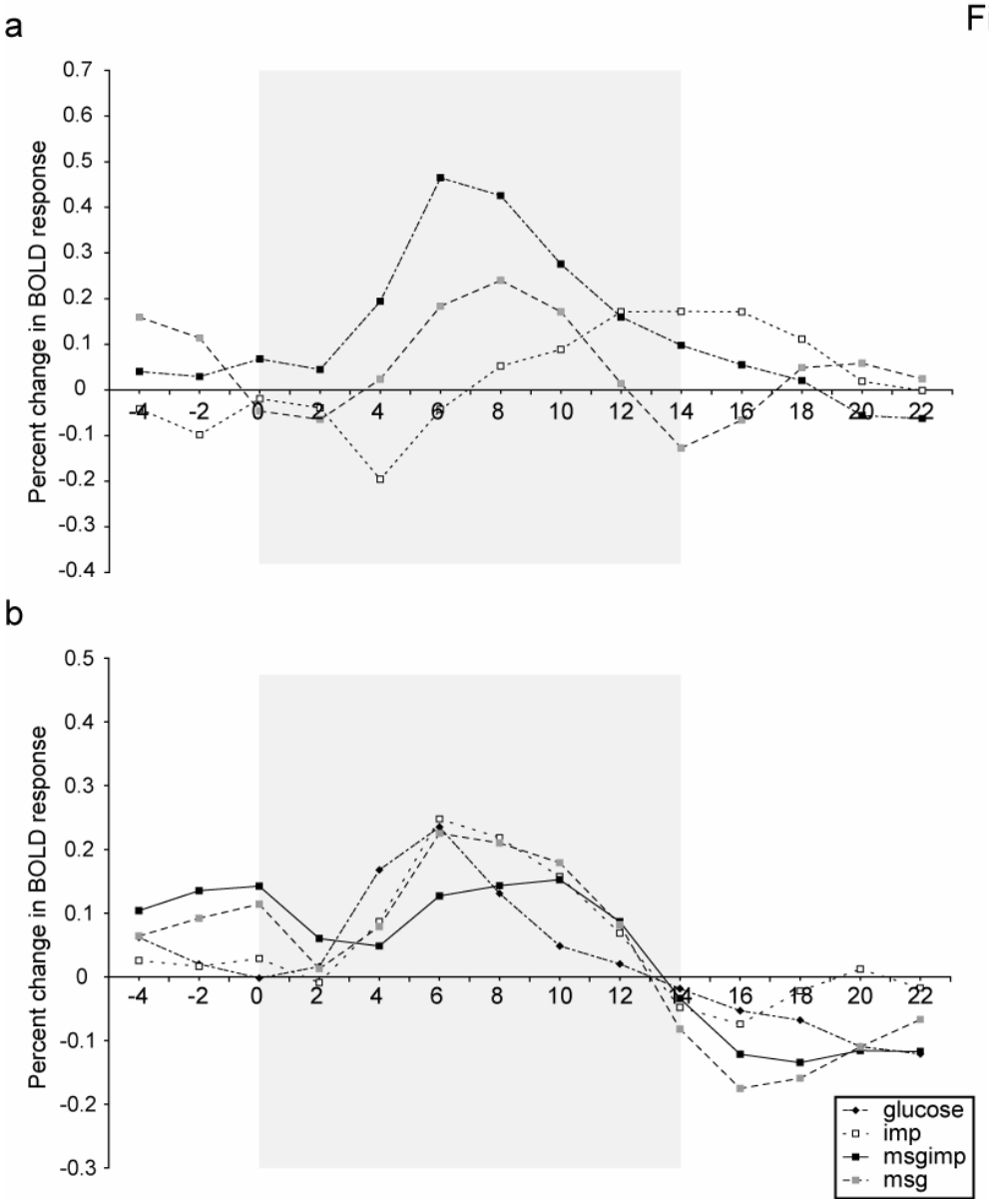


Figure 1.8. Timecourses of cortical activation to taste. (a) Time course (averaged across all 10 subjects) within the significant cluster of 30 activated voxels in the orbitofrontal cortex in the group analysis from the supra-additivity contrast showing the percent change in BOLD signal for MSGIMP, MSG and IMP compared to the tasteless control. The peak voxel of the cluster was at (-44,34,-18; with z=3.49). (b) Time course (averaged across all 10 subjects) within the significant cluster of voxels in the insular/opercular taste cortex (from the main effects of taste contrast shown in Fig. 1.6, group effect across all 10 subjects, p<0.05, corrected for multiple comparisons) averaged over a group of 53 voxels in the primary gustatory cortex (x,y,z=52,12,10; z=5.48). The percent changes in the BOLD signal for glucose, MSG, IMP and MSGIMP compared to the tasteless control are shown.

Discussion

The results of this study show first that the taste of umami activates generally similar brain regions to another and prototypical tastant, glucose, including the putative human primary taste cortex in the anterior insular/opercular region, and the putative secondary taste cortex in the orbitofrontal cortex. The taste effects of umami were shown to be independent of the necessity of administered sodium ion by our use as a stimulus of inosine 5'-monophosphate (Sigma I-2879, which contains no sodium ion). The fact that cortical taste areas shown to be activated by glucose were also activated by the umami stimuli provides additional evidence that umami works in generally the same way as other tastants, and is consistent with umami being considered as a "fifth taste".

The new findings described here in humans are supported by single-neuron recordings in non-human primates (macaques) which have shown that umami tastants activate single neurons in the primary and secondary taste cortices, and that these neurons can be shown to be tuned to umami tastants in a way that does not reflect their responsiveness to the sodium ion (Baylis and Rolls 1991; Rolls 2000a; Rolls et al. 1996a). The populations of neurons with responses to umami tastants such as MSG and IMP were shown to be separate from the populations activated by the four other prototypical tastants, sweet (glucose), salt (NaCl), bitter (quinine) and sour (HCl) (Rolls et al. 1996a).

Second, this study uncovered a part of the human orbitofrontal cortex that showed strong supralinear additivity in the BOLD signal produced by the combination of MSG and IMP (the MSGIMP condition) when compared to the sum of the MSG and IMP BOLD signals. This region was just anterior (with a peak at y=34) to the part of the orbitofrontal cortex showing effects in the main comparison between taste and tasteless solution (with a peak at y=26).

In the light of the much discussed issue of hemispheric specialisation (Davidson 1992; Small et al. 1999), it is potentially of interest to note that in the group analysis the region of the orbitofrontal cortex showing supra-linear additivity in the BOLD signal is on the left side of the human brain. This is consistent with the suggestion corroborated by clinical findings (Cereda et al. 2002; Pritchard et al. 1999) that gustatory processing involves the left side of the human brain (Craig 2002). However, it should be noted that in some of the individual subjects, the supra-linear additivity effects were also seen in the right orbitofrontal cortex. Further, we note that as shown in Figs. 1.5 and 1.6, there is very clear evidence of the representation of taste bilaterally in the human brain.

The relative activations by the different umami tastants (MSG, IMP, and the mixture) were similar in the insula/operculum and main area of the taste orbitofrontal cortex (peak at y=26), but were much larger to the MSGIMP combination in the more anterior area (peak at y=34), as shown by the timecourse data shown in Fig. 1.8. This supra-linear change in BOLD signal for the mixture MSGIMP compared with the MSG and IMP may reflect underlying supra-addivity effects in the neuronal firing rates. Although there is some evidence that the BOLD signal reflects the underlying neuronal firing rates (Smith et al. 2002), there is also evidence that the BOLD signal reflects in addition the inputs to and processing within a brain area (Logothetis 2002; Logothetis et al. 2001).

The actual interaction between MSG and IMP may be expressed in part in the taste receptors themselves, or there may be somewhat different receptors for the different umami tastants (Chaudhari 2001; Chaudhari et al. 2000; Lin and Kinnamon 1998), but in any case the results of the present study show that there is a part of the human orbitofrontal cortex in which supra-linear additivity shows up very strongly in the statistical analysis. The fact that this part of the human orbitofrontal cortex statistically reflects supra-additive effects between umami tastants evident in the BOLD signal, makes it likely that activity in this part of the orbitofrontal cortex is especially relevant to the perceived sensation of umami taste, and to the behavioral preferences for umami taste. The especial role of this part of the human cerebral cortex in the taste of umami could arise because it is able to provide a non-linear amplification of the MSG and IMP inputs already combined in the taste receptors, or it could be that this part of the cortex is able to combine information from partly separate umami channels to produce the large response to the combination of MSG and IMP. This will be an interesting issue for future investigations.

The evidence described here that the orbitofrontal cortex represents umami taste (literally 'delicious' in Japanese) is consistent with other evidence that the orbitofrontal cortex also represents information about the reward value of other primary and secondary reinforcers including taste (O'Doherty et al. 2001b; Small et al. 1999), odour (Zald and Pardo 1997; Zatorre et al. 1992) and even abstract monetary rewards (O'Doherty et al. 2001a).

The activation of the cingulate cortex found in this study by the taste stimuli is of interest. For example, we have found that pleasant olfactory stimuli activate a far anterior part of the anterior cingulate cortex, with aversive olfactory stimuli a slightly more posterior region (de Araujo et al. 2002). The far rostral anterior cingulate area activated by glucose shown in Fig. 1.5 is close to the area in which pleasant olfactory stimuli are represented. The cingulate area activated by umami taste is in the anterior cingulate cortex, a little behind the region activated by glucose (see Fig. 1.5). Further, the anterior cingulate cortex has been shown to be activated by motivationally

relevant affective stimuli including pleasant touch (Rolls et al. 2003b), and there is evidence from animal studies that it is involved in a range of motivationally oriented unconditioned behaviours and emotional learning (Cardinal et al. 2002; Devinsky et al. 1995). In addition the anterior, ventral cingulate cortex (Brodmann's areas 24a/b and 25) in humans seems to be involved in the pathology of depression in humans, as well as in the control of normal mood (Drevets 1999) and in responding to emotionally significant stimuli, such as cocaine-associated cues in drug abusers (Childress et al. 1999).

Other affective stimuli have been shown to activate nearby parts of the anterior cingulate (Bush et al. 2000). However, it is not clear from these imaging studies whether the cingulate activation reflects a sensory representation of the stimuli, or some more general affective or even arousal reaction to the stimuli, or some behavioral response or response selection or response inhibition. We now have reason to believe that the activation shown in the present study of the human cingulate cortex by taste stimuli reflects sensory inputs produced by the tastants, for in studies now in progress in macaques E.T.Rolls and P.Gabbott are now finding taste neurons with classical taste cell properties in a corresponding region of the macaque rostral anterior cingulate cortex, and interestingly these cingulate taste cells are hunger dependent, and in particular reflect sensory-specific satiety in the same way as orbitofrontal cortex taste neurons (Rolls et al. 1989).

Chapter II

Different representations of pleasant and unpleasant odours in the human brain

The olfactory system conveys a wide variety of information about the environment that is necessary for the location of biologically relevant stimuli such as food, mates, aversive events and danger. That's the likely reason why most odours are assigned hedonic and motivational value and why the main anatomical and physiological features of the olfactory system are roughly conserved across species. Yet, relatively little is known about the representations of the affective qualities of odours in the human brain. This Chapter describes an event-related fMRI study where was it found that three pleasant and three unpleasant odours activated dissociable parts of the human brain. In particular, pleasant but not unpleasant odours were found to activate a medial region of the rostral orbitofrontal cortex. Further, there was a correlation between the subjective pleasantness ratings of the six odours given during the investigation with activation of a medial region of the rostral orbitofrontal cortex. In contrast, a correlation between the subjective unpleasantness ratings of the six odours was found in regions of the left and more lateral orbitofrontal cortex. In addition, the subjective intensity ratings correlated with activity in the primary olfactory cortex, but not with activity in the orbitofrontal cortex. Thus dissociation was found in the human brain between the representations of the hedonic and intensity properties of odours. Activation was also found in the anterior cingulate cortex, with a middle part of the anterior cingulate activated by both pleasant and unpleasant odours, and a more anterior part of the anterior cingulate cortex showing a correlation with the subjective pleasantness ratings of the odours. Thus the results suggest that there is a hedonic map of the sense of smell in brain regions such as the orbitofrontal cortex, and these results have implications for understanding the psychiatric and related problems that follow damage to these brain areas.

The first section provides a brief description of the olfactory receptor physiology followed by a description of some of the main aspects of the primate olfactory system including its specific cortical structures. Then we proceed to describe in detail the fMRI study mentioned above.

The organisation of the primate olfactory system

Olfactory receptor neurons

The olfactory epithelium lies on the anterior surface of the nasal cavity and consists of three basic types of cells: olfactory receptor neurons (ORNs), supporting cells and basal cells (Graziadei 1973). The majority of the human olfactory epithelium consists of non-sensory (respiratory) ciliated columnar tissue (Rawson and Gomez 2002). In the posterior section of the nasal cavity, upper part, non-sensory gives place to the sensory epithelium, which is richly innervated by ORNs (Morrison and Constanzo 1990).

ORNs have a distinct morphology. They are bipolar cells with a non-branched dendrite process terminating in a knob (Morrison and Constanzo 1990). About 10 to 25 non-motile cilia extend from the knob, and are the site of the primary events in olfaction-related sensory transduction. The cilia extend then to the mucous nasal cavity constituting a dense formation in the sensory epithelium (Rawson and Gomez 2002). ORNs cell bodies are embedded in the epithelial layer, and ORNs axons project directly from the cell bodies into the olfactory bulb. Human ORNs have a generally similar morphology, although some species variation has been found (Schild and Restrepo 1998).

In non-human vertebrates, odour-related transduction processes have been the focus of considerable attention in the past decade. Odorants enter the nasal cavity and diffuse through the mucous reaching the cilia. Those contain G-protein-linked receptor molecules that bind to the odorants. In mammals specifically, this binding process triggers the activation of the G-protein Golf (Noe' and Breer 1998), which causes the activation of the second messenger generating enzyme adenylyl cyclase III, which in its turn leads to the formation of an specific ribonucleotide, the second messenger molecule cyclic adenosine 3'-monophosphate (cAMP, Schild and Restrepo 1998). cAMP formation then leads to the opening of cyclic nucleotide gated cation channels on the ORN membrane. Under physiological conditions, $Ca2^{+}$ has the highest permeability through these channels, and the increase in intracellular $Ca2^{+}$ concentration activates a Cl^{-} current, which owing to an elevated reversal potential for Cl^{-}, depolarises the olfactory neuron (Schild and Restrepo 1998). The receptor potential finally leads to the generation of action potentials conveying the chemosensory information to the olfactory bulb.

Schild and Restrepo (1998) give specific parameters for ORNs membrane cell properties. The capacitance and resting resistance of ORNs appear to be in the range from 0.7 to 35 pF and from 1 to 40 GΩ, respectively. Adjusting for artefacts that affect the measurement of the resting

potential, it seems to be between -85 and -70 mV. Also, membrane time constants range from ~40 to >100 ms. These membrane properties make ORNs extremely sensitive to external stimuli, so that binding of a few or maybe only one molecule can excite an ORN.

As shown by several studies conducted in human tissue, several aspects of the physiological properties of human ORNs are common to other mammals and in general to other vertebrate species (Rawson and Gomez 2002). However, given inter-specific variations, one should be cautious in generalising animal studies to human-specific psychophysical functions: it has been estimated that 400 000 compounds are odorous to the human nose.

Finally, it should be noted that although there has been some confusion with respect to the vomeronasal system, it is not part of the olfactory system and the vomeronasal organ does project to the olfactory cortex (Takami 2002).

Organisation of the olfactory cortex in primates

Action potentials in ORNs convey then chemosensory information to the olfactory bulb. In primates, the primary olfactory areas (including the primary olfactory cortex) can be defined as the (paleo)cortical areas receiving direct projections from the olfactory bulb (Carmichael et al. 1994). Carmichael and colleagues, using anterograde and retrograde axonal tracers, have determined (Carmichael et al. 1994) eight structures characterising the primary olfactory areas in the macaque monkey: the anterior olfactory nucleus, the ventral *tenia tecta*, the pyriform cortex, the olfactory tubercle, the periamygdaloid cortex, the nucleus of the lateral olfactory tract, the anterior cortical nucleus of the amygdala and the most rostral portion of the entorhinal cortex. The areas labelled in the anterograde studies revealed that projections from the olfactory bulb in monkeys are similar to those found in the rat (Price 1990).

The pyriform cortex is the largest primary cortical area in the olfactory system. Rostrally, it is situated on the posterior orbital surface caudal to the anterior olfactory nucleus and lateral to the olfactory tubercle (Price et al. 1991). At the limen insula (floor of basal part of the lateral fissure) it continues caudally and ventrally onto the dorsomedial border of the temporal lobe. The anterograde tracing studies revealed that the pyriform cortex is richly innervated by projections originating in the olfactory bulb.

In this study, anterograde tracers were injected in the pyriform cortex area, immediately caudal to the limen insula. In the prefrontal cortex, labelled fibres from the pyriform cortex reached the caudal orbitofrontal cortex (BAs 13a, 13m, 14c) and parts of the rostral cingulate cortex (BA 25). Of particular interest are the projections into the insular cortex. Fibres reached preferentially the agranular parts of the rostral insula, Iam, Iai, Ial, Iapl, and Iapm. In general, it was found the labelled fibres reach preferentially cortical areas neighbouring the pyriform cortex, and that projection density declines with distance. This is particularly the case for the insular cortex, where the most rostral (agranular) part was more clearly labelled. We show in Fig 2.1 a schematic view of the insular and prefrontal areas labelled by anterograde tracers in the pyriform cortex as determined by Carmichael *et al.* (1994) and depicted in their paper.

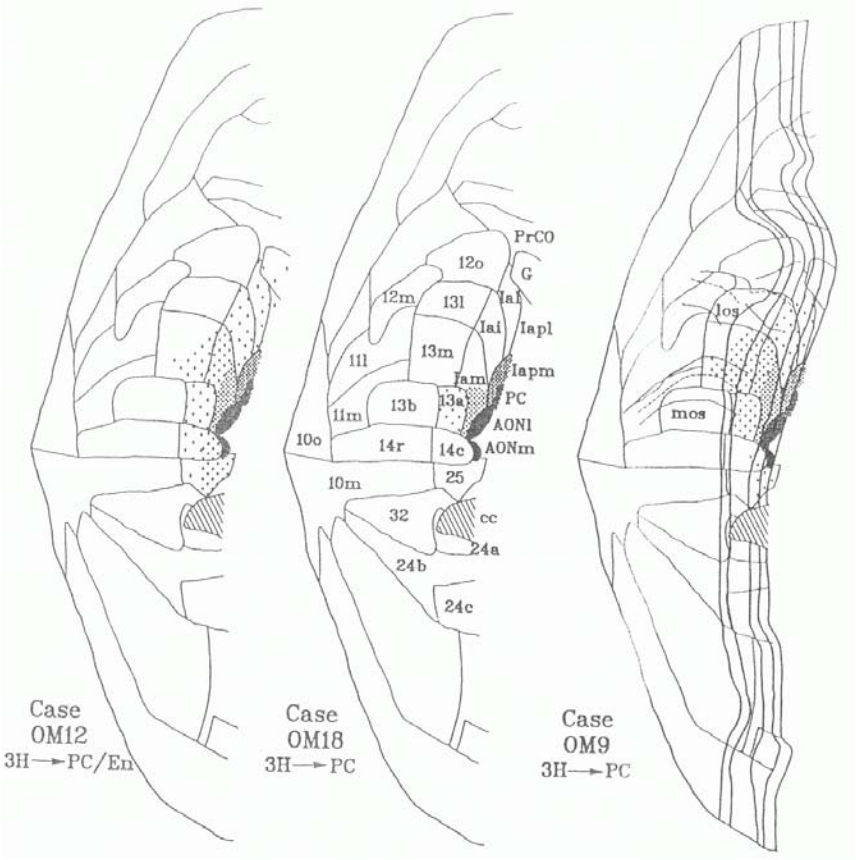


Fig 2.1 After Carmichael et al (1994). Distribution of fibres in the prefrontal and neighbouring insular cortices labelled from an injection of anterograde tracers in the pyriform cortex of three macaque monkeys, as determined by Carmichael et al (1994). Notice the heavy labelling in the rostral region of the insula, agranular part (Iam, Iai, Ial, Iapl, Iapm) and in the adjacent caudal part of the medial orbitofrontal cortex (13, 14). No such labelling was found for more posterior parts of the insula or operculum. Numeric labels in the cytoarchitectonic subdivisions denote Brodmann subareas: c, caudal; m, medial; l, lateral; o, orbital part; r rostral, except for 24a-c. 3H, ^{3}H-leucine (tracer); AONl, anterior olfactory nucleus, lateral division; AONm, anterior olfactory nucleus, medial division; cc, corpus callosum; En, endopyriform nucleus; G, gustatory cortex (frontal operculum); Iai, intermediate agranular insular area; Ial, lateral agranular insular area; Iam, medial agranular insular area; Iapl, posterolateral agranular insular area; Iapm, posteromedial agranular insular area; mos, medial orbital sulcus; los, lateral orbital sulcus; PC, pyriform cortex; PrCo, precentral opercular cortex.

Another structure of interest is the periamygdaloid cortex. It occupies the rostromedial surface of the temporal lobe just ventral to the pyriform cortex (Carmichael et al. 1994). It is a not precisely defined cortical structure and was found to have at least five distinct cytoarchitectural divisions (Amaral et al 1992). Also, the anterior cortical amygdaloid nucleus and the nucleus of the lateral olfactory tract are small areas situated in the rostrodorsal part of the amygdala and receive substantial projections from the olfactory bulb (Carmichael et al. 1994).

As in the case of the rat (Price 1990), there are substantial projections from the primary olfactory cortex into other cortical areas in the primate (Carmichael et al. 1994; Öngur and Price 2000). These were demonstrated with anterograde tracer injections into the pyriform cortex and retrograde tracer injections into the orbital and medial prefrontal cortices, and rostral insula. These injections labelled projections to nine areas in the caudal orbital cortex, including the adjacent agranular insula and (Brodmann) areas 14c, 25 (anterior cingulate cortex), 13a, and 13m. Areas Iam and Iapm receive the densiest projections from pyriform cortex. Areas Iam, Iapm, and 13a were also the only areas that responded with multiunit action potentials to olfactory bulb stimulation in anesthetized animals. Figure 2.2 shows the putative location of the agranular insula/pyriform cortex in humans as well as an axial view of the human orbitofrontal cortex and associated olfactory areas.

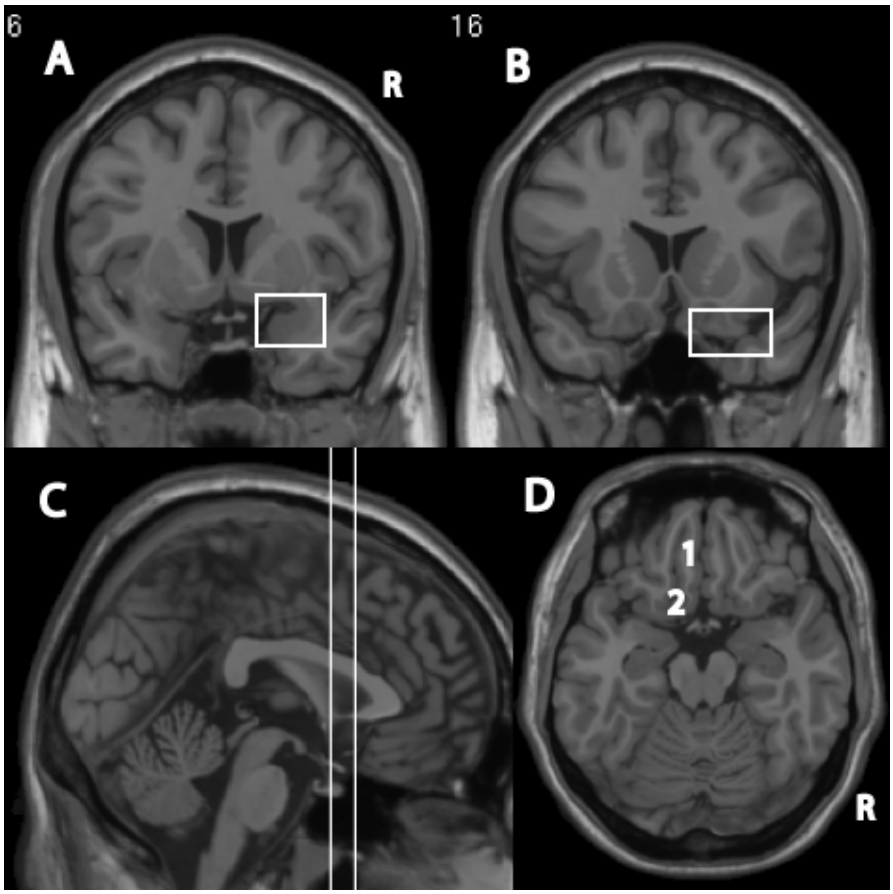


Fig 2.2 Putative location of the olfactory cortical areas in humans, as seen in an MRI T1 scan as compared to the rhesus monkey brain (Paxinos et al. 2000). (A): A region of the periamygdaloid cortex (at y = 6) which possibly includes part of the primary olfactory cortex (within white box).. (B): A more anterior region (at y = 16) just posterior to the caudal border of the orbitofrontal cortex/ agranular insula, including part of the pyriform cortex ; (C): A saggital slice is shown with the anterior-posterior locations of the regions depicted in (A) and (B). (D) (1) : The gyrus rectus within the orbitofrontal cortex (medial orbital sulcus) where the olfactory bulb lies ventrally in primates including humans ; (2) A caudal part of the medial orbitofrontal cortex putatively targeted by projections from the pyriform cortex, possibly including BA 13 (Carmichael et al. 1994; Ongur et al. 2003). This region is caudally contiguous with some parts of the agranular insular cortex.

Electrophysiology

Rolls and colleagues have performed considerable investigations on single-cell activity in olfactory cortical areas, specially the orbitofrontal cortex. As discussed above, in primates, the projections from the olfactory bulb reach the pyriform (primary olfactory) cortex, cortico-medial nucleus of the amygdala, and olfactory tubercle. From the pyriform cortex, projections reach area 13a, a part of the caudal orbitofrontal cortex, and from there project on to area 13 of the caudal orbitofrontal cortex, and then on to further orbitofrontal areas (Carmichael et al. 1994). A population of neurons in the primate (macaque) orbitofrontal cortex has olfactory responses tuned to different odours (Rolls et al. 1996b). The tuning of approximately 35% of these neurons

is in terms of the affective value of the odour as it is influenced by whether the odour is associated with the taste of glucose reward or saline punishment in an olfactory discrimination task (Critchley and Rolls 1996b). (12% responded to the reward-related set of odours; 23% to the punishment associated set of odours; and 65% did not discriminate between odours based on their taste association.) Very direct evidence that the affective value of odours is represented in the orbitofrontal cortex is that many orbitofrontal cortex olfactory neurons alter the odour to which they respond when the association of the odour with sweet vs salt taste is reversed during the reversal of an olfactory discrimination task (Rolls et al. 1996b). Further evidence that the reward value of olfactory stimuli is represented in the orbitofrontal cortex is that orbitofrontal cortex neurons that respond to the odour of a food decrease their responses (to zero) as the food is fed to satiety and the reward value of the food decreases to zero (Critchley and Rolls 1996a). This decrease is even sensory-specific, occurring more for the smell of a food eaten to satiety than for other food odours (Critchley and Rolls 1996a). This olfactory sensory-specific satiety effect has been described and analysed in humans (Rolls and Rolls 1997), and indeed in humans it has been shown that activation of the orbitofrontal cortex mirrors this olfactory sensory-specific satiety (O'Doherty et al. 2000).

Human studies

The role of genetics in human olfaction has been the focus of considerable attention (Amoore 1967; Rawson and Gomez 2002). For example, ~50% of the population is unable to detect the odour androstenone, and this specific anosmia is linked to a simple recessive trait. Other specific anosmias have been reported and support the idea that different individuals vary in the expression of different receptor genes (Rawson and Gomez 2002).

However, olfactory dysfunction might also originate from induced conditions. First, injuries to the neuroepithelium, central olfactory pathways and olfactory bulb impair odour discrimination; also, general loss of olfactory function follows with aging (Deems and Doty 1987). More recently, olfactory deficits have been linked with neurodegenerative diseases. Olfactory discrimination deficits were reported in Alzheimer's disease patients, and even support diagnostic (McCaffrey et al. 2000), probably due to the neuroanatomical changes in the central portions of the olfactory system in these patients.

In previous neuroimaging studies in humans, Zatorre *et al* (1992) showed in a PET study that the right orbitofrontal cortex as well as structures that receive direct inputs from the olfactory tract such as the pyriform cortex are activated by odours such as vanilla. Zald and Pardo (1997) reported that the orbitofrontal cortex was activated by an unpleasant odour, H_2S. Zatorre *et al* (1992) showed that orbitofrontal cortex activation was related to judgements of the hedonic

value given to a set of odours, but they did not describe any investigation of whether different brain regions were activated by pleasant and unpleasant odours, or covaried with subjective ratings of pleasantness vs unpleasantness. Recent studies have investigated the representation of the valence of odours in the human brain with fMRI (Anderson et al. 2003; Gottfried et al. 2002) and found a medial vs. lateral orbitofrotal cortex dissociation. However, given that in these two studies the authors have chosen to use one prototypical odour for each valence, it is not clear if the results obtained are due to the encoding of the valence or the indentity of these odours. It is thus an open question in humans whether there are systematic differences in the representation of pleasant and unpleasant odours, as for example obtained by using more than one prototypical odour for each valence. This was one of the issues addressed in the following investigation.

The representation of pleasant and unpleasant odours in the human brain: an event-related fMRI study

One of the most important features of odour perception is its hedonic or affective component. Most odours are labelled as "pleasant" (positive hedonic value) or "unpleasant" (negative hedonic value). The aim of this study is to investigate whether there are separate representations of pleasant and unpleasant odours in areas of the human brain that receive olfactory inputs, including in particular the orbitofrontal cortex, cingulate cortex, and subgenual cingulate cortex, as these areas are implicated in affect (Rolls 1999). An additional aim is to investigate brain areas involved in emotion, for emotions can be defined as states elicited by rewarding (generally subjectively pleasant) and punishing (generally subjectively unpleasant) stimuli, and the representation of pleasant and unpleasant olfactory stimuli thus provides one part of a systematic study of the brain regions involved in affect (Rolls 1999, 2000a).

In primates, the projections from the olfactory bulb reach medial olfactory areas including the pyriform (primary olfactory) cortex, entorhinal cortex, cortico-medial nucleus of the amygdala, and olfactory tubercle. From the pyriform cortex, projections reach area 13a, a part of the caudal orbitofrontal cortex, and from there project on to area 13 of the caudal orbitofrontal cortex, and then on to further orbitofrontal areas (Carmichael et al. 1994; Öngur and Price 2000). Populations of neurons in the primate (macaque) orbitofrontal cortex have olfactory responses to odours (Rolls et al. 1996b; Takagi 1986; Tanabe et al. 1975), which in many cases reflect the reward value of the odour (Critchley and Rolls 1996a, b; Rolls et al. 1996b).

In positron emission tomography (PET) neuroimaging studies in humans, Zatorre et al (1992)

and Zald and Pardo (1997) showed that the orbitofrontal cortex can be activated by odours such as vanilla and H_2S. Another PET study found that the perception, discrimination and recognition of odours activate the orbitofrontal, cingulate and insula cortices (Savic et al. 2000), while another PET study found that the right orbitofrontal cortex was associated with familiarity judgments (Royet et al. 1999). Zatorre et al (Zatorre et al. 2000) showed in a PET study that orbitofrontal cortex activation was related to judgements of the hedonic value of a set of odours, but they did not describe any investigation of whether different brain regions were activated by pleasant and unpleasant odours, or covaried with subjective ratings of pleasantness versus unpleasantness. A recent functional magnetic resonance neuroimaging (fMRI) study (Anderson et al. 2003) found that activation of the amygdala was associated with intensity and of the orbitofrontal cortex with the valence of two odours, but only two different odours (citral and valeric acid) were used so that inferences about whether brain activations reflect pleasant odours in general, or instead citral vs valeric acid, are unclear; and, also in contrast to the present study, subjects were asked to rate the odours for pleasantness and intensity *after (*and not during) collecting the neuroimaging data.

It is thus an open question in humans whether there are differences in the representation of pleasant and unpleasant odours. This issue was addressed in this investigation. We performed fMRI while three pleasant, and three unpleasant odours were delivered through an olfactometer. Each of the odours was a pure chemical, to ensure that the composition of each stimulus was constant throughout the experiment. To enable the brain activations to be directly related to the subjective affective value of the stimuli, pleasantness / unpleasantness ratings were taken during the neuroimaging, and we were able to perform a correlation between these ratings and the brain activations measured. Given the evidence from neurophysiological experiments (Rolls et al. 1996b) and from neuroimaging experiments (Anderson et al. 2003; O'Doherty et al. 2000), we hypothesized that the orbitofrontal cortex and the anterior cingulate cortex would be activated by the odours. Moreover we used special methods to ensure that activations in the orbitofrontal cortex could be measured (Wilson et al. 2002), as this region is implicated in the representation of the affective value of a variety of sensory stimuli.

Material and Methods

Experimental Subjects

Eleven healthy right-handed subjects (6 women and 5 men) participated in the experiment. Written informed consent from all subjects and ethical approval were obtained before the experiment. Prior to the scanning sessions subjects were exposed to each of the odours and trained to use a visual scale for rating the intensity and pleasantness of each of the odours.

Stimuli and experimental design

The odours were chosen from a pool of 18 carefully selected odours, which had undergone meticulous psychophysical investigations in 35 subjects at Firmenich (Switzerland) such that the odour concentrations were matched for similar intensity. The pleasant odours chosen were linalyl acetate (floral, sweet), geranyl acetate (floral) and alpha-ionone (woody, slightly food-related). (Chiral substances were used as racemates.) The unpleasant odours chosen were hexanoic acid, octanol and isovaleric acid. All odours were diluted at 5% in propylene glycol.

A purpose-built continuous airflow ten-channel computer-controlled olfactometer was constructed to allow odour stimuli to be delivered in the MRI scanner. The control and metal components of the system are kept outside the scanner room, and the system is free of any auditory, tactile or thermal shifts that could cue the subject to the onset of odour delivery. The flow of clean pressurized medical air is controlled using a pressure regulator and flow meter. The air is directed using solenoid-operated valves controlled by the stimulus computer using TTL pulses to either a clean air washbottle containing only solvent, propylene glycol, or to one of seven other washbottles each containing one odorant dissolved in the propylene glycol. Each washbottle is connected by its own teflon tube (to provide for low adhesion) to a delivery nozzle placed within 1 cm of the nose to minimize dead space. The delivery nozzle provided two types, one for each nostril, to produce birhinal stimulation. This provides seamless alternation between odorant and non-odorant conditions. The odour air stream was on for 8000 ms for any one odorant, and at all other times the clean air wash bottle and line were being used. The 24000 ms inter-trial interval with the stream of pure odourless air (passed through propylene glycol solvent) ensured the removal of the previous odorant before delivery of the next odorant. The flow-rate of the air supply was kept constant at 10 l/min such that the same degree of tactile somatosensory stimulation was delivered throughout. The olfactometer is the same design (apart from the longer teflon tubes) as that used to analyze the responses of single neurons in the orbitofrontal cortex to odours (Critchley and Rolls 1996b; Rolls et al. 1996b). All odours were presented birhinally in a randomised block design during the imaging with a total of 10 presentations of each odour. Subjects were instructed to keep their heads absolutely still, breathe normally and to smell but not sniff the visually cued odour. Subjects were pre-trained on the stimulation procedure where the onset of odour stimulation was visually cued and where after the 8000 ms stimulation period, the odour was rated using a button box for both pleasantness and intensity, using a visual rating scale from +2 (very pleasant/very strong) to -2 (very unpleasant/very weak).

fMRI data acquisition

Images were acquired with a 3.0-T VARIAN/SIEMENS whole-body scanner at FMRIB, Oxford. Local brain shim was performed using special weighting in the inferior frontal region before acquiring 840 volumes of 14 T2* weighted coronal EPI slices with TR=2 seconds and a TE of 25 ms. Slice thickness was 7 mm and in-plane resolution was 3 x 3 mm. Coverage was obtained from +60 (A/P) to –38 (A/P). The following parameters were carefully selected in order to minimize susceptibility and distortion artefact in the orbitofrontal cortex and are fully described in Wilson *et al.* (2002). Firstly, the data were acquired in a coronal rather than axial slicing direction, as this aligned the slices to be perpendicular to the predominant direction of the intrinsic susceptibility induced field gradients, and helps to minimize through-plane dephasing. Secondly, the voxel resolution was minimized by using 3 mm in-plane resolution and a 7 mm slice thickness, which results in less phase cancellation than would be produced by lower voxel resolutions. Thirdly, a relatively low TE of 25ms was selected to decrease the signal dropout, as less phase dispersion is created across the voxels. Fourthly, each subject was individually shimmed using both linear and second order shimming to minimize static field inhomogeneities in the orbitofrontal cortex. Finally, geometric distortion was minimised by using a specialist head insert gradient coil (Magnex SGRAD III) with a relatively high gradient switching frequency of 960 Hz.

fMRI data Analysis

Image pre-processing was performed with FLIRT (FMRIB Linear Registration Tool) (Jenkinson and Smith 2001) for realignment, reslicing with sinc interpolation and normalisation in stereotactic space. SPM99 (Wellcome Institute of Cognitive Neurology) was then used first in applying spatial smoothing with an 8 mm full width half maximum isotropic Gaussian kernel and global scaling. The time series at each voxel were high-pass and low-pass filtered with a haemodynamic response kernel. A general linear model was then applied to the time course of activation of each voxel and linear contrasts were defined to test the specific effects of each condition.

Specific effects were tested by performing conjunction analysis (Friston et al. 1999a) on individual linear contrasts corresponding to statistical parametric maps of the *t* statistic (then transformed into the unit normal distribution SPM Z). Conditions were established for each of the six odours and for each of the six control periods with pure air following each odour. The main effects of pleasant odours were established by the conjunction of the contrasts: [lynalyl acetate - control lynalyl acetate] AND [alpha-ionone - control alpha-ionone] AND [geranyl acetate - control geranyl acetate]. The main effects of unpleasant odours were established by the conjunction of the contrasts involving the subtraction of the remaining three unpleasant odours

minus their respective pure air control periods. In addition a correlation analysis based on the individual subjective ratings was performed in each subject revealing voxels representing a significant correlation between BOLD signal change and pleasantness ratings across all odours. Each individual subject-specific contrast was then entered into a second-level, random-effects group analysis (df=10). Reported p-values based on this group analysis for *a priori* regions of interest based on our prior hypothesis (i.e. that the orbitofrontal cortex and anterior cingulate cortex are involved in olfaction) were corrected for the number of comparisons made within each region (Worsley et al. 1996).

Results

The mean pleasantness ratings given by the 11 subjects through the experiment were 1.08 ± 0.26 (s.e.m.) for the pleasant odours, and –0.79 ± 0.27 for the unpleasant odours ($t=3.91$, $p < 0.006$, two-tailed; the rating scale was from +2 very pleasant to –2 very unpleasant). No significant differences were found with respect to the intensity ratings, which (on a scale of +2 very intense to -2 very weak) were 0.50 ± 0.41 (mean ± se) for the unpleasant odours, and 0.42 ± 0.44 for the pleasant odours.

Fig. 2.3 shows the brain regions activated by each of the odours with respect to the clean air control in a group analysis across all 11 subjects. It was notable that a part of the medial orbitofrontal cortex was activated by each of the three pleasant odours, and that similar activations were not produced by any of the three unpleasant odours. Some activation of regions of the cingulate cortex was also found.

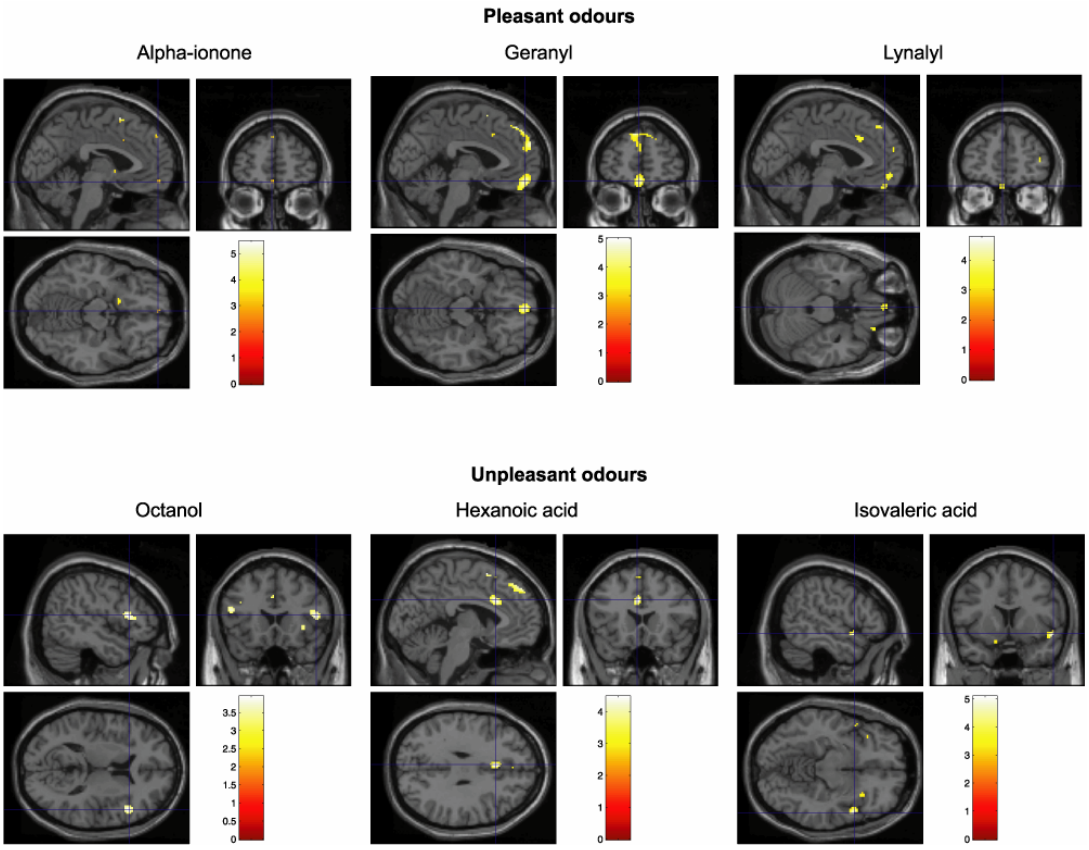


Figure 2.3. Individual pleasant and unpleasant odour activations. The figure shows the group activations to each individual odour across 11 subjects with representative sagittal, axial and coronal slices. The activations were thresholded at p<*0.001 to show the extent of the activations.*

To investigate the common brain areas activated by all 3 pleasant odours, we performed a group conjunction analysis across all three pleasant odours (Friston et al. 1999a)(see Methods). A large cluster of activated voxels (see Fig. 2.4) was found in the medial OFC with the voxel of highest significance located at MNI coordinates [0, 54, -12] and significance level Z =5.23 (p<0.05 corrected for multiple comparisons). Another significant cluster was found in the anterior cingulate cortex with peak at [2, 20, 32] (Z=5.44, p<0.05 corrected for multiple comparisons). This analysis was confirmed and extended by another conjunction which tested for voxels significantly activated by the average of the pleasant odours and not activated by the average of the three unpleasant odours (i.e. [(Pleasant) and (– Unpleasant)]. This also revealed a large cluster of activated voxels in the same part of the medial OFC (p<0.05 corrected for multiple comparisons). This shows that this medial orbitofrontal cortex region is selectively activated by the pleasant with respect to the unpleasant odours, and that the anterior cingulate region is not significantly differently activated by the pleasant and unpleasant odours.

Conjunction analysis was similarly applied to reveal activations common to the three unpleasant odours (Fig. 2.4, below). A lateral part of the orbitofrontal cortex was activated (-36,27,-8; Z=4.23, p < 0.05 S.V.C.). In addition, the sagittal view (left) in Fig. 2.4 (below) shows an activated region of the anterior cingulate cortex (x,y,z= 0, 18, 36; Z=4.42, p<0.05, S.V.C.), which is very similar to the region activated by the conjunction of the pleasant odours. Finally, a part of the anterior insula was activated by the conjunction of the three unpleasant odours (with a peak at [45 15 –9]; Z=3.79, p<0.0001 uncorrected), and the same region was activated by a conjunction of the 3 pleasant odours (Z=4.69, p<0.05 corrected for multiple comparisons).

A direct comparison between pleasant and unpleasant odours revealed only a region of the medial OFC (peak at [2, 52, -18]; Z =3.92, *p*<0.05, S.V.C), which was very similar to the region found when performing a conjunction of the three pleasant odours. Likewise, the comparison between unpleasant and pleasant odours revealed a region of more lateral OFC (peak at [26, 28, -8]; Z =3.90, *p*<0.05, S.V.C). Results are summarised in Table 2.1.

Side	MNI	Z	p
		Pleasant	
ACC	[0 26 38]	5.44	p<.01c
rACC	[-2 52 12]	3.9	p<.0001u
Medial OFC	[-2 52 -22]	4.63	p<.05c
Insula	[45 15 -9]	3.66	p<.0001u
		Unpleasant	
IFG	[42 42 8]	6.18	p<.01c
cACC	[-2 20 32]	4.42	p<.00001u
Lateral OFC	[-36 28 –8]	4.23	p<.00001u
Insula	[46 10 –2]	3.37	p<.001u

Table 2.1. Main effects of pleasantness and unpleasantness assessed through conjunction analysis. ACC, anterior cingulate cortex ; c, corrected for multiple comparisons ; OFC, orbitofrontal cortex ; rACC, rostral ACC ; u, uncorrected for multiple comparisons.

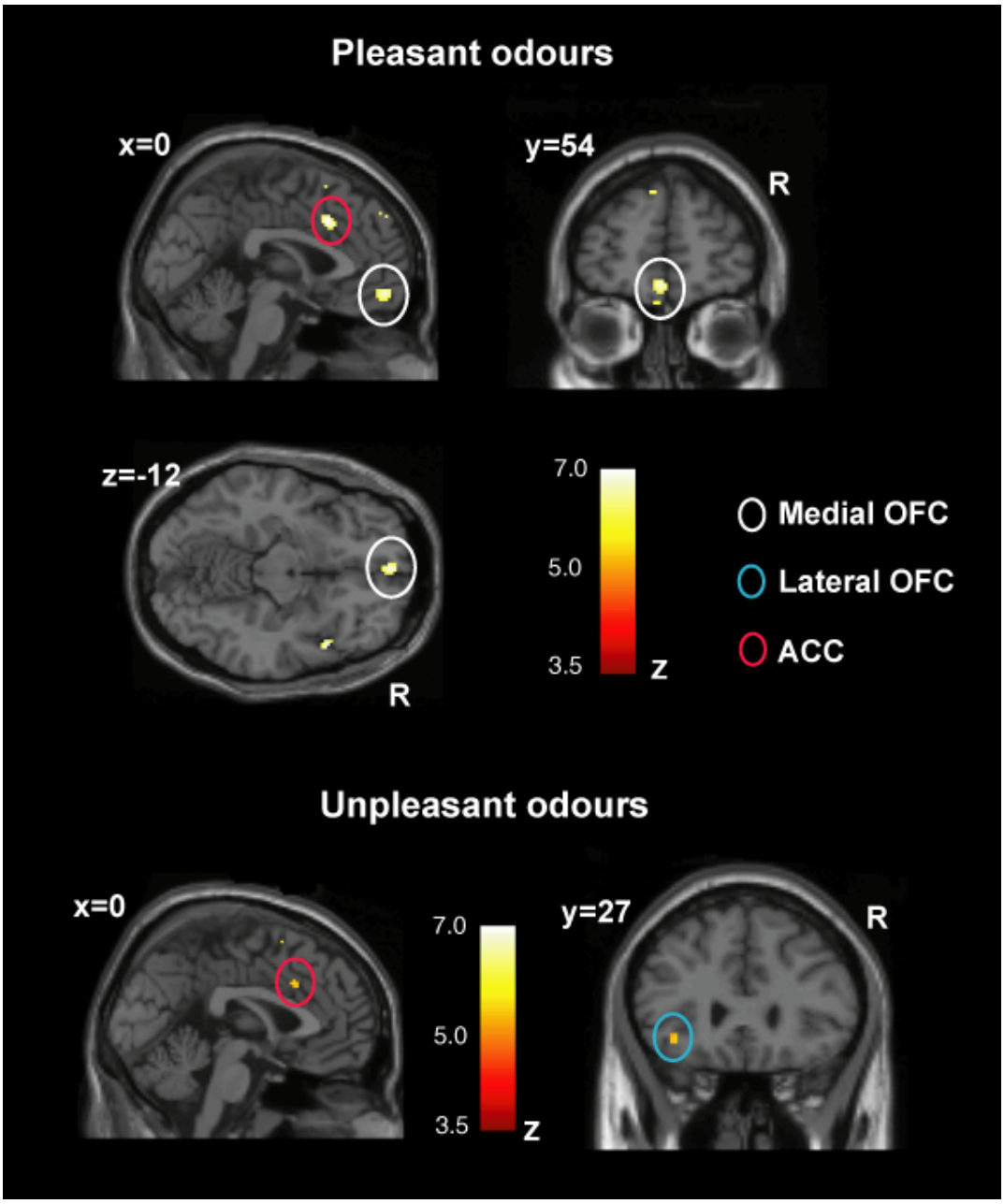


Figure 2.4. Above : Group conjunction results for the 3 pleasant odours. Sagittal, horizontal and coronal views are shown at the levels indicated, all including the same activation in the medial orbitofrontal cortex, OFC (x,y,z = 0,54,-12; Z=5.23). Also shown is activation for the 3 pleasant odours in the anterior cingulate cortex, ACC (x,y,z= 2, 20, 32; Z=5.44). These activations were significant at p<0.05 fully corrected for multiple comparisons. Below : Group conjunction results for the 3 unpleasant odours. The sagittal view (left) shows an activated region of the anterior cingulate cortex (x,y,z= 0, 18, 36; Z=4.42, p<0.05, S.V.C.). The coronal view (right) shows an activated region of the lateral orbitofrontal cortex (-36,27,-8; Z=4.23, p < 0.05 S.V.C.). All the activations were thresholded at p<0.00001 *to show the extent of the activations.*

Correlation analysis

The second part of the analysis concerns a correlation analysis of the BOLD signal (in each voxel) with the subjective pleasantness ratings given by the subjects after each odour presentation. The results show that BOLD responses in the rostral medial OFC correlate positively with the subjective ratings of pleasantness (see Fig. 2.5). The largest cluster of activation in a second-level random effects model extends bilaterally to the anterior portion of medial OFC, with peak activation at [-2, 52, -10], and significance level $Z = 4.28$ ($p < 0.05$, S.V.C.). A second cluster was found in the anterior cingulate gyrus, with its peak at [4, 42, 12] and $Z = 3.95$ ($p < 0.05$, S.V.C.). On the right of Fig. 2.5 we show the relation between the subjective pleasantness ratings and the BOLD signal from the first cluster (in the medial orbitofrontal cortex), together with the regression line.

Brain areas where activation correlated with the subjective unpleasantness ratings in a comparable analysis are also shown in Fig. 2.5. It is shown that activation of the lateral OFC correlates with the unpleasantness ratings and thus related to the negative hedonic values of the odours. The random effects model shows that one cluster is located in the left anterior OFC ([-20, 54, -14], $Z = 4.26$ $p < 0.05$, S.V.C.), and a second cluster is in a more posterior region in the left OFC ([-16, 28, -18], $Z = 4.08$, $p < 0.05$, S.V.C.). On the right of Fig. 2.5 we show the relation between the subjective unpleasantness ratings and the BOLD signal from the first cluster (in the lateral orbitofrontal cortex at $Y = 54$), together with the regression line. No significant correlation with the unpleasantness of the odours was found in the cingulate cortex, but a correlation was found in a part of the right caudate nucleus ([16, 8, 16], $Z = 4.08$ below the statistical significance used in this Chapter but included here for descriptive purposes only), which receives from the prefrontal cortex.

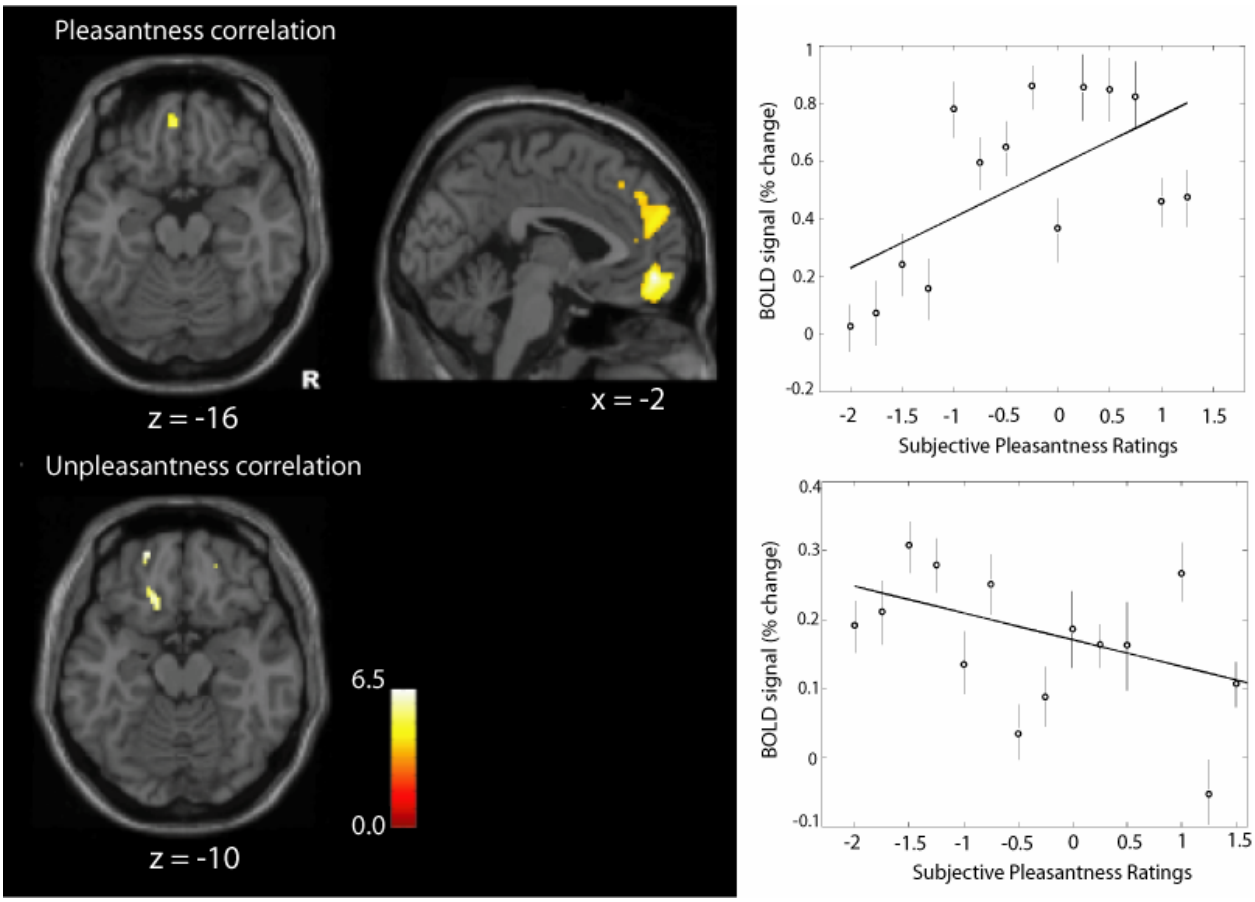


Figure 2.5. Random effects group analysis correlation analysis of the BOLD signal with the subjective pleasantness ratings. On the top left is shown the region of the medio-rostral orbitofrontal (peak at [-2, 52, -10]; z=4.28) correlating positively with pleasantness ratings, as well as the region of the anterior cingulate cortex in the top middle. On the far top-right of the figure is shown the relation between the subjective pleasantness ratings and the BOLD signal from this cluster (in the medial orbitofrontal cortex at Y = 52), together with the regression line. The means and sem across subjects are shown. At the bottom of the figure is shown the regions of left more lateral orbitofrontal cortex (peaks at [-20, 54, -14]; z=4.26 and [-16, 28, -18]; z=4.08) correlating negatively with pleasantness ratings. On the far bottom-right of the figure is shown the relation between the subjective pleasantness ratings and the BOLD signal from the first cluster (in the lateral orbitofrontal cortex at Y = 54), together with the regression line. The means and sem across subjects are shown. The activations were thresholded at p<0.0001 for extent.

A comparable correlation analysis was performed for the intensity ratings. The results are shown in Fig. 2.6. There was no correlation between the intensity ratings and the activation of the orbitofrontal cortex. However, very interestingly, much of the pyriform cortex and related medial areas that receive direct connections from the olfactory bulb did show correlations of their activations with the intensity ratings. In Fig. 2.6A we show from the random effects model across subjects at the level Y=16 that the BOLD signal in the pyriform cortex and immediately adjacent areas is correlated with the intensity ratings ([24, 16, -29], Z = 5.9, p < 0.05 corrected for

multiple comparisons across the whole brain). In Fig. 2.6B we show from the group random effects model at the level Y=6 that the BOLD signal in the medial olfactory areas including parts of the pyrifirm cortex and olfactory entorhinal cortex which lie at the rostral and anterior border of the amygdala is correlated with the intensity ratings ([20, 6, -31], Z = 5.2, $p < 0.05$ corrected for multiple comparisons). Although this cluster was on the right, a similar cluster was found (see Fig. 2.6C) on the left posterior to this in an entorhinal cortex / pyriform cortex area forming the ventral and medial border of the amygdala at its junction with the hippocampus ([-17, -10, -29], Z = 5.5, $p < 0.05$ corrected for multiple comparisons). We note that because the intensity ratings were being given on every trial during the scanning by the subjects, any variation of intensity on a trial by trial basis, or any habituation effect, are being utilized in the correlation analysis to enable the results shown to be revealed.

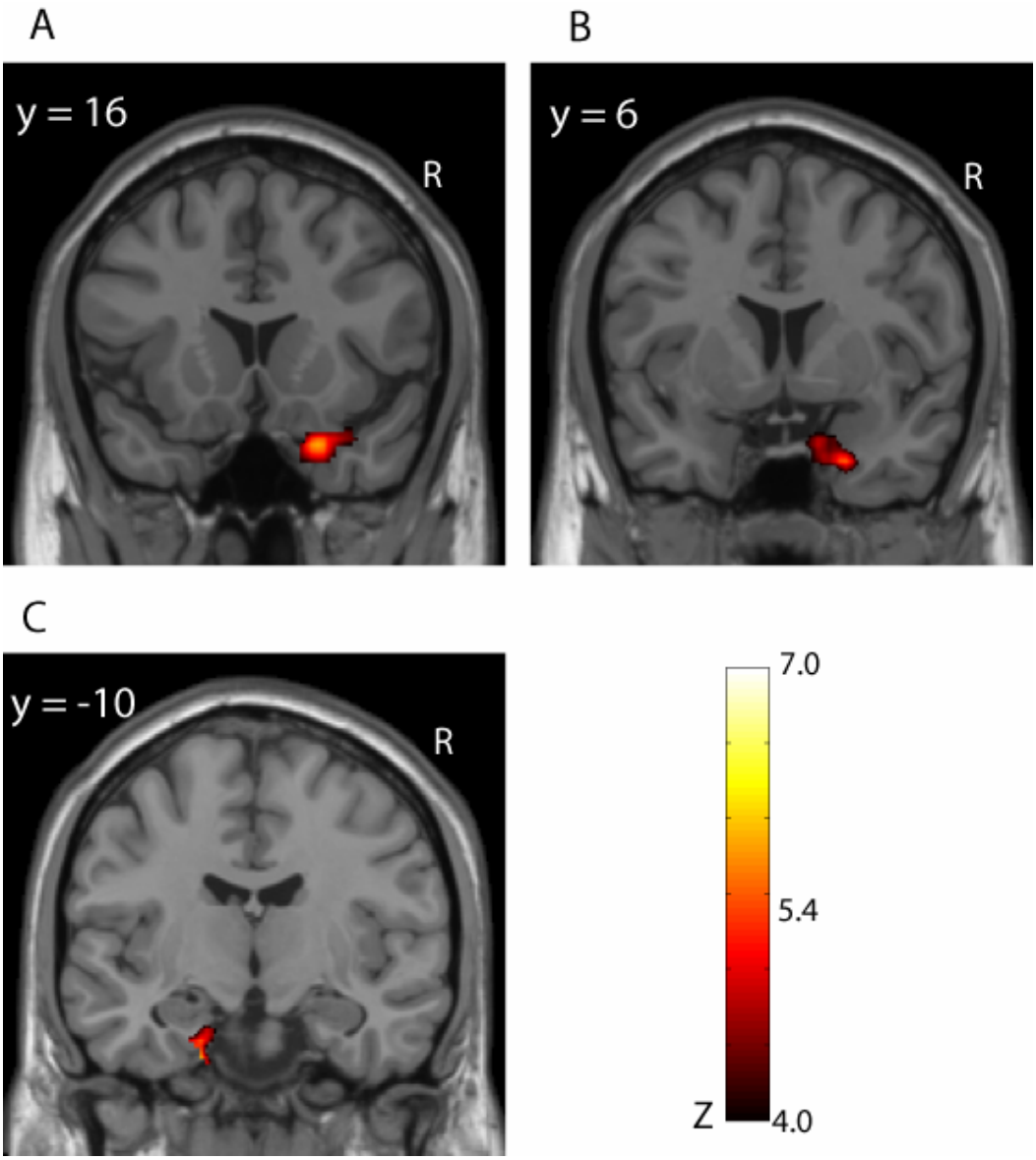


Figure 2.6. Random effects group analysis correlation analysis of the BOLD signal with the subjective intensity ratings. A: At the level Y=16 the BOLD signal in the pyriform cortex and immediately adjacent areas is correlated with the intensity ratings ([24, 16, -29], Z = 5.9, p < 0.05 corrected for multiple comparisons across the whole brain). B: At the level Y=6 the BOLD signal in the medial olfactory areas including parts of the pyrifirm cortex and olfactory entorhinal cortex which lie at the rostral and anterior border of the amygdala is correlated with the intensity ratings ([20, 6, -31], Z = 5.2, p < 0.05 corrected for multiple comparisons). C: A similar cluster was found on the left posterior to (B) in an entorhinal cortex / pyriform cortex area forming the ventral and medial border of the amygdala at its junction with the hippocampus ([-17, -10, -29], Z = 5.5, p < 0.05 corrected for multiple comparisons).

Discussion

The results of this study demonstrate that different brain areas were activated by the pleasant and the unpleasant odours. Pleasant odours activated a region of medio-rostral OFC, whereas no activity was observed in the OFC for the unpleasant odours (even when applying a much more liberal threshold of $p<0.001$).

The results of this study also show that there is a very significant correlation between a region of the medio-rostral OFC and the pleasantness ratings of the six different odours obtained a total of 60 times during the experiment for each of the 11 subjects. It is of interest that this region of medio-rostral orbitofrontal cortex is just anterior to the region found to correlate with monetary wins (O'Doherty et al. 2001a). The present study also demonstrates that different and more lateral regions of the left OFC were correlated with the subjective unpleasantness ratings of the odours. This is the first time that dissociations have been found between brain areas encoding the pleasantness and unpleasantness of odours. The foci in the more lateral parts of the orbitofrontal cortex correlating with unpleasantness are not as lateral as those reported in O'Doherty et al. (2001a) but are clearly dissociable from the medial foci correlating with subjective pleasantness ratings.

The finding that the orbitofrontal cortex was activated by odour is consistent with neurophysiological findings that a population of neurons in the non-human primate orbitofrontal cortex has olfactory responses tuned to different odours (Rolls et al. 1996b). The tuning of approximately 35% of these neurons is in terms of the affective value of the odour as it is influenced by whether the odour is associated with the taste of glucose reward or saline punishment in an olfactory discrimination task (Critchley and Rolls 1996a, b). (12% responded to the reward-related set of odours; 23% to the punishment associated set of odours; and 65% did not discriminate between odours based on their taste association.) Very direct evidence that the affective value of odours is represented in the orbitofrontal cortex is that many orbitofrontal

cortex olfactory neurons alter the odour to which they respond when the association of the odour with sweet vs salt taste is reversed during the reversal of an olfactory discrimination task (Rolls et al. 1996b). Further evidence that the reward value of olfactory stimuli is represented in the orbitofrontal cortex is that orbitofrontal cortex neurons that respond to the odour of a food decrease their responses (to zero) as the food is fed to satiety and the reward value of the food decreases to zero (Critchley and Rolls 1996a). This decrease is even sensory-specific, occurring more for the smell of a food eaten to satiety than for other food odours. This olfactory sensory-specific satiety effect has been described and analysed in humans (Rolls and Rolls 1997), and indeed in humans it has been shown that activation of the orbitofrontal cortex mirrors this olfactory sensory-specific satiety (O'Doherty et al. 2000). It is likely that activation of the orbitofrontal cortex is related to reward processing and the pleasantness of odours rather than to providing ratings about how rewarding an odour is, in that in the study by O'Doherty et al (2000) ratings were not being given throughout the neuroimaging. (We do note though that in one PET study some difference was found that appeared to be related to giving ratings (Zatorre et al. 2000)).

Both the pleasant and the unpleasant odours activated a middle part of the anterior cingulate cortex (Fig. 2.4). This was distinct from a more rostral part of the anterior cingulate cortex in which the activation was correlated with the subjective pleasantness ratings of the odours (Fig.2.5). This is of interest, because the rostral part of the anterior cingulate cortex is activated by pleasant touch (Rolls et al. 2003b), and this has been called the affective division of the cingulate in a meta-analysis of imaging studies (Bush et al. 2000). There is evidence from animal studies that it is involved in a range of motivationally oriented unconditioned behaviours and emotional learning (Cardinal et al. 2002; Devinsky et al. 1995). In addition the anterior, ventral cingulate cortex (Brodmann's areas 24a/b and 25) in humans seems to be involved in the pathology of depression in humans, as well as in the control of normal mood (Drevets 1999) and in responding to emotionally significant stimuli, such as cocaine-associated cues in drug abusers (Childress et al. 1999).

Some activation by pleasant odours was also found in the frontal operculum/anterior insula (with some activation also by some unpleasant odours, such as isovaleric acid as shown in Fig. 2.3). The far anterior, putatively agranular insula is known to receive olfactory inputs from the primary olfactory cortices in non-human primates (Carmichael et al. 1994; Carmichael and Price 1995a). The anterior insula of primates contains the primary taste cortex (Carmichael and Price 1995a; Rolls and Scott 2003), and it is of considerable interest that the part of the human insula activated by tastes such as glucose and umami as exemplified by monosodium glutamate (de Araujo et al. 2003a) is very close to the region found in this Thesis with the same imaging methods to be

activated by odours. This raises the possibility that at least part of the human anterior insula is a multimodal area, where taste and olfactory inputs may be brought together to represent flavour. It is know that in macaques such multimodal representations of the flavour of food are built by associative learning in the caudal orbitofrontal cortex (Critchley and Rolls 1996b), and it is possible that these region is located topologically a little more posteriorly in humans. Activation of the right inferior frontal gyrus by olfactory stimulation has been reported previously (Royet et al. 2001; Royet et al. 1999; Zald and Pardo 1997) and here we show that it is especially related to the delivery of unpleasant odours.

The activations described in this Chapter in the orbitofrontal cortex were related to the pleasantness and not to the intensity of the odours, in that the random effects group analysis described in the results section showed significant correlations in different parts of the orbitofrontal cortex with the pleasantness (medial OFC) or unpleasantness (lateral OFC) of the odours, whereas the corresponding analysis performed for intensity showed no BOLD signal correlation in the orbitofrontal or cingulate cortex (but did show a correlation with the BOLD signal in other brain areas as described in the Results section). These findings show that the BOLD signal in the OFC reflected the pleasantness vs the unpleasantness of the odours, but not their intensity. This conclusion is supported by the generally consistent evidence obtained by Anderson et al (2003) that a pleasant odour activated the medial orbitofrontal cortex, and an unpleasant odour activated the left lateral orbitofrontal cortex. However, the study described here goes considerably beyond the study of Anderson et al (2003) by testing whether it is generally the case that pleasant odours activate the medial orbitofrontal cortex, and unpleasant odours activate the lateral orbitofrontal cortex. With just one pleasant (citral) and one unpleasant odour (valeric acid), the localization found could have reflected just that the odours were different (Anderson et al. 2003). However, by using three pleasant odours and three unpleasant odours in the present study, we were able to show using conjunction analysis that all the pleasant odours activated the medial orbitofrontal cortex, a region not activated by the unpleasant odours; whereas the lateral orbitofrontal cortex was activated by a conjunction of the three unpleasant odours, and this lateral region was not activated by the pleasant odours. Moreover, we were able to show that the activation in the medial orbitofrontal cortex correlated with the pleasantness taken across all the 3 pleasant and 3 unpleasant odours, whereas activation of the lateral orbitofrontal cortex correlates with the unpleasantness taken across all these 6 odours. This design and the result found makes it unlikely that the correlations with pleasantness reflected correlations with just the chance identity of the odours, but instead reflect correlations with pleasantness independently of any particular odour being used in the test.

The correlations with the intensity ratings completed the dissociation to produce a double dissociation of intensity and pleasantness ratings. In particular, the BOLD signal in the medial olfactory areas such as the pyriform and entorhinal cortex in was correlated with the intensity ratings, and not with the pleasantness ratings of the olfactory stimuli. The strong conclusion is that the pyriform and entorhinal areas represent the intensity of odours, and the orbitofrontal cortex (at Y= 52 to Y = 54 and Y) represents the pleasantness (at Y = 52, and medially) and the unpleasantness (at Y = 54 and 28, and laterally) of the olfactory stimuli. We note that Anderson et al (2003) claimed that the amygdala itself (as well as a part of the pyriform cortex) represents the intensity of the odour. However, the correlations we found (see Figs. 2.6 and 2.5) were much better confined to particular regions than those shown in the Anderson et al (2003) paper (in which many activations are found outside the olfactory areas), and our results show rather clearly that it is the pyriform and entorhinal cortices which have activations correlated with intensity (see Fig. 2.6), rather than the body of the amygdala.

We note that the results described here were obtained when olfactory stimuli were delivered in a highly controlled way using a carefully designed olfactometer, which maintained a constant airstream when the odour was not being delivered, which switched to the odour without any change of pressure under computer control, so that the effects found are attributable to the odours being delivered, and not to somatosensory effects related to the presence of an air stream or not.

The correlation of activation of the caudate nucleus with unpleasantness ratings has not been observed before. However, there are projections from the prefrontal cortex to the caudate nucleus (Berendse et al. 1992; Öngur and Price 2000), and we did find activations by unpleasant odours in a part of the orbitofrontal cortex, as noted above. A previous study has also found activation of the caudate nucleus to the main effects of odours (Poellinger et al. 2001).

This study has demonstrated that the pleasant and unpleasant odours elicit activity in different parts of the human brain. One of the main findings of this study was that the brain activations produced by the pleasant odours were similar to each other, and that the brain activations produced by the unpleasant odours were also similar to each other, and that these different brain regions can be dissociated with fMRI. Importantly, it has been demonstrated that dissociable regions of human orbitofrontal cortex correlate with subjective pleasantness and unpleasantness ratings of the odours. This is further evidence that the orbitofrontal cortex is involved in representing the affective valence of emotional stimuli such as odours. Taken together with similar data linking the orbitofrontal cortex with the representation and processing of the reward value of other primary and secondary reinforcers, including taste and monetary reward

(O'Doherty et al. 2001a; O'Doherty et al. 2001b), the orbitofrontal cortex is therefore a prime candidate for subjective emotional processing in the human brain (Rolls 1999).

Chapter III

Taste-olfaction convergence and the representation of flavour in the human brain

In this Chapter we describe a study whose aim is to analyse specific interactions between different taste and olfactory stimuli at both the perceptual and brain activity levels. In particular we are interested in, first, assessing how flavour processing is represented in the human brain by comparing responses to taste, smell and their interactions. Second, we aim to compare the hedonic properties of particular combinations of stimuli meant to be *consonant*, (i.e. matching combinations of taste and olfactory stimuli) against *dissonant* combinations and how these properties might be represented in the brain. We are also interested in knowing, through psychophysical tests, if matching combinations facilitate the detection of particular olfactory stimuli presented at "sub-threshold" concentrations. In order to achieve these aims, we first ran a number of these psychophysical experiments to determine which compounds would be most appropriate for such studies. This is described in the first section of this Chapter. The second section describes thus the mentioned fMRI study.

The psychophysics of crossmodal taste-olfactory integration

In the following we present the results of two different psychophysical experiments. In the first experiment, the taste solutions (sucrose and quinine) were concomitantly presented with a given odour (either menthol or coffee flavour) delivered through a continuous air-flow olfactometer. Two of the possible four combinations (sucrose + menthol and quinine +coffee) would be matching combinations and the remaining two non-matching.

In the second experiment, which was informed by the results of the first study, different stimuli were chosen: sucrose and monosodium glutamate (MSG) for tastes and strawberry flavour and methional (chicken flavour) for odours, which were delivered in aqueous solutions. Olfactory stimulation was thus in this case retro-nasal, as these flavours were added to the mxtures containing the taste stimuli. The combination *sucrose* + *strawberry* flavour is a "sweet" matching combination, while *MSG+methional* is a "savoury" matching combination.

Experiment 1

In this first experiment, two taste (sucrose and quinine) and two olfactory (menthol and coffee flavour) stimuli were used. The combination *sucrose* + *menthol* was supposed to form a "sweet" matching combination, while the *quinine* + *coffee* flavour was supposed to form a "bitter" matching combination. The two remaining combinations (*sucrose* + *coffee* and *quinine* + *menthol*) were non-matching or dissonant.

The first part of the study aimed to investigate if a given odour stimuli presented at very weak sub-threshold concentrations would be more easily detected if combined with its matching taste (also presented at sub-threshold levels). The second part aimed to compare the hedonic values determined by the matching combinations as opposed to the non-matching ones.

Methods

The following stimuli and concentrations were used:

Saccharose $C_{12}H_{22}O_{11}$ (Sigma)	0.5M
Quinine $C_{20}H_{24}N_2O_2$ HCl (Sigma)	0.005M
Menthol (Sigma) *sub-threshold:* *supra-threshold*	 2% in Propylene Glycol 20% in Propylene Glycol
Coffee flavour (IFF) *sub-threshold* *supra-threshold*	 5% in Propylene Glycol 25% in Propylene Glycol
Control solutions: *Taste (tas): KCl + $NaCO_3$* *Odour: Propylene Glycol* *(DIPG, Sigma)*	 25mM + 2.5 mM

All the taste stimuli were diluted in deionised water.

Seventeen normal right-handed volunteers (mean age = 20) were tested. Taste solutions were delivered in 0.7ml aliquots through the use of a two-way valve attached to a standard 1ml syringe. Odour stimuli were concomitantly delivered through a continuous air-flow olfactometer at 10 litres/minute. Subjects were asked to give pleasantness and intensity ratings of the stimuli after each delivery anchored on the scale given by the limits –2 (very aversive/very weak) and +2 (very pleasant/very strong).

Results

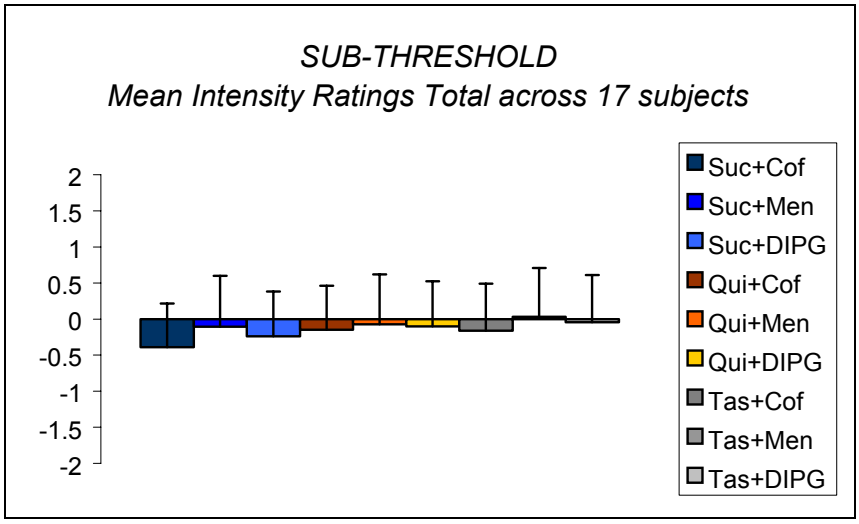
Sub-Threshold

We initially tested the hypothesis that the olfactory stimuli presented in sub-threshold concentrations would be more easily detected if combined with the matching tastes also presented in weak concentrations.

However, intensity rating values show comparable detection values for the combination sub-menthol + sub-sucrose with respect to sub-menthol + sub-quinine and to sub-coffee + sub-

sucrose. The same holds for sub-coffee + sub-quinine with respect to sub-coffee + sub-sucrose and to sub-menthol + sub-quinine. So combining stimuli under the matching criteria doesn't seem to facilitate odour or flavour detection. In fact, one-way, within-subjects ANOVA performed on these values showed no significant effects.

The intensity subjective rating values for this task are shown below:

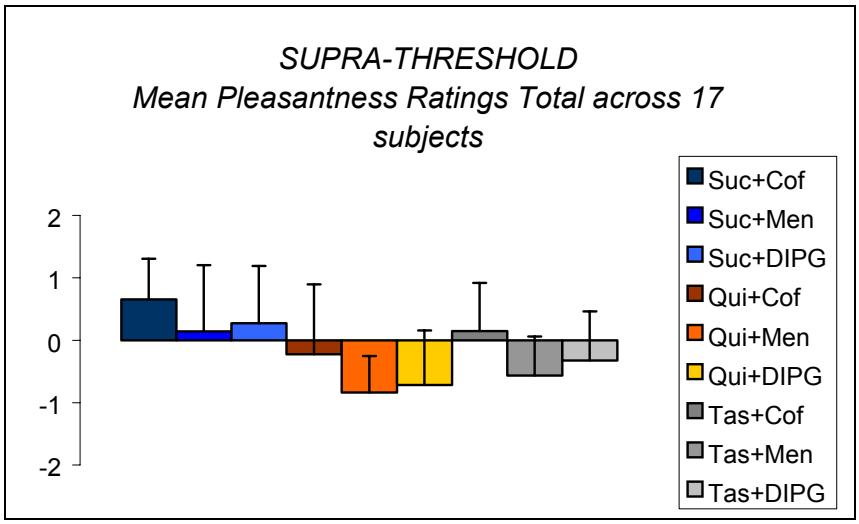


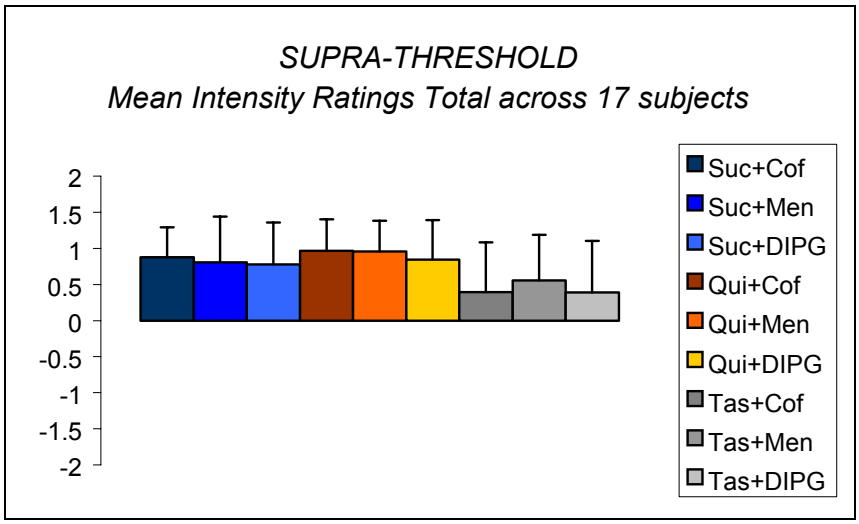
This indicates that interactions between taste and olfactory stimuli at sub-threshold levels are not at all obvious and if present will need further psychophysical investigations.

Supra-threshold

In this second part of the experiment we were interested in knowing if the hedonic values produced by the four combinations would be compatible with the consonance criteria, *i.e.* if menthol + sucrose would be found to be pleasant with respect to menthol + quinine and to coffee + sucrose and that coffee + quinine would be found pleasant with respect to coffee + sucrose and to menthol + quinine.

The values for the pleasant and intensity subjective ratings across the 17 subjects are shown below:





One-way, within subjects ANOVA performed on these values showed significant effects for both pleasantness and intensity. However, close inspection through individual t-test performed on each pair revealed that the matching/non-matching criteria did not determine the differences in score. Specifically, the hedonic effects produced by the taste stimuli determined the pleasantness ratings of the combinations, in that menthol + sucrose and coffee + sucrose (as much as sucrose + Propylene glycol) were found to be rather pleasant, while coffee + quinine and menthol + quinine (as well as quinine + Propylene glycol) were found aversive.

The results for the paired t-tests for both pleasantness and intensity are shown below:

Pairwise comparison	*Pleasantness*	*Intensity*
Suc+Cof vs. Suc+DIPH	P<.000	Non-Sig.
Suc+Cof vs. Tas+Cof	P<.002	P<.000
Suc+Men vs. Suc+DIPG	Non-Sig.	Non-Sig.
Suc+Men vs. Tas+Men	P<.000	Non-Sig.
Qui+Cof vs. Tas+Cof	P<.012	P<.000
Qui+Men vs. Qui+DIPG	Non-Sig.	Non-Sig.
Qui+Men vs. Tas+Men	P<.006	P<.001
Suc+DIPG vs. Tas+DIPG	P<.000	P<.000
Qui+DIPG vs. Tas+DIPG	P<.000	P<.000
Tas+Men vs. Tas+DIPG	P<.005	P<.001
Tas+Cof vs. Tas+DIPG	P<.000	Non-Sig.

Conclusion

Concerning the first part of the experiment, where stimuli were presented at sub-threshold levels, no significant effects were found, in that combining a given odour with its matching taste doesn't seem to facilitate or enhance its perception.

For the supra-threshold level, psychophysical tests performed so far indicate that the taste stimuli sucrose and quinine were determinant for the pleasantness ratings given by subjects. This shows that in order to be able to obtain interesting matching/non-matching effects on different combinations of taste and olfactory stimuli one needs to use combinations not involving quinine, given that it seems to be "dissonant" with respect to most odours. Also one would need to find a flavour that would "mismatch" with respect to sucrose in a clearer way, *e.g.* savoury/garlic odours.

Experiment 2

Informed by the results of the first experiment, we chose two taste (sucrose and monosodium glutamate, MSG) and two olfactory (strawberry and chicken flavour) stimuli. The combination sucrose + strawberry flavour formed a "sweet/fruity" matching combination as much as MSG + chicken flavour formed a "savoury" matching combination. The two remaining combinations (sucrose + chicken and MSG + strawberry) were non-matching or dissonant.

The first part of the study aimed to investigate if a given odour presented at very weak sub-threshold concentrations would be more easily detected if combined with its matching taste. The second part aimed to compare the hedonic values determined by the matching combinations as opposed to the non-matching ones. This includes comparing the degree of "consonance", as judged by the subjects, of these combinations.

Future investigations include a functional neuroimaging study (by using fMRI) of how taste and olfactory stimuli combination, as well as the matching properties of these combinations, are represented in the human brain (see next section of this Chapter).

Methods

The following stimuli and concentrations were used:

Saccharose ($C_{12}H_{22}O_{11}$, Sigma)	0.5M
L-glutamic salt (MSG, Sigma)	0.05M
Strawberry Flavour (Firmenich) *sub-threshold:* *supra-threshold*	 2 ppm 20 ppm
Chicken flavour, (1.9% Methional in Prop.Glycol, IFF) *sub-threshold* *supra-threshold*	 5 ppm 25 ppm
Tasteless control solution (KCl + $NaCO_3$)	25mM + 2.5 mM

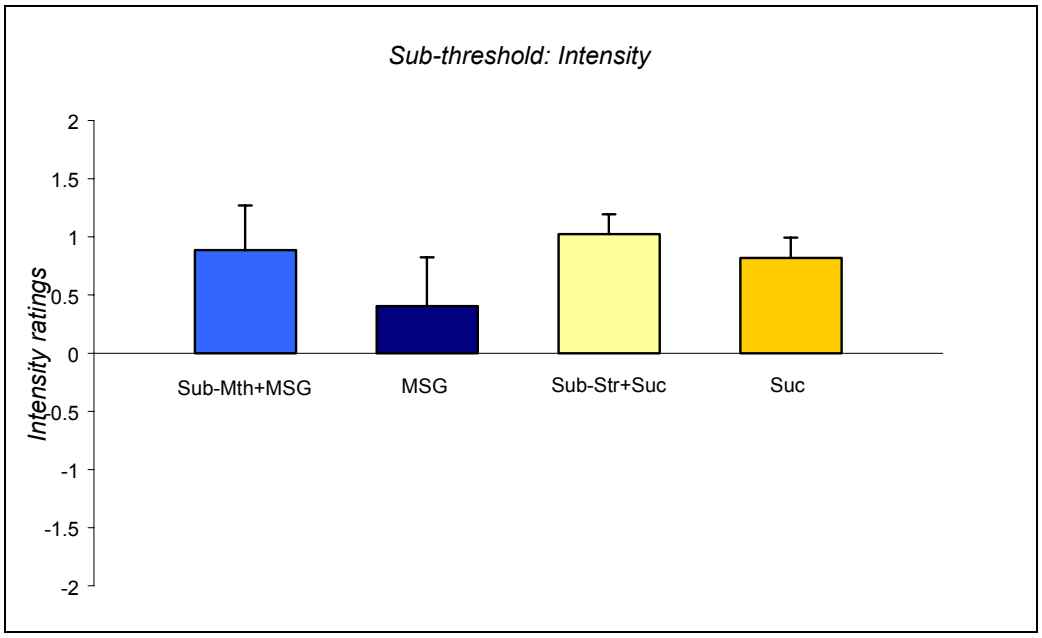
All stimuli were diluted in deionised water. Ten normal right-handed volunteers (mean age = 27.4) were tested. Solutions were delivered in 0.7ml aliquots through the use of a two-way valve attached to a standard 1ml syringe. Subjects were asked to give pleasantness and intensity ratings of the stimuli after each delivery anchored on the scale given by the limits –2 (very aversive/very weak) and +2 (very pleasant/very strong). For supra-threshold trials consonance/dissonance ratings, on the same scale, were also given.

Results

Sub-Threshold

We initially tested the hypothesis that the olfactory stimuli presented in sub-threshold concentrations would be (retro-nasally) more easily detected if combined with the matching tastes.

However intensity rating values show comparable detection values for the combination sub-strawberry + sucrose with respect to sucrose on its own; this also holds for sub-methional+MSG with respect to MSG on its own. The values are shown below (where Mth=Methional, Str = Strawberry flavour and Suc = Sucrose):

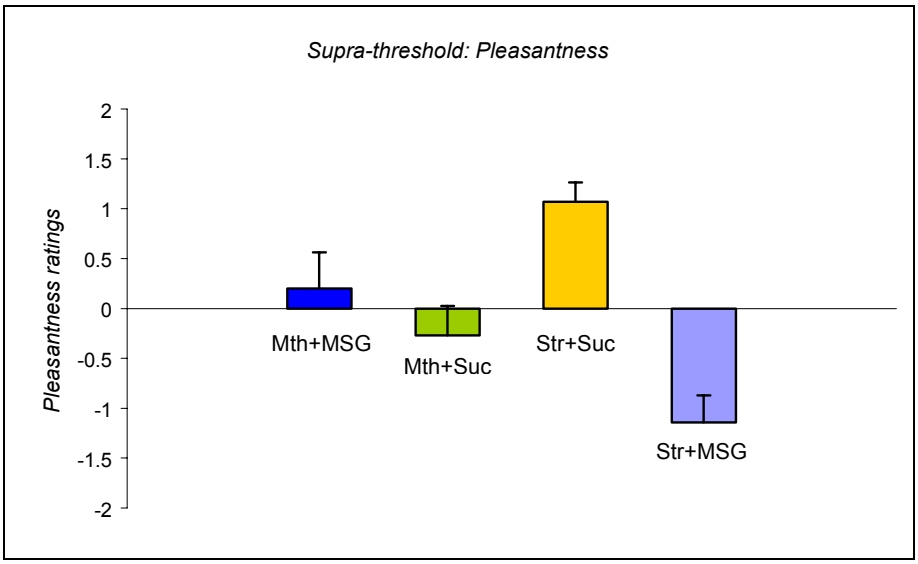


Pairwise t-tests were performed on these ratings. The null hypothesis was that the combination sub-methional+MSG (sub-strawberry+sucrose) was not stronger than MSG (sucrose). There was no basis for rejecting the null hypotheses, as shown in the table below. This indicates that interactions between taste and olfactory stimuli at sub-threshold levels do need further psychophysical investigations.

Pairwise comparison	*Intensity*
Sub-strawberry+sucrose *vs.* sucrose	Non-Sig. (P ~ 0.4122)
Sub-methional+msg *vs.* msg	Non-Sig. (P ~ 0.4089)

Supra-threshold

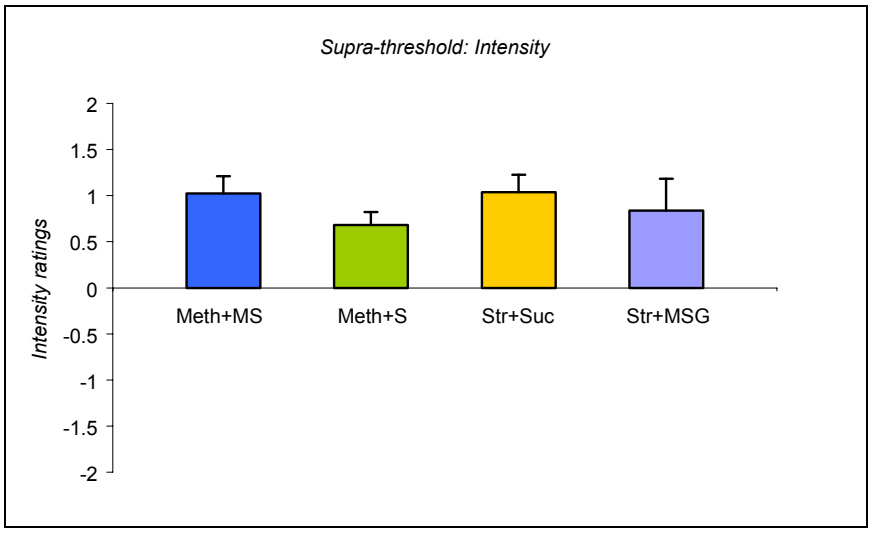
For the supra-threshold case, comparisons between the pleasantness, intensity and consonance ratings were performed. In general the results show that the matching combinations strawberry + sucrose and methional+ MSG are more pleasant than the non-matching combinations strawberry + MSG and methional + sucrose as shown below:



T-tests based on the above ratings show that in general matching combinations are significantly more pleasant than non-matching combinations with exception to the comparison (methional + msg) – (methional + sucrose) where the combination sweet/savoury was not found to be particularly unpleasant:

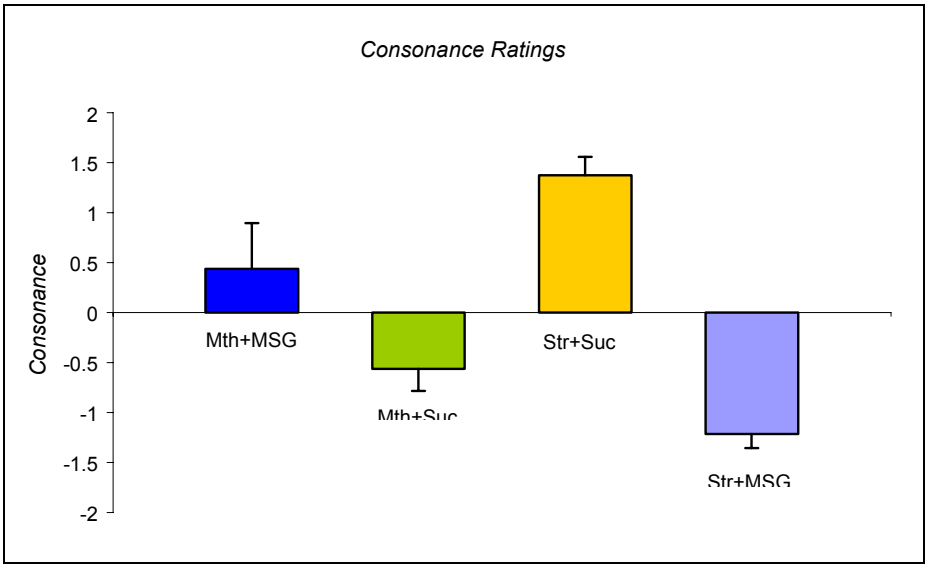
Pairwise comparison	*Pleasantness*	*Intensity*
Strawberry+sucrose *vs.* Strawberry+msg	P<0.001	Non-Sig.
Strawberry+sucrose *vs.* Methional+sucrose	P<0.002	Non-Sig.
Methional+msg *vs.* Strawberry+msg	P<0.007	Non-Sig.
Methional+msg *vs.* Methional + sucrose	Non-Sig.	Non-Sig.

Note that the difference in pleasantness ratings cannot be explained by differences in intensity values that showed no significant differences. The ratings are displayed below:



Consonance

There seems to be a clear correlation between pleasantness ratings and the consonance judgements given by the subjects. In particular sucrose and strawberry, in one hand, and MSG and methional, on the other, were judged to be highly consonant:



T-tests performed on these ratings are as follows:

Pairwise comparison	*Consonance*
Strawberry+sucrose *vs.* Strawberry+msg	P< 0.001

Strawberry+sucrose *vs.* Methional+sucrose	P< 0.001
Methional+msg *vs.* Strawberry+msg	P< 0.008
Methional+msg *vs.* Methional+sucrose	P<0.07

Conclusion

The psychophysical tests performed so far indicate that the combinations sucrose and strawberry, in one hand, and MSG and methional, on the other, were thought to be matching combinations and highly pleasant ones. The other two combinations were found to be significantly less pleasant, and in particular the combination strawberry + MSG was found to be aversive. Importantly, it has been shown that the pleasantness/consonance effects obtained for the matching combinations cannot be explained by intensity-related factors.

This set of stimuli is thus suitable for an fMRI study on taste-olfactory interactions in the human brain, which would allow an investigation on the representation in the brain of the hedonic properties of these interactions. Of particular interest would be a regression analysis of the BOLD signal with respect to the subjective pleasantness/consonance ratings of these combinations. Also, the taste and retronasal olfactory stimuli can be delivered separately, so that supra-additive interactions as well as common activations can be assessed from the BOLD signal data.

Designing an associated fMRI study

The above ratings indicate that the above four combinations would work as suitable stimuli for an event-related fMRI investigation on the cortical representations of taste-olfactory interactions and convergence in humans. Such a study is described in the remaining of this Chapter.

Taste-olfaction convergence in the human brain: an event-related fMRI study

Summary of the imaging study

The functional architecture of the central taste and olfactory systems in primates provides evidence that the convergence of taste and smell information onto single neurons is realized in the caudal orbitofrontal cortex (and immediately adjacent agranular insular). These higher-order association cortical areas thus support flavour processing. Much less is known, however, about homologous regions in the human cortex, or how taste-odour interactions, and thus flavour perception, are implemented in the human brain. We performed an event-related fMRI study to investigate where in the human brain these interactions between taste and odour stimuli (administered retronasally) may be realised. The brain regions that were activated by both taste and smell included parts of the caudal orbitofrontal cortex, amygdala, insular cortex and adjoining areas, and anterior cingulate cortex. A comparison with activations produced by orthonasal olfactory stimulation reveals a small part of the far anterior (probably agranular) insula that responds to unimodal taste and to both retronasal and orthonasal olfactory stimuli; and a part of the anterior frontal operculum that is a unimodal taste area. Supralinear activations to combined olfactory and taste stimuli (providing positive evidence for interactions between the olfactory and taste inputs) were found in a lateral anterior part of the orbitofrontal cortex. Correlations with consonance ratings for the smell and taste combinations, and for their pleasantness, were found in a medial anterior part of the orbitofrontal cortex. These results provide evidence on the neural substrate for the convergence of taste and olfactory stimuli to produce flavour in humans, and where the pleasantness of flavour is represented in the human brain.

Introduction

The primary cortical structures involved in gustatory and olfactory processing have been the focus of considerable investigation in humans, particularly through functional neuroimaging methods such as positron emission tomography (PET) and functional magnetic resonance imaging (O'Doherty et al. 2001b; Small et al. 1999; Zald and Pardo 2000b). Not much is known, however, about brain regions that receive both taste and olfactory input and about how these two neural systems interact and support psychophysical processes such as flavour perception (Small et al. 1997a).

In primates there are no known connections between the sub-cortical areas performing taste (e.g. the ventroposterior medial nucleus of thalamus, parvocellular part (VPMpc)) and olfactory (e.g. the olfactory bulb) processing (Sewards and Sewards 2001). Nor are there direct inputs from both of these regions into a common part of the amygdala. Thus convergence between taste and olfactory inputs must be implemented in the cortex. In primates, the primary taste cortex is in the frontal operculum and the anterior insula, in that it receives afferents from VPMpc, and contains taste neurons (Pritchard et al. 1986; Rolls and Scott 2003; Rolls et al. 1988; Yaxley et al. 1990). The primary taste cortex does not contain olfactory neurons (Kadohisa et al. 2003), and projects forward into a secondary cortical taste area in the caudal orbitofrontal cortex (Baylis et al. 1995), which contains taste neurons (Rolls et al. 1990). Olfactory inputs from the olfactory bulb reach a more anterior part of the insula than the primary taste cortex, the agranular insula, which is just at the caudal border of the orbitofrontal cortex, and from there connections reach the orbitofrontal cortex (Carmichael et al. 1994). In the orbitofrontal cortex, convergence onto single neurons occurs (Rolls and Baylis 1994) to build by slow learning a representation of flavour (Critchley and Rolls 1996b; Rolls et al. 1996b). Thus the caudal orbitofrontal cortex, and possibly the adjoining agranular part of the far anterior insula, is a candidate region to implement flavour processing in humans.

When food is consumed, first there is orthonasal stimulation by odour before the food is placed in the mouth, and then when the food is in the mouth there is retronasal stimulation from odour molecules via the posterior nares of the nasopharynx (Pierce and Halpern 1996). Cerf-Ducastel and Murphy (2001) studied the cortical representation of olfactory retronasal stimulation in the human brain using fMRI, but did not attempt to use an odourless taste stimulus, nor this in combination with retronasal olfactory stimulation, to define unimodal taste areas, unimodal olfactory areas, and areas where both stimuli activate and potentially interact. The investigation of such convergence interaction between taste and olfactory stimuli seems to be a necessary and important step towards disclosing the neural structures involved in flavour processing.

In this study we investigated, using event-related fMRI, three different aspects of taste and retronasal olfactory processing during flavour perception. First we aimed to reveal brain areas responding unimodally to taste stimuli, and to olfactory stimuli, and in addition, brain areas responding to both taste and olfactory stimuli. Second, we aimed to identify areas that responded non-linearly to combinations of taste and olfactory stimuli, using this as a sign that these stimuli were interacting. Third, we were interested in the brain correlates of the perception of these complex combinations that is the degree of consonance or congruence between the inputs produced through these two sensory modalities. These were assessed by a correlation analysis based on subjective ratings taken throughout the experiment. The taste and retronasal olfactory

stimuli were delivered orally in aqueous solution, either separately or as complex mixtures. The results were compared with olfactory stimuli delivered orthonasally in a separate study, in order to help identify areas responding to unimodal olfactory stimuli, to unimodal taste stimuli, and to the combination of olfactory and taste stimuli.

Materials and methods

Subjects

Eleven healthy right-handed subjects (of whom 6 were males) participated in the study. Written informed consent from all subjects and ethical approval were obtained before the experiment.

Stimuli

Two taste and two olfactory stimuli provided the basic set. The taste stimuli were 0.5M sucrose (SIGMA) and 0.05 M monosodium glutamate (MSG, SIGMA). The olfactory stimuli were 20 ppm strawberry odour (for use as a food flavour, and kindly supplied by Firmenich S.A.) and 25 ppm of 1.9% methional (a chicken-like flavour). The stimuli and concentrations were chosen based on psychophysical tests performed on a panel of subjects, and were in a mid-point of the response-intensity functions so that possible interactions could be revealed. All the stimuli were diluted and delivered in deionised water either as a taste + odour combination or as a simple stimulus. So in this case olfactory stimuli stimulated the retronasal pathway through the posterior nares of the nasopharynx. A tasteless solution (containing the main ionic components of saliva, 25 mM KCl + 2.5 mM $NaHCO_3$) was used as a control stimulus (de Araujo et al. 2003a; O'Doherty et al. 2001b). Tests were performed to verify that detection of olfactory stimuli was reliable only when the subjects' noses were open.

Experimental design

The experimental protocol consisted of an event-related interleaved design using in random order the four stimuli that consisted of taste + olfactory combinations (sucrose + strawberry, MSG + methional, sucrose + methional and MSG + strawberry); together with a taste-only stimulus, sucrose; an olfactory-only stimulus, strawberry odour; and a tasteless control solution. This set of stimuli was chosen in order to limit the number of stimuli to what was feasible given the number of repetitions of each needed and the length of time that subjects were in the magnet; to enable consonant (e.g. sucrose and strawberry) and dissonant (e.g. sucrose and methional) combinations of stimuli to be compared; and to enable a combination of stimuli, sucrose + strawberry, to be compared with each of its components, sucrose alone and strawberry alone. Stimuli were delivered to the subject's mouth through seven polythene tubes that were

held between the lips, and the odours were thus delivered by the retronasal route in aqueous solution. Each tube of approximately 1 meter in length was connected to a separate reservoir via a syringe and a one-way syringe valve (supplied by Fisher Scientific Ltd., UK), which allowed 0.75 ml of any stimulus to be delivered manually under computer instruction.

At the beginning of each taste delivery, one of the six stimuli chosen by random permutation was delivered in 0.75 ml aliquots to the subject's mouth. Swallowing was cued by a visual stimulus after 10 seconds (following initial instruction and training). After a delay of 3 seconds, the subject was asked to rate each of the taste stimuli three times for consonance, pleasantness and intensity by using 3 separate visual analog rating scales anchored at -2 for very incongruent/unpleasant/weak, and +2 for very congruent/pleasant/intense. Each rating period was 5 seconds long. The tasteless control solution containing the main ionic components of saliva (25 mM KCl + 2.5 mM $NaHCO_3$) was then administered in exactly the same way as the test stimulus and the subject was cued to swallow again after 10 seconds. The tasteless solution was used as the comparison condition for the taste solution, and allowed non-taste effects such as somatosensory effects produced by liquid in the mouth, and the single tongue movement made to distribute the liquid throughout the mouth, to be controlled for (de Araujo et al. 2003a; O'Doherty et al. 2001b). There was then a 3 second delay period allowed for swallowing followed by a one-second gap until the start of the next trial. This taste trial was repeated for each of the six stimuli, and the whole cycle was repeated 9 times.

fMRI data acquisition

Images were acquired with a 3.0-T VARIAN/SIEMENS whole-body scanner at the Centre for Functional Magnetic Resonance Imaging at Oxford (FMRIB), where 14 T2* weighted EPI slices were acquired every 2 seconds (TR=2). We used the techniques that we have developed over a number of years (e.g. O'Doherty et al. 2001a) to carefully select the imaging parameters in order to minimise susceptibility and distortion artefact in the orbitofrontal cortex as described in detail by Wilson *et al.* (2002). The relevant factors include imaging in the coronal plane, minimizing voxel size in the plane of the imaging, as high a gradient switching frequency as possible (960 Hz), a short echo time of 25 ms, and local shimming for the inferior frontal area.

The matrix size was 64 x 64 and the field of view was 192 x 192 mm. Continuous coverage was obtained from +60 (A/P) to –38 (A/P). Acquisition was carried out during the task performance yielding 1008 volumes in total. A whole brain T2* weighted EPI volume of the above dimensions and an anatomical T1 volume with slice thickness 1.5 mm and in-plane resolution of 1.5 x 1.5 mm was also acquired. The acquisition protocol used in this study is similar to that used in previous studies from our laboratory in which we used fMRI to image the orbitofrontal cortex.

fMRI data analysis

The imaging data were analysed using SPM99 (Wellcome Institute of Cognitive Neurology). Pre-processing of the data used SPM99 realignment, reslicing with sinc interpolation, normalisation to MNI coordinate system (Montreal Neurological Institute) (Collins et al. 1994), used throughout this Thesis and spatial smoothing with a 8 mm full width at half maximum isotropic Gaussian kernel and global scaling. The time series at each voxel were high-pass and low-pass filtered with a haemodynamic response kernel. A general linear model was then applied to the time course of activation of each voxel and linear contrasts were defined to test the specific effects of each condition. Voxel values for each contrast resulted in a statistical parametric map of the t statistic which was then transformed into the unit normal distribution (SPM z). Group effects were assessed by conjunction analyses across distinct stimulus conditions and second-level, random effects analysis. Reported p-values based on this group analysis for a priori regions of interest (e.g.. the insula and the orbitofrontal cortex) were corrected for the number of comparisons made within each region (Worsley et al. 1996). Checks were performed using the estimated motion as a covariate of no interest to rule out the possibility of the observed results being due to motion-correlated artifact. Reported p-values based on this group analysis for a priori regions of interest (e.g. the insula/operculum and the orbitofrontal cortex) were corrected for the number of comparisons made within each region using the small volume correction (S.V.C.) procedure (Worsley et al. 1996).

As mentioned above, subjects gave ratings for consonance, pleasantness and stimulus intensity on every trial. This allowed performance of a correlation analysis aiming to reveal brain areas significantly co-varying with the subjective ratings for stimuli congruence or consonance. This analysis was performed in each subject's individual data through a parametric modulation analysis and the resulting parametric maps were entered into a second-level, random effects analysis. Pleasantness and intensity ratings were modelled as effects of no interest by including the relevant parameters as columns in the design matrix.

Orthonasal olfactory stimulation through a continuous air-flow olfactometer

In order to determine that activations in the far anterior (agranular) insular and caudal orbitofrontal cortices could also be elicited through orthonasal olfactory stimulation, we analysed a dataset obtained from a previous fMRI study in which orthonasal olfactory stimulation was obtained through the use of a continuous air-flow olfactometer (the experiment described in Chapter II). Eleven healthy right-handed subjects (6 women and 5 men) participated in the experiment. Written informed consent from all subjects and ethical approval were obtained before the experiment. Prior to the scanning sessions subjects were exposed to each of the odours. These odours were chosen from a pool of 18 selected odours from Firmenich

(Switzerland) such that the odour concentrations were matched for similar intensity. The odours chosen were linalyl acetate (floral, sweet), geranyl acetate (floral) and alpha-ionone (woody, slightly food-related), hexanoic acid, octanol and isovaleric acid, the former three odours being considered to be "pleasant" and the latter three ones "unpleasant". All odours were diluted at 5% in propylene glycol.

A continuous airflow olfactometer was used to deliver a given odorant for a period of 8 seconds, followed by 24 seconds of pure air (control condition). All odours were presented birhinally in a randomised block design during the imaging with a total of 10 presentations of each odour. fMRI data acquisition was performed as described above, except that 840 volumes of 14 T2* weighted coronal EPI slices were acquired. All the other previous parameters apply. For all details on Methods and results, see Chapter II.

Results

Behavioural data

The consonance ratings given by the subjects for each stimulus delivered throughout the experiment were as follows (mean ± s.e.m): Sucrose 0.34 ± 0.08; Strawberry 0.16 ± 0.11; Sucrose + Strawberry 0.99 ± 0.11; MSG + Methional 0.17 ± 0.22; MSG + Strawberry –0.57 ± 0.17; Sucrose + Methional –0.38 ± 0.22. We note that the two consonant combinations (Sucrose + Strawberry, and MSG + Methional) were rated positively, while the dissonant combinations (Sucrose + Methional and MSG + Strawberry) were rated negatively. A pairwise comparison between the two classes of stimuli results in a t-value of 5.02, significant at $p<0.0001$. (Pairwise t-tests were performed to test particular hypotheses.) In addition, supra-additivity was found for some of the consonance ratings. For example, the consonance of the combination of Sucrose + Strawberry was significantly greater than the sum of the unimodal components Sucrose and 0Strawberry ($p<0.0001$).

The pleasantness ratings were as follows (mean ± s.e.m): Sucrose 0.6 ± 0.1; Strawberry 0.28 ±0.06; Sucrose + Strawberry 1.19 ± 0.11; MSG + Methional -0.8 ± 0.16; MSG + Strawberry -0.7 ± 0.14; Sucrose + Methional -0.01 ± 0.23. It is interesting to note that the above ratings show that while the combination MSG + methional was rated positively with respect to consonance it was perceived as rather unpleasant by the subjects. This shows that subjects were able to dissociate between consonance and pleasantness, perceiving them as distinct attributes of the stimuli. Thus potentially the experimental design could reveal parts of the brain in which the activation was correlated with either consonance or pleasantness. In addition, supra-additivity was found for some of the pleasantness ratings. For example, the pleasantness of the

combination of Sucrose + Strawberry was significantly greater than the sum of the unimodal components Sucrose and Strawberry ($p<0.001$).

The intensity ratings were as follows (mean ± s.e.m): Sucrose 2.6 ± 0.04; Strawberry 1.54 ± 0.23; Sucrose + Strawberry 2.95 ± 0.11; MSG + Methional 2.6 ± 0.19; MSG + Strawberry 2.38 ± 0.15; Sucrose + Methional 2.98 ± 0.1. These ratings were rescaled into the interval (0-4), where 0 = very weak and 4 = very intense. We found that the rated intensity of the combination Sucrose + Strawberry was greater than that of the unimodal Sucrose ($t= 2.95$, $p<0.01$). (Note that the intensity ratings were mapped into a (0-4) scale, and that the intensity of the stimulus was what was being rated.) While this effect is not surprising, it does show that the retronasal strawberry odour was significantly intense when present with sucrose to increase the intensity rating compared to that for sucrose alone.

fMRI data

Main effects

Initially a group analysis was performed on each individual stimulus in order to reveal the brain areas responding significantly to the stimuli. In general, activations were found for all six stimuli (bilaterally unless otherwise stated) in the amygdala, insular cortex and adjoining frontal operculum, ventral striatum, caudal orbitofrontal cortex, and an anterior region of the anterior cingulate cortex (ACC). Fig. 3.1 shows the effects of sucrose+strawberry, sucrose alone, and strawberry alone (all with the control subtraction of the effects of the tasteless solution) in four different brain regions: the amygdala and frontal operculum bilaterally (column 1), the caudal orbitofrontal cortex (second column), and the anterior ACC (third column). The third column also shows ventral forebrain activations (which extend for the Sucrose+Strawberry combination from the posterior end of the orbitofrontal cortex at Y=30 to Y=0 which is approximately 5 mm behind the anterior commissure). Table 3.1 summarizes the results of this main effects analysis. Most of the activations were found bilaterally.

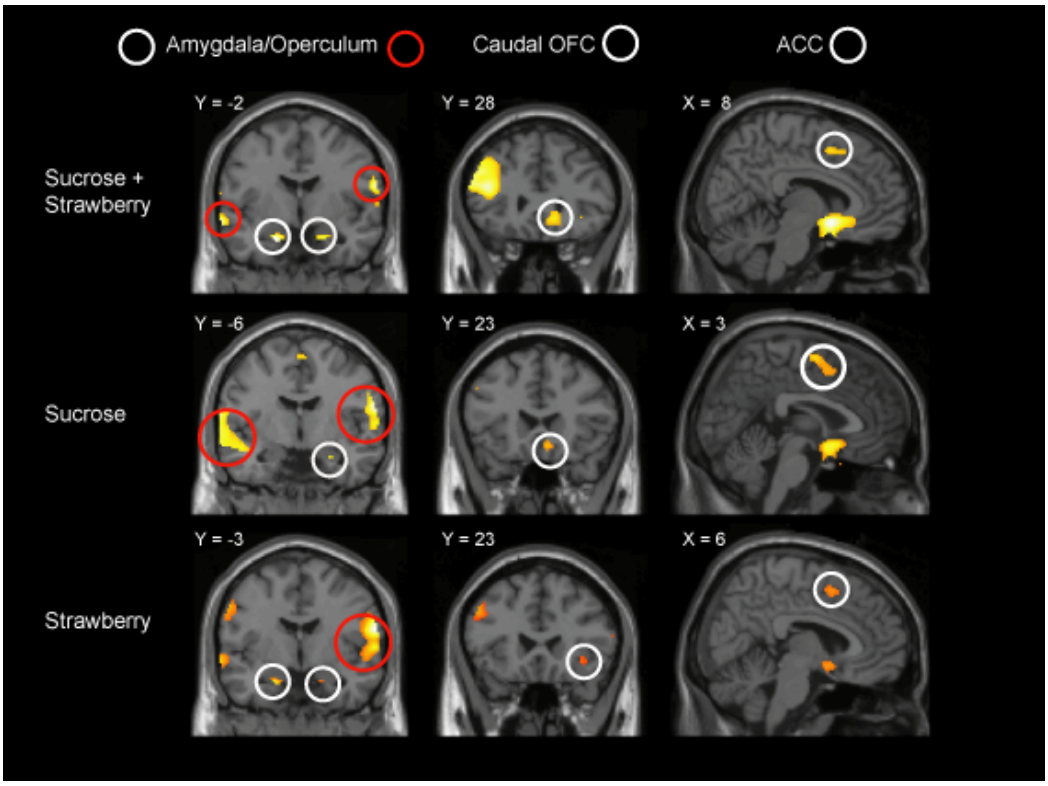


Figure 3.1. Main effects analyses: group effects for the comparisons (row 1) [Sucrose + Strawberry odour – Tasteless]; (row 2) [Sucrose – Tasteless]; (row 3) [Strawberry odour – Tasteless] in four different brain regions: (column 1) frontal operculum, and amygdala; (column 2) the caudal region of the orbitofrontal cortex (OFC); and (column 3) a posterior part of the anterior cingulate cortex region close to the supplementary motor cortex (ACC/SMA). The images were thresholded at p<0.0001 for illustration. In the coronal sections, R *indicates the right side of the brain. Column 3 also shows activation in the basal forebrain extending from the caudal orbitofrontal cortex to behind the anterior commissure. The middle column top row shows in addition an area of the left dorsolateral prefrontal cortex activated by the stimulus [Sucrose + Strawberry odour – Tasteless] (which was also activated in the other conditions at Y=28, not shown).*

(Sucrose + Strawberry) – Tasteless solution

Side / Location	MNI coordinates (peak)	Z-score	p-Value
R Caudomedial OFC	[14 26 –6]	3.94	p<0.05svc
R Anterior Insula	[42 18 –6]	4.02	p<0.01svc
L Anterior Insula	[-31 22 0]	4.13	p<0.01svc
R Operculum	[64 -4 20]	5.19	p<0.05c
R Frontal Operculum	[64 14 16]	4.29	p<0.01svc
RVentral Forebrain	[8 8 -10]	5.85	p<0.01c
L Amygdala	[-18 -2 -24]	5.91	p<0.01c
R Amygdala	[20 -4 -24]	4.35	p<0.01svc
R ACC	[8 11 49]	3.39	p<0.001u
L DLPFC	[-42 28 20]	5.38	p<0.01c

Sucrose – Tasteless solution

Side / Location	MNI coordinates (peak)	Z-score	p-Value
R Caudomedial OFC	[10 22 –12]	3.64	p<0.05svc
R Anterior Insula	[45 15 –9]	3.96	p<0.05svc
R Operculum	[64 -4 20]	6.67	p<0.01c
L Operculum	[-62 -10 14]	5.40	p<0.05c
R Ventral Forebrain	[8 8 -12]	6.10	p<0.01c
L Amygdala	[-18 0 -26]	3.40	p<0.001u
R Amygdala	[20 -4 -24]	5.52	p<0.05c
R ACC/SMA	[6 6 50]	3.54	p<0.0001u

Strawberry odour – Tasteless solution

Side / Location	MNI coordinates (peak)	Z-score	p-Value
R Caudolateral OFC	[38 23 -7]	3.10	p<0.001u
R Anterior Insula	[45 15 –8]	2.95	p<0.005u
R Operculum	[64 -4 20]	6.01	p<0.01c
R Ventral Forebrain	[8 8 -12]	3.89	p<0.001u
L Amygdala	[-20 -4 -24]	5.01	p<0.05c
R Amygdala	[18 –2 -26]	3.94	p<0.005svc
R ACC/SMA	[6 10 52]	3.63	p<0.001u

c = corrected for multiple comparisons; svc= Small Volume Correction (see Methods); u = uncorrected for multiple comparisons.

Table 3.1 Activations produced by unimodal taste (sucrose) and retronasal olfactory (strawberry) stimuli, and by their combination (cf Fig. 3.1)

Brain areas activated by both taste and olfactory stimuli

A systematic comparison between taste and olfactory activations was performed through conjunction analysis (Friston et al. 1999a), as follows. We first assessed common brain areas activated by sucrose (unimodal taste) and by strawberry (unimodal olfactory, using retronasal delivery) by performing a conjunction analysis across these two conditions (using a group analysis). This conjunction analysis showed significant activations by both the taste and the olfactory stimuli each delivered unimodally in the amygdala (bilaterally), right frontal operculum, right far anterior insula, and right caudal orbitofrontal cortex. The analysis revealed that right amygdala activations resulted in higher Z-scores than in the left amygdala ($Z = 5.39$, $p<0.05$ corrected for multiple comparisons for the peak voxel in the right amygdala and $Z = 4.17$, $p< 0.0001$ uncorrected in the left amygdala) (see Fig. 3.2A). Right frontal operculum activations were found at [62 1 18], $Z=5.4$, $p<0.05$ corrected (Fig. 3.2A), right far anterior (agranular) insular activations were found at [45 15 –8], $Z=3.2$, $p<0.001$ uncorrected (Fig. 3.2B, circled), and right caudolateral orbitofrontal cortex at [36 25 –6], $Z= 3.2$, $p<0.001$ uncorrected (see Fig. 3.2C).

To reveal areas activated by unimodal taste but not by unimodal olfactory stimuli, conjunction analysis was performed for the contrast ([Sucrose – Strawberry]) across all eleven subjects. Significant activations were found in the frontal operculum, as shown in Fig. 3.2D. This

activation is significant at $p<0.05$, corrected for small volume correction (by defining a 20 mm sphere around the peak voxel; MNI coordinates [-36 12 12], Z =4.06). The implication is that the frontal operculum / insula area at this level anterior (Y=3 to Y=14) is unimodal taste cortex. This area has been found to be consistently activated in previous taste imaging studies (de Araujo et al. 2003a; O'Doherty et al. 2001b; Small et al. 1999), and is thought to be not targeted by projections from primary olfactory areas (see Discussion and Sewards and Sewards 2001).

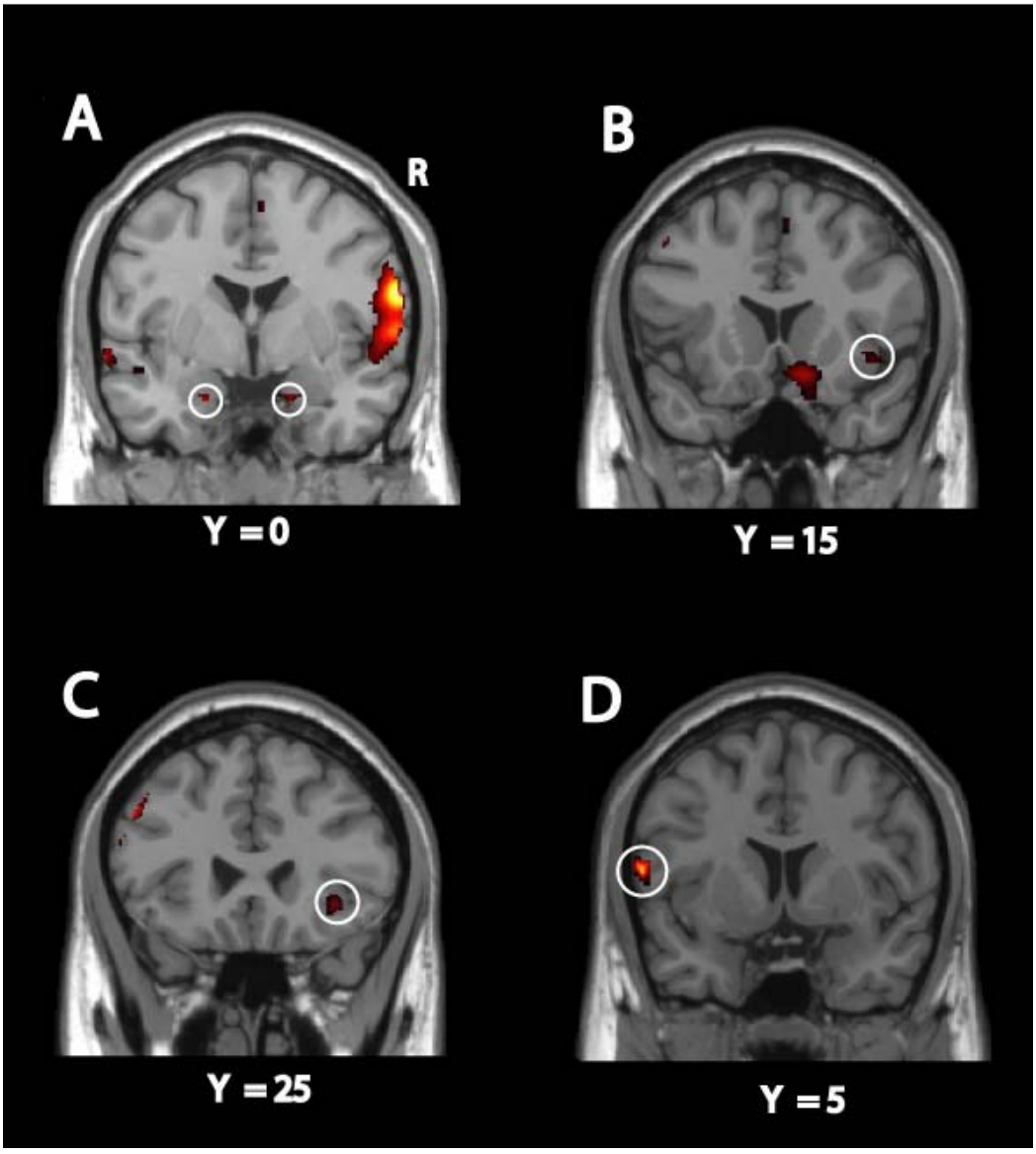


Figure 3.2. ***A-C****). Areas in the cortex activated by both unimodal taste and unimodal olfactory stimuli as revealed by conjunction analysis across all subjects for the comparison [Sucrose – Tasteless] AND [Strawberry odour – Tasteless]. Significant activations were found (A) in the frontal operculum and bilaterally in the amygdala (circled); (B) in the far anterior, agranular, insula (circled) (basal forebrain activation is also visible); (C) in the caudolateral orbitofrontal cortex (circled).* ***(D)*** *Conjunction analysis across all eleven subjects for the comparison [Sucrose taste – Strawberry odour] revealed a significant activation in the frontal operculum area (ranging from Y=3 to Y=14), providing evidence that this region is activated by taste and not by odour. Images were thresholded at p<0.0001 for illustration.*

Taste and olfaction interactions

To reveal brain areas responding to positive interactions between taste (sucrose) and olfactory (strawberry) stimuli, we defined the linear contrast [Sucrose + Strawberry mixture – (Sucrose alone + Strawberry alone)]. This contrast was applied to each individual subject data and the resulting statistical parametric maps were inserted into a second-level, random effects analysis (Worsley et al. 1996). Significant activations left from this contrast show brain areas that are activated more by the combined odour + taste stimulus than by the sum of the activations produced by each separately, and is a way in neuroimaging studies of detecting interactions between different stimuli due to their convergence onto the same neural processing system.

The random effects analysis revealed that an area of the left anterior orbitofrontal cortex was more strongly activated by the combination sucrose + strawberry odour than by the sum of the activations to the two stimuli (see Fig. 3.3). This activation is significant at $p<0.05$ corrected for small volume correction (by defining a 20mm sphere around the peak voxel; MNI coordinates [-32 50 –10], Z =3.92). No other cluster was found to be significant at this statistical threshold.

Brain areas with activations correlating with the consonance and pleasantness ratings

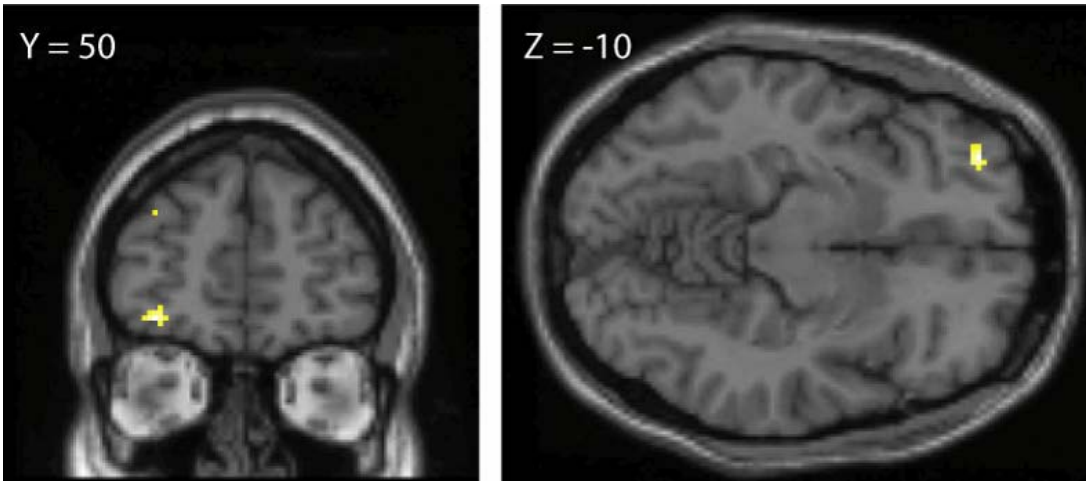


Figure 3.3. Interaction effects produced by adding strawberry odour to a sucrose solution. A second-level, random effects analysis based on individual contrasts (for the comparison [Sucrose/Strawberry mixture – (Sucrose alone + Strawberry odour alone]) revealed a significant activation in a lateral part of the left anterior orbitofrontal cortex. The images were thresholded at p<0.0001 for illustration.

Correlation analysis

A second-level (random-effects) analysis was performed to show brain areas with activations correlating with the subjective ratings taken during the experiment. Significant areas correlating with the consonance (Fig. 3.4A) and pleasantness (Fig. 3.4B) ratings were found in the rostral medial orbitofrontal cortex. For the consonance correlation the peak activation in the cluster was [0 46 –17], Z=5.09, significant at $p<0.05$ (corrected for multiple comparisons). In this case the pleasantness ratings were modelled as effects of no interest. For the pleasantness correlation the peak activation was found at [2 52 –15], Z = 4.14, $p<0.05$ S.V.C. Neither effect was due to any confound with intensity, for no correlations of brain activation with the stimulus intensities (which were deliberately kept within a limited range) were found. To elucidate further these results, Fig 3.4C shows the relation between the BOLD signal from the cluster of voxels in the medial orbitofrontal cortex shown in Fig 3.4A and the subjective consonance ratings. Fig 3.4C shows a very clear relation between the consonance ratings and the activations of these medial orbitofrontal cortex voxels (r=0.52).

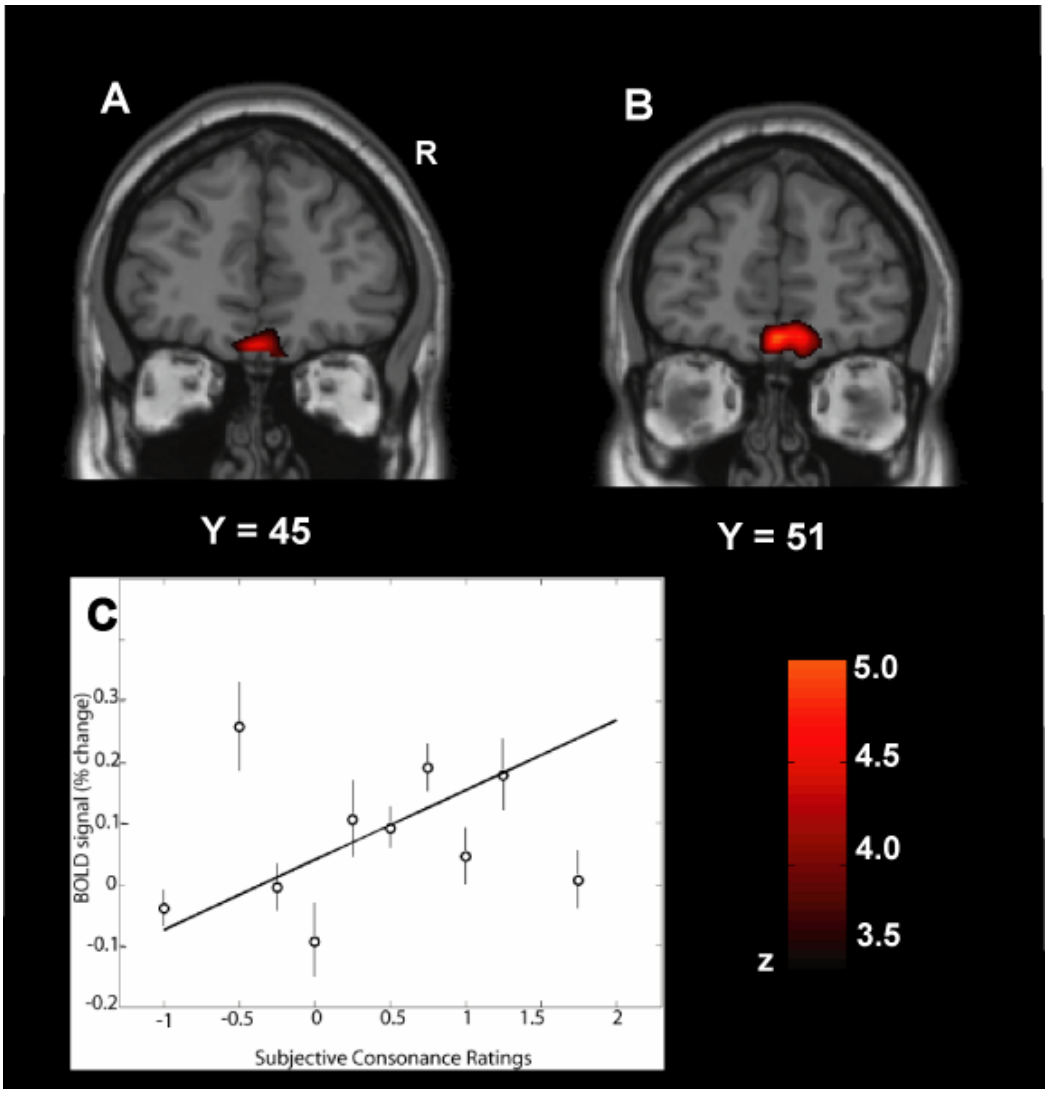


*Figure 3.4. Brain areas where activations were correlated with the subjective ratings for stimulus (taste-odour) consonance and pleasantness. (**A**) A second-level, random effects analysis based on individual contrasts (the consonance ratings being the only effect of interest) revealed a significant activation in a medial part of the anterior orbitofrontal cortex. (**B**) Random effects analysis based on the pleasantness ratings showed a significant cluster of activation located in a (nearby) medial part of the anterior orbitofrontal cortex. The images were thresholded at p<0.0001 for illustration. (**C**) The relation between the BOLD signal from the cluster of voxels in the medial orbitofrontal cortex shown in (A) and the subjective consonance ratings. The analyses shown included all the stimuli included in this investigation. The means and standard errors of the mean across subjects are shown, together with the regression line.*

Orthonasal olfactory stimulation

All the results presented so far for olfactory stimuli have been with retronasal delivery with the olfactory stimulus delivered intraorally in aqueous solution. To further clarify the activations produced by the retronasal olfactory stimulus strawberry in the anterior insula region shown in

the bottom left slice in Fig. 3.1A at Y=-3, and in other areas, further analysis was performed here of the orthonasal olfactory dataset obtained by Rolls et al (2003) using an olfactometer for stimulus delivery. In order to show brain areas activated by orthonasal olfactory stimuli, a conjunction analysis was performed across the six olfactory conditions [alpha-ionone – control] AND [lynalyl acetate – control] AND [geranyl acetate – control] AND [isovaleric acid – control] AND [octanol – control] AND [hexanoic acid – control]. The control condition was the clean air flow, and was used to remove possible effects of the orthonasal air stream. Orthonasal olfactory activations were found in the anterior cingulate cortex (Fig. 3.5 right panel) ([0 15 38], Z = 4.6 $p<0.05$ corrected for multiple comparisons), left caudolateral orbitofrontal cortex (Fig. 3.5 middle panel) ([-40 26 -10], Z = 4.53 $p<0.05$ corrected for multiple comparisons) and right far anterior (agranular) insular cortex (see Fig. 3.6A) ([45 15 -9], Z = 4.07 $p<0.01$ S.V.C.). The latter is the exact location found for activations in both sucrose – tasteless ($p<0.05$ corrected) and strawberry odour – tasteless ($p<0.001$ uncorrected) contrasts indicating that this region of the right far anterior (agranular) insula is a site of unimodal taste and (retronasal/orthonasal) olfactory co-activation and thus potentially of convergence [although it must be noted that this region is close to and adjoins the caudal orbitofrontal cortex region showing taste/olfactory convergence from which it is difficult to separate given the spatial filtering used of 8 mm in the anterior-posterior direction]. Interestingly, no activation by the orthonasal olfactory stimuli was found in the main part of the opercular/insular taste cortex (see Fig. 3.5 left panel) in the region where activation was produced by the retronasal strawberry stimulus shown in the bottom left slice in Fig. 3.1A at Y=-3. The implication is that this opercular/insular area around Y=0 is in fact not a region that can be activated by pure orthonasal olfactory stimuli alone. Its activation by the retronasal strawberry could be because when the odour is delivered in this way, and is combined with some intra-oral stimulation including somatosensory inputs which may be produced by the odours in solution or, though the concentration at 25 ppm is likely to be far too low, possibly by minimal taste inputs. (The same conclusion was reached when the 3 pleasant orthonasal odours were used in the conjunctional analysis just described instead of the 6 odours.)

To provide further evidence with respect to insular / opercular areas that receive both unimodal olfactory and taste inputs, we assessed further the results of the conjunction analysis performed to show brain areas activated by both retronasal olfactory stimulation by strawberry and by unimodal taste produced by sucrose (parts of which are illustrated in Fig. 3.2B). Fig. 3.6C shows that there is a part of the far anterior (agranular) insular cortex at Y=15 (and very close to the boundary with the caudal orbitofrontal cortex) that is activated by this retronasal strawberry AND unimodal sucrose (MNI coordinates [45, 15, -9]; this is the region marked by the cross-lines). Fig 3.6A shows that the same region is activated by orthonasal olfactory stimuli (revealed in a conjunction analysis across [lynalyl acetate – control], [alpha-ionone - control], [geranyl acetate – control], and [isovaleric acid – control]). Fig 3.6B shows that the same region is

activated by 0.5 M sucrose - tasteless. The timecourses of the activations measured in these voxels and corresponding to these effects are shown in Fig. 3.6D, to show that these three different stimulus conditions activate the same brain region in the far anterior (putatively agranular) insular cortex. Thus this far anterior, probably agranular, part of the insular cortex just where it joins the orbitofrontal cortex does receive both taste and olfactory (whether produced retronasally or orthonasally) inputs. Activations in Fig. 3.6B and C are also shown in the ventral forebrain.

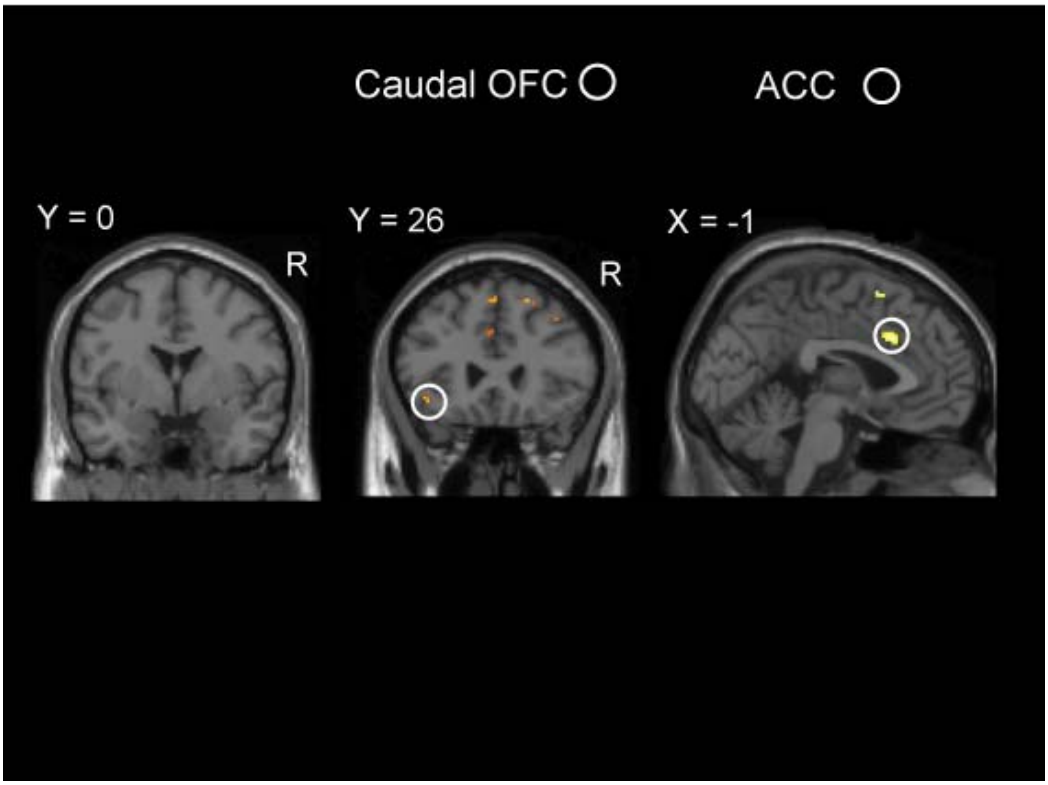


Fig. 3.5. Brain areas activated by six orthonasal olfactory stimuli. This is based on a conjunction analysis across the six olfactory conditions [alpha-ionone – control] AND [lynalyl acetate – control] AND [geranyl acetate – control] AND [isovaleric acid – control] AND [octanol – control] AND [hexanoic acid – control] AND [octanol – control] AND [hexanoic acid – control]. The control condition was the clean air flow, and was used to remove possible effects of the orthonasal air stream. Orthonasal olfactory activations were found in the anterior cingulate cortex (right panel) ([0 15 38], Z = 4.6 p<0.05 corrected for multiple comparisons), and right far anterior (agranular) insular cortex (Fig. 3.5, middle panel) ([45 15 -9], Z = 3.9 p<0.0001 uncorrected). Activations were not found in the main insular/opercular taste cortex at the level Y=0 shown in the left panel.

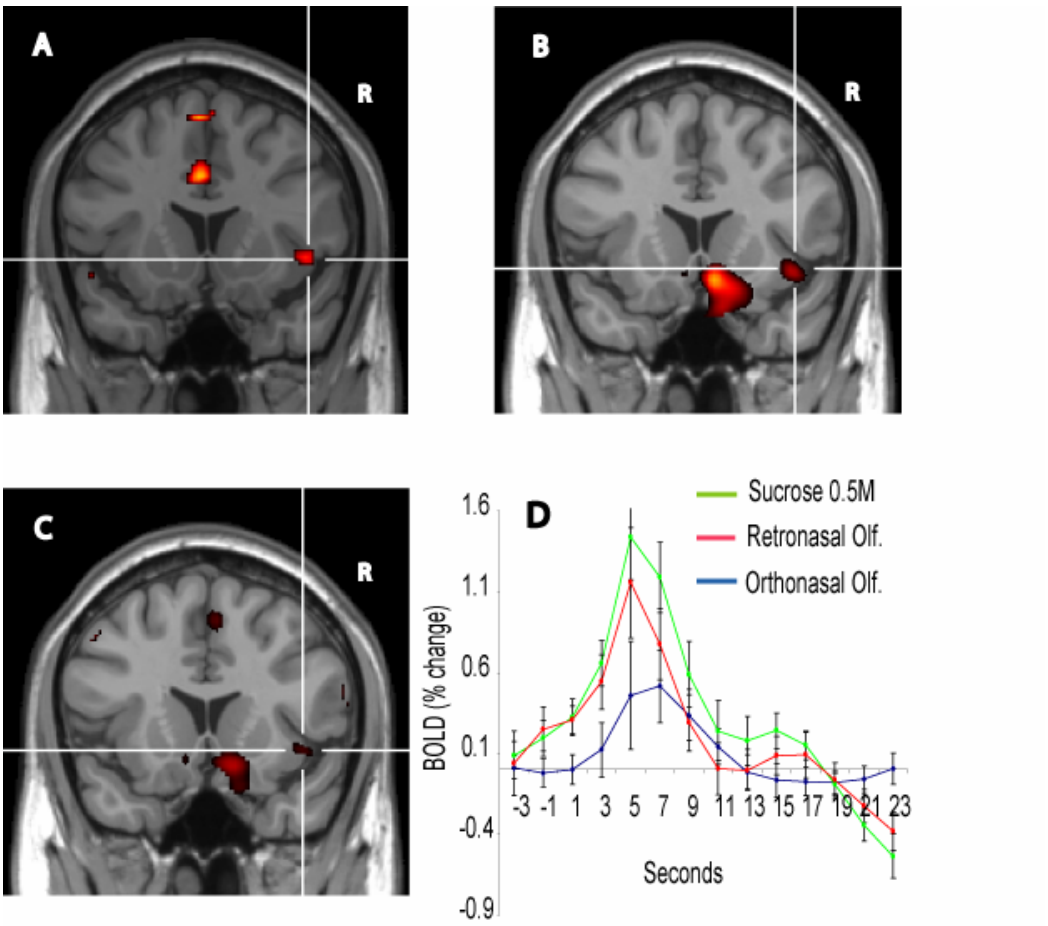


Fig 3.6. Coronal slices through the far anterior insular cortex showing small region in this brain area found to receive convergent ortho-nasal olfactory and gustatory input (MNI coordinates [45, 15, -9]; this is the region marked by the cross-lines). A Responses to orthonasal olfactory stimuli (revealed in a conjunction analysis across [lynalyl acetate – control] AND [alpha-ionone - control] AND [geranyl acetate – control] AND [isovaleric acid – control]) AND [octanol – control] AND [hexanoic acid – control]. B Responses to [0.5 M sucrose - tasteless]. C The same brain region is activated by a conjunctive comparison of [sucrose - tasteless] AND [retronasally administered strawberry odour - tasteless]. D: Timecourses of activation corresponding to these effects, showing that these three different stimuli activate the same site in the far anterior (putatively agranular) insular cortex at Y=15. The units on the abscissa are in seconds, and on the ordinate are percent of BOLD signal change. Activation in B and C is also shown in the ventral striatum.

Discussion

This study aimed to reveal how the human brain represents flavour, by disclosing which areas respond to either taste or retronasal olfactory stimuli, and which brain areas respond to both. In particular we were interested in knowing if the findings could be compared with what is known about taste-odour interactions in non-human primates. We have shown that taste and olfactory inputs in the human brain converge in particular in the far anterior (putatively agranular) insular cortex, the caudal orbitofrontal cortex, the amygdala, the ventral forebrain (a region extending from the far caudal orbitofrontal cortex to 5 mm behind the anterior commissure), and in the anterior cingulate cortex (ACC) and adjoining areas. We have also shown that positive interactions between taste and (retronasally delivered) odour stimuli are represented in a lateral part of the anterior orbitofrontal cortex, and that subjective judgements of congruence between taste and smell stimuli correlate with activity in a medial part of the anterior orbitofrontal cortex. Further confirmation that a specific location of the far anterior (putatively agranular) insular cortex (shown in this study to be activated by both taste and a retronasally presented odorant) is activated by olfactory stimuli was provided by analysis of an orthonasal olfactory stimulation dataset. Although there has been a previous neuroimaging study on retronasal olfactory stimulation (Cerf-Ducastel and Murphy 2001), the study described here is the first we know to have analysed activations using both unimodal and bimodal taste and olfactory stimuli, and to have compared retronasal with orthonasal application of olfactory stimuli.

The part of the insular/opercular taste cortex shown to be activated by sucrose in Fig. 3.1 middle row left centered on the anterior-posterior region Y=0 to Y=5 may be a part of the taste cortex which is unimodal and not activated at least by orthonasal olfactory stimuli (see Fig. 3.5 left). This region was activated by the retronasally delivered strawberry olfactory stimulus in aqueous solution (Fig. 3.1 bottom row left), but this activation may, by comparison with the effects of orthonasally delivered olfactory stimuli, be ascribable to the combination of a retronasal odour AND somatosensory inputs produced by liquids in the mouth with a further possible contribution of minor taste or somatosensory inputs produced by the olfactory stimulus in the mouth. (We did control for non-taste related inputs in this study by always using a tasteless control which produced similar somatosensory and tongue movements.) It may be that even that at the very low concentration of odour used, 25 ppm of strawberry odour, there was some somatosensory input, and this may be difficult to eliminate if the stimuli are delivered in aqueous solution, as inevitably they will be when eating a real food, the situation at which this study is aimed. Our suggestion thus is that the insular/opercular region at Y=0 in humans is a taste and not olfactory area. It is in the same brain region in humans as the primary taste cortex of macaques to which we believe it corresponds. To enable these areas to be understood in humans by reference to macaques in which the anatomy and physiology has been well established, we

show coronal sections through these regions in macaques in Fig 3.7. The primary taste cortex of macaques, as defined by anterograde tracing from the taste thalamus (Pritchard et al. 1986) and by the presence of taste neurons (Rolls and Scott 2003; Rolls et al. 1988; Scott and Plata-Salaman 1999; Yaxley et al. 1990), and labelled "G" in Fig. 3.7, is in the anterior insular and adjacent frontal opercular cortex. The primary taste cortex of macaques is now known to contain neurons that respond to taste and/or somatosensory inputs which convey information about the texture of food in the mouth, and does not have olfactory or visual responses (Kadohisa et al. 2003). In these respects it may be very similar to the human insular/opercular taste cortex at Y=0. Activation in this region by unimodal taste stimuli has also been found by de Araujo et al. (2003a), O'Doherty et al. (2001b) and Small et al. (1999).

A far anterior, cytoarchitectonically agranular, part of the macaque insula (labelled "Ia" in Fig. 3.7) where it adjoins the caudal orbitofrontal cortex receives anatomical connections from the primary olfactory system, as demonstrated by anterograde tracer injections in the macaque pyriform cortex (Carmichael et al. 1994). This region is very close to the caudal orbitofrontal cortex area that has been defined as the secondary taste cortex by virtue of receiving direct projections from the primary taste cortex (Baylis et al. 1995). This secondary cortical taste area is in area 12 and 12/PrCo according to the labelling used in Fig. 3.7. This same general region is known to contain single neurons in macaques that respond to both taste and olfactory stimuli (Rolls and Baylis 1994) and where olfactory-taste association learning to produce flavour representations occurs (Rolls 1997; Rolls et al. 1996b). (The area extends anteriorly well into the orbitofrontal cortex, as shown by Rolls and Baylis (1994), Rolls *et al.* (1996b), and Critchley and Rolls (1996b). This transitional agranular far anterior insular / caudal orbitofrontal cortex area (labelled "Ia" in Fig. 3.7) probably corresponds to the region shown to receive olfactory (as confirmed by orthonasal as well as retronasal delivery) and taste inputs in this investigation in humans (see Fig 3.6)).

The caudal orbitofrontal cortex, a main site for olfactory/gustatory convergence in macaques as just described, contains in humans a posterior part (close to Y=25) that responds to sucrose taste and to the sucrose+strawberry combined stimulus (see Fig. 3.1 middle column). At a more anterior level of the orbitofrontal cortex (at Y=50) is the region where there is supralinear additivity of the combined [sucrose + strawberry] stimulus with respect to the sum of the components (see Fig. 3.3), and at a similar level (Y=45, but more medially) is the region where the BOLD signal correlates with the subjective rating of the consonance of the stimuli (Fig. 3.4A). At a similar level anteriorly (Y=50, and again medially) is the part of the orbitofrontal cortex where the BOLD signal correlates with the subjective rating of the pleasantness of the stimuli (Fig. 3.4B). This medial orbitofrontal cortex region is close to that which activation has

been shown to be related to other affectively positive stimuli such as pleasant odours (Anderson et al. 2003; Zald and Pardo 1997; Zatorre et al. 1992), taste (O'Doherty et al. 2001b; Small et al. 2001), pleasant touch (Rolls et al. 2003b), and monetary reward (O'Doherty et al. 2001a). There is additional strong evidence at the level of the single neuron that neurons in the orbitofrontal cortex respond in relation to the reward value of taste (Rolls et al. 1989), olfactory, and visual stimuli (Critchley and Rolls 1996a; Rolls 1999, 2000a; Rolls et al. 1996b).

With respect to the amygdala, anterograde tracers placed into the olfactory bulb label axons in the anterior cortical nucleus of the amygdala and periamygdaloid cortex (Carmichael et al. 1994); and projections from the primary taste cortex reach the central nucleus of the amygdala (Scott and Plata-Salaman 1999). The primate amygdala contains taste neurons (Rolls and Scott 2003), and activation of the human amygdala by a pleasant taste, glucose, and an aversive taste, saline, has been described (O'Doherty et al. 2001b). Activation of the human amygdala by both olfactory and taste stimuli is described here for the first time.

The anterior cingulate activations shown in this study are in regions known to respond to odours (Chapter II) and taste stimuli (Chapter I and de Araujo et al. 2003a). It is known that areas 23/24 of the anterior cingulate cortex receive projections from the agranular part of the insula as shown by axonal tracer methods (Vogt and Pandya 1987), and this could be one source of such inputs. Another possible source is the orbitofrontal cortex (Cavada et al. 2000).

One of the goals of our study was to determine which brain areas respond non-linear interactions between taste and olfactory stimuli, i.e. which areas are more strongly activated by the combination sucrose + strawberry odour than by the sum of the two stimuli. The analysis reveals significant supralinear activation in a part of the left anterior orbitofrontal cortex. Interestingly, an adjacent region was shown to respond to the enhancement of umami taste produced by adding 5'-ribonucleotides to monosodium glutamate (de Araujo et al. 2003a). The primate orbitofrontal cortex is known to be a site of multimodal integration (Rolls 1999, 2000a) and neurons in this area are involved in encoding information about the sensory properties of complex combinations of stimuli. The supralinear activation produced by the olfactory-taste combination stimulus in this study is the type of evidence obtainable by fMRI that two stimuli interact, and thus provides evidence that this region is an important area in humans too not only of functional convergence of taste and olfactory stimuli, but also of effects produced by particular combinations of taste and olfactory stimuli.

Finally, we aimed in this study to assess the representation in the human brain of the affective and hedonic properties of taste-olfactory stimulus combinations. In particular we were interested

in determining which brain areas are involved in representing the degree of "consonance" or "matching" between taste and olfactory stimuli. A correlation analysis using the subjective ratings as parameters revealed a significant activation in the anterior medial orbitofrontal cortex (Fig. 3.4). This result is consistent with other evidence that the orbitofrontal cortex also represents information about the reward value of primary and secondary reinforcers including taste (O'Doherty et al. 2001b; Small et al. 2001), odour (see Discussion in Chapter II), somatosensory (Rolls et al. 2003b) and even abstract monetary rewards (O'Doherty et al. 2001a). Also, we have found that pleasant olfactory stimuli activate a far anterior part of the medial orbitofrontal cortex, with aversive olfactory stimuli a slightly more posterior region compared to the one found in Chapter II. The area activated in the correlation analysis shown in Fig. 3.4 is close to the area in which pleasant olfactory stimuli are represented.

In conclusion, the far anterior (putatively agranular) insular cortex, the caudal orbitofrontal cortex, the amygdala, and the anterior cingulate cortex seem likely from this investigation to support flavour perception. Of these, it is the orbitofrontal cortex which shows the most interesting evidence of being closely related to the representation of flavour, in that a part of this region showed supra-linear additivity between olfactory and taste stimuli, and a nearby part of the medial orbitofrontal cortex has activations that are correlated with the subjective consonance between olfactory and taste stimuli (such as sweet and strawberry), and with the pleasantness of the olfactory and taste stimuli and their combination.

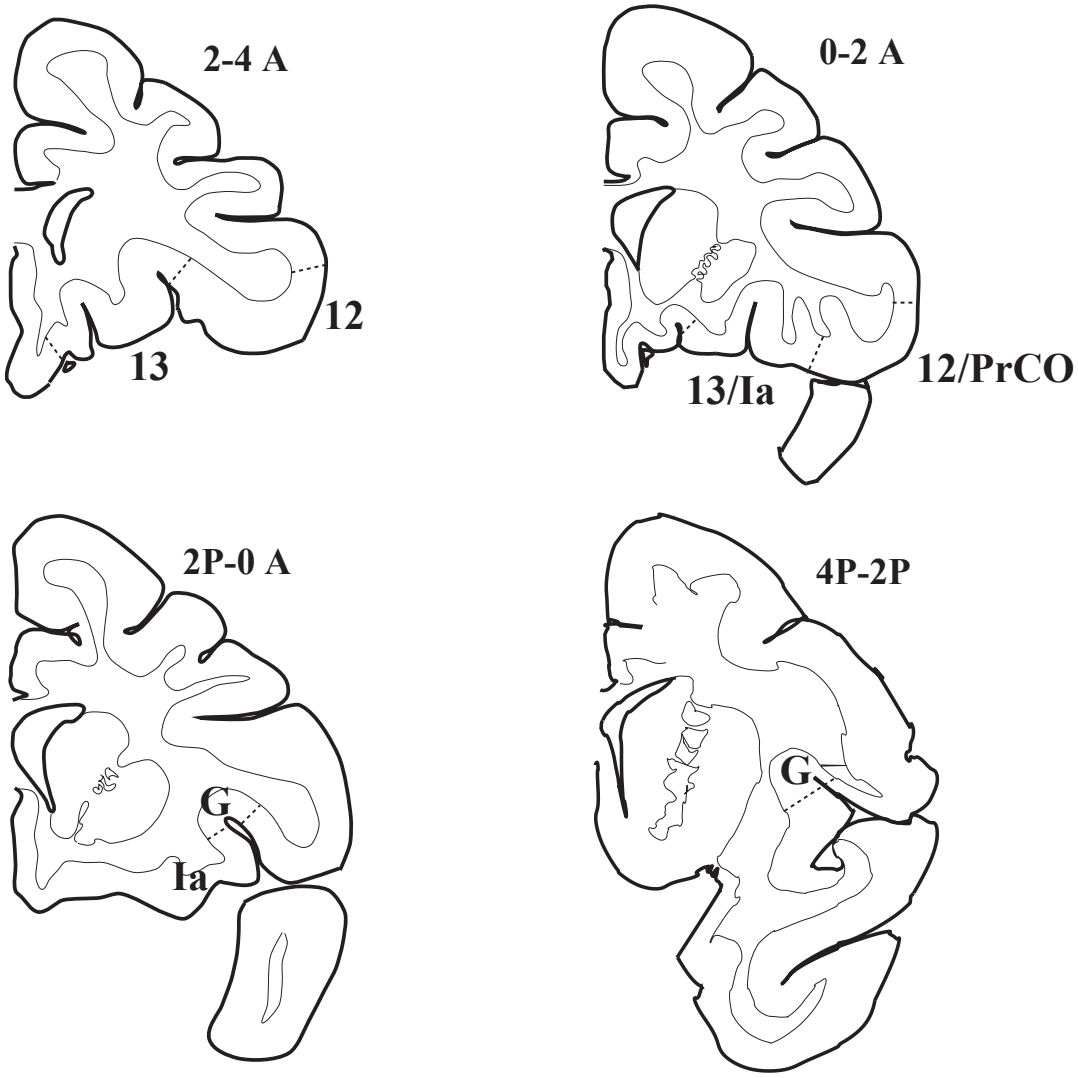


Fig 3.7. Coronal slices through the transition area between the caudal part of the orbitofrontal cortex and the far anterior insula in the rhesus monkey. Coordinates in the anterior-posterior direction are with respect to the sphenoid (see Aggleton and Passingham 1981). G, primary taste cortex (extends posterior); Ia, agranular part of the insula; PrCO, precentral opercular cortex; 12, 13, areas of the orbitofrontal cortex. The approximate boundaries of the regions are indicated by dashed lines. The regions are labelled using the nomenclature of Carmichael and Price (1994).

Chapter IV

Cortical responses to intra-venous amphetamine in naïve subjects

Intra-venous (i.v.) administration of amphetamine produces a number of known neuropsychological effects, including hedonic and cognitive effects such as the one assessed here by a measure of "mind-racing". At higher doses, i.v. amphetamine administration produces symptoms that might reflect executive dysfunction, including some of those found in paranoid schizophrenia. The aim of the study described in this Chapter was to investigate the areas of the human brain activated by i.v. M-amphetamine, and in addition, to relate the brain activation to subjective reports of the degree of mind-racing made every minute during scanning. Amphetamine (and similar substances of abuse known to increase extra-cellular dopamine concentrations) is a potent primary reinforcer, in that animals will work to perform self-administration, and repeated intake eventually leads to addiction. Thus amphetamine (in particular when administered intra-venously) should rely on reward-related brain circuitry to produce its effects. Using i.v. M-amphetamine in naïve subjects, we will be able to assess whether cortical areas reflecting the reinforcing properties of taste and smell stimuli (such as the medial orbitofrontal cortex) are also activated by reinforcers other than tastants and odours, and if this is the case to demonstrate thus that taste and olfactory representations involve the processing of general reward-related information. Psychiatrists B. Voellm and P. Cowen from Oxford University performed subject preparation and i.v. drug administration.

Two different image analysis models were used to reveal the brain areas modulated by amphetamine. The first was a simple subtractive, categorical analysis designed to show which areas of the brain were activated by amphetamine. The second was a correlation analysis, of brain areas where the activation was correlated with the degree of "mind-racing" being reported throughout the experiment. Although the concept of mind racing is a rather imprecise one, it has been useful in helping to define the perceived effects of amphetamine in otherwise naïve subjects. In any case, an interesting aspect of this study was the use of healthy naïve subjects,

which might help in disclosing brain areas involved in the initial stages of drug abuse leading to addiction.

This Chapter briefly introduces the basic psychopharmacology of the mesocortical dopamine system, with emphasis on some of the current psychological theories on the function of the dopaminergic system. We proceed then to a description of the abovementioned study.

Amphetamine and the dopaminergic system

The mesocortical dopamine system

The administration of a considerable number of drugs of abuse, including amphetamine, cocaine, heroin, nicotine, cannabis and alcohol have as a common consequence the activation of dopaminergic terminals in the nucleus accumbens (Everitt et al. 2001), leading to the hypothesis that the mesocortical dopaminergic system plays a crucial role in the reinforcing and ultimately addictive properties of these substances.

Dopamine (DA), together with noradrenaline and serotonine, is one of the major amine transmitters, known as monoamines. Monoamines are derived from tyrosine, and are also called catecholamines, given the catechol nucleus forming each of these molecules. The monoamines are synthesised through a series of reactions starting with the monoamine tyrosine: tyrosine hydroxylase leads to the production of dihydroxyphenylalanine (DOPA), which in its turn through decarboxylase leads to the DA compound (see Fig 4.1).

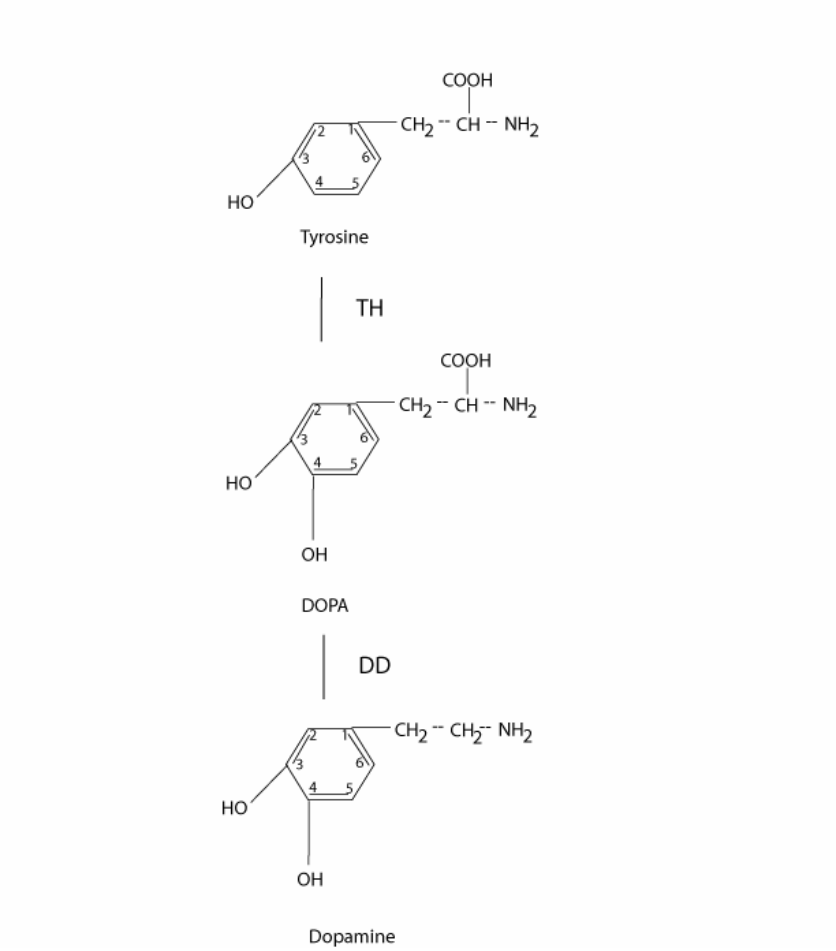


Fig 4.1*: Schematic representation of the monoamine transmitter dopamine. Top: amino acid tyrosine; Middle: dihydroxyphenylalanine (DOPA) structure; Bottom: dopamine structure. TH = tyrosine hydroxylase; DD = dihydroxyphenylalanine decarboxylase.*

In rats, dopaminergic projections to the cortex - in particular the prefrontal cortex - arise mainly from the ventral tegmental area (VTA) and the medial extent of the substantia nigra, *pars compacta*. This innervation displays a laminar-dependent pattern, with layers V and VI receiving denser projections than more superficial ones (Tzschentke 2001). The primary targets of DA cells in the medial prefrontal cortex are pyramidal cells, although the DA receptors D1 and D2 are also found in other cell types such as GABAergic cells (Vincent et al. 1993). Concerning specifically VTA DA projections, there is a specific subcortical/cortical dissociation, with cells in the nucleus paranigralis of the VTA projecting to subcortical sites while cells in the nucleus parabrachialis

pigmentosus predominantly projecting to cortical areas, in particular the medial prefrontal cortex (Berger et al. 1976).

Different hypotheses have been formulated concerning the functional role of the dopaminergic system in the mammalian brain. The anhedonia hypothesis (actually, an "hedonia hypothesis") suggests that brain dopamine systems mediate the "pleasure", or more precisely the hedonic impact produced by primary rewards or incentives such as food, sex and drugs of abuse as well as the pleasure produced by secondary reinforcers (Wise 1982). Some authors, based on biochemical markers studies, even suggest that the hedonic impact of primary incentives such as food can be quantified through measurements of dopamine release in specific sites such as the nucleus accumbens shell (Di Chiara and Tanda 1997). Alternatives however have been proposed to the anhedonia hypothesis based on the fact that dopamine function in reward seems rather to involve anticipatory or approach phases of motivated behaviours (Berridge and Robinson 1998). Two of these alternatives have received much attention. First, it has been claimed that dopamine mediates specific aspects of reward learning through the computation of reward prediction errors (Schultz et al. 1997). In the experiments described by Schultz and colleagues, DA cells are initially activated by primary unpredicted rewards, and inversely their activity decreases when a fully predicted reward fails to occur. These same cells, following learning, respond to previously neutral stimuli fully predicting reward, and decrease their activity to baseline levels when predicted primary rewards occur at the expected time. A similar effect has been observed in humans as assessed through fMRI (O'Doherty et al. 2002). In particular, DA cell responses in reward-related learning tasks have been modelled by using the temporal-difference learning algorithm ("TD-learning") derived from the computational theory of reinforcement learning and Markov chains (Schultz et al. 1997; Schultz et al. 2000). Second, Berridge and Robinson (1998) proposed that DA systems mediate the attribution of incentive salience to otherwise neutral stimuli by suggesting that reward processes can be separated in "wanting" and "liking" subprocesses that would be mediated by different neural structures. DA would then mediate the "wanting" (anticipatory, approach-related) but not the "liking" (consummatory) processes. It differs from the reward learning hypothesis in that 6-hydroxydopamine lesions impaired the attribution of incentive salience, but not the associative learning aspects of a Pavlovian task (Berridge and Robinson 1998).

Effects of amphetamine administration

While either acute systemic or intra-nucleus accumbens shell administration of amphetamine are known to elicit hyperlocomotion (through increases in extra-cellular DA concetration), this effect was reversed by intra-medial prefrontal cortex amphetamine injections (Tzschentke 2001), leading to the hypothesis that acute amphetamine effects might be independent of medial

prefrontal function. In fact, single intra-medial prefrontal cortex amphetamine injections do not affect spontaneous locomotor activity or the locomotor –induced activity produced by systemic acute amphetamine administration (Hooks et al. 1992). It is interesting to note that amphetamine administration seems to produce different effects from those produced by cocaine with respect to cortical activity. So, while both drugs do activate mesoaccumbal neurons, only amphetamine inhibits firing of mesocortical neurons (White et al. 1995).

The acute locomotor effects of amphetamine administration seem however to interact in a complex way with behavioural processes in reinforcement-related tasks, in that increasing in motor response under amphetamine administration might be modulated by the presentation of reward-predicting stimuli. So, both Pavlovian-to-Instrumental transfer (PIT) and Conditioned Reinforcement (CRf) tasks are potentiated by amphetamine administration (Cardinal et al. 2002). Potentiation of CRf by amphetamine is known to depend on DA innervation of the nucleus accumbens (Taylor and Robbins 1986) while non-contingent presentation of an appetitive conditioned stimulus elevates accumbens DA levels, in particular in the core region (Ito et al. 2000) and PIT may also depend on the accumbens DA innervation, in that it is abolished by systemic DA antagonist administration (Dickinson et al. 2000) and enhanced by intra-accumbens amphetamine (Wyvell and Berridge 2000). It is also known that both CRf and PIT potentiation by amphetamine depend on the central nucleus of the amygdala (Hall et al. 1999), and this is supported by the fact that this amygdalar region projects to dopamine cells in VTA and so modulates dopaminergic terminals in the nucleus accumbens (Fudge and Haber 2000). Lesions in the accumbens core impair the ability of amphetamine to potentiate responding in CRf (Parkinson et al. 1999), as well as shell lesions abolish the amphetamine potentiation of PIT (Corbit et al. 2001). These data show that psychostimulants such as amphetamine do involve accumbal dopaminergic terminals, giving evidence on the role of DA in the development of sensitisation and addiction.

Previous human studies

A number of previous studies on the effects of amphetamine on brain activity in humans have been performed, in particular through the use of functional neuroimaging (while normally PET is used for non-human primates, (e.g. Price et al. 2002), fMRI has become increasingly common in research with humans). A brief account of those follows.

Amphetamine has been shown to induce anxiety and fear in humans, and the elicitation of this type of affective response seems to correlate with activations in the amygdala. In fact, Hariri *et al* (2002) have shown in a double-blind placebo controlled study, that dextroamphetamine potentiated the response of the amygdala during the perceptual processing of angry and fearful

facial expressions. These results provide evidence of a specific neural correlate for the anxiogenic effects of amphetamine, which also confirms previous animal studies on amygdala activation by amphetamine.

Amphetamine seems in a more general way to be involved in prefrontal dysfunction in humans. In particular, the performance of amphetamine-dependent subjects in decision making tasks seem to mirror the impairments previously observed in ventro-medial prefrontal patients in this type of tasks (e.g. Bechara et al. 1998). Paulus *et al* (2002) designed an fMRI) study to determine the relationship between decision-making dysfunction and neural activation in different prefrontal areas so that the behavioural hypothesis that methamphetamine-dependent subjects in early sustained remission show decision-making dysfunctions could be tested. It was shown that, first, methamphetamine-dependent subjects were more influenced by the immediately preceding outcome during a two-choice prediction task relative to normal comparison subjects. Second, methamphetamine-dependent subjects activated less dorsolateral prefrontal cortex (BA 9) and failed to activate ventromedial cortex (actually, the frontopolar and orbitofrontal cortices, BA 10 and 11) during the two-choice prediction task compared with the two-choice response task. Thus the authors concluded that abnormal activity in dorsolateral (in particular area 9 of Brodman) and ventral medial prefrontal cortices underlies the decision-making impairments in these patients.

However, the relationship between amphetamine abuse and cognitive performance is not so direct. Previously, Mattay *et al* (2000) have examined the physiological correlates of the effects of dextroamphetamine on working-memory performance in healthy controls with fMRI. Interestingly, d-amphetamine improved performance only in those subjects who had relatively low working-memory capacity at baseline, whereas in the subjects who had high working-memory capacity at baseline, it worsened performance. In particular, in subjects whose performance deteriorated, signal change was greater than that in subjects who had an improvement in performance, and these variations were correlated. The authors come to the point of speculating that these heterogeneous effects of d-amphetamine may be explained by genetic variations that interact with the effects of the drug.

The observation of the direct effects of amphetamine in the human brain has been assessed with fMRI previously. Uftring *et al* (2001) used fMRI to evaluate the effects of oral d-amphetamine on brain activation elicited by auditory and simple motor tasks Compared to a placebo pill, amphetamine significantly increased the number of activated voxels in the left and right primary auditory cortices during the tone discrimination task as well as increased the number of activated voxels in the ipsilateral primary sensorimotor cortex and right middle frontal area during the motor task. Although the authors could not rule out completely vascular effects related to amphetamine administration during the task, this study gives good indication that oral

amphetamine administration increases neuronal activity associated with sensory-motor-related tasks. It should be noted that motor areas in the human cortex receive dense DA innervation (Gaspar et al. 1989), and these DA innervations could thus be the substrate for the enhancement of neuronal activity for the case of the motor task.

The psychological and affective aspects of amphetamine administration in humans have also been explored with PET, such mania-like symptoms and euphoria. A study by Vollenweider *et al.* (1998) showed that d-amphetamine produced a mania-like syndrome concomitantly with a widespread increase in absolute cerebral metabolism, which was significant in the anterior cingulate cortex, caudate nucleus, putamen and thalamus. These structures have strong connections with DA structures in the mid-brain, and also with the prefrontal cortex. Drevets *et al* (Drevets et al. 2001) correlated the change in endogenous dopamine concentrations following d-amphetamine administration with the associated hedonic response in human subjects and compared the strength of this correlation specifically across striatal subregions. The d-amphetamine induced changes in euphoria scores correlated with activity in the ventral striatum. Thus this study provides evidence that the magnitude of ventral striatal DA release correlates positively with the hedonic response to amphetamine administration in humans.

However, none of these studies focused on intra-venous systemic administration, or on subjective measures of amphetamine effects that could be used as parameter in analysing activated brain areas.

Intra-venous administration of amphetamine: an event-related fMRI study

We now proceed to describe the fMRI study where intra-venous amphetamine (0.15mg/kg) was administered in naïve subjects. The aim was to investigate the areas of the human brain activated by i.v. M (metha)-amphetamine, and in addition, to relate the brain activation to subjective reports of the degree of "mind-racing" made every minute during scanning. Psychiatrists B. Voellm and P. Cowen from Oxford University performed subject preparation and drug administration. One specific aim of this study was to reveal human brain areas responsive to psychostimulants such as amphetamine before sensitisation and craving takes place.

Materials and methods

Subjects

Seven right-handed healthy subjects were scanned, and the results of analysis of the activations in these subjects are described. [Data from two additional subjects tested with administration of a placebo, one of whom the subjective ratings are available, are not described here. The subjective ratings remained at baseline in the subject who gave ratings].

Protocol

The investigation was run as a single-blind amphetamine/saline study, in that the subjects were not informed when the injection was being given. Saline was infused intravenously for a random period of 10-15 minutes, followed by m-amphetamine (0.15 mg per kg) delivered over a 1 min period, followed by saline for a further period of 20-25 min. The subjects were asked to give ratings of "mind-racing" (on a scale between 0 and 4) every 60 seconds through the use of a button box used by the right hand. The ratings were cued by a visual stimulus, a spot on the screen. These ratings were found in a pilot study to co-vary well with the subjective "rush" effect produced by amphetamine (Voellm and Cowan, personal communication).

Image Analysis

In order to investigate the brain activations related to amphetamine, two different models were constructed: an *on-off design*; and *correlation analysis* using the "mind-racing" ratings. These models and their results are described in detail in the following.

Model 1: On-Off comparison, amphetamine – saline

An on-off model was designed to test for the main effects of amphetamine injection on the BOLD response (see Fig 4.2). Based on inspection of the changes in subjective ratings correlating with drug delivery, the 'on' period was set to have its onset 5 minutes after the start of the amphetamine injection and to last for 10 minutes. The comparison 'off' period was the period of 10-15 min during the initial saline infusion before the amphetamine infusion started.

Pre-processing of the data was performed with SPM99 (Welcome Dep. of Cognitive Neurology, London) for volume realignment, FLIRT (FMRIB, Oxford) was used to perform inter-modal registration and spatial normalisation to the MNI-brain (Collins et al. 1994); spatial smoothing was performed by applying a 8 mm Gaussian filter. Temporal filtering used the HRF (haemodynamic response function) for low-pass filtering and 100 sec for high-pass filtering.

Results

A group fixed effects model was used. The statistics threshold was set to $p<0.05$, corrected for multiple comparisons corresponding to a z value of $z = 4.5$. The contrast of the amphetamine condition against saline revealed a cluster of (30) activated voxels in the medial orbitofrontal cortex (MNI coordinates [12,42,-14], $p<0.05$ corrected for multiple comparisons). These activations are shown in Fig 4.2.

Another significant cluster was found in a rostral region of the anterior cingulate cortex [14 62 2], $z= 6.6$, and [12 56 26], $z=5.4$, $p<0.05$ corrected for multiple comparisons). Significant activations were also found at the (ventral) striatum, MNI coordinates [-4 10 –4], $z = 6.54$. These activations are also shown in Fig. 4.2.

Activations were also found, as evident in the glass brain part of Fig. 4.2, in areas of the motor cortex, the parietal cortex, and the cerebellum. The effects of intra-venous amphetamine were found to be particularly significant in the motor cortex area, MNI coordinates [-30,-2,60], with $Z=6.07$, $p<0.01$ corrected for multiple comparisons. Subjects were asked to produce a "mind-racing" rating at every minute, and this suggests that i.v. amphetamine enhances the effects produced by motor responses in the motor cortex.

The contributions of motor responses in the activations observed will be discussed in sections *Further analyses: identifying motor contributions* and *The activations in the medial orbitofrontal cortex are not motor-dependent*, below. In the latter, it will be discussed the possibily that motor responses do not contribute equally, throughout the cortex, to the activations produced by intra-venous administration of amphetamine, in that motor cortex, but not orbitofrontal cortex activations depict significative interactions with motor responses.

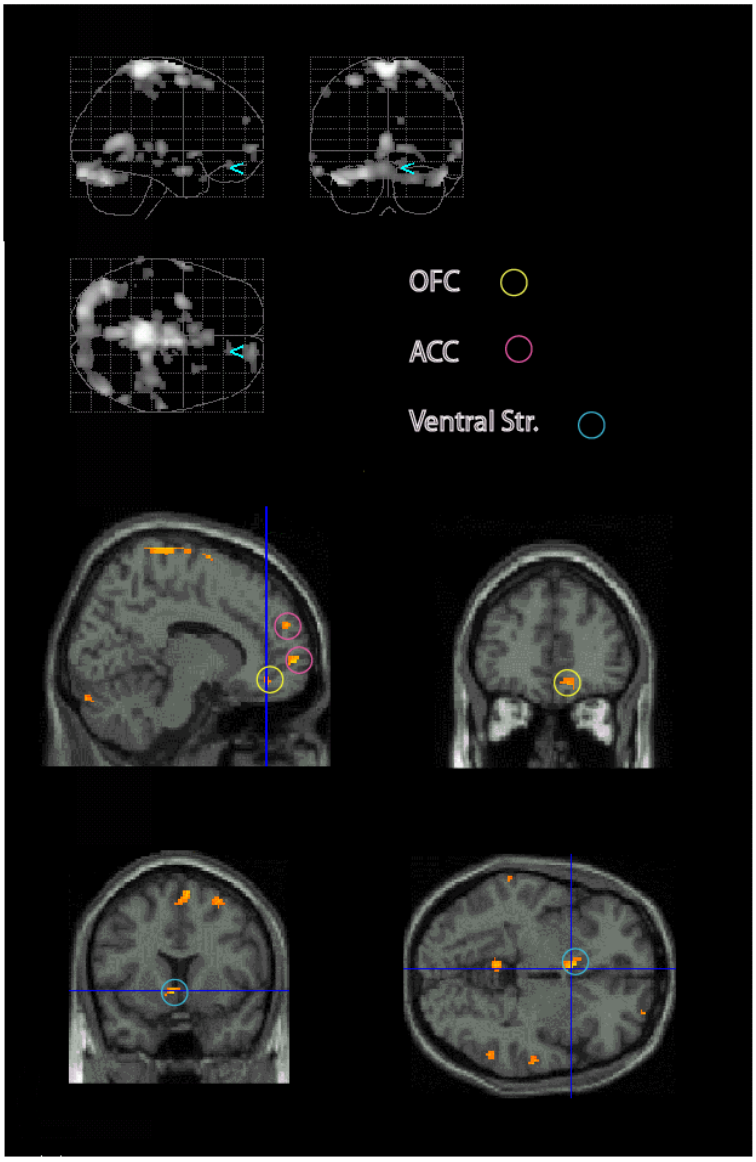


Fig 4.2. Results of on-off comparison between (i.v.) amphetamine and saline. On the top left, the SPM99 glass brain shows the main results. At the middle left is shown a saggital slice with the activations in the medial orbitofrontal cortex (OFC, yellow circle) (x,y,z: [12,42,-14]) shown also at middle right) and anterior cingulate cortex (ACC, yellow circle) (x,y,z: [14, 62, 2], and [12, 56, 26]. At the bottom left is shown a coronal slice with activation in the ventral striatum (Ventral Str., blue circle) (x,y,z: -4,10,-4). The same activation is shown in an axial slice at bottom right. The image was thresholded at , p<0.05 corrected for multiple comparisons,

Model 2: Correlation analysis

In this model the Haemodynamic Response Function (HRF) basis functions used in the SPM analysis were 'parametrically modulated' by the subjective "mind-racing" ratings, and the analysis

showed which voxels had activations that were correlated with the subjective ratings. The BOLD signal that was correlated with the subjective ratings was that obtained at the time each rating was given, using the standard parametric modulation of the HRF basis function. (The SPM design matrix contained four columns with one column designating the button-press event (plus another column for its time derivative), and one column representing the basis functions modelling this event as being modulated by the rating values (and a column for the time derivatives). Because the ratings were made using the right hand and a button box, the analysis subtracted any effect in the BOLD signal that might be related to the button press itself, by subtracting the main effects in the design matrix of the button press.

Pre-processing of the data was performed with SPM99 (Welcome Dep. of Cognitive Neurology, London) for volume realignment, FLIRT (FMRIB, Oxford) was used to perform inter-modal registration and spatial normalisation to the MNI-brain; and spatial smoothing was performed by applying a 8 mm Gaussian filter. Temporal filtering used the HRF for low-pass filtering and 100 s for high-pass filtering.

Results

The correlation analysis just described showed with a fixed-effects group analysis (n=7) significant at $p<0.05$ activation using the small volume correction (S.V.C.) in a number of different brain regions. The activations in each of these regions are illustrated in Fig. 4.3 to show the extent of each significantly activated region at $p<0.0001$ uncorrected.

Activations were found in the medial orbitofrontal cortex (peak at x,y,z=[0,54,-8]; z=3.66); bilateral striatum (putamen/ventral striatum [-18,12,-6]; z=3.95); medio-dorsal thalamus/pulvinar (-4,-12,6; z=6.53); and anterior cingulate cortex (areas 23/24; [0,4,46]; z=5.40).

Further significant activations were found bilaterally in the primary motor cortex ([44,-18,50]; z=5.62 and [–60,16,40]; z=5.17). In addition activations were seen in visual cortical region, probably V5/MT ([50,-74,-4]; z=4.70).

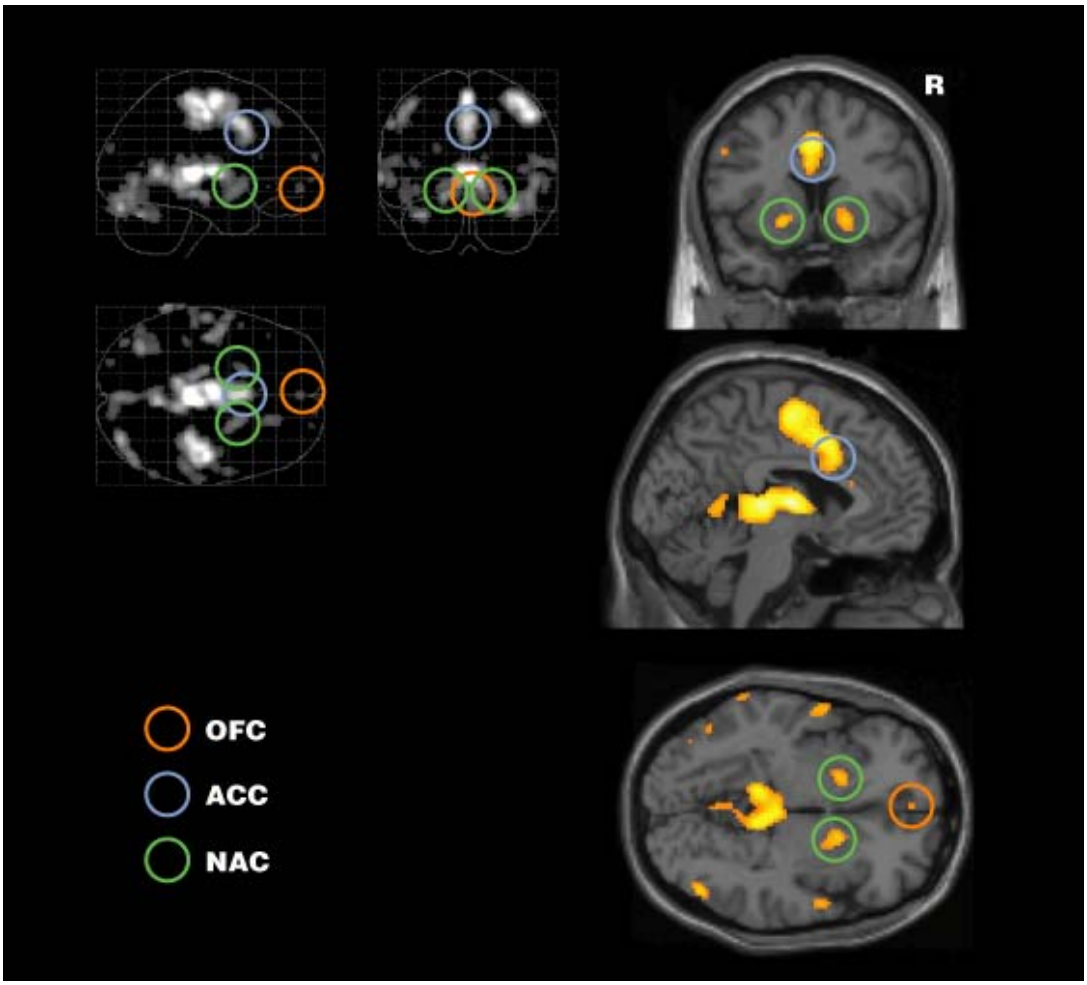


Fig 4.3. Results of correlation analysis with subjective "mind-racing" ratings induced by i.v. amphetamine. On the left, the SPM99 glass brain shows the main results. At the top right is shown a coronal slice with the activation in the ventral striatum/nucleus accumbens (NAC, green circle) (-18, 12, -6; z=3.95). In the middle right is shown a sagittal slice with activation in the anterior cingulate cortex (ACC, blue circle) (areas 23/24; peak at 0,4,46; z=5.40). At the bottom right is shown an axial slice with activations in the NAC and in the medial orbitofrontal cortex (OFC, red circle) (peak at x,y,z=0,54,-8; z=3.66).

Further analyses: identifying motor contributions

A series of three different models was designed to reveal the amphetamine-specific effects in such a way that motor-related effects could be factored out. Given that subjects performed the

"mind-racing" ratings every minute, we decided to delay the relevant onsets for 30 seconds with respect to the button press event.

Model A consisted of an (event-related) parametric-modulation analysis where the relevant parameters were defined as being the mean of two consecutive "mind-racing" ratings and the trial being defined by a 30 seconds delay with respect to the button press event.

Model B consisted of a simple (event-related) on-off design with the two trials being "amphetamine" and "saline". Each of the trial event onsets was defined with a delay of 30 seconds with respect to the button press event. The canonical HRF function (with its time derivative) was selected as the basis function. Simple subtractive contrasts would then reveal the significant activations.

Model C consisted of an epoch-based design with two trials, "amphetamine" and "saline". The trial onsets were defined with a delay of 30 seconds with respect to the button press event. In this case a box-car basis function was used with a fixed duration of 30 seconds. As above, significant activations would be revealed by relevant subtractive contrasts.

The three models were estimated as fixed-effects statistical models. Models A-B revealed similar results in that no significant activations were found at the (relatively low) threshold of $p<0.001$, uncorrected for multiple comparisons.

However, in Model C, when the high-pass temporal filter cut-off is set to 1200s, a significant activation is observed in the medial orbitofrontal cortex, MNI coordinates being [14 48 -12], $Z=5.09$, corrected for multiple comparisons. This cluster of activation (with 150 voxels) overlaps spatially with the medial orbitofrontal cortex cluster found in Model 1.

The results of the analysis with Models A and B lead to the conclusion that the amphetamine-specific effects obtained in models 1 and 2 result mainly from modulation by amphetamine of events happening at the time of the button press event. At the time of the button press, there are movements; and the ratings are being made. In principle, the greater activations occurring at this time could thus reflect modulation of movements, or of more cognitive processes involved in assessing the current state of "mind-racing". However, the results from Model C imply that the activation found in the medial orbitofrontal cortex was not dependent on movement. Moreover, it should be noticed that the activations found in regions such as the medial orbitofrontal cortex, rostral anterior cingulate cortex (ACC), and the ventral striatum have been implicated by other evidence in reward and affect rather than just motor function (Parkinson et al. 1999), and the

activation of these areas produced by amphetamine in this study may thus be related to cognitive (including reward) rather than just motor effects. Further, activation of these areas by amphetamine could play a role in the addiction that can result from repeated use. It should be noted that the subjects participating in this study are (healthy) non-abusers. The analysis below performed on the raw data further confirms the result from Model C above.

The activations in medial orbitofrontal cortex are not motor-dependent

To further clarify the issue of potential motor contributions to the activations observed in the medial orbitofrontal cortex, a region of special interest in this Thesis, the raw fMRI data was extracted from the medial orbitofrontal cluster found to be significant (centred at [12,42,-14]) and from the most significant cluster in the motor cortex (centred at [-30,-2,60]). The data locked to the events where mind-racing ratings were given were separated from those where subjects were at rest in the scanner, so that the contributions made by motor responses to the activations found could be assessed. A two-way ANOVA was performed on the data and revealed that motor responses affected differently the activity in the medial orbitofrontal cortex and in the motor cortex. In the medial orbitofrontal cortex, it was found that the main effects of drug administration was significant at $p<0.03$ ($F[2,4]= 4.1$) whereas no significant effects were found for motor responses ($p>0.1$). In addition, no significant interactions between drug administration and motor responses were found ($p>0.7$). This implies thus that the medial orbitofrontal cortex represents the effects of intra-venous M-amphetamine even if no motor response is required.

However, in the motor cortex, a significant interaction between drug administration and motor responses were found ($F[2,6]= 4.64$, $p<0.03$), suggesting thus that intra-venous amphetamine modulates the responses in motor-related areas of the human cortex.

The above gives further confirmation to the result of inspecting the average level of activity, as measured by the (raw) BOLD signal, in the medial orbitofrontal cortex. The average BOLD signal change across the period (and across all seven subjects) in which subjects have higher concentrations of the drug in the plasma (the "on" period defined in the on-off analysis above) is significantly higher than the saline period. In fact, a pairwise t-test performed on the BOLD signal measures between the on (amphetamine) and off (saline) periods produces a t score of 5.13, significant at $p<0.001$. This is shown in Fig 4.4.

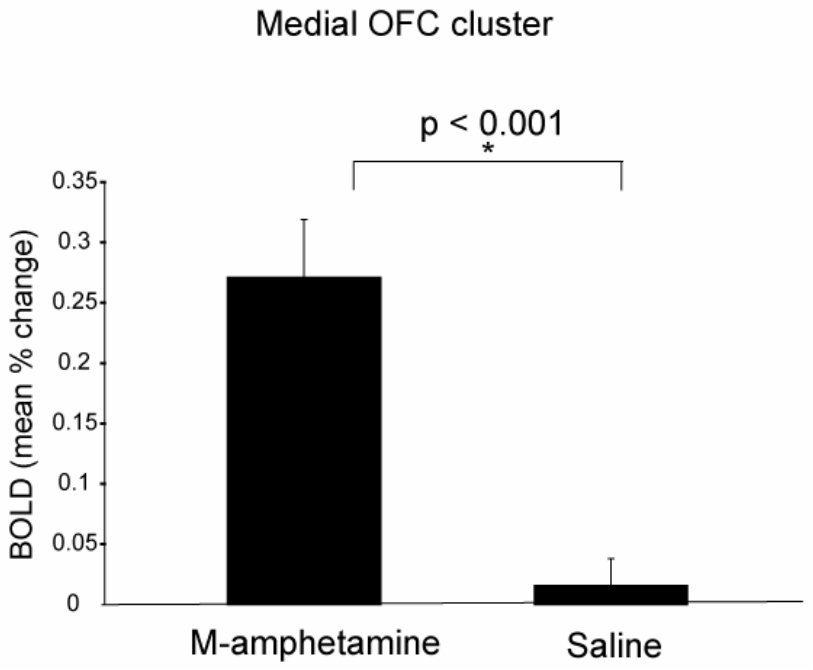


Fig 4.4 The effects of intra-venous amphetamine administration in the levels of activity in the medial orbitofrontal cortex. The figure shows the average BOLD signal (mean % change) across the "on" period in comparison to the "off" (saline) control period. The average was taken across all seven non-placebo subjects.

Discussion

In the on-off analysis (Model 1), the orbitofrontal cortex activation produced by amphetamine is in a similar region to that where the correlation analysis (Model 2) showed that the BOLD signal is directly related to the subjective ratings of mind-racing. The orbitofrontal cortex region is in an area in which there are high concentrations of D1 receptors, as shown in post mortem binding studies in humans (Hurd et al. 2001). Other investigations show that this is in or near an area of the orbitofrontal cortex in which activation can be produced by pleasant odour (Gottfried et al. 2002), monetary reward (O'Doherty et al. 2001a), and pleasant touch (Rolls et al. 2003b). Based on these comparisons, we suggest that the activation of the orbitofrontal cortex by amphetamine may be one of the areas in the brain where amphetamine produces rewarding effects and the associated subjective states. This is in line with the evidence that macaques will learn to self-administer very small quantities of amphetamine to this region (Phillips et al. 1979), and that this is a region where electrical stimulation in macaques is rewarding (Rolls 2000a).

The cingulate, ventral striatum, and thalamic activations found in the correlation analysis (Model 2) are in agreement with the study by Vollenweider *et al.* (Vollenweider et al. 1998) showing with PET that d-amphetamine produced a mania-like syndrome concomitantly with a widespread increase in absolute cerebral metabolism, which was significant in the anterior cingulate cortex,

caudate nucleus, putamen, and thalamus. Dopamine in the ventral striatum is linked to the rewarding and locomotor-stimulant effects of abused drugs like amphetamine (Parkinson et al. 1999). The part of the mid cingulate area revealed in the correlation analysis is in or near to the cingulate motor area (Picard and Strick 2001). Dopaminergic projections to this area are very prominent (Gaspar et al. 1989), and these may be related to the activations shown. The thalamic areas activated include the medial thalamic nucleus (which projects to the prefrontal cortex), and/or the pulvinar, the medial divisions of which have strong connections with the cingulate cortex. These regions may be part of a thalamic-cingulate network processing sensory-motor information.

The correlations revealed in the hand area of the motor cortex (Fig. 4.3) reflect increased activation produced by amphetamine of areas involved in moving the hand to provide the ratings. The finding is in agreement with other studies showing that amphetamine significantly increased the number of activated voxels in primary sensorimotor cortex and right middle frontal area during a finger tapping (motor) task (Uftring et al. 2001). It should be also noted that motor areas in the human cortex receive dense DA innervation (Gaspar et al. 1989).

The results just described based on the analysis using Models 1 and 2 are due largely to an effect of amphetamine on brain processes that occur at about the time the ratings are given. This is what is shown using Models A-B, in which the analysis of the activation was for periods offset by 30 s from when the rating was being given. In these analyses, much smaller effects of the amphetamine were identified. (A control analysis not illustrated of activations of similar duration but not offset from the time of the button press did show similar effects of amphetamine to those identified with Models 1 and 2). Thus the main effect of the amphetamine identified in this study, in areas such as motor cingulate and motor cortex, was to produce changes in brain activations that occur when the ratings are being given and the button press response is being made. Whether these effects of amphetamine (apart from those in the motor areas) are related to the cognitive evaluation of the current state of mind racing, or to the movements being made to press the button, are difficult to establish in this study. This was not the case, however, for the medial orbitofrontal cortex, as shown using Model C above in addition to the raw data analisis of variance, in that the activations in this region do not depend on motor responses given during rating. The fact that areas such as the rostral anterior cingulate cortex and medial orbitofrontal cortex do not respond generally in simple movement tasks does imply that the effects of amphetamine on these regions are related to effects on reward or cognitive processing, and not to effects on movements.

The above was further analysed by inspecting the BOLD signal data extracted from clusters located in the medial orbitofrontal cortex and in the motor cortex. No significant interactions were found between drug administration and motor responses in the medial orbitofrontal cortex whereas this was the case for the motor cortex. This gives an indication that the activations in the orbitofrontal cortex result mainly from the reinforcing properties of amphetamine, as suggested by the involvement of this area of the cortex in general reward-related processing (Rolls 2000a) and the rich dopaminergic innervation in this region (Hurd et al. 2001).

In general, it is worth noting that areas such as the medial orbitofrontal cortex, rostral ACC or ventral striatum are not normally found to be activated in simple motor tasks such as finger tapping. Activity in these areas seem to correlate well with motor response (rating) but could be due to an interaction between motor activity and the activation of dopaminergic terminals in these areas. In fact, CRf and PIT potentiation by amphetamine administration (see above) show exactly that increases in locomotor activity, although normally following this type of treatment, can also indicate that the DA system plays a role in sensitisation processes characteristic of drugs of abuse. The extent to which motor activity contributes to the development of incentive sensitisation and addiction remains to be determined by more precise techniques such as electrophysiological recordings.

In conclusion, M-amphetamine was used in this study as a direct contrast allowing for the characterisation of reward-related areas in the human brain. Of particular interest are the activations in the medial part of the orbitofrontal cortex and in the rostral part of the cingulate cortex (and adjoining areas) whereas no activation was found in more lateral areas of the orbitofrontal cortex (in particular more caudally) and adjoining anterior insular/opercular cortex.

Chapter V
Dehydration and the Taste of Water

In this Chapter we describe an event-related fMRI study in which we investigated the brain responses to the oral presentation of water under different physiological states (*i.e.* dehydrated/sated) in normal human subjects. The rationale behind this study is that different degrees of hydration induce different motivational states in normal subjects so that under dehydration water acquires (primary) rewarding properties. Also, this will help to reveal brain areas involved in monitoring fluid homeostasis.

In this study water-deprived subjects were scanned while being presented water (as well as salt and glucose) orally. They were then removed from the scanner and given water to drink to satiety. After approximately 30 minutes the scanning session was repeated, allowing direct comparison between dehydrated and sated (hydrated) states. As described later in this Chapter, significant differences in brain activation were found for the presentation of water during dehydration in the right mid insular cortex and subgenual cingulate/caudomedial orbitofrontal cortex, with respect to the sated state. In general (*i.e.* not with respect to stimuli presentation) it was found that the (rostral) anterior cingulate cortex was significantly more activated during the dehydration state in comparison to the sated state.

Another finding of interest was that water, when compared to the tasteless control solution containing the main ionic components of saliva, activated primary and secondary taste cortical regions, including the frontal operculum/anterior insula and caudolateral orbitofrontal cortex. These areas activated by water are basically similar to the ones activated by the other tastants, *i.e.* glucose and salt.

In the following we first describe some of the current knowledge on the central mechanisms controlling fluid homeostasis, in particular the role of the peptide angiotensin II and of neural structures located in the anterior wall of the third ventricle (*lamina terminalis*). We then proceed to a description of the abovementioned fMRI study and a discussion of the results.

Introduction: Neural mechanisms of thirst

Monitoring the integrity of the fluid compartment is a fundamental function for homeostatic equilibrium. Changes in the composition of the fluid compartment can be detected by the central nervous system through two parameters (Rolls and Rolls 1982; Watts 2001): plasma osmolarity and extracellular fluid volume. Osmolarity increases, causing cellular dehydration, are detected by osmoreceptors, and possibly Na receptors, located primarily at the rostral end of the third ventricle. Extracellular fluid volume decrease signals are transduced (i.e. transformed into electrical signals conveying information to the brain) by two mechanisms (Grossman 1990): the first one involves the renal juxtaglomerular apparatus and elevates the circulating peptide angiotensin II through the release of renin; the second involves low-pressure baroreceptors in the venous circulation that are capable of altering afferent input to the nucleus of the solitary tract.

Cellular dehydration

Disruption of the correct equilibrium in the fluid compartment can be caused by increased osmotic pressure, leading to intra-cellular dehydration. The mechanism underlying increases in osmotic pressure is an increase in the levels of extracellular sodium-ion concentrations (Rolls and Rolls 1982). It has been postulated that osmoreceptors exist in the central nervous system. In fact, it has been shown that increases in fluid osmolality depolarise hypothalamic supraoptic neurons (Oliet and Bourque 1993). This supraoptic activity will influence the release of vasopressin (also called Anti-Diuretic Hormone, ADH), a peptide hormone synthesized by neurons of the (hypothalamic) supraoptic and paraventricular nuclei. Vasopressin is the major hormone for fluid homeostasis in that it is an anti-diuretic hormone (Fitzsimons 1998; Rolls and Rolls 1982). The supraoptic and paraventricular nuclei influence vasopressin release through the projection of axon terminals to the neurohypophysis.

More recently, it has been demonstrated the existence of a specific sodium receptor candidate located in the circumventricular organs, named "Na_x channel" (Hiyama et al. 2002). This channel has been formerly called NaG/SCL11 in rats and Nav2.1 in humans and has been classified as a subfamily of voltage-gated sodium channels (Hiyama et al. 2002). As will be described in the following paragraphs, activity in the circumventricular organs influences the compensatory autonomic responses to changes in fluid homeostasis, so that the Na_x channel could work as the sodium-level sensor in the brain responsible for the initiation of these autonomic responses in the event of increased osmolarity.

Hypovolemia and the renin-angiotensin system

Information from baroreceptors that monitor vascular wall stretch in the aortic arch and the carotid sinus converges into the central nervous system through projections to the nucleus of the solitary tract in the rostral part of the medulla, and is conveyed from there to the ventrolateral medulla (Saper 2002). A fall in arterial pressure causes reduced net excitatory input from the nucleus of the solitary tract into cardiovagal motor neurons located in the nucleus ambiguus, reducing then vagal firing and thus increasing heart rate (Saper 2002). There is also reduced excitation of inhibitory interneurons in the caudal part of the ventrolateral medulla that project to a population of neurons in the rostral ventrolateral medulla that regulate vasoconstrictor sympathetic tone. The disinhibition of these rostral ventrolateral medullary neurons increases their excitation of vasoconstrictor sympathetic preganglionic neurons, resulting in elevated arterial blood pressure.

Neurons in the caudal ventrolateral medulla project to the hypothalamic area, where they regulate the release of vasopressin. Magno and parvo-cellular vasopressin containing neurons are present in the SON, PVN and supra-chiasmatic nucleus in the hypothalamus. Magnocellular neurons terminate in the posterior pituitary (hypophysis), where vasopressin is stored and released in the bloodstream. A fall in baroreceptor input results then in the release of vasopressin through medullar-hypothalamic projections, thus increasing fluid retention and causing vasoconstriction (Blessing and Willoughby 1985).

The kidney is also sensitive to decreases in blood volume. In fact, a reduction in intra-arteriolar pressure as sensed by the afferent intra-arteriolar baroreceptors at the level of the juxtaglomerular cells leads to the release of renin (Rolls and Rolls 1982). The juxtaglomerular apparatus is the main source of renin, consisting of renin-producing cells in the media of the afferent glomerular arterioles and extraglomerular mesangial cells lying between the glomerulus and the distal tubule of the same nephron (Fitzsimons 1998). Renin is also released when changes are detected in sodium plasma concentration reaching the macula densa, a renal region neighbouring the juxtaglomerular apparatus.

Renin then acts in the plasma as an acid protease, forming angiotensin I which the angiotensin converting enzyme (ACE) transforms into angiotensin II (Rolls and Rolls 1982). Injections of angiotensin II into sensitive areas in the brain produce a vigourous, fast increase in drinking in several mammals, particularly rats and primates, including humans (Fitzsimons 1998). For example, a male Wistar rat will drink ~15ml of water within 15 min of injecting 10 pM angiotensin II in the region of the anterior third ventricle.

The second behavioural response to hypovolemia is increase in sodium appetite. Physiologically, this is mainly the result of activating the renin-angiotensin system. In fact, angiotensin II causes a delayed but robust increase in sodium appetite following the primary manifestation of thirst. NaCl intake is necessary under hypovolemia because not only water, but also the extracellular solute is necessary to restore blood volume at normal levels (Fitzsimons 1998). Normal blood volume levels are eventually restored because increases in angiotensin II are detected by the juxtaglomerular apparatus and inhibit further renin release, acting then as a negative-feedback loop (Rolls and Rolls 1982).

The Lamina terminalis

The circumventricular organs, median preoptic nucleus, and tissue surrounding the anteroventral third ventricle in the lamina terminalis (AV3V region) provide the neural support for thirst and sodium appetite related behaviours, having extensive connections with the hypothalamus, limbic cortex, and brain stem (Fitzsimons 1998). In particular, the lamina terminalis express a high concentration of the angiotensin receptor AT_1 (McKinley et al. 2001).

The lamina terminalis, which forms most of the anterior wall of the third ventricle, consists of the median preoptic nucleus and two circumventricular organs (CVOs), the subfornical organ (SFO) and organum vasculosum of the lamina terminalis (OVLT). These latter two regions lack a blood-brain barrier and, unlike other regions of the brain, are influenced by the hormonal and ionic composition of the blood (McKinley et al. 1999). In particular, this allows these two lamina terminalis organs (*i.e.* SFO and OVLT) to detect changes in plasma angiotensin II concentrations and osmolarity, implying this region in the initiation of drinking behaviour under hypertonic or hypovolemic thirst.

SFO and OVLT have a number of common efferent projections (McKinley et al. 2001). Besides reciprocal projections and efferent targets to the neighbouring median preoptic nucleus, they project into magno and parvocellular regions of the (hypothalamic) paraventricular nucleus (PVN). The PVN supports then lamina terminalis influence on vasopressin release (Miselis et al 1979, 1981) through its efferent terminals in the neurohipophysis. Additional SFO and OVLT efferent projections include lateral and dorsomedial hypothalamic regions, the bed nucleus of the stria terminalis, the periaqueductal grey and, importantly for the fMRI study to be described below, the cingulate cortex (McKinley et al. 2001; Miselis 1981).

SFO and OVLT are also characterised by their dense expression of angiotensin AT_1 receptors, as revealed by *in situ* hybridisation and immunohistochemical studies (Lenkei et al. 1997). Through activation of these receptors, detection of increased levels of circulating angiotensin II by AV3V

organs in the lamina terminalis influences the initiation of compensatory autonomic responses to hypertonicity and /or hypovolemia. In fact, rats undergoing AV3V lesions showed attenuated responses to experimentally induced hypertension (Haywood et al. 1983). Also, direct injection of angiotensin II into the SFO increases arterial pressure (Mangiapane and Simpson 1980). Retrograde tracing injections in the kidney, heart and sympathetic ganglia (Sly et al. 1999) revealed synaptic junctions back to the lamina terminalis, as well as to areas such as the hypothalamus and the nucleus of the solitary tract in the rostral part of the medulla. Besides these direct AV3V-sympathetic connections, circulating angiotensin II influences, through its projections to the (hypothalamic) PVN, sympathetic responses such as cardiovascular rhythm and vasopressin release. In fact, parvocellular neurons in PVN project to sympathetic pre-ganglionic neurons in the intermediolateral column of the spinal cord, so that hypertensive responses produced by SFO stimulation are attenuated by PVN ablation (Ferguson and Renaud 1984).

Interoception

Although the mechanisms underlying autonomic responses to imbalances in the fluid compartment are reasonably well known, thirst remains a behavioural concept, in that it is defined as a motivational state of the organism eliciting drinking behaviour. So, a crucial problem for understanding the neural mechanisms of thirst is the cortical representation of the physiological state of the body under hypertonicity and/or hypovolemia.

The cortical representation of the ongoing physiological state of the organism has been investigated, mainly through anatomical tracing studies focusing on the efferent terminals of the autonomic nervous system (for reviews Craig 2002; Saper 2002). Less precisely, it has been claimed that visceral sensation reaches "conscious appreciation" through these autonomic-cortical projections (Saper 2002).

In fact, the lamina I spinothalamocortical pathway is being shown to convey information to the cortex on several aspects of the physiological condition of the physical body (Craig 2002) through afferent small-diameter fibres that innervate body tissues. Anterolateral cordotomy, when localised to the ascending lamina I pathway, disrupts (contralateral) temperature, pain and visceral sensations (Craig et al. 2000). It is known that in primates the lamina I pathway projects to a specific thalamic nucleus, the posterior part of the ventromedial nucleus (VMpo, Craig et al. 1994), caudal to the basal part of the ventromedial nucleus (VMb) (also known as VPMpc). The VMb receives gustatory and more general visceral information (through vagal and glossopharingeal cranial nerves) from the nucleus of the solitary tract. What is to be noticed is that these two thalamic nuclei are conveyed direct information on the homeostatic state of the

body, through sympathetic (in case of the VMpo) and parasympathetic (VMb) pathways (Craig 2002). This rostrocaudal thalamic organisation reflecting parasympathetic and sympathetic information, respectively, seems to be further represented in the insular cortex. In fact, single cell recordings in alert monkeys show that primary cortical taste areas (*i.e.* receiving parasympathetic cranial nerve inputs through the gustatory part of the nucleus of the solitary tract) are located in the frontal (rostral) opercular cortex extending to the neighbouring anterior insular region (Scott and Plata-Salaman 1999; Yaxley et al. 1990) which constitutes a dysgranular insular region. Recordings from insular regions caudal to the taste area report activity elicited by stimulation of the cervical vagus nerve (Radna and MacLean 1981), indicating then general visceral input in this area. Anatomically, it has been shown that the VMb and the VMpo project in a rostrocaudal topographic organisation into the insular cortex, with the VMb projecting to more rostral regions of the insula including dygranular taste areas (Craig et al. 2000; Pritchard et al. 1986; Yaxley et al. 1990). This topographic organisation in thalamo-insular pathways could then subserve as the substrate for different representations in the cortex of the ongoing homeostatic state of the body, through sympathetic and parasympathetic pathways.

It is important to note however that sympathetic and parasympathetic autonomic information are not completely segregated, in that a characteristic of the lamina I (as well as lamina V, VII and X) pathway is the provision of collaterals converging with cranial nerve parasympathetic input in several levels (Saper 2002). For example, ~80% of lamina I spinothalamic axons send collaterals to the parabrachial nucleus (Hylden et al. 1989) and antidromic activation of spinal dorsal hornal neurons have been obtained from the parabrachial nucleus (Foreman 1999). So, sympathetic and parasympathetic systems might interact in complex ways and such interactions might be reflected in the insular representaion of visceral inputs to these systems.

The functional segregation within the mid and posterior insular cortex suggested by the results of Craig and colleagues may be partially explained by the functional organisation of the posterior thalamic nuclei in humans. In a cytoarchitectonic and immunohistochemical characterisation of the ventral medial nucleus of the human thalamus, (Blomqvist et al. 2000) have demonstrated different reactivity for the calcitonin gene-related peptide (CGRP, an important visceral-related modulator Yasui et al. 1991) within posterior regions of this nucleus. In particular CGRP-positive fibres were observed in an intermediate region located adjacent, but distinct to, VMpc and the posterior ventral medial nucleus of the thalamus (VMpo), named by these authors the posterior nucleus (Po). In fact, this organisational feature of the human thalamus will prove to be important for interpreting any results suggesting segregation within the insular cortex. See Discussion below.

Previous imaging studies

Denton and colleagues have performed a series of PET studies on the brain representation of the genesis and satiation of thirst (Denton et al. 1999a; Denton et al. 1999b). Thirst was induced by infusion of hypertonic saline and subjects were also scanned after drinking water to satiation. In general, correlation between thirst score and regional cerebral blood flow was particularly significant in the cingulate cortex. Also "maximum thirst" activations were found in several cingulate areas, as well as the thalamus and insular regions. Interestingly, most cingulate activations decreased to sub-significant levels after satiation.

However, as seen previously, injecting saline to induce thirst alters only one of the parameters used by the central nervous system to detect changes in the fluid compartment, that is, osmotic pressure due to changes in extra-cellular Na concentrations. So, induced thirst through hypovolemia might result in different cortical representations for the changes in fluid homeostasis. As we will see, the most straightforward way to induce hypovolemic (additional to osmotic) thirst is to deprive subjects from fluids for a minimum amount of time.

In the following, we describe an event-related fMRI study in which we investigated the brain responses to the oral presentation of water (as well as glucose and salt) under different physiological states (*i.e.* dehydrated/hydrated) in normal human subjects. This study intends to reveal the cortical representations of (i) the "taste" of water under different physiological conditions and (ii) the central monitoring of fluid homeostasis.

Cortical responses to water in the mouth and its modulation by the level of thirst: an event-related fMRI study

Summary of the study

In an event-related fMRI study in humans it was shown, first, that water produces activations in cortical taste areas (in particular the frontal operculum/anterior insula which is the primate primary taste cortex, and the caudal orbitofrontal / secondary taste cortex) comparable to those produced by the prototypical tastants salt and glucose. Second, the activations in the frontal operculum/anterior insula produced by water when thirsty were still as large after the subjects had consumed water to satiety. Third, in contrast, the responses to water in the caudal orbitofrontal cortex were modulated by the physiological state of the body, in that responses to the oral delivery of water in this region were not found after the subjects had drunk water to satiety. Fourth, further evidence that the reward value or pleasantness of water is represented in the orbitofrontal cortex was that a positive correlation with the subjective ratings of the pleasantness of the water was found with activations in the caudal and anterior orbitofrontal cortex, and also in the anterior cingulate cortex. Fifth, it was found that a region of the mid part of the insula was also activated by water in the mouth, and further that this activation only occurred when thirsty. Sixth, analyses comparing pre- and post-satiety periods (i.e. when thirsty and when not thirsty) independently of stimulus delivery revealed higher activity levels in the rostral anterior cingulate cortex. The activity of the rostral anterior cingulate cortex thus appears to reflect the thirst level or motivational state of the subjects.

Introduction

Thirst is a subjective sensation aroused by the lack of water. Thirst is sensed by an increase in the tonicity of the body fluids by receptors in the preoptic area, and by a decrease in the body fluid volume (Fitzsimons 1998; Rolls and Rolls 1982). Water in the mouth tastes pleasant when thirsty but not when satiated (Rolls 1981), and this alteration in the reward or affective value of the water is thought to be part of the control mechanism by which water is consumed when thirsty, but not after water has been drunk to satiety (Rolls 1999).

It has been shown in macaques that water in the mouth activates neurons in the primary taste cortex in the anterior insula and adjoining frontal operculum (Scott et al. 1986a; Yaxley et al. 1990), and in the secondary taste cortex in the caudal orbitofrontal region (Rolls et al. 1990). In the primary taste cortex the responses to taste stimuli are not decreased after satiety (Rolls et al. 1988; Yaxley et al. 1988), but in the secondary taste cortex the neuronal responses to water in the

mouth are large when thirst is present, and decrease to zero during drinking to satiety (Rolls et al. 1989). Thus the reward value of water in the mouth is correlated with the responses of single neurons in the orbitofrontal cortex, but the responses of neurons in the macaque primary taste cortex reflect the identity and concentration of the tastant, but not its affective value.

In humans, much less is known of the neural mechanisms underlying thirst and the reward value of water intake. In a PET (positron emission tomography) study, Denton and colleagues investigated the brain representation of the genesis and satiation of thirst (Denton et al. 1999a; Denton et al. 1999b). The conditions investigated included the initial state, a state after thirst was induced by infusion of i.v. hypertonic saline, and a state after the subjects had drunk to satiety. A correlation between the thirst scores and regional cerebral blood flow was reported in the anterior cingulate cortex. This study did not investigate neural responses to the delivery of water in the mouth, or with any modulation of that response by the level of thirst. In another PET study, water has been shown to activate taste-related cortical areas in humans (Zald and Pardo 2000a), but there was no condition to control for placing a fluid in the mouth that was similar to saliva. The aims of the investigation described here were to investigate cortical areas of the human brain activated by the delivery of small quantities of water to the mouth with an adequate control for non-specific effects of placing a fluid in the mouth provided by a tasteless solution with the main ionic components of saliva; to compare these areas with known taste cortical areas identified by prototypical taste stimuli such as sweet (glucose) and salt (NaCl) incorporated into the experimental design; to investigate which cortical areas were activated by water in the mouth independently of thirst, and which cortical areas only respond to water in the mouth when thirst was present; to investigate the brain areas in which the activation is correlated with the subjective pleasantness and refreshment value of water in the mouth; and to investigate brain areas in which the level of activity even in the absence of any oral stimulation was different during thirst produced by mild water deprivation as compared to the satiated state produced after water had been drunk to satiety. How water in the mouth is sensed, and whether it should be classified as a taste, is considered in the Discussion. A wider aim of this study was to provide further evidence on the brain areas involved in emotion, for emotions can be defined as states elicited by rewarding (generally subjectively pleasant) and punishing (generally subjectively unpleasant) stimuli, and the investigation of where the pleasantness of water is represented in the brain thus provides one part of a systematic study of the brain regions involved in affect (Rolls 1999).

Materials and Methods

Subjects

Eleven healthy right-handed subjects (of which 5 were males) participated in the study. Written informed consent from all subjects and ethical approval from the Central Oxford Research Ethics Committee were obtained before the experiment. Subjects were asked to arrive at the scanning session (which was generally between 5 and 8 pm) after 6-8 hours of fluid deprivation. They were allowed during this time to take a light meal (e.g. a light sandwich) and to drink one cup of coffee or tea.

Stimuli

Three different stimuli were used: mineral water (Evian, France), 0.5 M glucose (Sigma), and 0.05 M salt (NaCl, Sigma). The glucose was chosen in preference to sucrose for direct comparison with the neurophysiological studies described in the Introduction in which an aim was sometimes to produce rapid satiety during investigations of hunger. The concentrations of the two prototypical tastants were chosen to be approximately equally intense based on psychophysical tests performed on a panel of subjects. All stimuli were diluted and delivered in the mineral water, and were delivered at room temperature. A tasteless solution (containing the main ionic components of saliva, 25 mM KCl + 2.5 mM $NaCO_3$) was used as a control stimulus.

Experimental design

The experimental protocol consisted of an event-related interleaved design using four stimulus conditions (the three stimuli described above, and the tasteless control solution). Stimuli were delivered to the subject's mouth through four polythene tubes that were held between the lips. Each tube of approximately 1 meter in length was connected to a separate reservoir via a syringe and a one-way syringe valve (supplied by Fisher Scientific Ltd., UK).

Initially, subjects were scanned when mildly fluid deprived as described above. At the beginning of each trial (the timing of which is shown in Fig. 5.1), one of the four stimuli chosen by random permutation was delivered in a 0.75 ml aliquot to the subject's mouth. The subject was instructed to make one tongue movement to distribute the fluid in the oral cavity, then 11 sec after the delivery of the stimulus, swallowing was cued by a visual stimulus (following initial instruction and training). The swallowing period was three seconds long, followed by three rating periods over a period of 21 seconds. In the first rating period the pleasantness of the stimulus was rated,

in the second intensity, and in the third the refreshment value. Each rating was cued by a question on the screen for two seconds, and was made during five seconds using a button box on a visual analog rating scale shown on the screen anchored at +2 for very pleasant/ intense/refreshing, and at -2 for very unpleasant/weak/non-refreshing. After the three ratings, the tasteless control solution was administered in exactly the same way as the main stimulus with the same single tongue movement being made, and the subject was cued to swallow again after 11 seconds. The next trial started after a three second interval for swallowing, and a one second inter-trial gap.

The tasteless solution was used as the comparison condition for the stimulus solution delivered first in each trial, and allowed effects such as somatosensory effects produced by liquid in the mouth, and the single tongue movement made to distribute the liquid throughout the mouth, to be controlled for. The tasteless solution also provided a rinse before the oral stimulus provided on the next trial. A taste trial was performed permutatively for each of the four stimuli, and the whole cycle was repeated 9 times.

After the first scanning session, the subjects were taken out of the scanner and allowed to drink mineral water to satiety. Subjects drank on average 1.6 litres of water (sd = 0.46), although care was taken to ensure that they could not count how many cups they had consumed by providing the water in a large (0.5 litre) jug. A second and identical scanning session was then run.

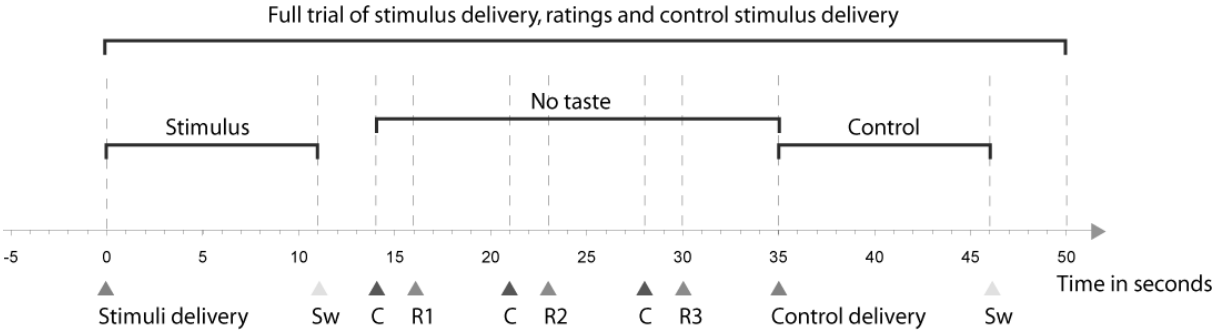


Fig. 5.1. Each full trial lasts 50 seconds as shown in the figure. The stimulus is delivered at time 0 and swallowing (Sw) is cued after 11 seconds and completed within a period of three seconds. The three subjective ratings are then taken during a non-taste period of 21 seconds. Each rating begins with a cue (C) which is on for two seconds, and each of the subjective ratings of pleasantness, intensity and refreshment (R1, R2 and R3, respectively) are taken during a period of five seconds (subjects are pretrained). The tasteless control solution is delivered at time 35, and 11 seconds later swallowing is cued for a period of three seconds, which is followed by a one second intertrial gap period.

fMRI data acquisition

Images were acquired with a 3.0-T VARIAN/SIEMENS whole-body scanner at the Centre for Functional Magnetic Resonance Imaging at Oxford (FMRIB), where 14 T2* weighted EPI slices were acquired every 2 seconds (TR=2). We used the techniques that we have developed over a number of years to carefully select the imaging parameters in order to minimise susceptibility and distortion artefact in the orbitofrontal cortex as described in detail by Wilson et al. (2002). The relevant factors include imaging in the coronal plane, minimizing voxel size in the plane of the imaging, as high a gradient switching frequency as possible (960 Hz), a short echo time of 25 ms, and local shimming for the inferior frontal area.

The matrix size was 64 x 64 and the field of view was 192 x 192 mm yielding 3 mm x 3 mm in-plane resolution. Continuous coverage was obtained in 14 slices from +60 (A/P) to –38 (A/P). Acquisition was carried out during the task performance yielding 900 volumes in total for each session. A whole brain T2* weighted EPI volume of the above dimensions and an anatomical T1 volume with slice thickness 1.5 mm and in-plane resolution of 1.5 x 1.5 mm was also acquired.

fMRI data analysis

The imaging data were analysed using SPM99 (Wellcome Department of Cognitive Neurology, Institute of Neurology, London). Pre-processing of the data used SPM99 realignment, reslicing with sinc interpolation, normalization to MNI coordinates (Collins et al. 1994) (the coordinate system used throughout this Thesis) and spatial smoothing with a 10 mm full width at half maximum isotropic Gaussian kernel and global scaling. The time series at each voxel were high-pass and low-pass filtered with a haemodynamic response kernel. A general linear model was then applied to the time course of activation of each voxel and linear contrasts were defined to test the specific effects of each condition. Voxel values for each contrast resulted in a statistical parametric map of the t statistic which was then transformed into the unit normal distribution (SPM Z).

Comparisons were defined between each of the stimuli and its corresponding control stimulus within a trial. Conditions were thus defined for water delivery (water) and for the control trial-specific tasteless delivery following each water delivery (control_water). This way the statistical parametric maps for effects of water could be defined by the comparison: [water - control_water]. Similarly, comparisons were defined for salt and glucose with respect to their corresponding control conditions (control_salt and control_glucose). Thus the contrasts for each of these comparisons were mutually orthogonal. In addition, these conditions were defined for both the pre- and post-satiety periods.

Group effects were assessed by conjunction analyses across different stimulus conditions and second-level, random effects analysis. The main effects of taste was defined as the conjunction contrast: [water - control_water] AND [salt – control_salt] AND [glucose – control_glucose]. Reported p-values based on this group analysis for a priori regions of interest (e.g. the insula/operculum and the orbitofrontal cortex) were corrected for the number of comparisons made within each region using the small volume correction (S.V.C.) procedure (Worsley et al. 1996). Checks were performed using the estimated motion as a covariate of no interest to rule out the possibility of the observed results being due to motion-related artifacts.

Results

Behavioural data

The ratings given by subjects to the pleasantness of water during the first (pre-satiety) period are significantly higher than the ones given during the post-satiety period (mean ± sem): 0.76 ± 0.18 for the pre period and 0.1 ± 0.15 for the post period. A one-tailed pairwise Student's t-test performed on these ratings resulted in a t-value of $t=2.48$ ($p<0.03$, $df=10$). No significant differences were found with respect to the other stimuli used, that is the pleasantness of the glucose (0.74 ± 0.20) and of the salt (-1.14 ± 0.15) were not altered by drinking water to satiety (Rolls et al. 1983).

To complement these pleasantness ratings, refreshment ratings were also taken throughout the experiment. As expected, the water was rated as more refreshing while thirsty than after satiety. Indeed, t-test comparisons between pre-satiety and post-satiety refreshment ratings revealed that water was found to be significantly more refreshing before drinking water to satiety (0.90 ± 0.14) than during the post period (0.09 ± 0.2). A one-tailed pairwise Student's t-test performed on these ratings resulted in a $t=2.78$ ($p<0.02$, $df=10$). No significant differences were found with respect to the other stimuli used. (The refreshment ratings were +0.41 ± 0.22 for the glucose, and -1.11 ± 0.20 for the NaCl.) We found that the refreshment ratings correlated highly with the pleasantness ratings ($r=0.89$, calculated over all subjects and all stimuli), and also that the correlations with the brain activations (see Fig. 5.8) were similar for pleasantness and refreshment, and therefore focus for the remainder of this Chapter on the pleasantness rather than the refreshment ratings.

No significant differences for intensity were found with respect to any of the stimuli, as expected (Rolls et al. 1983), indicating that the hedonic response to water is independent of any simple, perhaps peripheral, gating of the neural response, which would have altered the perceived

intensity. (The intensity ratings were -1.15 ± 0.14 for water, +1.28 ± 0.14 for the glucose, and +1.38 ± 0.16 for the NaCl.)

fMRI data analyses

To meet the aims of this investigation, the analyses described next included the following. First, we describe the cortical responses to water in order to compare them with those produced by prototypical tastants such as salt and glucose. Second, we describe the similarities and differences in the neural activity produced by water when thirsty and when satiated. Third, we correlated the subjective ratings of the pleasantness, refreshment, and intensity with the activation produced in different cortical areas. Fourth, we compare the level of activity (that is independent of any stimulus being delivered) in different brain areas while thirsty and after drinking to satiety.

The taste of water

In order to establish the cortical regions activated by water (including the two phases of the experiment) we initially performed a group analysis to reveal which voxels were significantly activated by the comparison [Water – Tasteless solution] including both the pre- and post-satiety sessions. This analysis revealed activations illustrated in Fig. 5.2 bilaterally extending from the anterior insula / frontal opercular cortex (e.g. [37 22 3], $Z = 4.98$, $p<0.05$ corrected for multiple comparisons; and [-33 22 3], $Z = 4.67$, $p<0.05$ corrected for multiple comparisons) (see coronal sections at top left of Fig. 5.2) to a more mid insular / opercular region (e.g. [-60 –2 18], $Z = 5.05$, $p<0.05$ corrected for multiple comparisons; and [37 6 -4], $Z = 4.84$, $p<0.05$ corrected for multiple comparisons) (see horizontal sections in the bottom right of Fig. 5.2); in medial parts of the caudal orbitofrontal cortex (OFC) ([-1 35 -16], $Z = 3.9$, $p<0.03$ S.V.C.; and [9 19 -16], $Z = 3.7$, $p<0.05$ S.V.C.); and in the two parts of the rostral anterior cingulate cortex and adjoining cortex (e.g. [1 24 39], $Z = 4.82$, $p<0.05$ corrected for multiple comparisons) (labelled ACC in the upper left part of Fig. 5.2).

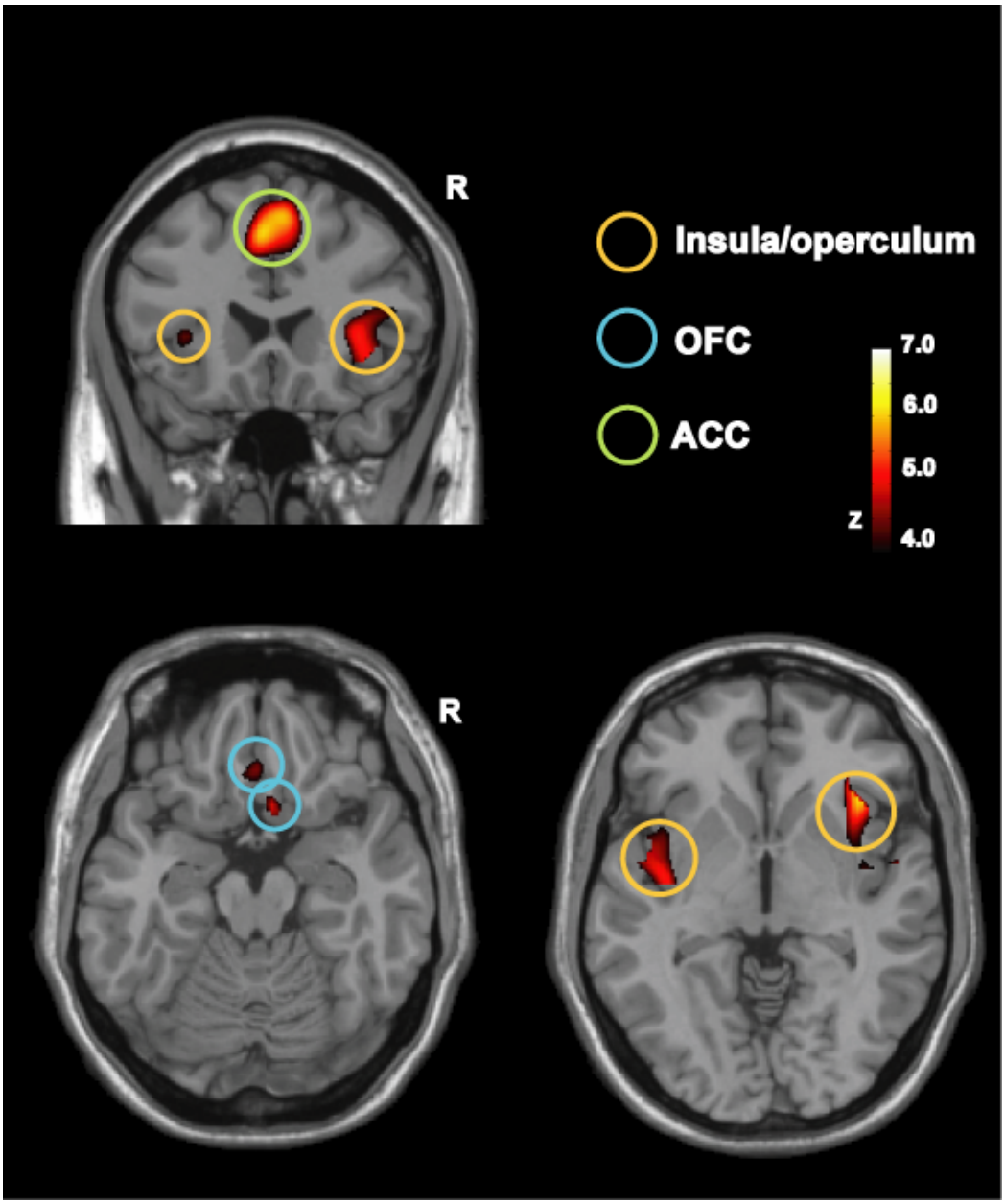


Fig. 5.2. Analysis showing the group main effect for the comparison (water - control_water). Significant activations were found in the insular / opercular cortex, the orbitofrontal cortex (OFC), and the anterior cingulate cortex (ACC) (see text for details). The activations were thresholded at p<0.0001, uncorrected for multiple comparisons, to show their extent. The scale shows the z scores (uncorrected for multiple comparisons). Values greater than 4.54 are significant at P < 0.05 corrected for multiple comparisons.

To determine if water does activate similar areas to those activated by the prototypical tastants glucose and salt, we performed the conjunction analysis described in the Materials and Methods section. This conjunction analysis revealed significant activations in the bilateral operculum/insula ([39 24 4], Z = 5.17, p<0.05 corrected for multiple comparisons), caudal

orbitofrontal cortex ([2 30 -18], Z = 4.53, p<0.05 corrected for multiple comparisons), and in two parts of the rostral anterior cingulate and adjoining cortex ([2 40 16], Z = 7.17, p<0.05 corrected for multiple comparisons; and [-2 32 37], Z = 4.47, p<0.05 corrected for multiple comparisons). The results of this conjunction analysis are shown in Fig. 5.3. This conjunction analysis thus shows that water elicits responses in similar cortical areas to those activated by prototypical tastants such as glucose and salt. The timecourse of activation for an anterior right insula cluster ([40 20 0]) for water, glucose and salt are shown in Fig. 5.5 (lower). The responses to the different stimuli are similar.

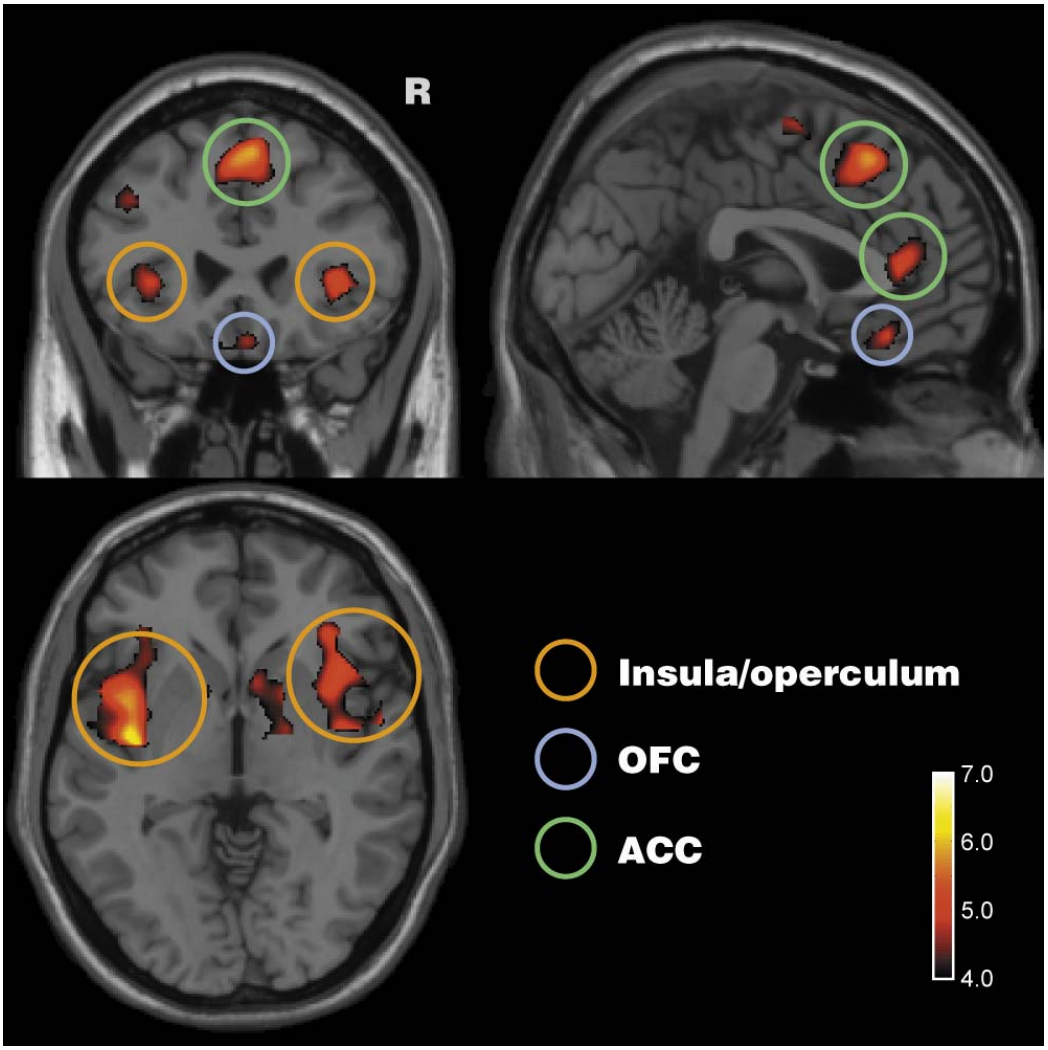


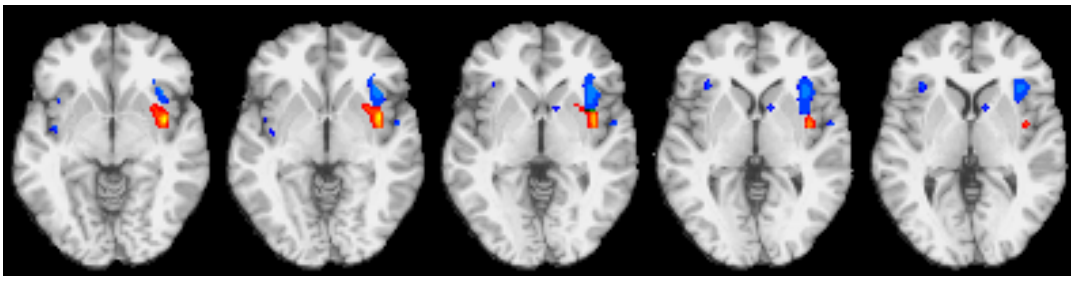
Fig. 5.3. Conjunction analysis revealing the main effects of taste across the comparisons (water- control_water) AND (glucose-control_glucose) AND (salt-control_salt). Significant activations were found in the insular, opercular, anterior cingulate and orbitofrontal cortices (see text for details). The activations were thresholded at p<0.0001, uncorrected for multiple comparisons, to show their extent.

Modulation of water in the mouth by the level of thirst

Second, we investigated how the physiological state of the organism modulates the brain responses to the oral delivery of water. We first aimed to reveal which brain areas responding to water in the mouth are not modulated by the level of thirst. We thus performed a conjunction analysis across the conditions [water pre – tasteless pre] AND [water post – tasteless post]. This revealed significant bilateral activations by water when both thirsty and satiated in the anterior part of the insular / frontal opercular area (*e.g.* [± 40 20 0] $Z = 4.8$, $p<0.05$ corrected for multiple comparisons). These activations are depicted in *blue* in Fig 5.4a. The timecourses of these activations produced by water for a cluster centred in the right anterior part of the insula, for both pre- and post-satiety periods, are shown in Fig 5.5 (upper), and confirm that the activations produced by water are similar when thirsty and when satiated. As shown in Fig. 5.4a, this region extends anteriorly to include some voxels in the caudolateral part of the orbitofrontal cortex which adjoins the frontal operculum and insula.

To uncover brain areas where the activation produced by water in the mouth is modulated by the level of thirst, the contrast [water pre – water post] was computed in each individual subject. A second-level, random effects analysis performed on these contrasts revealed a significant cluster of voxels in the caudomedial orbitofrontal cortex (areas 25/11, [6,22,-7], $p<0.005$ uncorrected for multiple comparisons), as shown in Fig. 5.4b. This cluster adjoined and may have included some voxels in the subgenual anterior cingulate cortex. In addition, the second-level, random effects analysis performed on these contrasts revealed a significant cluster of voxels in the right mid insula ([34 –4 -4], $Z = 3.55$, $p<0.05$ corrected with S.V.C.), as shown in *red* in Fig. 5.4a. The corresponding timecourses for this right mid insula region (centred at [34 –4 -4]) are shown in Fig. 5.6. Thus in both the medial orbitofrontal cortex, and a mid part of the right insular cortex, the oral delivery of water produced smaller effects when satiated than when thirsty.

A



B

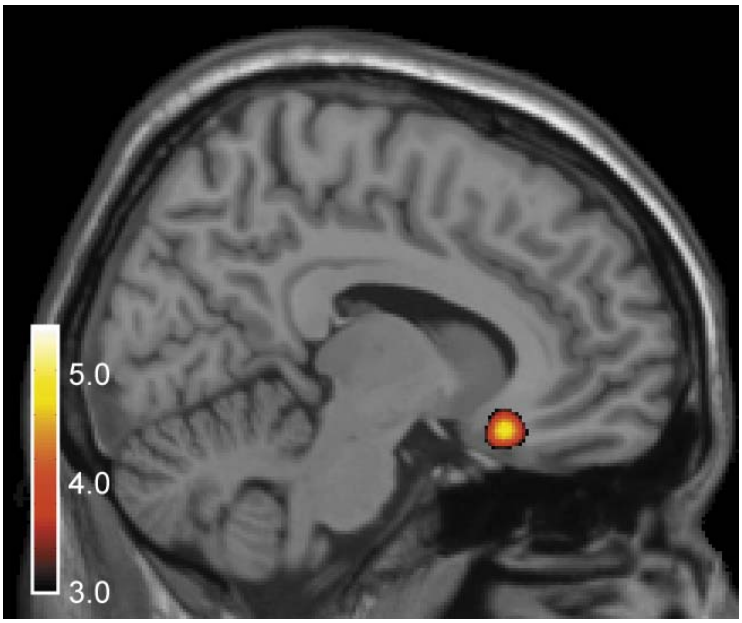


Fig. 5.4. Comparison of the effects of delivering water in the mouth during the pre (dehydrated) period against the post (hydrated) period (water pre – water post satiation). a) Axial sections through the insular cortex showing the main effects of water through conjunction analysis : [water_pre – control water_pre] AND [water_post – control_post], in blue); and the results of [water_pre – water_post] satiation (in red) as revealed through second-order, random effects analysis. Activations were thresholded at p< 0.001 uncorrected to show their extent. b) Sub-genual cingulate/medial orbitofrontal cortex activation in the [water_pre – water_post] comparison as revealed through second-order, random effects analysis. Activations were thresholded at p< 0.001 uncorrected to show their extent.

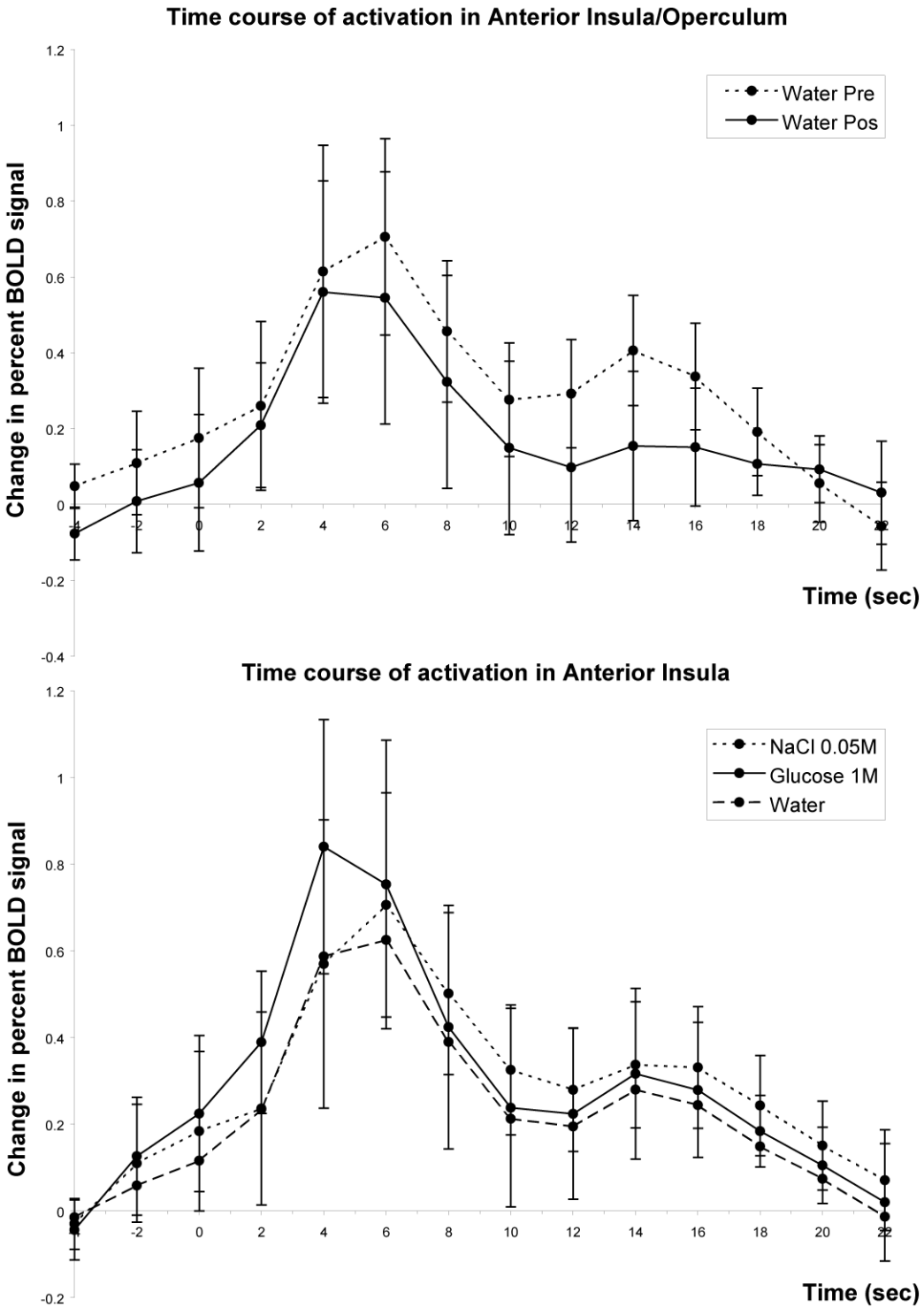


Fig. 5.5. Timecourses of activation extracted from a cluster in the right anterior insula (MNI coordinates [40,20,0]) with respect to the delivery of ***a)*** *Water, with the response shown separately for the presatiety and postsatiety states and* ***b)*** *Water (throughout the experiment), salt and glucose.*

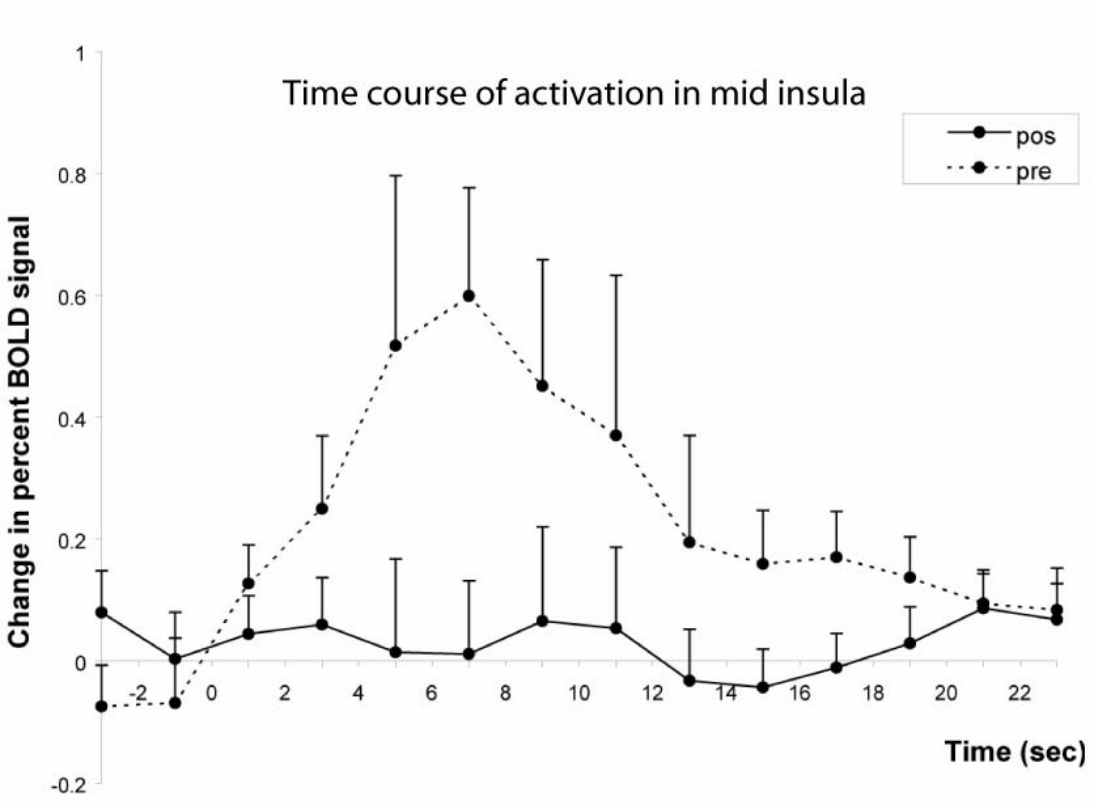


Fig. 5.6. Timecourses of activation extracted from a cluster in the right mid insula (MNI coordinates [34,-4,-4]) with respect to the delivery of water, shown separately for presatiety and postsatiety states. This region (Y=-4) was acquired coronally after 1 second from the start of volume acquisition, and this is reflected in the time axis scale.

To provide further evidence on the activations produced by placing water in the mouth before and after satiation with water, we show in Fig. 5.7 the BOLD signals (mean across subjects +/- sem), obtained from the timecourse of the activations in the reported main clusters. This analysis confirms what was found in the main random effects and conjunction analyses illustrated in Fig. 5.4. In particular, Fig. 5.7 shows that there was no significant reduction in the BOLD signal in the clusters illustrated in blue in Fig. 5.4a in the anterior insula/opercular taste area. On the other hand, there was a significant reduction in the activations produced by drinking water to satiety in the medial orbitofrontal cortex (the area illustrated in Fig. 5.4b); and also in the right mid insula region shown in red in Fig. 5.4a. This analysis helps to confirm that the anterior insula / opercular area behaves differently to the mid-insular area in this paradigm. These conclusions were supported by a 2-way ANOVA on the data shown in Fig. 5.7 (for the time period 4-12 s post stimulus delivery), with one factor dehydrated vs hydrated, and the other factor the brain region, and the interaction was significant ($F[2,6]= 40.8$, $p< 0.001$), providing further evidence that the activations produced by water in the different brain regions were differently affected by whether thirst was present.

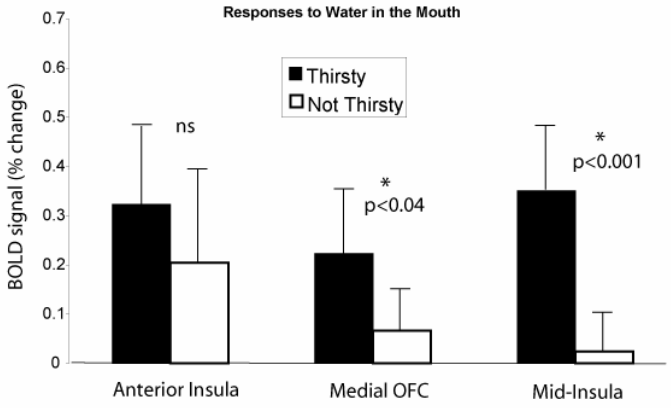
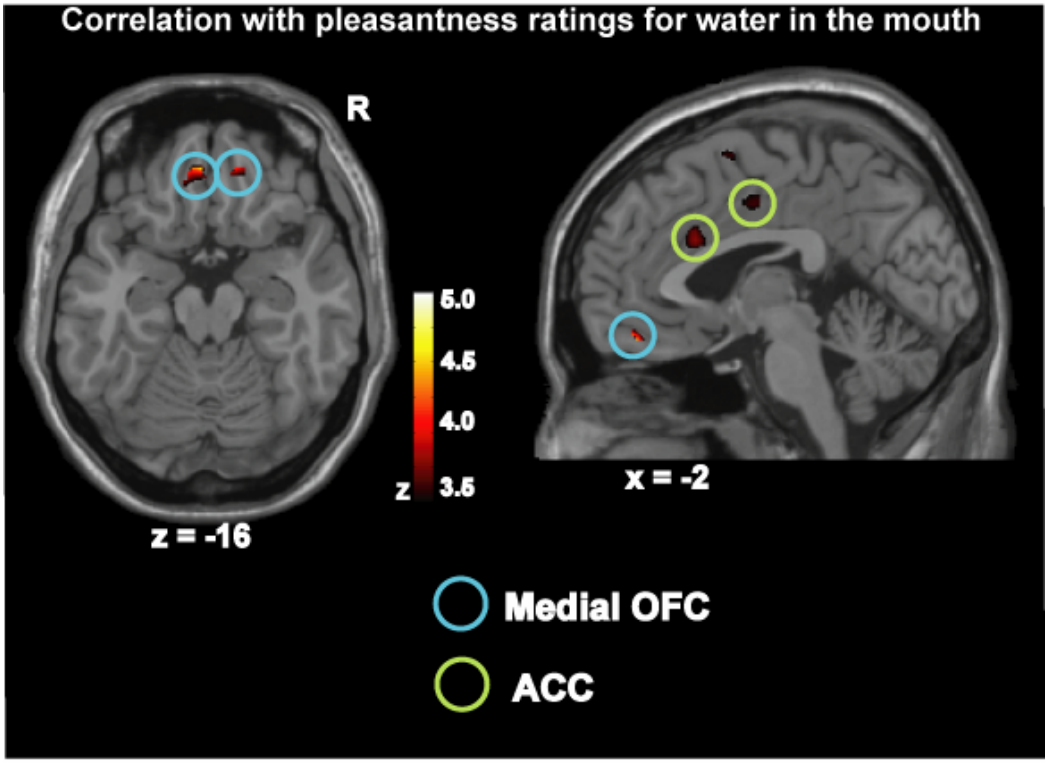


Fig. 5.7. The change in the BOLD signal produced by water in the mouth when thirsty, and when not thirsty following drinking water to satiety, in three different regions. The mean and standard error of the mean across 11 subjects is shown, measured from the time course in the relevant clusters of voxels.

Correlations with subjective ratings

We correlated brain activity with the subjective pleasantness ratings for the water stimulus taken across the whole experiment. Most importantly we found (in a group random effects analysis) that a region of the medial orbitofrontal cortex ([-3,45,-16]; $z=3.92$, $p<0.05$ S.V.C.); and ([16,46,-16]; $z=3.42$, $p<0.001$) was significantly correlated with the pleasantness ratings of water (see Fig. 5.8 left top), which is quite close to the region illustrated in Fig. 5.4b which describes a related comparison. A scatter plot showing the values of the BOLD signal in the first medial orbitofrontal cluster of voxels described is shown in Fig. 5.8 below, with the regression line shown. This emphasizes the strong relation between the pleasantness ratings of water and the activation in this medial orbitofrontal cortex region. We also found that regions of the anterior cingulate cortex (ACC) at [-2,19,28] and [-2,-5,43] were significantly correlated ($p<0.0001$) with the pleasantness ratings of water across the whole experiment (see Fig. 5.8). In addition (not shown in Fig. 5.8), inspection at lower thresholds showed that there was some correlation with the pleasantness ratings for water in a part of the mid insula close to that illustrated in Fig. 5.4a in

red [47,-1,6, z=2.9, p<0.005]. No significant correlations were found with the intensity ratings. The finding that there is no correlation of the activation of any brain area in this study with the intensity ratings is important, for it shows that the correlations of activation of the medial orbitofrontal cortex with pleasantness cannot be ascribed to a different factor such as intensity.



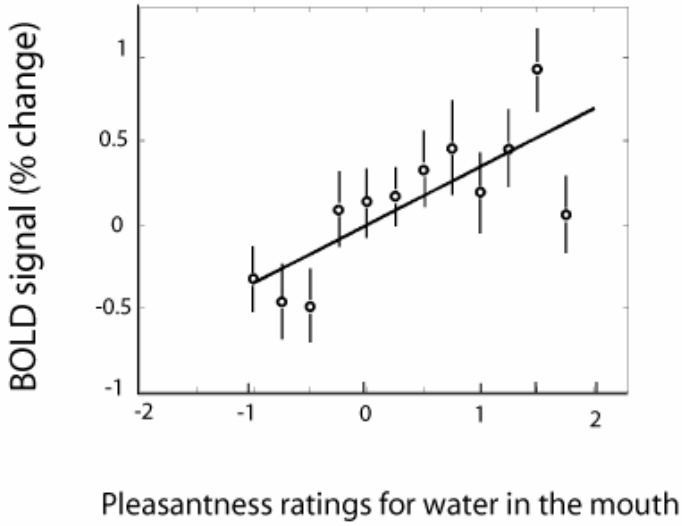


Fig. 5.8. Correlations with the pleasantness of the taste of water in a group random effects analysis. Top left: Regions of the medial caudal orbitofrontal where the activation was correlated with the subjective pleasantness ratings of water throughout the experiment. Bottom: A scatter plot showing the values of the BOLD signal in the medial orbitofrontal cortex (mean across subjects, +/- sem), with the regression line shown (r = 0.79). Top right: The regions of anterior cingulate cortex (ACC) where activation was correlated with the subjective pleasantness ratings of water given throughout the experiment.

Levels of brain activity that were different in the pre and post satiation state measured when stimuli were not being delivered

We created a comparison between pre-satiation and post-satiation periods independently of stimulus delivery events. The analysis was performed for the period 14 – 35 sec with respect to the onset of the stimulus in each trial, which is, as shown in Fig. 5.1, a time when no stimuli were being delivered. This comparison revealed significant activity differences in the rostral anterior cingulate cortex (Brodmann area 32, [-8 46 16], Z = 4.96, $p<0.05$ corrected for multiple comparisons, see Fig. 5.9).

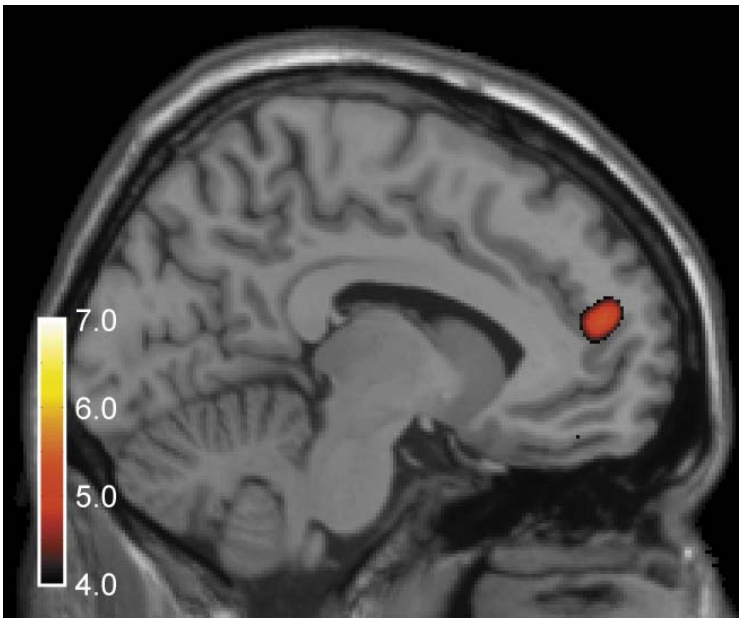


Fig. 5.9. Rostral anterior cingulate cortex activation revealed in the group effects analysis for the presatiety – postsatiety comparison, when the stimulus delivery events are not taken into account. The activations were thresholded at p<0.05, corrected for multiple comparisons.

Discussion

The results show that the oral delivery of water activated a part of the human anterior insular and frontal opercular cortex (see Fig. 5.2). Moreover, the results shown in Fig. 5.3 indicate that the same region activated by water is also activated by the prototypical tastants glucose and NaCl. This brain region corresponds with the anterior insular and adjoining anterior opercular cortex of macaques which is the primary taste cortical area in that it receives direct projections from the taste thalamic nucleus, VPMpc (the parvocellular part of the ventro-postero-medial thalamic nucleus, Pritchard et al. 1986), and has taste-responsive neurons (Scott et al. 1986a; Yaxley et al. 1990). On these grounds, the anterior insular and frontal opercular region shown in Figs. 5.2 and 5.3 is the putative human primary taste cortex. Also consistent with the macaque (Rolls et al. 1988; Yaxley et al. 1988) is the finding that the homeostatic need state, in this case thirst, does not modulate the responsiveness to oral water, as shown in Fig. 5.4a in blue). The representation in this primary taste cortical area in humans as well as in macaques appears to be of the identity and intensity of the oral taste stimulus, and not of the reward value or the correlated affective value, both of which decrease to zero when water is drunk to satiety, as confirmed in this study. Individual neurons in the macaque primary taste cortex are tuned to respond best to each of the prototypical stimuli sweet (glucose), salt (NaCl), bitter (quinine) and sour (HCl), and also to water (Rolls et al. 1988; Scott et al. 1986a), with each neuron showing a distributed representation in that each typically responds to several stimuli in the set. The finding that the same region of the human brain is activated by water, glucose, and NaCl is consistent with this evidence that water responses form a continuous part of what is represented in the primary taste cortex, although of course the fMRI methodology is too insensitive to reveal directly anything about the nature of the encoding used by the neurons. In humans, as in macaques, it is notable that this primary taste cortical area extends right to the anterior border of the far anterior insula and adjoining frontal operculum into the transitional region which topologically might be described as a far caudal part of the orbitofrontal cortex but which architectonically can be classified as PrCO, Iai and 12o (Carmichael and Price 1994; Öngur and Price 2000; Petrides and Pandya 1994). Although it has been shown previously that oral water activates the insular and opercular cortices in humans (Zald and Pardo 2000a), that study did not use a tasteless control for non-specific including somatosensory effects produced by placing a fluid into the mouth. The present finding constitutes the first report that water activates taste-related cortical areas in humans when contrasted to a tasteless control solution, which includes the ionic components of saliva.

The results also show that a part of the caudomedial human orbitofrontal cortex is activated by water and by the taste stimuli sweet and salt (Fig. 5.3, OFC). In this region, the activation produced by the delivery of water is high when the subjects are thirsty, and decreases to baseline

after the subjects have drunk water to satiety (Figs. 5.4b and 5.7). Thus the activation of this caudomedial part of the human orbitofrontal cortex is large when the subjects find the water rewarding (in that the subjects want to drink the water), and when they find its taste pleasant and refreshing as shown by the subjective ratings. Moreover, the same location shows activation that is correlated with the refreshing value and pleasantness of the water delivered into the mouth (Fig. 5.8). This region may thus be the human secondary taste cortex, corresponding to the macaque secondary taste cortex, defined by its projections from the primary taste cortex (Baylis et al. 1995), and which also contains single neurons that only respond to water delivered into the mouth when thirst is present (Rolls et al. 1989). The human caudomedial orbitofrontal cortex also shows a motivation-selective decrease in its responsiveness to oral stimuli, in that its activation to water but not to glucose or salt decreased after the subjects had consumed water to satiety. This directly parallels the motivation-selective decrease in the pleasantness of water but not glucose after water has been consumed to satiety, shown by Rolls, Rolls and Rowe (1983) and confirmed in this investigation. It is notable that the part of the human orbitofrontal cortex showing these effects is far medial, whereas in the macaque the region is more lateral in the caudal orbitofrontal cortex (Rolls et al 1990; Rolls et al, 1989). However, in macaques, taste neurons are not confined to this lateral part of the orbitofrontal cortex, and indeed are found in smaller numbers widely in the orbitofrontal cortex, mixed in with neurons responding to stimuli in other modalities, including olfactory and visual (Rolls and Baylis 1994). The finding that pleasantness (and refreshment) ratings for water are correlated with activations in the medial orbitofrontal cortex (Fig. 5.8) is consistent with previous studies implicating the medial part of the orbitofrontal cortex in the representation of the affective properties of primary and secondary reinforcers including pleasant touch, monetary reward, and pleasant touch (de Araujo et al. 2003a; O'Doherty et al. 2001a; Rolls et al. 2003b); and even face attractiveness (Aharon et al. 2001), in addition to the pleasantness of odours (Chapter II), of flavour (Chapter III) and the consonance of the taste-odour mixture (Chapter III).

In this investigation, we found a region of the insula that is midway between the anterior and the posterior insula, and which we refer to as mid insula, which was activated by water but not by sweet and salt stimuli, and which further was only activated by water when thirst was present and not after satiation (see Fig. 5.4a, red). This region has not been investigated neurophysiologically in macaques. A simple explanation for this activation which is anatomically plausible (Jain et al. 2001; Kaas 1993) refers to somatosensory effects produced by a dry mouth, in that in thirsty subjects intra-oral saliva becomes more viscuous (Rolls and Rolls 1982; Rolls et al. 1983) and the mouth feel of a more viscous saliva might be a motivational factor leading to water intake.

However, it is possible that responses to intra-oral stimuli in this mid region of the insula are modulated by the current physiological or homeostatic state of the body. In fact, previous functional neuroimaging studies in humans have demonstrated that regions located in the mid and posterior insular cortex are consistently activated by general visceral and homeostatic-related stimuli such as temperature (Craig 2002), nociceptive stimulation (Craig 2002), fasting (Tataranni et al. 1999), and isometric and dynamic exercise (King et al. 1999). Indeed, we have found activation by painful stimuli applied to the hand of a part of the mid insula which is quite close (Rolls et al. 2003b). However, we think it unlikely that exactly the same mid-insula area is activated by pain and by water, because the activations we describe were larger when the water was rewarding and pleasant than after drinking water to satiety when the water was less pleasant (Figs. 5.4a and 5.7). A similar region was shown to have activations that correlate with mean arterial pressure in humans (Critchley et al. 2000a). Activations in the insula were also produced by hypertonic saline injection, leading to thirst (Denton et al. 1999a; Denton et al. 1999b). The functional segregation within the mid and posterior insular cortex suggested by the results of Craig and colleagues may be partially explained by the functional organisation of the posterior thalamic nuclei in humans. In a cytoarchitectonic and immunohistochemical characterisation of the ventral medial nucleus of the human thalamus, Blomqvist et al (2000) have demonstrated different reactivity for the calcitonin gene-related peptide (CGRP, an important visceral-related modulator, Yasui et al. 1989) within posterior regions of this nucleus. In particular CGRP-positive fibres were observed in an intermediate region located adjacent, but distinct to, VMpc and the posterior ventral medial nucleus of the thalamus (VMpo), named by these authors the posterior nucleus (Po). In the rat (similar data is presently unavailable in non-human primates), CGRP-positive terminal fibres in the thalamus originate (preferentially) from the external medial parabrachial subnucleus and convey general visceral-related information (Blomqvist et al. 2000; Yasui et al. 1989) whereas CGRP-negative terminals originate from the central medial parabrachial subnucleus, a gustatory relay receiving taste-related information from the NST. In addition, different thalamic regions in the macaque monkey appear to represent either general visceral or gustatory information (Pritchard et al. 1989). Taking also into consideration the non-peptidergic structure of the taste pathway (Kruger et al. 1988), Blomqvist and colleagues (2000) conclude thus that a clear separation exists between gustatory and visceral-dedicated thalamic nuclei in humans as determined by the distinct immunoreactivity to CGRP in VPMpc and Po. This separation could thus be further represented in the human insular cortex, in that more anterior regions seem to be dedicated preferentially to gustatory processing, whereas a more posterior region seems to respond to water delivered into the mouth when thirst is present. Given the lack of relevant neurophysiology on this region to date, we are not sure how to interpret the activation found in this study to water when thirst is present, but note that autonomic and endocrine responses will be elicited by water delivered under these conditions,

and suggest that the activations we found in the mid insula could be related to the initiation of these autonomic and endocrine responses. Neurophysiological investigations in macaques are likely to be revealing with respect to this issue.

We also found that parts of the anterior cingulate and adjoining cortex showed activation to water and to the tastants sweet and salt (Fig. 5.3, ACC). Moreover, when no oral stimuli were being delivered, it was found that the level of activity in a part of the anterior cingulate cortex was higher when thirsty than when satiated (see Fig. 5.9). This is consistent with previous findings showing that the primate ACC is also involved in autonomic and emotional control (Devinsky et al. 1995), and in particular is a target in rats of projections from circumventricular organs (McKinley et al. 2001), and has been shown in a PET study to have blood flow that correlates with thirst produced by hypertonic stimuli in humans (Denton et al. 1999a; Denton et al. 1999b).

The question arises about how water delivered into the mouth produces its effects found at the neuronal level in the insular and orbitofrontal cortices (Scott et al. 1986a; Yaxley et al. 1990), at the psychophysical level (Bartoshuk 1974), and at the neuroimaging level in humans as described in this Chapter. One possibility is that the water acts through a taste sensitive system. In particular, salt-best neurons might decrease their firing rate below the spontaneous level when water is placed on the tongue. Such salt-best neurons may be sufficiently sensitive to respond to the decrease of a few mM in the concentration of Na^+ (and other cations) when the saliva in the mouth is replaced by water. Another possibility is that water-best neurons in the cortex respond to a combination of fluid of a low viscosity in the mouth and the lack of taste neurons firing. Neurophysiological investigations are required to resolve this issue. With respect to human psychophysics, it is notable that whereas the subjects of Bartoshuk (1974) reported after adaptation to 10 mM NaCl that water in the mouth tasted bitter-sour, our subjects found that taste of water pleasant. The difference is almost certainly due to the fact that the pleasantness of water is high when subjects are slightly water-deprived as in the present study, and indeed the findings described in this Thesis underline the point that the pleasantness of water in the mouth is a function of need state.

In the context of the much discussed issue of hemispheric specialisation (Davidson 1992; Small et al. 1999), we found little evidence for lateralisation of the taste effects described in this Thesis. For example, the activation of the anterior insular/opercular (primary) taste cortex by water (Fig. 5.2) and by other tastes (Fig. 5.3) is clearly bilateral. Also, the activation of the orbitofrontal cortex by water was to at least some extent bilateral (see Figs 5.2 and 5.3), and the representation of the pleasantness of the taste of water in the medial orbitofrontal cortex was clearly bilateral

(Fig. 5.8). The only indication of any laterality we found was in the contrast of the effects of water delivery when thirsty – the effects of water delivery when not thirsty, which did produce more signal on the right mid insula (see Fig. 5.4a, activations shown in red). Certainly in macaques the representation of taste is bilateral (Rolls and Scott 2003 for review), and, when a representation of a part of the body surface is being considered, there is little theoretical advantage of lateralization (Rolls and Deco 2002). Clinical findings (Cereda et al. 2002; Pritchard et al. 1999) and other evidence (Craig 2002) also suggest bilateral functions of the insula in taste processing. The evidence in this study shows that taste is in general represented bilaterally in the insular/opercular cortex and in the orbitofrontal cortex.

Throughout this Chapter we have presented the results of the group analyses (including conjunction and second level random effects analyses), as this is statistically very powerful (Friston et al. 1999a ; Worsley et al. 1996). However, we note that all the effects described were present at the individual subject level.

In conclusion, the results provide evidence not only for where the stimulus of water in the mouth is represented in the brain, but also on the medial orbitofrontal cortex region where the activations produced by water in the mouth are larger when thirsty than when satiated, and where the pleasantness and refreshing value or water are represented in the brain. As such, the investigation advances our understanding of where affect and emotion are represented in the brain (Rolls 1999). Moreover, the findings provide evidence that, as in macaques, in humans there are separate representations of the identity of tastes and oral stimuli in the mouth (in the anterior insular/opercular cortex), and of their hedonic value (in the medial orbitofrontal cortex). Further, the findings provide new evidence on the functions of the mid part of the human insula, and are consistent with the hypothesis that it may be related to autonomic function as part of an interoceptive network (Craig 2002). Finally, we note that the temperature of water may influence its pleasantness. We already know that some single neurons in the primate orbitofrontal cortex do respond to the temperature of liquids in the mouth (Kadohisa, Verhagen and Rolls, in preparation), and believe that the same could be true in humans.

Conclusion

The five experimental Chapters described so far lead to two overall conclusions, with respect to the functional organisation of the human insular and adjoining orbitofrontal cortex (specific considerations on the implications of the findings presented in each Chapter can be found in the corresponding Discussion section):

– The frontal opercular, anterior insular (including its agranular extension into the orbital surface and the posterior end of the agranular insula which includes the primary olfactory cortex) and the adjacent caudolateral orbitofrontal cortices are part of a network processing information on the sensory aspects of taste and olfactory stimuli (including water in the mouth) in humans; the far anterior (agranular) insular cortex, close to its junction with the caudolateral orbitofrontal cortex, is a site for crossmodal (taste-olfaction) integration whereas the frontal opercular cortex is a unimodal area in that it receives taste, but not olfactory, inputs; the anterior insular, frontal opercular, primary olfactory and in particular the far anterior (agranular) insular cortex do not correlate with the reward or motivational value of these stimuli;

– Activity in medial parts of the human orbitofrontal cortex (scattered across the anterior-posterior axis) and in the adjacent rostral region of the anterior cingulate cortex is modulated by the reward value of specific stimuli including taste, olfactory (and their combinations) and psychostimulants. Moreover, along with a part of the mid-insula, the medial orbitofrontal and the rostral anterior cingulate cortex respond to intra-oral water as a function of the need state of the body.

Convergence of taste and olfactory inputs into the far anterior, agranular insula

As was reviewed in Chapter I, in primates, gustatory afferents proceed through cranial nerves VII, IX, and X to terminate in the rostral division of the nucleus of the solitary tract (Pritchard et al. 1986; Scott and Plata-Salaman 1999). In contrast to the rat case, in primates second-order fibres bypass the parabrachial nucleus of the brainstem (Pritchard et al. 2000; Rolls and Scott 2003) only to project through the central tegmental tract and distribute within the parvicellular division of thalamic ventroposterior medial nucleus (VPMpc, Beckstead et al. 1980; Pritchard et al. 1986) (this nucleus is also called the basal ventromedial thalamic nucleus, VMb, in Craig et al. 1994; Craig et al. 2000). In *Macaca fascicularis* the VPMpc projects ipsilaterally to the insulo-opercular cortex adjacent to the superior limiting sulcus and extends anteriorly (including thus the anterior areas of the insula) to reach the caudolateral orbitofrontal cortex (Baylis et al. 1995; Pritchard et al. 1986).

Olfactory input reaches the more anterior (agranular) part of the primate insula through projections from pyriform cortex, as reviewed in Chapter II. These were demonstrated in (Carmichael et al. 1994) with anterograde tracer injections (into the pyriform cortex) and retrograde tracer injections (into the orbital and medial prefrontal cortices, and rostral insula). The anterograde injections labelled projections to the caudal orbitofrontal cortex, as well as the adjacent agranular insula. Importantly, areas Iam (medial agranular insula) and Iapm (posteromedial agranular insula) receive the densiest projections from pyriform cortex. It should be noticed that taste projections into the agranular extension of the insula have also been reported, in that retrograde injections in areas Iapm and Ial of the macaque monkey labelled cells located dorsomedially in VPMpc (Carmichael and Price 1995b). Notice that Iapm (a part of the far anterior, agranular insula) thus emerges as a candidate for primary taste-olfaction convergence in the macaque monkey cortex.

The available anatomical data on taste and olfactory inputs into the (non-human) primate cortex imply thus that medial and anterior regions of the insular cortex (along with the caudal orbitofrontal cortex), which includes possibly granular, dysgranular and agranular parts of the insula (Sewards and Sewards 2001), are sites receiving taste input whereas only the anterior (putatively) agranular insula (along with the adjacent caudal orbitofrontal cortex) receives olfactory inputs. So, it has been hypothesised in this Thesis that the anterior agranular insula and its extension to the adjoining caudal orbitofrontal cortex would be a primary site for taste-

olfaction integration in humans and would provide the neural substrate for flavour perception (for a review, Sewards and Sewards 2001).

The fMRI experiments described in Chapters I, II and III substantiate this claim. The experiment described in Chapter I has shown that the frontal opercular cortex, the anterior insula and the orbitofrontal cortex were significantly activated both by umami (monosodium glutamate, MSG) taste and a prototypical tastant, glucose. In the experiment described in Chapter II, orthonasal olfactory input (*e.g.* alpha-ionone, lynalil acetate and geranyl acetate delivered through a continuous air-flow olfactometer) was shown to activate anterior (putatively agranular) parts of the right insula only. Thus, Chapters I and II present evidence for responses to unimodal taste and unimodal orthonasal olftory stimuli in a far anterior, putatively agranular part of the insula in humans where it adjoins the caudal region of orbitofrontal cortex, as would be predicted from a homology with the non-human primate brain. It remained however open the question of determining which regions in the human brain would be targeted by both taste and olfactory input and thus support flavour perception.

The study described in Chapter III aimed, first, to reveal how the human brain represents flavour, by disclosing which areas respond to either taste or retronasal olfactory stimuli (in acqueous solution), and which brain areas respond to both. Second, it attempted to determine if the findings could be compared with what is known about taste-odour interactions in non-human primates. It has been shown that taste and olfactory inputs in the human brain converge in particular in the far anterior (putatively agranular) insular cortex, precisely in the site found to respond to orthonasal olfactory stimuli (in a way which is independent of the hedonic value of the stimuli). This region of the far anterior (agranular) insula (labelled "Ia" in Fig. 3.7) is close to the part of the insular cortex where it adjoins the caudal orbitofrontal cortex, a region also found to respond to taste (this secondary cortical taste area is in area 12 and 12/PrCo according to the labelling used in Fig. 3.7) and retronasal olfactory input (in addition to the responses found to orthonasal olfactory stimuli described in Chapter II).

A homology between the rodent and primate cases with respect to the central anatomy of taste and olfactory integration has been previously suggested, and it is being proposed here thus that this homology would extend to humans. In fact, Shi and Cassell (1998) reported that in rats both the granular and dysgranular zones in the posterior insula are part of the gustatory cortex (see also Cechetto and Saper 1987). Moreover, based on the projection patterns between the granular, dysgranular and agranular parts of the rat insula (as well as on the projection patterns from VPMpc, Cechetto and Saper 1987), Shi and Cassell (1998) claimed that the dysgranular insular cortex constitutes a secondary taste association cortex (in contrast to the lower-order granular

zone). They further hypothetise that the agranular part of the insular cortex is a tertiary taste association cortex supporting flavour perception (given its afferent projections from the olfactory bulb and pyriform/endopyriform cortices, see also Sewards and Sewards 2001). In primates, Ogawa (e.g. Ogawa et al. 1989) proposed (based on anatomical and electrophysiological studies on squirrel or macaque monkeys) that the primary gustatory cortex is located at the buried frontal operculum and dorsal (granular) insula. Benjamin and colleagues (Benjamin and Burton 1968; Benjamin et al. 1968) also claim the primate primary taste cortex is located in the fronto-parietal opercular area. Since the primate opercular cortex is granular (Sanides 1968), this area along with the adjacent dorsal granular insula might constitute the homologue in primates of the rat gustatory cortex. Sewards and Sewards (2001) propose thus that this homology between the rodent and primate cases holds also for the secondary (dysgranular) and tertiary (agranular) taste association area. In particular, the agranular insula and the adjoining caudal part of the orbitofrontal cortex would support flavour perception given the convergence of olfactory and taste inputs in these areas. Although the available anatomical studies in primates (e.g. Baylis et al. 1995) do not completely support such a general claim, the imaging studies presented in this Thesis lead to the possibility that the homology could be extended to humans as previously hypothesised by Ogawa (1994). Notice however that the "tertiary association cortex" (Sewards and Sewards 2001) concept is misleading at least for the primate (including humans) case in that, as mentioned above, at least one part of the far anterior agranular insula, Iapm, is thought to receive projections from both the primary olfactory cortex (Carmichael et al. 1994) and VPMpc (Carmichael and Price 1995b). For this reason such terminology won't be adopted in what follows.

In addition, Carmichael and Price (1995b) have more clearly hypothetised that the far anterior, agranular insula is the earlierst stage in which taste and olfactory inputs converge in the primate cortex, given the gustatory and olfactory projections into the medial part of the agranular insula (Iam). Chapter III in this Thesis gives evidence for that for the human case.

Further regions of taste/retronasal odour convergence found in the study described in Chapter III include the amygdala, the ventral forebrain (a region extending from the far caudal orbitofrontal cortex to 5 mm behind the anterior commissure), and the anterior cingulate cortex (ACC) and adjoining areas. In fact, anterograde tracers placed in the olfactory bulb of the macaque monkey labelled neurons in the anterior cortical nucleus of the amygdala (Carmichael et al. 1994); moreover, the central nucleus of the amygdala is targeted by projections from the primary taste cortex (Rolls and Scott 2003; Scott and Plata-Salaman 1999). Previous functional neuroimaging studies have reported amygdalar activations for both taste (O'Doherty et al. 2001b) and smell (Zald and Pardo 1997). Analogously, the primate anterior cingulate cortex is targeted

by regions of the anterior insula, possibly including taste cortex (Vogt and Pandya 1987) and in addition the more ventral areas of the cingulate cortex receive projections from the agranular part of the caudomedial orbitofrontal cortex (area 13a), which is targeted by projections from the primary olfactory cortex (Carmichael et al. 1994). Finally, the role of the ventral forebrain in taste-olfactory integration remains to be determined by further investigations to be performed in both human and non-human primates. However, it should be noticed that regions of the ventral forebrain are known to respond to food-related stimuli in a sensory-specific satiety way (Rolls et al. 1986), which demonstrates the importance of this region in the control of food intake and thus leads to the hypothesis that this region is involved in flavour perception.

Unimodal taste and olfactory areas

An important complementary issue concerns the determination in the human brain of unimodal taste and unimodal olfactory areas. In Chapter III, a group conjunction analysis across all 11 subjects in this study was performed with respect to the comparison taste (sucrose) – odour (strawberry odour). This analysis revealed significant activations only in the frontal opercular cortex. In contrast, the more anterior parts of the insular cortex were not found to respond significantly to this comparison. In fact Kinney (1978), after having identified the fronto-parietal opercular complex as the primary taste area, proposed that an anterior, dysgranular part of the primate insula constitutes a secondary taste area given its projections from the operculum through short inter- and intracortical association fibres. This is in general agreement with the ideas by Ogawa (e.g. Ogawa et al. 1989) and Benjamin (Benjamin and Burton 1968; Benjamin et al. 1968), reported in the previous section, that more rostral parts of the insular cortex are likely to perform multimodal integration. Thus these authors suggest that insular areas rostral to the fronto-parietal operculum constitute higher-order gustatory areas and are not unimodal (*i.e.* taste only) areas, whereas unimodality would be a property of the frontal opercular and adjoining (probably granular) insula only. However, it should be noticed that it is unlikely that the primate dysgranular insula could constitute a site for the convergence of taste and olfactory inputs as proposed in Kinney (1978), given the absence of olfactory input to that region, as mentioned above.

In fact, in Chapter III, the part of the insular/opercular taste cortex shown to be activated by sucrose in Fig. 3.1 (middle row left) centered on the anterior-posterior region Y=0 to Y=5 may be a part of the taste cortex which is unimodal and not activated at least by orthonasal olfactory stimuli (see Fig. 3.5 left). This region was activated by a retronasally delivered strawberry olfactory stimulus in aqueous solution (Fig. 3.1 bottom row left), but this activation may, by comparison with the effects of orthonasally delivered olfactory stimuli, be ascribable to the combination of a retronasal odour AND somatosensory inputs produced by liquids in the mouth

with a further possible contribution of minor taste or somatosensory inputs produced by the olfactory stimulus in the mouth. (non-taste related inputs in this study were controlled for by always using a tasteless control which produced similar somatosensory and tongue movements.) It may be that even that at the very low concentration of odour used, 25 ppm of strawberry odour, there was some somatosensory input, and this may be difficult to eliminate if the stimuli are delivered in aqueous solution, as inevitably they will be when eating a real food, the situation at which this study is aimed. It is being suggested here thus that the insular/opercular region at Y=0 in humans is a taste and not olfactory area. It is in the same brain region in humans as the primary taste cortex of macaques to which we believe it corresponds. For a reference to the macaque case, see Fig 3.7, Chapter III. The primary taste cortex of macaques, as defined by anterograde tracing from the taste thalamus (Pritchard et al. 1986) and by the presence of taste neurons (Rolls 1997; Rolls and Scott 2003; Scott and Plata-Salaman 1999; Scott et al. 1986a; Yaxley et al. 1990) and labelled "G" in Fig. 3.7, is in the anterior insular and adjacent frontal opercular cortex. The primary taste cortex of macaques is now known to contain neurons that respond to taste and/or somatosensory inputs which convey information about the texture of food in the mouth, and does not have olfactory or visual responses (Kadohisa, Rolls and Verhagen, in preparation). In these respects it may be very similar to the human insular/opercular taste cortex at Y=0. Activation in this region by unimodal taste stimuli has also been found by de Araujo et al. (2003a) (and Chapter I in this Thesis), O'Doherty et al. (2001b) and Small et al. (1999).

In addition, Chapter II provided a characterisation of the putative primary olfactory cortical areas in humans (see Fig 2.6). The human primary olfactory cortex, which includes the pyriform cortex and the anterior olfactory nucleus, lies on the caudal border of the agranular part of the insula (Ongur et al. 2003). It has been found in the study described in Chapter II that the BOLD signal in the medial olfactory areas such as the pyriform and entorhinal cortex was correlated with the intensity ratings, and not with the pleasantness ratings of the olfactory stimuli (further on the correlation with the hedonic values of stimuli in Section II below). Notice that Anderson et al (2003) claimed that the amygdala itself (as well as a part of the pyriform cortex) represents the intensity of the odour. However, the correlations we found (see Fig. 2.6) were much better confined to particular regions than those shown in the Anderson et al (2003) paper (in which many activations are found outside the olfactory areas), and results presented in Chapter II show rather clearly that it is the pyriform and entorhinal cortices which have activations correlated with intensity (see Fig. 2.6), rather than the body of the amygdala. This is an important finding, in that it implies that the hedonic aspects of odours are encoded in a reward-related region whereas the primary olfactory cortex encodes for other aspects of odours such as itsidentity and intensity. Overall, it should to be noticed that no areas ascribed to the primary taste cortex have correlated

significantly with the odour intensity ratings, providing further evidence that taste-olfactory convergence is first implemented in more anterior parts of the insular and caudal orbitofrontal cortices. It is interesting to note that, in Fig 2.6A the correlation analysis with the intensity ratings reveals an area of the anterior prefrontal cortex, probably the transition zone between areas 13a and 13b, which is partially agranular (Ongur et al. 2003), implying that the agranular posterior orbital cortex, including its insular extension, seems to be targeted by olfactory inputs in multiple sites, as it was found for the macaque monkey case (Carmichael et al. 1994; Carmichael and Price 1995b).

The orbitofrontal cortex responses to taste

In addition to the robust activations produced by the delivery of taste stimuli found in the caudal parts of the orbitofrontal cortex as reported in Chapters I, II and V, a lateral, more anterior, part of the (left) orbitofrontal cortex was found to represent positive interactions between the umami tastants monosodium glutamate (MSG) and inosine 5'-monophosphate (IMP) as well as between unimodal taste (sucrose) and (retronasally delivered) odour stimuli. This part of the human orbitofrontal cortex (centered at MNI coordinates [-44 34 –18]) showed strong supralinear additivity in the BOLD signal produced by the combination of MSG and IMP (the MSGIMP condition) when compared to the sum of the MSG and IMP BOLD signals, and this region is just anterior to the part of the orbitofrontal cortex showing effects in the main comparison between taste and tasteless solution (with a peak at y=26). Moreover, this same general area (however more anterior) was found to respond significantly to the comparison which tests for supra-linear interactions between unimodal taste (sucrose) and retronasal olfactory stimuli (peak at [-32 50 -10]). As in the case of umami stimuli, this was the only cluster of activation at this level of significance ($p<0.05$, corrected for the number of comparisons made within a region of interest defined by a sphere with a 10mm radius). In particular no activations were found in other the other brain regions imaged in these studies, *e.g.* the primary taste cortex.

The abovementioned results might be revealing about the relative role of the orbitofrontal cortex in gustatory/flavour processing in humans in comparison to the primary taste cortex and adjoining areas. The primate orbitofrontal cortex is a multi-modal integration site, where taste, olfactory, visual, somatosensory and homeostatic information converge (Rolls 2000a; Rolls and Baylis 1994). In the primate orbitofrontal cortex might thus be represented specific interactions between the sensory properties of these stimuli, characterising the specific function of the secondary taste and olfactory cortices as the sites processing information on higher-order properties of these stimuli. This would include their reinforcing or motivational value (Critchley and Rolls 1996b; Rolls 2000a) (see also section *Medial orbitofrontal cortex and reward* below).

The above also concerns the issue of hemispheric specialisation in taste processing (Small et al. 1997a; Small et al. 1999). It is of interest to note that in the group analyses presented in Chapter I and Chapter III the region of the orbitofrontal cortex showing supra-linear additivity in the BOLD signal is on the left side of the human brain. This is consistent with the suggestion corroborated by clinical findings (Cereda et al. 2002; Pritchard et al. 1999) that gustatory processing involves the also the left side of the human brain (Craig 2002). However, it should be noted that in some of the individual subjects, the supra-linear additivity effects were also seen in the right orbitofrontal cortex for the case of MSG and IMP interactions. Further, the analyses performed in Chapters I, III and V to reveal the main effects of taste, including water in the mouth, revealed strong evidence that the representation of taste is bilateral in the human brain.

Summary

The far anterior (putatively agranular) insular cortex, the caudal orbitofrontal cortex, the amygdala, and the anterior cingulate cortex seem likely from the investigations described in Chapters I, II and III to support flavour perception. The far anterior (putatively agranular) insula was concluded from these investigations to be the primary site for taste-olfactory convergence in the human cortex. Information from this region of the insular cortex is further conveyed to the caudal part of the orbitofrontal cortex. The orbitofrontal cortex shows the most interesting evidence of being closely related to the representation of flavour, in that a part of this region showed supra-linear additivity between olfactory and taste stimuli, and a nearby part of the medial orbitofrontal cortex has activations that are correlated with the subjective consonance between olfactory and taste stimuli (such as sweet and strawberry), and with the pleasantness of the olfactory and taste stimuli and their combination (further on the representation of of the hedonic value of stimuli in section *Medial orbitofrontal cortex and reward* below). Further confirmation that the far anterior insula site evidencing convergence for sucrose taste and retronasal strawberry odour also responds to orthonasal olfactory stimulation came thus from Chapter II, where a range of differently valenced odours were used. In order to control for hedonic intensity and trigeminality factors, a conjunction analysis was performed across the conditions [alpha-ionone – control] AND [lynalyl acetate – control] AND [geranyl acetate – control] AND [isovaleric acid – control] AND [hexanoic acid – control] AND [octanol – control]. Activations were found particularly in right far anterior insular cortex, in the exact location (MNI [45 15 -9]) found to respond for both sucrose – tasteless and strawberry odour – tasteless.

The claim that the frontal opercular (or PrCO as defined in macaque monkeys, pre-central opercular region), far anterior (putatively agranular) insular and caudolateral orbitofrontal cortex form part of a network involved in decoding the sensory aspects of intra-oral stimuli as well as

olfactory stimuli is substantiated by the known anatomy of the homologue region in macaques, as reviewed in detail in Chapter III. A far anterior, cytoarchitectonically agranular, part of the macaque insula (labelled "Ia" in Fig. 3.7) where it adjoins the caudal orbitofrontal cortex receives anatomical connections from the primary olfactory system, as demonstrated by anterograde tracer injections in the macaque pyriform cortex (Carmichael et al. 1994). This region is very close to the caudal orbitofrontal cortex area that has been defined as the secondary taste cortex by virtue of receiving direct projections from the primary taste cortex (Baylis et al. 1995). This secondary cortical taste area is in area 12 and 12/PrCo according to the labelling used in Fig. 3.7. This same general region is known to contain single neurons in macaques that respond to both taste and olfactory stimuli (Rolls and Baylis 1994) and where in macaques olfactory-taste association learning occurs so that flavour representations are formed (Rolls 1997; Rolls et al. 1996b). (The area extends anteriorly to reach the caudal part of the orbitofrontal cortex, as shown by Rolls and Baylis (1994), Rolls *et al.* (1996b), and Critchley and Rolls (1996b). This transitional agranular far anterior insular / caudal orbitofrontal cortex area (labelled "Ia" in Fig. 3.7) probably corresponds to the region shown to receive olfactory (as confirmed by orthonasal as well as retronasal delivery) and taste inputs in this investigation in humans (see Fig 3.6)). With respect to the recent histological and immunohistochemical study of the human orbital and medial prefrontal areas by Ongur et al (2003), the insular region found to respond to both taste and olfactory inputs depicted in Fig. 3.6 seems to correspond to region Iai ("intermediate agranular insula"), extending posteriorly to Ial ("lateral agranular insula") and anteriorly to 47/12, which is equivalent to 12o and 12/PrCO in the macaque monkey (Carmichael et al. 1994), thus further elucidating the claim outlined in Chapter III. This is further corroborated by the available anatomical data on the far anterior agranular insula of the macaque monkey, in that areas Ial (a putative target of gustatory input) and Iam (a target of olfactory input) are strongly reciprocally connected, along with area Iapm (Carmichael and Price 1996).

Medial orbitofrontal cortex and reward

An overall conclusion from the five experimental Chapters presented in this Thesis was that activity in the far anterior insular cortex which was found to respond to taste and olfactory stimuli was not dependent on the reinforcing or motivational value of these stimuli (in addition to the fact that these regions were not found to respond to intra-venous M-amphetamine) in that the correlation analyses performed with respect to the subjective ratings of pleasantness (and consonance) given to those stimuli did not reveal activations in these areas. This region of anterior insular cortex includes its agranular extension into the posterior part of the orbital cortex, as characterised previously in both macaque monkeys (Carmichael and Price 1994) and humans (Ongur et al. 2003) and the caudal border of the agranular insula, which includes the

primate primary olfactory cortex (Carmichael et al. 1994). Moreover, Chapter V (where the homeostatic states of subjects were explicitly manipulated) described a (bilateral) region of the far anterior insula including its extension into the caudal part of the lateral orbitofrontal cortex which was activated by water in the mouth during both water deprived and sated periods. Thus in this case reponses to water in the mouth produced independently from thirst levels most likely included agranular areas Iai, Ial and the orbital area 47/12l, following the characterisation proposed by (Ongur et al. 2003). These same regions, in particular, were not found to correlate significantly with the pleasantness ratings given by subjects. In contrast, the medial part of the orbitofrontal cortex, (along with rostral regions of the anterior cingulate cortex) were found to correlate with the reward value of these stimuli (including responses to intra-venous M-amphetamine). Modulation of responses by the reward value of water in the mouth was also found in a part of the right mid-insula, in a region which in monkeys is mostly dysgranular and distinct from the anterior agranular portion (Mesulam and Mufson 1982a). Thus these latter regions are involved in encoding the reward or motivational value of the presented stimuli.

In Chapter II, it has been demonstrated that activations in the orbitofrontal cortex were correlated with the pleasantness ratings given by the subjects and not with the intensity of the odours, in that significant correlations in different parts of the orbitofrontal cortex with the pleasantness (medial orbitofrontal cortex) or unpleasantness (lateral orbitofrontal cortex) of the odours were found, whereas the corresponding analysis performed for intensity showed no BOLD signal correlation in the orbitofrontal or cingulate cortex (but did show a correlation with the BOLD signal in other brain areas as described in the Results section). These findings show that the BOLD signal in the orbitofrontal cortex reflected the pleasantness vs the unpleasantness of the odours, but not their intensity. This conclusion is supported by recent evidence obtained by Anderson et al (2003) and by Gottfried et al. (2002) that a pleasant odour activated the medial orbitofrontal cortex, and an unpleasant odour activated the left lateral orbitofrontal cortex. However, the study described in Chapter II goes considerably beyond the study of Anderson et al (2003) by testing whether it is generally the case that pleasant odours activate the medial orbitofrontal cortex, and unpleasant odours activate the lateral orbitofrontal cortex. It is possible that, with just one pleasant (citral) and one unpleasant odour (valeric acid), the localization found in the Anderson et al. (2003) study could have simply reflected the identity rather than the valence properties of the odours. The same holds true for the Gottfried et al. (2002) study. However, by using three pleasant odours and three unpleasant odours in the study described in Chapter III, it has been shown by using conjunction analysis that all the pleasant odours activated the medial orbitofrontal cortex, a region not activated by the unpleasant odours; whereas the lateral orbitofrontal cortex was activated by a conjunction of the three unpleasant odours, and this lateral region was not activated by the pleasant odours. Moreover, we were able to show that

the activation in the medial orbitofrontal cortex correlated with the pleasantness taken across all the 3 pleasant and 3 unpleasant odours, whereas activation of the lateral orbitofrontal cortex correlates with the unpleasantness taken across all these 6 odours. This design and the result found makes it unlikely that the correlations with pleasantness reflected correlations with just the chance identity of the odours, but instead reflect correlations with pleasantness independently of identity. More precisely, the medial orbitofrontal cortex represents the pleasantness (at Y = 52) and more lateral parts of the orbitofrontal cortex represent unpleasantness (at Y = 54 and 28) of the orthonasal olfactory stimuli.

The finding that medial regions of the orbitofrontal cortex represent the reward value of stimuli was further confirmed for the case of taste-odour complex mixtures, as described in Chapter III. At a more anterior level (Y=45) is the region where the BOLD signal in the medial orbitofrontal cortex correlates with the subjective ratings of the consonance of the stimuli (Fig. 3.4A). More anteriorly (Y=50) is the part of the medial orbitofrontal cortex where the BOLD signal correlates with the subjective ratings of the pleasantness of the stimuli (Fig. 3.4B). So, the correlation analyses described in Chapters II and III (in both cases based on stringent group random-effects analyses) reveal two very close medial orbitofrontal cortex regions where activation has been shown to relate to the positive affective properties of stimuli.

Moreover, in Chapter IV, intra-venous administration of M-amphetamine was shown to elicit significant responses in the medial orbitofrontal cortex, in both the amphetamine-saline comparison (with the cluster of activation centred at [12 42 –14]) and in the correlation analysis based on the "mind-racing" ratings given by subjects (centred at [0 54 –8]). Notice that amphetamine is known to produce pleasant and even euphoria-like subjective feelings in humans (Tremblay et al. 2002) and that this latter location almost coincides with those found to correlate with the pleasantness (and consonance) of odours and flavour mixtures. This result is important because it demonstrates that the prefrontal cortex areas involved in the representation of the reinforcing value of taste, olfactory and flavour-related stimuli are part of a more general circuit involved in reward processing. In fact, it has been suggested previously that the circuitry involved in drug addiction and craving actually developed as part of an ingestion-related network in the brain (Wise 1997).

The reward value of water in the mouth is also represented in the medial orbitofrontal cortex, providing further evidence on the above characterisation. In the study described in Chapter V, water in the mouth was found to produce activations in the medial orbitofrontal cortex only when subjects were thirsty, thus further demonstrating that activations in the medial region of the orbitofrontal cortex can reflect the motivational properties of the stimulus. Interestingly, this

activation was found in a more caudal region of the medial orbitofrontal cortex, where it adjoins the subgenual cingulate cortex (areas 25/11, centred at [6,22,-7]). This was further confirmed by performing a correlation analysis with the subjective ratings for the pleasantness of water in the mouth. The medial orbitofrontal cortex was activated in two neighbouring sites (centred at [-3,45,-16] and [16,46,-16]). In this case the activations are more anterior with respect to the activations produced by the main effects of water in the mouth when thirsty, closer thus to the sites described in the preceding Chapters.

The role of the primate orbitofrontal cortex in reward processing has been consistently established by a number of different lines of evidence. In non-human primates, there is strong evidence at the single-neuron level that the orbitofrontal cortex responds as a function of the reward value of taste (Rolls et al. 1989), olfactory (Critchley and Rolls 1996b), and visual stimuli (Critchley and Rolls 1996b; Rolls 2000a; Rolls et al. 1996b). In the specific case of neurons responding to the reward value of taste stimuli, neurons in the macaque monkey orbitofrontal cortex have been shown to respond in a sensory-specific satiety manner (Rolls et al. 1989). Reward-related learning and expectation is also encoded at the single-neuron level in the primate orbitofrontal cortex (Schultz et al. 2000), probably involving the midbrain dopaminergic system. Moreover, it has been shown that macaques will learn to self-administer very small quantities of amphetamine to this region (Phillips et al. 1979), and that this is a region where electrical stimulation in macaques is rewarding (Rolls 2000a). In humans, the medial orbitofrontal cortex region is in an area in which there are high concentrations of D1 receptors, as shown in post mortem immunohistochemical studies (Hurd et al. 2001), which is particularly relevant for the interpretation of the results obtained in Chapter IV. Evidence that, in humans, that the orbitofrontal cortex is involved in reward processing comes from studies making use of a variety of stimuli, such as odour (Anderson et al. 2003; Gottfried et al. 2002; Zald and Pardo 1997, 2000b; Zatorre et al. 1992), olfactory stimuli in a sensory-specific satiety paradigm (O'Doherty et al. 2000), positive and negative feedback (Elliott et al. 1997), taste (O'Doherty et al. 2001b; Small et al. 2001), face attractiveness (Aharon et al. 2001; O'Doherty et al. 2003), sexually arousing stimuli (Redoute et al. 2000), consonant music sequences (Blood et al. 1999) and reward-related learning and expectation (O'Doherty et al. 2002).

Findings from non-human primates (Critchley and Rolls 1996a, b; Rolls et al. 1989; Tremblay and Schultz 1999) provide evidence for reward-dependent responses more specifically in the medial part of the orbitofrontal cortex. These studies reported neurons located in posteriomedial area 11, close to area 14, and in area 12 and 13 that reflect reward preferences. More generally, neurons responding to taste and smell combinations, and to fat in the mouth, were found throughout the caudal part of the orbitofrontal cortex, including its medial region (Rolls and

Baylis 1994; Rolls et al. 1999). Moreover, these results were further corroborated by functional neuroimaging in humans. Medial orbitofrontal cortex activity was found to correlate with the pleasantness of musical sequences (Blood et al. 1999), monetary reward (O'Doherty et al. 2001a) and face actrativeness (O'Doherty et al. 2003). Concerning taste-related responses in this area in humans, O'Doherty et al. (2000) reported sensory-specific responses in medial orbitofrontal cortex to the smell of a food eaten to satiety, whereas Small et al. (2001) found that the caudomedial part of the orbitofrontal cortex represents the changing reward value of a food (chocolate) eaten to satiety. It is important to note that these activations are found across the anterior-posterior axis of the orbitofrontal cortex, consistent with the findings presented in this Thesis.

The mid part of the insular cortex

The region of the mid-insula found to respond to the delivery of water in the mouth when the subject is thirsty, but not sated, hasn't been the focus of substantial electrophysiological investigation to date. In Chapter V, we investigated how the physiological state of the organism modulates the brain responses to the oral delivery of water. In particular we aimed to reveal which brain areas responding to water in the mouth are not modulated by the level of thirst by performing a conjunction analysis across the conditions [Water Pre – Tasteless Pre] AND [Water Post – Tasteless Post]. This analysis revealed significant bilateral activations in the frontal operculum and in the anterior part of the insula possibly including its far anterior, agranular part, extending to the caudal part of the orbitofrontal cortex. In contrast, no activations were found in more medial or posterior parts of the insular cortex. This leads then to the conclusion that primary gustatory areas located in frontal opercular and anterior insular cortices are not modulated by the physiological or motivational state of the organism. This is in agreement with earlier recording studies in primates (Rolls et al. 1988; Yaxley et al. 1988) where it has been shown that primary cortical gustatory areas in non-human primates are not modulated by the level of hunger.

The findings reported in Chapter V, on the other hand, are more complex in that an interaction between taste responses and the need state of the body was found in the mid-insular cortex in contrast to more anterior insular regions. A possible explanation for the thirst-dependent activation in this mid part of the insular cortex is that these responses are caused by somatosensory effects produced by a dry mouth, in that thirsty subjects will experience a particular mouth feel resulting from a more viscuous saliva (Jain et al. 2001; Kaas 1993; Rolls and Rolls 1982; Rolls et al. 1983). We did not, however, control explicitly for this specific type of somatosensory effect by using a more viscuous tasteless control solution, so that it remains possible that these activations were produced by a more complex mechanism, namely that

responses to water in the mouth in this region of the mid insula are modulated by the current physiological or need state of the body, in contrast to the far anterior, agranular part of the insular cortex.

Assuming that this second possibility is the case, it will be hypothetised here that such functional internal organisation depends on the type of thalamic information being conveyed to the human forebrain.

There is evidence that in the human thalamus there exists a clearer distinction between taste and visceral-dedicated thalamic nuclei as compared to those found in other primates. In fact, a cytoarchitectonic and immunohistochemical study of the posterior regions of the human thalamus performed by Blomqvist *et al* (2000) has characterised an intermediate nucleus with respect to VPM and VMpo (called by the authors the *posterior nucleus*, Po), highly responsive to the calcitonin gene-related peptide (CGRP). CGRP-responsive thalamic nuclei have been previously studied only in the rat (Kruger et al. 1988; Yasui et al. 1991) where it has been observed CGRP staining in VPMpc. However, the afferent fibres terminanting in VPMpc that responded densely to CGRP originated preferentially from the external medial subnucleus of the PBN (Kruger et al. 1988; Yasui et al. 1991), a parabrachial site conveying (general) visceral-related information (Cechetto and Saper 1987). On the other hand fibres originating from the central medial subnucleus of PBN (a subnucleus projecting to different termination sites with respect to the external medial subnucleus in VPMpc) did not present CGRP staining, and this subnucleus is preferentially involved in transmitting gustatory information into the thalamus as it receives gustatory information from the nucleus of the solitary tract (Norgren and Leonard 1973). This pattern was also reported in primates where it was found that different thalamic nuclei convey either general visceral or gustatory information (Pritchard et al. 1989). In addition to that the gustatory pathway seems to be selectively non-peptidergic in rats (Kruger et al. 1988), and primates, where there are direct gustatory projections from the NTS into VPMpc bypassing the PBN (Pritchard et al. 2000). The data reported in Blomqvist et al (Blomqvist et al. 2000) thus provide evidence for an even more specialised differentiation between general visceral and gustatory relay nuclei in the human thalamus. The data lead the authors to conclude that the CGRP-positive area Po, located between VPM and VMpo, might constitute a vagal-related visceral afferent in the human thalamus.

Water is a physiologically relevant stimulus in that it acquires motivational properties when fluid compartment homeostasis is challenged (the behavioural correlate of this being thirst). This change in motivational properties has been directly observed in the pleasantness subjective ratings given by the subjects through the experiment described in Chapter V. Water-responsive

cells should thus contain information on both the current physiological state of the body and the somatosensory (possibly also gustatory) properties of water. It is being proposed here that a part of the right mid-insula contains cells with these characteristics.

The water deprivation study presented in Chapter V provides further evidence that, in fact, the insular cortex activity is signalling imbalances in the fluid compartment and that this activity is also being modulated by water intake. In a recent study Johnson and colleagues (Pastuskovas et al. 2003) have studied the differences in the pattern of *c-fos* expression in the rat insular cortex consequent to acute depletion of body water (and sodium), followed by ingestion of water and sodium-rich fluids. One fluid-replete group of animals, as well as a fluid-deplete group having no access to fluid intake, were used for the comparisons. With respect to the subdivision of the rat insular cortex in terms of granule cell density, Fos staining varied as a function of hydration and access to fluids. In general, dehydration increased neuronal activity across all areas of the insular cortex, as shown by the Fos staining patterns found in fluid-deplete animals that had no access to fluids in comparison to fluid-replete animals, in particular in anterior and mid areas. The authors raise the hypothesis that this reflects the representation of visceral activity related to hypovolemia, as we did in our study. In any case this provides direct evidence of the involvement of the insula in sensing decreases in body fluid volume. More interestingly, deplete rats with fluid access presented elevated Fos expression in middle and posterior areas of the insula, compared to deplete rats with no fluid access. This is in line with our finding in that water intake seems to amplify the activity of neurons in the middle (and possibly posterior) parts of the insula, which also signal hypovolemia. In the Pastuskovas et al (2003) study fluid-replete rats did not engage in fluid intake (due of course to low motivational salience of fluid stimuli), limiting thus the parallel with our own study. In any case this work reports increased levels of insular activity under dehydration, and that this is further amplified by subsequent fluid intake, implying a possible extension of the functions of the rat insula to the primate case.

In humans, it is being suggested thus that one possible explanation for the type of activation found in Chapter V in this part of the insular cortex is the processing of combined information from two different thalamic regions, namely VPMpc and Po, the latter putatively involved in processing vagal-related information. The rat thalamus probably lacks such a rich chemo and cytoarchitectonic parcellation, limiting thus the extent to which the rat case could be compared to the primate (including human) one. In addition to that, the involvement of the PBN in the central taste pathways of the rat implicates that the mechanisms involved in conveying both taste and visceral-related information to the insular cortex are different in rats from the primate case. Further electrophysiological and cytoarchitectonic research in non-human primates is required. However, in rats, Hanamori et al (1998) studied the responses in the insular cortex to gustatory,

visceral, and nociceptive inputs. Following confirmation of a dissociation between special and general visceral representations across the anterior/posterior axis of the insula, Hanamori et al (1998) reports cells receiving convergent inputs from gustatory, general visceral and nociceptive related sensory organs. Gustatory responses were obtained through stimulation of the posterior part of the tongue (probably eliciting activity in the IXth nerve). These cells are located ~1.0mm anterior to the anterior commisure, posterior to "prototypical" taste areas and anterior to "prototypical" general visceral-related cells and might thus constitute part of an area receiving projections from functionally distinct thalamic nuclei. The human insular areas responsive to water in the mouth in a thirst-dependent way could constitute a homologous area in humans.

Mid insula, orbitofrontal and anterior cingulate cortex network

Data from experiment V also suggest that there might exist a shared network involving the mid (and possibly also posterior, Craig et al. 2000) insular and the anterior cingulate (including BA areas 24, 25 and 32) cortices where visceral and homeostatic information is represented in the human brain. Moreover, the results presented in Chapters II, III, IV and V of this Thesis provides clear evidence that an anterior cingulate/orbitofrontal cortex network is involved in processing reward-related information on a range of stimuli. First, there are two lines of anatomical evidence that would support the existence of a network involving specific areas of the insular cortex and the anterior cingulate cortex. First, it has been shown that in rhesus monkeys specific insular fields project to the cingulate area (see also Introduction). Morecraft and Van Hoesen (1998) used anterograde and retrograde labelling to study inputs into areas 24c and 23c. Retrogradelly, insular projections to area 24c were robust with cells of origin occupying layers III, V and VI. Labelling at more anterior levels of the insula were only moderate and restricted to inferior levels (Iap and Idg). At more medial levels, substantial labelling was observed for inferior levels in Idg. Retrograde tracing applied to 23c revealed that most anterior areas of the insula were label-free. More posteriorly, at medial levels, moderate labelling was found at superior parts of Idg (layer III). However, at more posterior areas of the insula, heavy labelling was found in superior parts of Ig (which might indicate some granular-granular preferential connectivity). Thus, insular projections into cingulate areas 23c and 24c, preferentially originate in mid and posterior parts (including both dysgranular and granular parts) whereas very weak, if any, anterior (including agranular) projections were found. There is also evidence on cingulo-insular projections. Chiba et al (2001) studied the efferent projections of areas 25 and 32 in the Japanese monkey (*macaca fuscata*). In particular it was found that cingulate areas 25 and 32 project into agranular areas of the insula Ial and Iai, and adjacent orbitofrontal BA 12.

The second line of evidence comes from shared projections from insular and cingulate cortices into the hypothalamus in primates. It has been previously shown in rats that the insular cortex projects directly to the lateral hypothalamic area (Cechetto and Chen 1990), giving direct access (through the lateral hypothalamic area) from the insular cortex to the sympathetic nervous system. Using retrograde injections in the posterior part of the rhesus monkey hypothalamus (more precisely in the caudal edge of the ventral medial hypothalamic nucleus), Öngur and Price (1998) have observed strong labelling cingulate areas 24b, 25 and 32 and also in the insular areas Iai, Iapm, Iam and Ial and Idg (including adjacent orbital areas 13b,m,l.). Further labelling was found in more posterior areas of the agranular insular cortex and cingulate cortices No data were available concerning more posterior regions of the insular cortex. It should be observed that in this study the heaviest projections to all areas in the hypothalamus were observed to originate in cingulate areas 25 and 32 (see also Introduction). These common projections to autonomic, visceral and homeostatic related sites such as the hypothalamus from the primate insular and cingulate cortices leads thus to the hypothesis that these areas might be part of a common network involved in the regulation and monitoring of physiological states in humans.

Moreover, the orbitofrontal cortex is heavily connected with medial prefrontal areas, in particular the anterior cingulate cortex, areas 25, 24a, 24b, 23a and 23b (Cavada et al. 2000). Connections with areas 24a and 25 are particularly marked with respect to the medial orbitofrontal cortex. The role of the primate anterior cingulate cortex in affective processing in humans is well-established (Devinsky et al. 1995), including a functional characterisation of its subdivision "affective" or "cognitive" regions (See Introduction and Bush et al. 2000; Paus 2001). More recent studies have further confirmed the role of the primate cingulate cortex in affective processing and autonomic/homeostatic regulation (Craig 2002; Craig et al. 2000; Critchley et al. 2000a; Denton et al. 1999b). In addition, macaque monkeys sustaining cingulate lesions were impaired in social interaction-related activities, as measured for example by the time spent in contact with other individuals (Hadland et al. 2003b). Impairements were also found with respect to vocalisation and facial expressions. Finally, recent studies in primates (Hadland et al. 2003a) and humans (Rushworth et al. 2002) have demonstrated that the cingulate cortex is involved in action-reward associations, which leads to the hypothesis that the representation of primary rewards such as taste or drugs of abuse in the cingulate cortex is required for further action selection-related responses, as evidenced in this Thesis.

Overall Summary

The conclusions delineated in the two main sections above describe thus the functional organisation of the human orbitofrontal and adjoining cortex in terms of two distinct subregions. After having established the location (within the fMRI resolution) of the taste and olfactory cortices through unimodal stimulation, we found in a separate study a bimodal (taste-smell) responsive area in a part of the far anterior, agranular insula located at the anterior border of a network which includes the anterior insular and opercular cortex involved in encoding the sensory aspects of intra-oral taste and olfactory stimuli. This bimodal area contains the agranular extension of the insula into the orbital cortex, as well as an area at the more posterior part of the lateral orbitofrontal cortex. More generally the anterior insular-opercular cortex, including its agranular orbital extension into the immediately adjacent posterior part of the lateral orbital surface as well as the caudal border of the agranular insular cortex (which adjoins the primary olfactory cortex) were found to encode sensory aspects of taste and olfactory stimuli, but not to respond as a function of the reward or motivational value of these stimuli. In contrast, the medial part of the orbitofrontal cortex, including its anterior and posterior portions as well as its dorsal extension into the rostral anterior cingulate cortex, was modulated by the reward value of taste and olfactory stimuli, and was in addition activated by amphetamine. These medial, reward-related parts on the orbital surface do not seem to include the agranular extensions of the far anterior insular cortex or the more caudal, olfactory cortical areas.

In a recent study, Ongur et al. (2003) investigated the structure of the human orbital and medial prefrontal cortex using five histological and immunohistochemical stains and the results were correlated with the previous analysis in macaque monkeys (Carmichael and Price 1994), which was reviewed in the Introduction. Ongur et al. (2003) found that all of the areas recognized in the macaque orbital and medial prefrontal cortex have counterparts in humans. Of particular importance to the studies presented here, areas 47/12r, 47/12m, 47/12l, and 47/12s (see Fig C.1 legend below for abbreviation) occupy the lateral orbital cortex, corresponding to monkey areas 12r, 12m, 12l, and 12o. The agranular insula (areas Iam, Iapm, Iai, and Ial) extends anteriorly into the caudal orbital surface and posterior-laterally into the horizontal ramus of the lateral sulcus just to reach caudally parts of the primary olfactory cortex, the difference with the monkey being the relative smaller size of the more caudal orbital agranular areas at the expense of a relative increase of the granular areas around the frontal pole. Their description is also based on a distinction between orbital and medial networks as proposed previously for the macaque monkey case (Carmichael and Price 1994). The orbital network, involving most of the areas on the orbital

surface (areas Iam, Iapm, Ial, 13m, 13l, 47/12m, 47/12l, 47/12r, 11l), receives and integrates sensory information from several modalities including visual, somatosensory, gustatory and olfactory, whereas the medial network involves areas located closer to the medial wall (areas 25, 32pl, 24b, 10m, 10r, 10p) as well as areas Iai and 47/12s at the lateral edge of the orbital cortex. They notice that the orbital network, in humans, seems to be involved in the analysis of food-related sensation including reward-related processing whereas the medial network is known to project to visceral control centers in the hypothalamus and some brainstem centers (see also Öngur and Price 2000).

The prefrontal areas studied in this Thesis found to be involved in the sensory encoding of taste and olfactory stimuli in a way which seems to be not dependent on the reward value of these stimuli, seem to include areas Iam, Iai, Iapm and Ial, and then to extend posteriorly into the horizontal ramus of the lateral sulcus (in a region that might correspond to area Iapl in the macaque monkey, Carmichael and Price 1994) to reach the more dorsal and lateral primary taste areas. It also seems to include the areas adjoining the primary olfactory cortex at the caudal edge of the agranular insula and possibly also extends anteriorly, into orbitofrontal areas 47/12l and 47/12s. These areas do not seem to include the caudomedial parts of the orbitofrontal cortex, including areas 13a, 13b, 13m, 13l, 14c or 14r, in that they seem to be limited to the orbital agranular areas that have been grouped as part of the lateral agranular insula in macaque monkeys (Carmichael and Price 1994; Price 1999). On the other hand these more medial areas, in addition to the more rostromedial regions 10m, 10r, 10p, 11m, as well as areas 25 and 32ac seem to correlate with the reward value of the stimuli, and in addition to respond reliably to intra-venous amphetamine.

In the Ongur et al. (2003) study, some parts of the anterior agranular insula and caudolateral orbitofrontal cortex were classified as reward-related or visceral related areas (i.e. as being part of the medial network), in particular areas Iai and 47/12s. Some fMRI studies have been cited as providing evidence for this classification (Critchley et al. 2000a; Critchley et al. 2000b; Drevets 1999; Mayberg et al. 1997). However, the agranular areas of the human insula are small compared to the extension of (spatial) resolution elements in fMRI, so it is possible that the sensory network that seems to include the far anterior (agranular) insular areas and adjoining tissue of the caudolateral orbitofrontal cortex does not coincide entirely with the concept of orbital network proposed by Ongur et al. (2003). In addition, the mentioned fMRI studies reported anterior insular activations that are not centred at the agranular extension of the insula into the orbital surface, but more posteriorly, in a region that we distinguished from this agranular extension (see Introduction) as having the general name of "anterior insula". What seems clear, however, is that most of the areas classified as being part of the medial network in Ongur et al. (2003) were

shown in the experiments described in this Thesis to correlate with the reported affective state of the subjects, or with their physiological state as in the case of water deprivation.

The above characterisation is supported by the available anatomical data on macaque monkeys, in that projections from primary sensory areas into the orbital surface, including its agranular posterior part, seem to target preferentially posterior and lateral areas (Carmichael and Price 1995b). Of special interest here is that agranular areas Ial and Iapm of the macaque monkey are targeted by projections from VPMpc, and in addition the gustatory cortex (area G of Carmichael and Price 1995b) projects to both Ial and to the lateral, but not medial, part of area 13 (*i.e.* area 13l but not 13m). Gustatory projection into the lateral part of the orbitofrontal cortex, including areas 12 and 12/PrCO have also been reported (Baylis et al. 1995). Area 12m is a target of somatosensory input whereas area 12l receives visual information from the inferotemporal cortex (Carmichael and Price 1995b). Thus the hypothesis presented in Carmichael and Price (1995b) that the agranular insula, in the orbital network, is the earliest stage of taste-olfactory convergence in the primate cortex, has been corroborated here for the human case. In contrast, the study by Carmichael and Price (1995b) segregates the more medial areas from the orbital areas on the basis that this medial network is less heavily targeted by direct sensory inputs.

The results presented in this Thesis lead to a similar, but somewhat distinct, conclusion. Whereas the more medial parts of the orbitofrontal cortex (and its dorsal extension into the rostral anterior cingulate cortex) do not seem to be preferentially targeted by primary sensory cortical areas, sensory information is processed in this area (in that these areas were found to respond to taste and olfactory inputs), but as a function of the reinforcing or reward value of the stimulus. This higher-order sensory processing probably requires further input into this area, including general visceral or homestatic inputs (as conveyed, for example, by the hypothalamus and brainstem) and possibly strong dopaminergic innervation. The sensory information conveyed to these medial areas (which approximately coincide with the "medial network" concept of Price and colleagues, Carmichael and Price 1994; Ongur et al. 2003; Price 1999) probably originates mainly from the adjoining orbital areas receiving primary sensory information (Carmichael and Price 1995b).

More generally, it has been recently suggested that there is a functional segregation between the lateral and medial parts of the orbitofrontal cortex, as evidenced by the respective cortical (Barbas 1988, 1993; Baylis et al. 1995; Carmichael and Price 1995b; Cavada et al. 2000; Morecraft and Van Hoesen 1993) and subcortical (Carmichael and Price 1995b; Cavada et al. 2000) connectivity patterns of these regions. Further evidence comes from functional neuroimaging studies performed in humans, where it has been found that medial areas correlate with the

reward value or positive affect of a stimulus and lateral areas with negative affect (see also Elliott et al. 2000; O'Doherty et al. 2001a). Elliott et al (2000) have found that the lateral regions of the orbitofrontal cortex are more likely to be involved when action selection requires the suppression of previously rewarded responses, which migh reflect specific projections of the lateral part with action-selection related regions in the basal ganglia. However, the task performed by the subjects in this experiment involved a number of ill-defined entities such as "guessing" which makes the intepretation of the results rather difficult. In a more well-defined behavioural task, O'Doherty et al (2001a) have found that a correlation between the magnitude of the brain activation and the magnitude of the (monetary) rewards was significant in the medial anterior orbitofrontal cortex whereas the analogous correlation for monetary losses was found to be significant only in the lateral part of the orbitofrontal cortex. However, we notice that these lateral areas found in humans to correlate with negative affect or punishment are more anterior to the areas in the lateral cortex we propose to subserve sensory processing. These more anterior lateral areas on the orbital surface seem to be involved in the suppression of previously rewarded responses, as evidenced in Elliott et al (2000). This might also be the case for the O'Doherty et al (2001a) study, in that subjects in this task learned to reverse their behavioural response in the same events as punishment was being detected.

The distinction proposed here between a sensory-related network involving the anterior insular-opercular cortex including its agranular extension into the orbital cortex and a medial, reward-related area is also at least partially distinct from the "sensory-limbic" network concept proposed by Small et al. (2001). Small and colleagues have found that the anterior insula and the lateral orbitofrontal cortex were modulated by changes in the reward value of chocolate in the mouth, which was eaten to satiety throughout the experiment. This led them to suggest that cortical areas such as the insular and orbitofrontal cortices are integrative networks processing "limbic" and sensory information, as this would be required for the cortical encoding of primary reinforcers such as tastants. A similar view concerning pain processing had also been proposed in Coghill et al. (1999). However, electrophysiological studies in macaque monkeys have previously shown that single-neuron responses to taste in the primary taste cortex, including the operculum and the anterior insula, are not modulated by satiety (Rolls 1997; Rolls et al. 1988; Yaxley et al. 1988) suggesting thus a segregation between the pure sensory and reward-related aspects of taste. Moreover, this concept does not take into account the anatomical (including the cytoarchitectonical) variability within these areas, in particular with respect to the insular cortex. In fact the rat and primate insula, across its antero-posterior axis, is targeted by distinct thalamic nuclei conveying different types of information such as taste-, visceral- or nociceptive-related input (Cechetto and Saper 1987; Craig 2002; Craig et al. 2000; Hanamori et al. 1998; Saper 2002), as discussed above. Small and colleagues did not explicitly assessed the cortical areas responding

to the taste of chocolate (or to chocolate in the mouth) that would be significantly activated across the whole experiment (evidencing thus the taste-responsive areas not being modulated by the reward value of chocolate) as achieved in Chapter V with respect to water in the mouth under different need states by using conjunction analysis. Finally, some of the insular areas named "anterior insula" in Small et al. (2001) would actually be classified as part of the "mid-insula" following the terminology proposed in this Thesis, implying that the "sensory-limbic" concept might have to be partially reassessed. If taken into account the results obtained in this Thesis, the "sensory-limbic" properties would be restricted to the medial parts of the orbitofrontal cortex and its dorsal extension into the rostral anterior cingulate cortex, possibly also including the mid part of the insula.

The above points can be further clarified with the Table presented below, where the main orbitofrontal cortex activations found in the studies presented in this Thesis are listed (notice thus that this is only a sample of the activations found). Reward-related responses are marked with (■), and its corresponding *x* MNI coordinate is highlighted in bold. It can be noticed that these activations are concentrated in the medial part of the orbitofrontal cortex, across its anterior-posterior dimension. In contrast, the activations found in the orbitofrontal cortex to intra-oral (including tastants and water) and olfactory stimuli are marked with (‡) and its *x* MNI coordinate is underlined. In this case activations are concentrated in more caudolateral areas of the orbitofrontal cortex.

Table: Summary of orbitofrontal cortex (OFC) activations

Side / Location	MNI coordinates (peak)	Z-score	p-value
	Ch. I - Umami taste		
	‡Main effects produced by umami tastants		
L Caudal OFC	[-34 26 -6]	4.84	p<0.05c
	‡Supra-additivity		
L mid-anter. OFC	[-44 34 -18]	3.49	p<0.05svc
	Ch II - Orthonasal olfaction		
	■ Main effects produced by pleasant odours		
Medial ant. OFC	[**0** 54 -12]	5.23	p<0.05c
	Main effects produced by unpleasant odours		
L caudal OFC	[-36 27 -8]	4.23	p<0.05svc
	■ Correlation with pleasantness ratings		
L medial-ant. OFC	[**-2** 52 -10]	4.28	p<0.01svc
	Anti-correlation with pleasantness ratings		
L ant. OFC	[-20 54 -14]	4.26	p<0.01svc
L caudal OFC	[-16 28 -18]	4.08	p<0.05svc
	‡ Main effects produced by all odours		
L caudal OFC	[-40 26 -10]	4.53	p<0.05c

Side / Location	MNI coordinates (peak)	Z-score	p-value
	Ch. III - Crossmodal		
	Sucrose+Strawberry - tasteless		
R Caudomedial OFC	[14 26 –6]	3.94	p<0.05svc
	Sucrose - tasteless		
R Caudomedial OFC	[10 22 –12]	3.64	p<0.05svc
	Strawberry retro odour - tasteless		
R Caudolateral OFC	[38 23 -7]	3.10	p<0.001u
	‡ Conjunction sucrose AND retro strawberry		
R Caudolateral OFC	[36 25 -6]	3.20	p<0.001u
	‡ Supra-additivity		
L Anterior OFC	[-32 50 -10]	3.92	p<0.05svc
	■ Correlation with consonance ratings		
Medial ant. OFC	[**0** 46 -17]	5.09	p<0.05c
	■ Correlation with pleasantness ratings		
R Med-ant. OFC	[**2** 52 -15]	4.14	p<0.05svc
	Ch IV - i.v. M-Amphetamine		
	■ Amphetamine - saline		
R Medial ant. OFC	[**12** 42 -14]	5.10	p<0.05c
	■ Correlation with "mind-racing" ratings		
Medial ant. OFC	[**0** 54 -8]	3.66	p<0.001u
	Ch. V - Thirst		
	Water – tasteless (across experiment)		
L Caudomedial OFC	[-1 35 –16]	3.9	p<0.03svc
R Caudomedial OFC	[9 19 –16]	3.7	p<0.05svc

Side / Location	MNI coordinates (peak)	Z-score	p-value
Main effects of taste (– interaction) (water AND glucose AND salt)			
R Caudomedial OFC	[2 30 –18]	4.53	p<0.05c
‡ Main effects (– interaction) of water pre –tasteless AND water pos-tasteless			
R/L Caudolateral OFC	[±34 22 –8]	4.8	p<0.05c
■ Water – tasteless (thirsty - sated)			
R Caudomedial OFC/BA 25	[**6** 22 –7]	3.1	p<0.005u
■ Correlation with pleasantness ratings for water in the mouth			
L Med-ant. OFC	[**-3** 45 -16]	3.92	p<0.05svc
R Med-ant. OFC	[**16** 46 -16]	3.42	p<0.001u

Finally, with respect to the recent cytoarchitectonic characterisation of the human medial and orbital networks (Ongur et al. 2003) we show in Fig C.1 some exemplar peaks of activation obtained in this Thesis overlayed on the Talairach and Tournoux (1988) map, which had its frontal sections labelled with the corresponding cytoarchitectonic divisions by Ongur et al. (2003). It should be noticed that these are approximate locations, also because there is a slight discrepancy between the MNI and the Talairach and Tournoux coordinate systems (Collins et al. 1994).

Fig C.1 shows, first, that unimodal taste and unimodal olfactory (all odours independently of valence) inputs activate preferentially areas (as defined in Ongur et al. 2003) 47/12(r,s,l,m), PrCO, G, 45, 13(a,b) and the agranular extension of the insular cortex into the orbital surface Iai, Ial, Iam, Iapm. In particular, the intensity judgements for orthonasal odours correlated with activity in the primary olfactory cortex (PC and AON). In contrast, the activations reflecting the reward value of the stimuli (including the effects of intra-venous amphetamine) clearly activate preferentially the medial areas 10p, 10r, 11m, 24, 25, and 32ac. These medial areas could thus be characterised as sensory-motivational areas, in that sensory encoding is modulated by the reward or motivational value of stimuli.

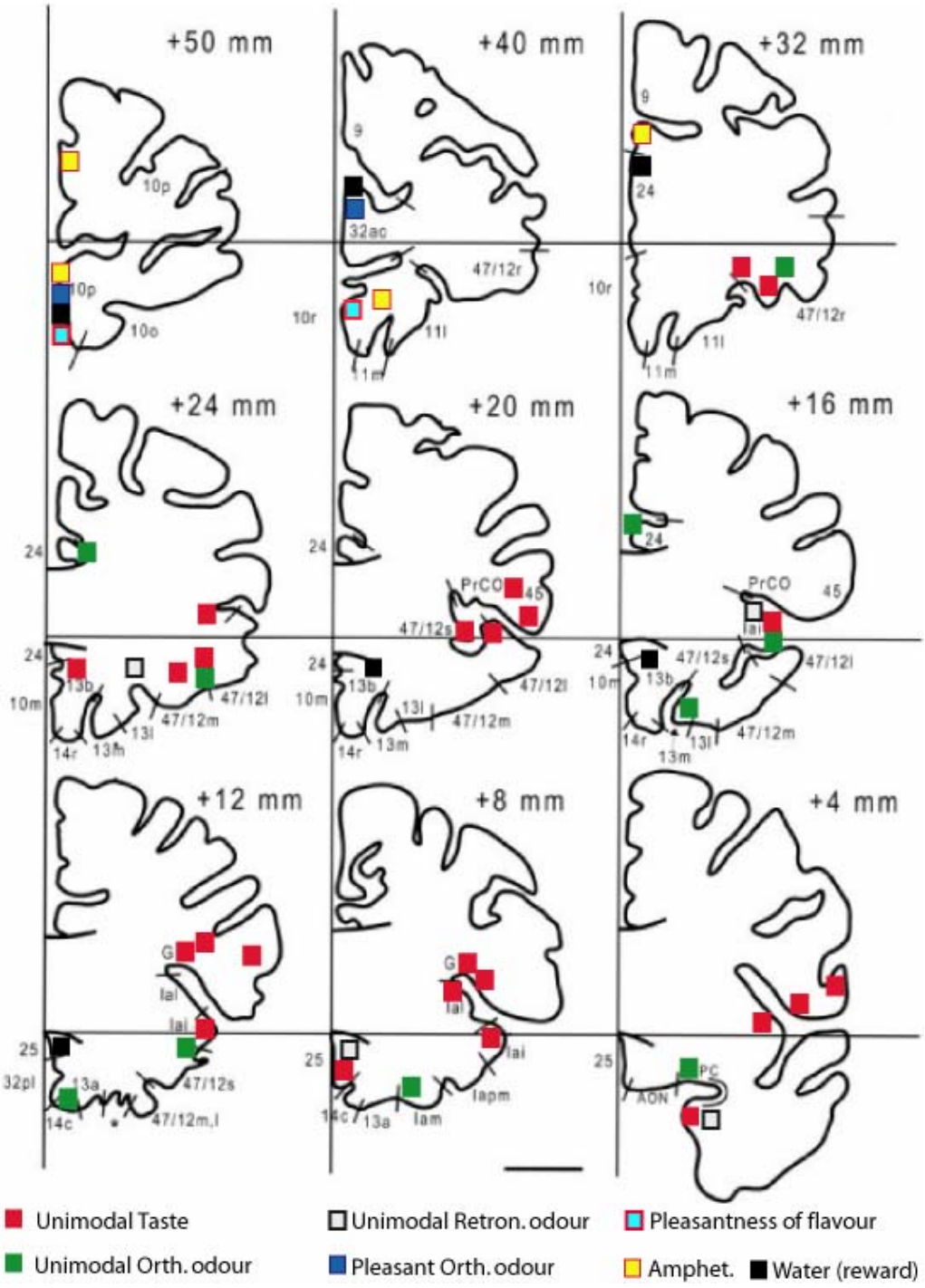


Fig C.1. Exemplar peaks of activation from the experimental Chapters overlayed on the Talairach and Tournoux (1988) map, as labelled by Ongur et al. (2003). Numbers denote cytoarchitecnonic areas and their subdivisions as labelled by the authors (ac, anterior cingulate; c, caudal; l, lateral; m, medial; o, orbital; p, polar; pl, prelimbic; r, rostral; s, sulcal). G, gustatory cortex; Iai, intermediate agranular insular area; Ial, lateral agranular insular area; Iam, medial agranular insular area; Iapl, posterolateral agranular insular area; Iapm, posteromedial agranular insular area; PrCO, precentral opercular cortex.

To some extent, thus, the characteristics of the activations reported in this Thesis seem to be in agreement not only with the data on taste and smell responses at the single-neuron level in macaque monkeys (e.g. Critchley and Rolls 1996b; Rolls 1997) but also with the "medial" and "orbital" network distinction proposed by Price and colleagues (Carmichael and Price 1994; Carmichael and Price 1996; Ongur et al. 2003; Price 1999). A minor discrepancy concerns the far anterior, agranular insular area Iai. In the original monkey studies of Carmichael and Price (1994; 1996) this area stands out as the single agranular extension of the anterior insula not found to be located in the orbital network, in that connections between Iai and Ial, Iam or Iapm were strinkingly weak (Carmichael and Price 1996). In contrast, the medial network areas 10m and 25 are strongly connected with Iai. However, it should be noticed that within fMRI spatial resolution, it is rather difficult to ascertain which area of the agranular cortex was activated by a given taste or olfactory stimulus; it may well be that the areas activated include more posterior regions such as Ial or Iapm so that no strong claims about the functional properties of Iai should be made based only on fMRI data. In any event we suggest here that further single- or multi-cell recordings in area Iai, and adjoining agranular areas, should reveal new aspects on the functions of the orbitofrontal cortex.

References

Aggleton JP and Passingham RE. Syndrome produced by lesions of the amygdala in monkeys (Macaca mulatta). *J Comp Physiol Psychol* 95: 961-977, 1981.

Aharon I, Etcoff N, Ariely D, Chabris CF, O'Connor E and Breiter HC. Beautiful faces have variable reward value: fMRI and behavioral evidence. *Neuron* 32: 537-551, 2001.

Amaral DG and Price JL. Amygdalo-cortical projections in the monkey (Macaca fascicularis). *J. Comp. Neurol.* 230: 465-496, 1984.

Amoore JE. Specific anosmia: a clue to the olfactory code. *Nature* 214: 1095-1098, 1967.

Anderson AK, Christoff K, Stappen I, Panitz D, Ghahremani DG, Glover G, Gabrieli JD and Sobel N. Dissociated neural representations of intensity and valence in human olfaction. *Nat Neurosci* 6: 196-202, 2003.

Augustine JR. Circuitry and functional aspects of the insular lobe in primates including humans. *Brain Res Rev* 22: 229-244, 1996.

Barbas H. Anatomic organization of basoventral and mediodorsal visual recipient prefrontal regions in the rhesus monkey. *J. Comp. Neurol.* 276: 313-342, 1988.

Barbas H. Organization of cortical afferent input to the orbitofrontal area in the rhesus monkey. *Neuroscience* 56: 841-864, 1993.

Bartoshuk LM. NaCl thresholds in man: thresholds for water taste or NaCl taste? *J Comp Physiol Psychol* 87: 310-325, 1974.

Baylis LL and Rolls ET. Responses of neurons in the primate taste cortex to glutamate. *Physiol Behav* 49: 973-979, 1991.

Baylis LL, Rolls ET and Baylis GC. Afferent connections of the orbitofrontal cortex taste area of the primate. *Neuroscience* 64: 801-812, 1995.

Bechara A, Damasio H, Tranel D and Anderson SW. Dissociation of working memory from decision making within the human prefrontal cortex. *J Neurosci* 18: 428-437, 1998.

Beckstead RM, Morse JR and Norgren R. The nucleus of the solitary tract in the monkey: projections to the thalamus and brainstem nuclei. *J. Comp. Neurol.* 190: 259-282, 1980.

Behan M and Haberly LB. Intrinsic and efferent connections of the endopiriform nucleus in rat. *J Comp Neurol* 408: 532-548, 1999.

Benjamin RM and Burton H. Projection of taste nerve afferents to anterior opercular-insular cortex in squirrel monkey (Saimiri sciureus). *Brain Res* 7: 221-231, 1968.

Benjamin RM, Emmers R and Blomquist AJ. Projection of tongue nerve afferents to somatic sensory area I in squirrel monkey (Saimiri sciureus). *Brain Res* 7: 208-220, 1968.

Bennarroch EE. *Central Autonomic Network: Functional Organization and Clinical Correlations*. Armonk, NY: Futura Publishing Company Inc,, 1997.

Berendse HW, Galis-de Graaf Y and Groenewegen HJ. Topographical organization and relationship with ventral striatal compartments of prefrontal corticostriatal projections in the rat. *J Comp Neurol* 316: 314-347, 1992.

Berger B, Thierry AM, Tassin JP and Moyne MA. Dopaminergic innervation of the rat prefrontal cortex: a fluorescence histochemical study. *Brain Res* 106: 133-145, 1976.

Berridge KC and Robinson TE. What is the role of dopamine in reward: hedonic impact, reward learning, or incentive salience? *Brain Res Rev* 28: 309-369, 1998.

Blessing WW and Willoughby JO. Excitation of neuronal function in rabbit caudal ventrolateral medulla elevates plasma vasopressin. *Neurosci Lett* 58: 189-194, 1985.

Bloch F. Nuclear induction. *Phys Rev* 70: 460-474, 1946.

Bloch F, Hansen WW and Packard M. The Nuclear Induction Experiment. *Phys Rev* 70: 474-485, 1946.

Blomqvist A, Zhang ET and Craig AD. Cytoarchitectonic and immunohistochemical characterization of a specific pain and temperature relay, the posterior portion of the ventral medial nucleus, in the human thalamus. *Brain* 123: 601-619, 2000.

Blood AJ, Zatorre RJ, Bermudez P and Evans AC. Emotional responses to pleasant and unpleasant music correlate with activity in paralimbic brain regions. *Nat Neurosci* 2: 382-387., 1999.

Brodmann K. *Vergleichende Lokalisationslehre der Grosshirnrinde in ihren Prinzipien dargestellt auf Grund des Zellenbaues*. Leipzip: Barth, 1909.

Bush G, Luu P and Posner MI. Cognitive and emotional influences in anterior cingulate cortex. *Trends Cogn Sci* 4: 215-222, 2000.

Cardinal R, Parkinson JA, Hall J and Everitt BJ. Emotion and motivation: the role of the amygdala, ventral striatum, and prefrontal cortex. *Neurosci Biobehav Rev* 26: 321-352, 2002.

Carmichael ST, Clugnet M-C and Price JL. Central olfactory connections in the macaque monkey. *J. Comp. Neurol.* 346: 403-434, 1994.

Carmichael ST and Price JL. Architectonic subdivision of the orbital and medial prefrontal cortex in the macaque monkey. *J. Comp. Neurol.* 346: 366-402, 1994.

Carmichael ST and Price JL. Limbic connections of the orbital and medial prefrontal cortex in macaque monkeys. *Journal of Comparative Neurol* 363: 615-641, 1995a.

Carmichael ST and Price JL. Sensory and premotor connections of the orbital and medial prefrontal cortex of macaque monkeys. *J. Comp. Neurol.* 363: 642-664, 1995b.

Carmichael ST and Price JL. Connectional networks within the orbital and medial prefrontal cortex of macaque monkeys. *J. Comp. Neurol.* 371: 179-207, 1996.

Cascino G and Karnes W. Gustatory and second sensory seizures associated with lesions in the insular cortex seen on magnetic resonance imaging. *J. Epilepsy* 3: 185-187, 1990.

Cavada C, Company T, Tejedor J, Cruz Rizzolo RJ and Reinoso Suarez F. The anatomical connections of the macaque monkey orbitofrontal cortex. A review. *Cereb Cortex* 10: 220-242, 2000.

Cechetto DF and Chen SJ. Subcortical sites mediating sympathetic responses from insular cortex in rats. *Am J Physiol* 258: R245-255, 1990.

Cechetto DF and Saper CB. Evidence for a viscerotopic sensory representation in the cortex and thalamus in the rat. *J. Comp. Neurol.* 262: 27-45, 1987.

Cereda C, Ghika J, Maeder P and Bogousslavsky J. Strokes restricted to the insular cortex. *Neurology* 59: 1950-1955, 2002.

Cerf-Ducastel B and Murphy C. fMRI activation in response to odorants orally delivered in aqueous solutions. *Chem Senses* 26: 625-637, 2001.

Cerf-Ducastel B, Van de Moortele PF, MacLeod P, Le Bihan D and Faurion A. Interaction of gustatory and lingual somatosensory perceptions at the cortical level in the human: a functional magnetic resonance imaging study. *Chem Senses* 26: 371-383, 2001.

Chaudhari N. Umami taste transduction: multiple receptors and pathways? *Sensory Neuron* 3: 129-138, 2001.

Chaudhari N, Landin AM and Roper SD. A metabotropic glutamate receptor variant functions as a taste receptor. *Nat Neurosci* 3: 113-119, 2000.

Chiba T, Kayahara T and Nakano K. Efferent projections of infralimbic and prelimbic areas of the medial prefrontal cortex in the Japanese monkey, Macaca fuscata. *Brain Res* 888: 83-101, 2001.

Childress AR, Mozley PD, McElgin W, Fitzgerald J, Reivich M and O'Brien CP. Limbic activation during cue-induced cocaine craving. *Am J Psychiatry* 156: 11-18, 1999.

Christersson CE, Lindh L and Arnebrant T. Film-forming properties and viscosities of saliva substitutes and human whole saliva. *Eur J Oral Sci* 108: 418-425, 2000.

Cipolloni PB and Pandya DN. Cortical connections of the frontoparietal opercular areas in the rhesus monkey. *J Comp Neurol* 403: 431-458, 1999.

Coghill RC, Sang CN, Maisog JM and Iadarola MJ. Pain intensity processing within the human brain: a bilateral, distributed mechanism. *J Neurophysiol* 82: 1934-1943., 1999.

Collins DL, Neelin P, Peters TM and Evans AC. Automatic 3D intersubject registration of MR volumetric data in standardized Talairach space. *J Comput Assist Tomogr* 18: 192-205, 1994.

Corbit LH, Muir JL and Balleine BW. The role of the nucleus accumbens in instrumental conditioning: evidence of a functional dissociation between accumbens core and shell. *J Neurosci* 21: 3251-3260, 2001.

Craig AD. How do you feel? Interoception: the sense of the physiological condition of the body. *Nat Rev Neurosci* 3: 655-666, 2002.

Craig AD, Bushnell MC, Zhang ET and Blomqvist A. A thalamic nucleus specific for pain and temperature sensation. *Nature* 372: 770-773, 1994.

Craig AD, Chen K, Bandy D and Reiman EM. Thermosensory activation of insular cortex. *Nat Neurosci* 3: 184-190., 2000.

Critchley HD, Corfield DR, Chandler MP, Mathias CJ and Dolan RJ. Cerebral correlates of autonomic cardiovascular arousal: a functional neuroimaging investigation in humans. *J Physiol* 523: 259-270, 2000a.

Critchley HD, Elliott R, Mathias CJ and Dolan RJ. Neural activity relating to generation and representation of galvanic skin conductance responses: a functional magnetic resonance imaging study. *J Neurosci* 20: 3033-3040., 2000b.

Critchley HD and Rolls ET. Hunger and satiety modify the responses of olfactory and visual neurons in the primate orbitofrontal cortex. *J Neurophysiol* 75: 1673-1686, 1996a.

Critchley HD and Rolls ET. Olfactory neuronal responses in the primate orbitofrontal cortex: analysis in an olfactory discrimination task. *J Neurophysiol* 75: 1659-1672, 1996b.

Davidson RJ. Anterior cerebral asymmetry and the nature of emotion. *Brain Cogn.* 6: 245-268, 1992.

Davis TL, Kwong KK, Weisskoff RM and Rosen BR. Calibrated functional MRI: mapping the dynamics of oxidative metabolism. *Proc Natl Acad Sci U S A* 95: 1834-1839, 1998.

de Araujo IE, Kringelbach ML and Rolls ET. Different areas of the human orbitofrontal and cingulate cortex activated by pleasant and unpleasant odors. *Soc Neurosci Abstr*, Orlando, FL, 2002.

de Araujo IE, Kringelbach ML, Rolls ET and Hobden P. Representation of umami taste in the human brain. *J Neurophysiol* 90: 313-319, 2003a.

de Araujo IE, Kringelbach ML, Rolls ET and McGlone F. Human cortical responses to water in the mouth, and the effects of thirst. *J Neurophysiol* 90: 1865-1876, 2003b.

de Araujo IE, Rolls ET, Kringelbach ML, McGlone F and Phillips N. Taste-olfactory convergence, and the representation of the pleasantness of flavour, in the human brain. *Eur J Neurosci* 18: In Press, 2003c.

de Araujo IE, Rolls ET and Stringer SM. A view model which accounts for the spatial fields of hippocampal primate spatial view cells and rat place cells. *Hippocampus* 11: 699-706, 2001.

Deems DA and Doty RL. Age-related changes in phenyl ethyl alcohol odor detection threshold. *Trans PA Acad Ophtamol Otolaryngol* 39: 646-650, 1987.

Denton D, Shade R, Zamarippa F, Egan G, Blair-West J, McKinley M and Fox P. Correlation of regional cerebral blood flow and change of plasma sodium concentration during genesis and satiation of thirst. *Proc Natl Acad Sci U S A* 96: 2532-2537, 1999a.

Denton D, Shade R, Zamarippa F, Egan G, Blair-West J, McKinley M, Lancaster J and Fox P. Neuroimaging of genesis and satiation of thirst and an interoceptor- driven theory of origins of primary consciousness. *Proc Natl Acad Sci U S A* 96: 5304-5309, 1999b.

Devinsky O, Morrell MJ and Vogt BA. Contributions of anterior cingulate cortex to behaviour. *Brain* 118: 279-306, 1995.

Di Chiara G and Tanda G. Blunting of reactivity of dopamine transmission to palatable food: a biochemical marker of anhedonia in the CMS model? *Psychopharmacology* 134: 351-353, 1997.

Dickinson A, Smith J and Mirenowicz J. Dissociation of Pavlovian and Instrumental incentive learning under dopamine antagonists. *Behav Neurosci* 114: 468-483, 2000.

Drevets WC. Prefrontal cortical-amygdalar metabolism in major depression. *Ann N Y Acad Sci* 877: 614-637, 1999.

Drevets WC, Gautier C, Price JC, Kupfer DJ, Kinahan PE, Grace AA, Price JL and Mathis CA. Amphetamine-induced dopamine release in human ventral striatum correlates with euphoria. *Biol Psychiatry* 49: 81-96, 2001.

Elliott R, Baker SC, Rogers RD, O'Leary DA, Paykel ES, Frith CD, Dolan RJ and Sahakian BJ. Prefrontal dysfunction in depressed patients performing a complex planning task: a study using positron emission tomography. *Psychol Med* 27: 931-942., 1997.

Elliott R, Dolan RJ and Frith CD. Dissociable functions in the medial and lateral orbitofrontal cortex: evidence from human neuroimaging studies. *Cereb Cortex* 10: 308-317., 2000.

Everitt BJ, Dickinson A and Robbins TW. The neuropsychological basis of addictive behaviour. *Brain Res Rev* 36: 129-138, 2001.

Ferguson AV and Renaud LP. Hypothalamic paraventricular nucleus lesions decrease pressor responses to subfornical organ stimulation. *Brain Res* 305: 361-364, 1984.

Fiol ME, Leppik IE, Mireles R and Maxwell R. Ictus emeticus and the insular cortex. *Epilepsy Res* 2: 127-131, 1988.

Fitzsimons JT. Angiotensin, thirst, and sodium appetite. *Physiol Rev* 78: 583-686, 1998.

Foreman RD. Mechanisms of cardiac pain. *Annu Rev Physiol* 61: 143-167, 1999.

Fox PT, Burton H and Raichle ME. Mapping human somatosensory cortex with positron emission tomography. *J Neurosurg* 67: 34-43, 1987.

Friston K, Ashburner J, Poline JB, Frith CD, Heather JD and Frackowiak RSJ. Spatial registration and normalization of images. *Human Brain Mapp* 2: 165-189, 1995a.

Friston KJ, Holmes A, Poline JB, Price CJ and Frith CD. Detecting activations in PET and fMRI: levels of inference and power. *Neuroimage* 4: 223-235, 1996.

Friston KJ, Holmes AP, Price CJ, Buchel C and Worsley KJ. Multisubject fMRI studies and conjunction analyses. *Neuroimage* 10: 385-396, 1999a.

Friston KJ, Holmes AP and Worsley KJ. How many subjects constitute a study? *Neuroimage* 10: 1-5, 1999b.

Friston KJ, Holmes AP, Worsley KJ, Poline JP, Frith CD and Frackowiak RSJ. Statistical parametric maps in functional imaging: A general linear approach. *Human Brain Mapp* 2: 189-210, 1995b.

Fudge JL and Haber SN. The central nucleus of the amygdala projection to dopamine subpopulations in primates. *Neuroscience* 97: 479-494, 2000.

Gaspar P, Berger B, Febvret A, Vigny A and Henry JP. Catecholamine innervation of the human cerebral cortex as revealed by comparative immunohistochemistry of tyrosine hydroxylase and dopamine-beta-hydroxylase. *J Comp Neurol* 279: 249-271, 1989.

Glenn JF and Erickson RP. Gastric modulation of gustatory afferent activity. *Physiol Behav* 16: 561-568, 1976.

Gottfried JA, Deichmann R, Winston JS and Dolan RJ. Functional heterogeneity in human olfactory cortex: an event-related functional magnetic resonance imaging study. *J Neurosci* 22: 10819-10828, 2002.

Grafton ST, Woods RP, Mazziotta JC and Phelps ME. Somatotopic mapping of the primary motor cortex in humans: activation studies with cerebral blood flow and positron emission tomography. *J Neurophysiol* 66: 735-743, 1991.

Graziadei PP. The ultrastructure of vertebrates olfactory mucosa. In: *The ultrastructure of sensory organs*, edited by Friedman I. Oxford: Elsevier Co., 1973, p. 267-305.

Grossman S-P. *Thirst and sodium appetite*. San Diego: Academic, 1990.

Hadland KA, Rushworth MF, Gaffan D and Passingham RE. The anterior cingulate and reward-guided selection of actions. *J Neurophysiol* 89: 1161-1164, 2003a.

Hadland KA, Rushworth MF, Gaffan D and Passingham RE. The effect of cingulate lesions on social behaviour and emotion. *Neuropsychologia* 41: 919-931, 2003b.

Hall J, Parkinson JA, Connor TM, Di Ciano P, Dickinson A and Everitt BJ. The role of amygdala-ventral striatal sub-systems in Pavlovian-to-instrumental transfer. *Soc. Neurosci. Abstr.* 25, 1999.

Hanamori T, Kunitake T, Kato K and Kannan H. Responses of neurons in the insular cortex to gustatory, visceral, and nociceptive stimuli in rats. *J Neurophysiol* 79: 2535-2545, 1998.

Hariri AR, Mattay VS, Tessitore A, Fera F, Smith WG and Weinberger DR. Dextroamphetamine modulates the response of the human amygdala. *Neuropsychopharmacology* 27: 1036-1040, 2002.

Haywood JR, Fink GD, Buggy J, Boutelle S, Johnson AK and Brody MJ. Prevention of two-kidney, one-clip renal hypertension in rat by ablation of AV3V tissue. *Am J Physiol* 245: H683-689, 1983.

Heeger DJ and Ress D. What does fMRI tell us about neuronal activity? *Nat Rev Neurosci* 3: 142-151, 2002.

Hiyama TY, Watanabe E, Ono K, Inenaga K, Tamkun MM, Yoshida S and Noda M. Na(x) channel involved in CNS sodium-level sensing. *Nat Neurosci* 5: 511-512, 2002.

Hooks MS, Jones GH, Liem BJ and Justice JB. Sensitization and individual differences to IP amphetamine, cocaine, or caffeine following repeated intracranial amphetamine infusions. *Pharmacol. Biochem. Behav.* 43: 815-823, 1992.

Hu J, Javaid T, Arias-Mendoza F, Liu Z, McNamara R and Brown TR. A fast, reliable, automatic shimming procedure using 1H chemical-shift-imaging spectroscopy. *J Magn Reson, Series B* 108: 213-219, 1995.

Hurd YL, Suzuki M and Sedvall GC. D1 and D2 dopamine receptor mRNA expression in whole hemisphere sections of the human brain. *J Chem Neuroanat* 22: 127-137, 2001.

Hurley KM, Herbert H, Moga MM and Saper CB. Efferent projections of the infralimbic cortex of the rat. *J Comp Neurol* 308: 249-276, 1991.

Hylden JL, Anton F and Nahin RL. Spinal lamina I projection neurons in the rat: collateral innervation of parabrachial area and thalamus. *Neuroscience* 28: 27-37, 1989.

Ito R, Dalley JW, Howes SR, Robbins TW and Everitt BJ. Dissociation in conditioned dopamine release in the nucleus accumbens core and shell in response to cocaine cues and during cocaine-seeking behaviour in rats. *J Neurosci* 20: 7489-7495, 2000.

Jain N, Qi HX, Catania KC and Kaas JH. Anatomic correlates of the face and oral cavity representations in the somatosensory cortical area 3b of monkeys. *J Comp Neurol* 429: 455-468, 2001.

Jenkinson M and Smith S. A global optimisation method for robust affine registration of brain images. *Med Im Analysis* 5: 143-156, 2001.

Kaas JH. The functional organization of the somatosensory cortex in primates. *Anat. Anz.* 175: 509-518, 1993.

Kadohisa M, Verhagen JV and Rolls ET. Taste, texture, and temperature but not olfactory or visual inputs to the primate primary taste cortex. *Chem Senses* In Press., 2003.

Kalk WW, Vissink A, Spijkervet FK, Bootsma H, Kallenberg CG and Nieuw Amerongen AV. Sialometry and sialochemistry: diagnostic tools for Sjogren's syndrome. *Ann Rheum Dis* 60: 1110-1116, 2001.

Kawamura Y and Kare M. *Umami: a basic taste*. New York: Marcel Dekker, 1987.

King AB, Menon R, Hachinski V and Cechetto DF. Human forebrain activation by visceral stimuli. *J. Comp. Neurol.* 413: 572-582, 1999.

Kinney FC. An experimental study of the central gustatory pathways in the monkey, Macaca mulatta and Cercopithecus aethiops. *J Hirnforsch* 19: 21-43, 1978.

Kosar E, Grill HJ and Norgren R. Gustatory cortex in the rat. I. Physiological properties and cytoarchitecture. *Brain Res* 379: 329-341, 1986a.

Kosar E, Grill HJ and Norgren R. Gustatory cortex in the rat. II. Thalamocortical projections. *Brain Res* 379: 342-352, 1986b.

Kruger L, Mantyh PW, Sternini C, Brecha NC and Mantyh CR. Calcitonin gene-related peptide (CGRP) in the rat central nervous system: patterns of immunoreactivity and receptor binding sites. *Brain Res* 463: 223-244, 1988.

Lenkei Z, Palkovits M, Corvol P and Llorens-Cortes C. Expression of angiotensin type-1 (AT1) and type-2 (AT2) receptor mRNAs in the adult rat brain: a functional neuroanatomical review. *Front Neuroendocrinol* 18: 383-439, 1997.

Li S, Dardzinski BJ, Collins CM, Yang QX and Smith MB. Three-dimensional mapping of the static magnetic field inside the human head. *Magn Reson Med* 36: 705-714, 1996.

Lin C and Kinnamon SC. Responses to monosodium glutamate and guanosine 5'-monophosphate in rat fungiform taste cells. *Ann N Y Acad Sci* 855: 407-411, 1998.

Logothetis NK. The neural basis of the blood-oxygen-level-dependent functional magnetic resonance imaging signal. *Philos Trans R Soc Lond B Biol Sci* 357: 1003-1037, 2002.

Logothetis NK, Pauls J, Augath M, Trinath T and Oeltermann A. Neurophysiological investigation of the basis of the fMRI signal. *Nature* 412: 150-157, 2001.

Manger PR, Woods TM and Jones EG. Representation of face and intra-oral structures in area 3b of macaque monkey somatosensory cortex. *J Comp Neurol* 371: 513-521, 1996.

Mangiapane ML and Simpson JB. Subfornical organ lesions reduce the pressor effect of systemic angiotensin II. *Neuroendocrinology* 31: 380-384, 1980.

Mansfield P, Coxon R and Glover P. Echo-planar imaging of the brain at 3.0 T: first normal volunteer results. *J Comput Assist Tomogr* 18: 339-343, 1994.

Mansfield P and Harvey PR. Limits to neural stimulation in echo-planar imaging. *Magn Reson Med* 29: 746-758, 1993.

Matsunami H, Montmayeur JP and Buck LB. A family of candidate taste receptors in human and mouse. *Nature* 404: 601-604, 2000.

Matsuo R. Role of saliva in the maintenance of taste sensitivity. *Crit Rev Oral Biol Med* 11: 216-229, 2000.

Mattay VS, Callicott JH, Bertolino A, Heaton I, Frank JA, Coppola R, Berman KF, Goldberg TE and Weinberger DR. Effects of dextroamphetamine on cognitive performance and cortical activation. *Neuroimage* 12: 268-275, 2000.

Mayberg HS, Brannan SK and Mahurin. Cingulate function in depression: a potential predictor of treatment response. *Neuroreport* 8: 1057-1061, 1997.

McCaffrey RJ, Duff K and Solomon GS. Olfactory dysfunction discriminates probable Alzheimer's dementia from major depression: a cross-validation and extension. *J Neuropsychiatry Clin Neurosci* 12: 29-33, 2000.

McKinley MJ, Allen AM, May CN, McAllen RM, Oldfield BJ, Sly D and Mendelsohn FA. Neural pathways from the lamina terminalis influencing cardiovascular and body fluid homeostasis. *Clin Exp Pharmacol Physiol* 28: 990-992, 2001.

McKinley MJ, Mathai ML, Pennington G, Rundgren M and Vivas L. Effect of individual or combined ablation of the nuclear groups of the lamina terminalis on water drinking in sheep. *Am J Physiol* 276: R673-683, 1999.

Mesulam M-M and Mufson EJ. Insula of the Old World Monkey. I. Architectonics in the insulo-orbito-temporal component of the paralimbic brain. *J Comp Neurol* 212: 1-22, 1982a.

Mesulam M-M and Mufson EJ. Insula of the old world monkey. III Efferent cortical output and comments on function. *J. Comp. Neurol.* 212: 38-52, 1982b.

Miselis RR. The efferent projections of the subfornical organ of the rat: a circumventricular organ within a neural network subserving water balance. *Brain Res* 230: 1-23, 1981.

Montmayeur JP, Liberles SD, Matsunami H and Buck LB. A candidate taste receptor gene near a sweet taste locus. *Nat Neurosci* 4: 492-498, 2001.

Montmayeur JP and Matsunami H. Receptors for bitter and sweet taste. *Curr Opin Neurobiol* 12: 366-371, 2002.

Morecraft R and Van Hoesen G. Frontal granular cortex input to the cingulate (M3), supplementary (M2) and primary (M1) motor cortices in the rhesus monkey. *J Comp Neurol* 337: 669–689, 1993.

Morecraft RJ, Louie JL, Schroeder CM and Avramov K. Segregated parallel inputs to the brachial spinal cord from the cingulate motor cortex in the monkey. *Neuroreport* 8: 3933-3938, 1997.

Morecraft RJ and Van Hoesen GW. Convergence of limbic input to the cingulate motor cortex in the rhesus monkey. *Brain Res Bull* 45: 209-232, 1998.

Morrison EE and Constanzo RM. Morphology of the human olfactory epithelium. *J. Comp. Neurol.* 297: 1-13, 1990.

Mufson EJ and Mesulam M-M. Insula of the old world monkey: II: Afferent cortical input and comments on the claustrum. *J. Comp. Neurol.* 212: 23-37, 1982.

Nagler RM and Nagler A. The effect of pilocarpine on salivary constituents in patients with chronic graft-versus-host disease. *Arch Oral Biol* 46: 689-695, 2001.

Ninomiya Y and Funakoshi M. Qualitative discrimination among 'umami' and the four basic taste substances in mice. In: *Umami: A Basic Taste*, edited by Kawamura Y and Kare MR. New York: Dekker, 1987, p. 365-385.

Noe' J and Breer H. Functional and molecular characterization of individual olfactory neurons. *J Neurochem* 71: 2286-2293, 1998.

Norgren R. Gustatory system. In: *The Human Nervous System*, edited by Paxinos G. New York: Academic Press, 1990, p. 845-861.

Norgren R and Leonard CM. Ascending central gustatory pathways. *J. Comp. Neurol.* 150: 217-238, 1973.

O'Doherty J, Deichmann R, Critchley HD and Dolan RJ. Neural responses during anticipation of a primary taste reward. *Neuron* 33: 815-826, 2002.

O'Doherty J, Kringelbach ML, Rolls ET, Hornak J and Andrews C. Abstract reward and punishment representations in the human orbitofrontal cortex. *Nat Neurosci* 4: 95-102., 2001a.

O'Doherty J, Rolls ET, Francis S, Bowtell R and McGlone F. Representation of pleasant and aversive taste in the human brain. *J Neurophysiol* 85: 1315-1321., 2001b.

O'Doherty J, Rolls ET, Francis S, Bowtell R, McGlone F, Kobal G, Renner B and Ahne G. Sensory-specific satiety-related olfactory activation of the human orbitofrontal cortex. *Neuroreport* 11: 399-403., 2000.

O'Doherty J, Winston J, Critchley H, Perrett D, Burt DM and Dolan RJ. Beauty in a smile: the role of medial orbitofrontal cortex in facial attractiveness. *Neuropsychologia* 41: 147-155, 2003.

Ogawa H. Gustatory cortex of primates: anatomy and physiology. *Neurosci Res* 20: 1-13, 1994.

Ogawa H, Ito SL and Nomura T. Oral cavity representation at the frontal operculum of macaque monkeys. *Neurosci. Res.* 6: 283-298, 1989.

Ogawa H and Wang XD. Neurons in the cortical taste area receive nociceptive inputs from the whole body as well as the oral cavity in the rat. *Neurosci Lett* 322: 87-90, 2002.

Ogawa S, Lee TM, Kay AR and Tank DW. Brain magnetic resonance imaging with contrast dependent on blood oxygenation. *Proc Natl Acad Sci U S A* 87: 9868-9872, 1990.

Ogawa S, Tank DW, Menon R, Ellermann JM, Kim SG, Merkle H and Ugurbil K. Intrinsic signal changes accompanying sensory stimulation: Functional brain mapping with magnetic resonance imaging. *Proc Natl Acad Sci U S A* 89: 5951-5955, 1992.

Ojemann JG, Akbudak E, Snyder AZ, McKinstry RC, Raichle ME and Conturo TE. Anatomic localization and quantitative analysis of gradient refocused echo-planar fMRI susceptibility artifacts. *Neuroimage* 6: 156-167, 1997.

Oliet SH and Bourque CW. Mechanosensitive channels transduce osmosensitivity in supraoptic neurons. *Nature* 364: 341-343, 1993.

Ongur D, An X and Price JL. Prefrontal cortical projections to the hypothalamus in macaque monkeys. *J Comp Neurol* 401: 480-505, 1998.

Ongur D, Ferry AT and Price JL. Architectonic subdivision of the human orbital and medial prefrontal cortex. *J Comp Neurol* 460: 425-449, 2003.

Öngur D and Price JL. Prefrontal cortical projections to the hypothalamus in macaque monkeys. *J Comp Neurol* 401: 480-505, 1998.

Öngur D and Price JL. The organization of networks within the orbital and medial prefrontal cortex of rats, monkeys and humans. *Cereb Cortex* 10: 206-219, 2000.

Oppenheimer SM, Gelb A, Girvin JP and Hashinki VC. Cardiovascular effects of human insular cortex stimulation. *Neurology* 42: 1727-1732, 1992.

Pardo JV, Wood TD, Costello PA, Pardo PJ and Lee JT. PET study of the localization and laterality of lingual somatosensory processing in humans. *Neurosci Lett* 234: 23-26, 1997.

Parkinson JA, Olmstead MC, Burns LH, Robbins TW and Everitt BJ. Dissociation in effects of lesions of the nucleus accumbens core and shell on appetitive Pavlovian approach

behavior and the potentiation of conditioned reinforcement and locomotor activity by D-amphetamine. *J Neurosci* 19: 2401-2411, 1999.

Pastuskovas CV, Cassell MD, Johnson AK and Thunhorst RL. Increased cellular activity in rat insular cortex after water and salt ingestion induced by fluid depletion. *Am J Physiol Regul Integr Comp Physiol* 284: R1119-1125, 2003.

Paulus MP, Hozack NE, Zauscher BE, Frank L, Brown GG, Braff DL and Schuckit MA. Behavioral and functional neuroimaging evidence for prefrontal dysfunction in methamphetamine-dependent subjects. *Neuropsychopharmacology* 26: 53-63, 2002.

Paus T. Primate anterior cingulate cortex: where motor control, drive and cognition interface. *Nat Rev Neurosci* 2: 417-424, 2001.

Paxinos G, Huang X-F and Toga AW. *The Rhesus Monkey Brain in Stereotaxic Coordinates*. San Diego: Academic Press, 2000.

Penfield W and Faulk M. The insula. Further observations on its function. *Brain* 78: 445-470, 1955.

Penfield W and Jasper H. *Epilepsy and the Functional Anatomy of the Human Brain*. Boston, MA: Little, Brown, and Co., 1954.

Petrides M and Pandya DN. Comparative cytoarchitectonic analysis of the human and the macaque frontal cortex. In: *Handbook of neuropsychology*, edited by Boller F and Grafman J. Amsterdam: Elsevier, 1994, p. 17-58.

Petrovic P, Kalso E, Petersson KM and Ingvar M. Placebo and opioid analgesia-- imaging a shared neuronal network. *Science* 295: 1737-1740, 2002.

Petrovic P, Petersson KM, Ghatan PH, Stone-Elander S and Ingvar M. Pain-related cerebral activation is altered by a distracting cognitive task. *Pain* 85: 19-30., 2000.

Phillips AG, Mora F and Rolls ET. Intracranial self-stimulation in orbitofrontal cortex and caudate nucleus of rhesus monkey: effects of apomorphine, pimozide, and spiroperidol. *Psychopharmacology (Berl)* 62: 79-82, 1979.

Picard N and Strick PL. Imaging the premotor areas. *Curr Opin Neurobiol* 11: 663-672, 2001.

Pierce J and Halpern BP. Orthonasal and retronasal odorant identification based upon vapor phase input from common substances. *Chem Senses* 21: 529-543, 1996.

Poellinger A, Thomas R, Lio P, Lee A, Makris N, Rosen BR and Kwong KK. Activation and habituation in olfaction--an fMRI study. *Neuroimage* 13: 547-560, 2001.

Prammer MG, Haselgrove JC, Shinnar M and Leigh JS. A new approach to automatic shimming. *J Magn Reson* 77: 40-52, 1988.

Preuss TM and Goldman Rakic PS. Conections of the ventral granular frontal cortex of macaques with perisylvian premotor and somatosensory areas: anatomical evidence for somatic representation in primate frontal association areas. *J. Comp. Neurol.* 282: 293-316, 1989.

Price CJ and Friston K. Cognitive Conjunction: A new approach to brain activation experiments. *Neuroimage* 5, 1997.

Price JC, Drevets WC, Ruszkiewicz J, Greer PJ, Villemagne VL, Xu L, Mazumdar S, Cantwell MN and Mathis CA. Sequential H(2)(15)O PET studies in baboons: before and after amphetamine. *J Nucl Med* 43: 1090-1100, 2002.

Price JL. Olfactory system. In: *The Human Nervous System*, edited by Paxinos G. New York: Academic Press, 1990, p. 979-998.

Price JL. Prefrontal cortical networks related to visceral function and mood. *Ann N Y Acad Sci* 877: 383-396, 1999.

Price JL and Amaral DG. An autoradiographic study of the projections of the central nucleus of the monkey amygdala. *J Neurosci* 1: 1242-1259, 1981.

Price JL, Carmichael ST, Carnes KM, Clugnet M-C, Kuroda M and Ray JP. Olfactory input to the prefrontal cortex. In: *Olfaction: A Model System for Computational Neuroscience*, edited by Davis JL and Eichenbaum H. Cambridge, Mass.: MIT Press, 1991, p. 101-120.

Pritchard TC, Hamilton RB, Morse JR and Norgren R. Projections of thalamic gustatory and lingual areas in the monkey, Macaca fascicularis. *J. Comp. Neurol.* 244: 213-228, 1986.

Pritchard TC, Hamilton RB and Norgren R. Neural coding of gustatory information in the thalamus of Macaca mulatta. *J Neurophysiol* 61: 1-14, 1989.

Pritchard TC, Hamilton RB and Norgren R. Projections of the parabrachial nucleus in the old world monkey. *Exp Neurol* 165: 101-117, 2000.

Pritchard TC, Macaluso DA and Eslinger PJ. Taste perception in patients with insular cortex lesions. *Behav Neurosci* 113: 663-671, 1999.

Radna RJ and MacLean PD. Vagal elicitation of respiratory-type and other unit responses in basal limbic structures of squirrel monkeys. *Brain Res* 213: 45-61, 1981.

Rawson NE and Gomez G. Cell and molecular biology of human olfaction. *Microsc. Res. Tech.* 58: 142-151, 2002.

Redoute J, Stoleru S, Gregoire MC, Costes N, Cinotti L, Lavenne F, Le Bars D, Forest MG and Pujol JF. Brain processing of visual sexual stimuli in human males. *Hum Brain Mapp* 11: 162-177, 2000.

Reese TG, Davis TL and Weisskoff RM. Automated shimming at 1.5 T using echo-planar image frequency maps. *J Magn Reson Imaging* 5: 739-745, 1995.

Rifkin B and Bartoshuk LM. Taste synergism between monosodium glutamate and disodium 5'-guanylate. *Physiol Behav* 24: 1169-1172, 1980.

Rolls BJ and Rolls ET. *Thirst*. Cambridge: Cambridge University Press, 1982.

Rolls ET. Central nervous mechanisms related to feeding and appetite. *Br Med Bull* 37: 131-134, 1981.

Rolls ET. Taste and olfactory processing in the brain and its relation to the control of eating. *Crit Rev Neurobiol* 11: 263-287, 1997.

Rolls ET. *The Brain and Emotion*. Oxford: Oxford University Press, 1999.

Rolls ET. The orbitofrontal cortex and reward. *Cereb Cortex* 10: 284-294, 2000a.

Rolls ET. The representation of umami taste in the taste cortex. *J Nutr* 130: S960-965, 2000b.

Rolls ET and Baylis LL. Gustatory, olfactory, and visual convergence within the primate orbitofrontal cortex. *J Neurosci* 14: 5437-5452, 1994.

Rolls ET, Critchley H, Wakeman EA and Mason R. Responses of neurons in the primate taste cortex to the glutamate ion and to inosine 5'-monophosphate. *Physiol Behav* 59: 991-1000, 1996a.

Rolls ET, Critchley HD, Browning AS, Hernadi A and Lenard L. Responses to the sensory properties of fat of neurons in the primate orbitofrontal cortex. *J Neurosci* 19: 1532-1540, 1999.

Rolls ET, Critchley HD, Mason R and Wakeman EA. Orbitofrontal cortex neurons: role in olfactory and visual association learning. *J Neurophysiol* 75: 1970-1981, 1996b.

Rolls ET and Deco G. *Computational Neuroscience of Vision*. Oxford: Oxford University Press, 2002.

Rolls ET, Kringelbach ML and de Araujo IE. Different representations of pleasant and unpleasant odours in the human brain. *Eur J Neurosci* 18: 695-703, 2003a.

Rolls ET, Murzi E, Yaxley S, Thorpe SJ and Simpson SJ. Sensory-specific satiety: food-specific reduction in responsiveness of ventral forebrain neurons after feeding in the monkey. *Brain Res* 368: 79-86, 1986.

Rolls ET, O'Doherty J, Kringelbach ML, Francis S, Bowtell R and McGlone F. Representations of pleasant and painful touch in the human orbitofrontal and cingulate cortices. *Cereb Cortex* 13: 308-317, 2003b.

Rolls ET, Rolls BJ and Rowe EA. Sensory-specific and motivation-specific satiety for the sight and taste of food and water in man. *Physiol Behav* 30: 185-192, 1983.

Rolls ET and Rolls JH. Olfactory sensory-specific satiety in humans. *Physiol Behav* 61: 461-473, 1997.

Rolls ET and Scott TR. Central taste anatomy and neurophysiology. In: *Handbook of Olfaction and Gustation* (2nd (Revised) ed.), edited by R.L.Doty. New York: Marcel Dekker, 2003.

Rolls ET, Scott TR, Sienkiewicz ZJ and Yaxley S. The responsiveness of neurones in the frontal opercular gustatory cortex of the macaque monkey is independent of hunger. *J Physiol* 397: 1-12, 1988.

Rolls ET, Sienkiewicz ZJ and Yaxley S. Hunger modulates the responses to gustatory stimuli of single neurons in the caudolateral orbitofrontal cortex of the macaque monkey. *Eur J Neurosci* 1: 53-60, 1989.

Rolls ET, Yaxley S and Sienkiewicz ZJ. Gustatory responses of single neurons in the caudolateral orbitofrontal cortex of the macaque monkey. *J Neurophysiol* 64: 1055-1066, 1990.

Royet JP, Hudry J, Zald DH, Godinot D, Gregoire MC, Lavenne F, Costes N and Holley A. Functional neuroanatomy of different olfactory judgments. *Neuroimage* 13: 506-519., 2001.

Royet JP, Koenig O, Gregoire MC, Cinotti L, Lavenne F, Le Bars D, Costes N, Vigouroux M, Farget V, Sicard G, Holley A, Mauguiere F, Comar D and Froment JC. Functional anatomy of perceptual and semantic processing for odors. *J Cogn Neurosci* 11: 94-109, 1999.

Rushworth MF, Hadland KA, Paus T and Sipila PK. Role of the human medial frontal cortex in task switching: a combined fMRI and TMS study. *J Neurophysiol* 87: 2577-2592, 2002.

Sakai K, Watanabe E, Onodera Y, Itagaki H, Yamamoto E, Koizumi H and Miyashita Y. Functional mapping of the human somatosensory cortex with echo-planar MRI. *Magn Reson Med* 33: 736-743, 1995.

Sanides F. The architecture of the cortical taste nerve areas in squirrel monkey (Saimiri sciureus) and their relationships to insular, sensorimotor and prefrontal regions. *Brain Res* 8: 97-124, 1968.

Saper CB. The central autonomic nervous system: conscious visceral perception and autonomic pattern generation. *Annu Rev Neurosci* 25: 433-469, 2002.

Savic I, Gulyas B, Larsson M and Roland P. Olfactory functions are mediated by parallel and hierarchical processing. *Neuron* 26: 735-745, 2000.

Schild D and Restrepo D. Transduction mechanisms in vertebrate olfactory receptor cells. *Physiol Rev* 78: 429-466, 1998.

Schneider E and Glover G. Rapid in vivo proton shimming. *Magn Reson Med* 18: 335-347, 1991.

Schultz W, Dayan P and Montague PR. A neural substrate of prediction and reward. *Science* 275: 1593-1599, 1997.

Schultz W, Tremblay L and Hollerman JR. Reward processing in primate orbitofrontal cortex and basal ganglia. *Cereb Cortex* 10: 272-284, 2000.

Schwartz JH, Shkolnik LJ and Goldberg DJ. Specific association of neurotransmitter with somatic lysosomes in an identified serotonergic neuron of Aplysia californica. *Proc Natl Acad Sci U S A* 76: 5967-5971, 1979.

Scott TR, Karadi Z, Oomura Y, Nishino H, Plata-Salaman CR, Lenard L, Giza BK and Ao S. Gustatory neural coding in the amygdala of the alert monkey. *J Neurophysiol* 69: 1810-1820, 1993.

Scott TR and Plata-Salaman CR. Taste in the monkey cortex. *Physiol Behav* 67: 489-511, 1999.

Scott TR, Yaxley S, Sienkiewicz ZJ and Rolls ET. Gustatory responses in the frontal opercular cortex of the alert cynomolgus monkey. *J Neurophysiol* 56: 876-890, 1986a.

Scott TR, Yaxley S, Sienkiewicz ZJ and Rolls ET. Taste responses in the nucleus tractus solitarius of the behaving monkey. *J Neurophysiol* 55: 182-200, 1986b.

Sewards TV and Sewards MA. Cortical association areas in the gustatory system. *Neurosci Biobehav Rev* 25: 395-407, 2001.

Shi CJ and Cassell MD. Cortical, thalamic, and amygdaloid connections of the anterior and posterior insular cortices. *J Comp Neurol* 399: 440-468, 1998.

Skinner K, Basbaum AI and Fields HL. Cholecystokinin and enkephalin in brain stem pain modulating circuits. *Neuroreport* 8: 2995-2998, 1997.

Sly DJ, Colvill L, McKinley MJ and Oldfield BJ. Identification of neural projections from the forebrain to the kidney, using the virus pseudorabies. *J Auton Nerv Syst* 77: 73-82, 1999.

Small DM, Jones-Gotman M, Zatorre RJ, Petrides M and Evans AC. Flavor processing: more than the sum of its parts. *Neuroreport* 8: 3913-3917., 1997a.

Small DM, Jones-Gotman M, Zatorre RJ, Petrides M and Evans AC. A role for the right anterior temporal lobe in taste quality recognition. *J Neurosci* 17: 5136-5142, 1997b.

Small DM, Zald DH, Jones-Gotman M, Zatorre RJ, Pardo JV, Frey S and Petrides M. Human cortical gustatory areas: a review of functional neuroimaging data. *Neuroreport* 10: 7-14., 1999.

Small DM, Zatorre RJ, Dagher A, Evans AC and Jones-Gotman M. Changes in brain activity related to eating chocolate: From pleasure to aversion. *Brain* 124: 1720-1733., 2001.

Smith AJ, Blumenfeld H, Behar KL, Rothman DL, Shulman RG and Hyder F. Cerebral energetics and spiking frequency: the neurophysiological basis of fMRI. *Proc Natl Acad Sci U S A* 99: 10765-10770, 2002.

Stehling MK, Turner R and Mansfield P. Echo-planar imaging: magnetic resonance imaging in a fraction of a second. *Science* 254: 43-50, 1991.

Takagi SF. Studies on the olfactory nervous system of the old world monkey. *Prog. Neurobiol.* 27: 195-249, 1986.

Takami S. Recent progress in the neurobiology of the vomeronasal organ. *Microsc. Res. Tech.* 58: 228-250, 2002.

Talairach J and Tournoux P. *Co-Planar Stereotaxic Atlas of the Human Brain*. Stuttgart: Thieme, 1988.

Tanabe T, Iino M and Takagi SF. Discrimination of odors in olfactory bulb, pyriform-amygdaloid areas, and orbitofrontal cortex of the monkey. *J Neurophysiol* 38: 1284-1296, 1975.

Tataranni PA, Gautier J-F, Chen K, Uecker A, Bandy D, Salbe AD, Pratley RE, Lawson M, Reiman EM and Ravussin E. Neuroanatomical correlates of hunger and satiation in humans using positron emission tomography. *Proc Natl Acad Sci U S A* 96: 4569-4574, 1999.

Taylor JR and Robbins TW. 6-Hydroxydopamine lesions of the nucleus accumbens, but not of the caudate nucleus, attenuate enhanced responding with reward-related stimuli produced by intra-accumbens D-amphetamine. *Psychopharmacology* 90: 390-397, 1986.

Thompson JK, Peterson MR and Freeman RD. Single-neuron activity and tissue oxygenation in the cerebral cortex. *Science* 299: 1070-1072, 2003.

Tremblay L and Schultz W. Relative reward preference in primate orbitofrontal cortex. *Nature* 398: 704-708, 1999.

Tremblay LK, Naranjo CA, Cardenas L, Herrmann N and Busto UE. Probing brain reward system function in major depressive disorder: altered response to dextroamphetamine. *Arch Gen Psychiat* 59: 409-416, 2002.

Tropp J, Derby KA and Hawryszko C. Automated shimming of B0 for spectroscopic imaging. *J Magn Reson* 85: 244-254, 1989.

Tzschentke TM. Pharmacology and behavioral pharmacology of the mesocortical dopamine system. *Prog. Neurobiol.* 63: 241-320, 2001.

Uftring SJ, Wachtel SR, Chu D, McCandless C, Levin DN and de Wit H. An fMRI study of the effect of amphetamine on brain activity. *Neuropsychopharmacology* 25: 925-935, 2001.

Urasaki E, Uematsu S, Gordon B and Lesser RP. Cortical tongue area studied by chronically implanted subdural electrodes--with special reference to parietal motor and frontal sensory responses. *Brain* 117 (Pt 1): 117-132, 1994.

Vincent SL, Khan Y and Benes FM. Cellular distribution of dopamine D1 and D2 receptors in rat medial prefrontal cortex. *J Neurosci* 13: 2551-2564, 1993.

Vogt BA and Pandya DN. Cingulate cortex of the rhesus monkey: II. Cortical afferents. *J. Comp. Neurol.* 262: 271-289, 1987.

Vogt BA, Pandya DN and Rosene DL. Cingulate cortex of the rhesus monkey: I. Cytoarchitecture and thalamic afferents. *J. Comp. Neurol.* 262: 256-270, 1987.

Vollenweider FX, Maguire RP, Leenders KL, Mathys K and Angst J. Effects of high amphetamine dose on mood and cerebral glucose metabolism in normal volunteers using positron emission tomography (PET). *Psychiatry Res* 83: 149-162, 1998.

Walker AE. A cytoarchitectural study of the prefrontal area of the macaque monkey. *J. Comp. Neurol.* 73: 59-86, 1940.

Watts AG. Neuropeptides and the integration of motor responses to dehydration. *Annu Rev Neurosci* 24: 357-384, 2001.

Webb P and Macovski A. Rapid, fully automatic, arbitrary-volume in vivo shimming. *Magn Reson Med* 20: 113-122, 1991.

Wen H and Jaffer FA. An in vivo automated shimming method taking into account shim current constraints. *Magn Reson Med* 34: 898-904, 1995.

White FJ, Xiu-Ti HU, Zhang XF and Wolf ME. Repeated administration of cocaine or amphetamine alters neuronal responses to glutamate in the mesoaccumbens system. *J. Pharmacol. Exp. Ther.* 273: 445-454, 1995.

Wilson JL, Jenkinson M, de Araujo I, Kringelbach ML, Rolls ET and Jezzard P. Fast, fully automated global and local magnetic field optimization for fMRI of the human brain. *Neuroimage* 17: 967-976, 2002.

Winston JS, Strange BA, O'Doherty J and Dolan RJ. Automatic and intentional brain responses during evaluation of trustworthiness of faces. *Nat Neurosci* 5: 277-283, 2002.

Wise RA. Neuroleptics and operant behavior: the anhedonia hypothesis. *Behav. Brain Sci.* 5: 39-87, 1982.

Wise RA. Drug self-administration viewed as ingestive behaviour. *Appetite* 28: 1-5, 1997.

Worsley KJ. Statistical analysis of activation images. In: *Functional MRI: An introduction to methods*, edited by Jezzard P, Matthews PM and Smith SM. Oxford: Oxford University Press, 2001, p. 251-270.

Worsley KJ, Evans AC, Marrett S and Neelin P. A three-dimensional statistical analysis for CBF activation studies in human brain. *J Cereb Blood Flow Metab* 12: 900-918, 1992.

Worsley KJ, Marrett P, Neelin AC, Friston KJ and Evans AC. A unified statistical approach for determining significant signals in images of cerebral activation. *Hum Brain Mapp* 4: 58-73, 1996.

Wyvell CL and Berridge KC. Intra-accumbens amphetamine increases the condioned incentive salience of sucrose reward: enhancement of reward wanting without enhanced liking or response reinforcement. *J Neurosci* 20: 8122-8130, 2000.

Yamaguchi S. The synergistic taste effect of monosodium glutamate and disodium 5'-inosinate. *J. Food Sci.* 32: 473-478, 1967.

Yamaguchi S and Kimizuka A. Psychometric studies on the taste of monosodium glutamate. In: *Glutamic Acid: Advances in Biochemistry and Physiology*, edited by Filler LJ, Garattini S, Kare MR, Reynolds WA and Wurtman RJ. New York: Raven, 1979, p. 35-54.

Yamaguchi S and Ninomiya K. Umami and food palatability. *J Nutr* 130: 921S-926S, 2000.

Yan J and Scott TR. The effect of satiety on taste cells in the amygdala of the alert monkey. *Brain Res* 740: 193-200, 1996.

Yasui Y, Breder CD, Saper CB and Cechetto DF. Autonomic responses and efferent pathways from the insular cortex in the rat. *J Comp Neurol* 303: 355-374, 1991.

Yasui Y, Saper CB and Cechetto DF. Calcitonin gene-related peptide immunoreactivity in the visceral sensory cortex, thalamus, and related pathways in the rat. *J Comp Neurol* 290: 487-501, 1989.

Yaxley S, Rolls ET and Sienkiewicz Z. The responsiveness of neurons in the insular gustatory cortex of the macaque monkey is independent of hunger. *Physiol Behav* 42: 223-229, 1988.

Yaxley S, Rolls ET, Sienkiewicz Z and Scott TR. Satiety does not affect gustatory activity in the nucleus of the solitary tract of the alert monkey. *Brain Res* 347: 85-93, 1985.

Yaxley S, Rolls ET and Sienkiewicz ZJ. Gustatory responses of single neurons in the insula of the macaque monkey. *J Neurophysiol* 63: 689-700, 1990.

Yoshida M and Saito S. Multidimensional scaling of the taste of amino acids. *Jpn Psych Res* 11: 149-166, 1969.

Zald DH, Hagen MC and Pardo JV. Neural correlates of tasting concentrated quinine and sugar solutions. *J Neurophysiol* 87: 1068-1075, 2002.

Zald DH, Lee JT, Fluegel KW and Pardo JV. Aversive gustatory stimulation activates limbic circuits in humans. *Brain* 121: 1143-1154, 1998.

Zald DH and Pardo JV. Emotion, olfaction, and the human amygdala: amygdala activation during aversive olfactory stimulation. *Proc Natl Acad Sci U S A* 94: 4119-4124, 1997.

Zald DH and Pardo JV. Cortical activation induced by intraoral stimulation with water in humans. *Chem Senses* 25: 267-275, 2000a.

Zald DH and Pardo JV. Functional neuroimaging of the olfactory system in humans. *Int J Psychophysiol* 36: 165-181, 2000b.

Zatorre RJ, Jones-Gotman M, Evans AC and Meyer E. Functional localization and lateralization of human olfactory cortex. *Nature* 360: 339-340, 1992.

Zatorre RJ, Jones-Gotman M and Rouby C. Neural mechanisms involved in odor pleasantness and intensity judgments. *Neuroreport* 11: 2711-2716., 2000.

Zhang ZH, Dougherty PM and Oppenheimer SM. Characterization of baroreceptor-related neurons in the monkey insular cortex. *Brain Res* 796: 303-306, 1998.

Zhang ZH and Oppenheimer SM. Baroreceptive and somatosensory convergent thalamic neurons project to the posterior insular cortex in the rat. *Brain Res* 861: 241-256, 2000.